THE RELEVANCE OF MICRORNAS AND CIRCADIAN RHYTHMS IN DRUG SAFETY

Thesis submitted in accordance with the requirements of the University of Liverpool for the degree of Doctor in Philosophy

By

Philip James Starkey Lewis

September 2012

DECLARATION

This thesis is the result of my own work. The material contained within this thesis has not been presented, nor is currently being presented wholly, or in part, for any other degree of qualification.

Philip James Starkey Lewis

This research was undertaken at the Department of Molecular & Clinical Pharmacology, at the Centre for Drug Safety Science, University of Liverpool.

CONTENTS

ABSTRACT

Drug-induced liver injury (DILI) is a serious adverse drug reaction (ADR) that is frequently encountered during drug development, representing a major cause of drug attrition. Furthermore, DILI is also a serious concern in the clinic, accounting for approximately half of all acute liver failure cases. Paracetamol overdose (acetaminophen; APAP) accounts for the majority of DILI-associated cases of ALF encountered in patients. The identification and development of novel biomarkers of DILI that are sensitive, specific, and rise early during hepatotoxicity are urgently required in the clinic and in the laboratory. Two liver-specific microRNAs (miRNAs) have recently been described that serve as sensitive and early markers of APAP-induced acute liver injury (APAP-induced ALI) in a mouse model. Together with the superior liver-enrichment of some liver-enriched miRNAs, these potential markers need to be assessed in patients for the clinical promise. Moreover, further work is warranted to test these potential markers in alternative pre-clinical models with other compounds to gain a better understanding regarding sensitivity of release, mechanism of release and circulatory kinetics. Furthermore, in separate work discussed in this thesis, the mammalian biological clock has been found to exert a powerful influence on the physiology of mammalian systems. This regulation hinges on the complex interplay between the clock genes and their products that oscillate over a twenty-four hour period and promote a diurnal variation in numerous output pathways. Emerging evidence suggests that the efficacy and toxicity of many drugs follow a diurnal rhythm and that this may be at least partly attributable to the clock-mediated regulation of drug targets and pathways of drug metabolism. APAP and FS represent two compounds that elicit hepatotoxicity in the mouse through two distinct mechanisms. Both APAP and FS are known to exhibit circadian variation in their toxicology and/or pharmacology. However, little is known about the molecular mechanisms that govern these differences in circadian variation.

Two liver-enriched miRNAs (miR-122 and miR-192) were tested alongside serum ALT activity, the gold-standard marker of ALI, for sensitivity and time of release in a mouse model of APAP-induced ALI. At 2 hours after APAP administration, miR-122 (ΔΔCt 75.0, *P*=0.02) was significantly higher compared to controls (ΔΔCt 4.1) while ALT levels were in the normal range (21 U/L) indicating earlier release of miR-122. In a sensitivity study, miR-122 was not more sensitive than ALT at a 300 mg/kg dose of APAP compared to controls (mean values 300 mg/kg vs 0 mg/kg: ALT = 491 U/L vs 38.1 U/L; miR-122 = ΔΔCt 572.9 vs ΔΔCt 209.4). In patients, serum miR-122 and miR-192 were substantially higher in APAP-induced ALI patients, compared to healthy controls (median ΔΔCt miR-122: 1,265 versus 12.1, P < 0.0001; miR-192: 6.9 versus 0.44 P < 0.0001). A heart-enriched miR-1 showed no difference between APAP-ALI patients and controls, whereas miR-218 (brain-enriched) was slightly higher in the APAP-ALI cohort (ΔΔCt 0.17 versus ΔΔCt 0.07 P = 0.01). In a cohort comprised of patients who presented early (median time of presentation since APAP overdose = 8 hours), miR-122 was significantly raised in patients who develop ALI (> 3 x ULN serum ALT activity) compared to those that did not (median ΔΔCt 3.48 vs ΔΔCt 0.16, P<0.0001). In contrast, presentation ALT levels were not different between patients who developed ALI compared to those that did not (median ALT = 21 U/L vs 19 U/L). Moreover, miR-122 was significantly raised in patients who develop coagulopathy (INR > 1.3) compared to those that did not (ΔΔCt vs 3.48 vs ΔΔCt 0.17, P=0.0004). In contrast, presentation ALT levels were not different between patients who developed ALI

compared to those that did not (median ALT = 21 U/L vs 19 U/L). In chronotoxicity studies, both APAP exhibited greater toxicity in the evening (mean ALT = 12785, 66% survival) compared to morning (mean ALT = 380, 100% survival) whereas FS showed greater toxicity after morning administration (mean ALT=561, 100% survival) compared to evening administration (mean ALT = 69.2, 100% survival). Circadian variation in APAP-induced ALI was associated with 38% lower (P=0.003) GSH levels and 20% higher (P=0.024) Cyp2e1 levels at 21:00h compared to 09:00.

This work confirms that miR-122 is released earlier than ALT in a young mouse model of APAP-induced ALI. Furthermore, it is shown for the first time that circulating liver enriched miRNAs are higher in patients following an APAP overdose. Also, plasma miR-122 is raised at emergency room presentation when serum ALT activity is in the normal range. Further clinical development of blood-based miR-122 is warranted, this work suggests that miR-122 analysis at the point of hospital admission can predict risk of subsequent liver injury in patients. Finally, APAP and FS exhibit circadian variation in their toxicity in a mouse model associated with circadian variation with genes involved in drug metabolism and drug detoxification. Profiling of the hepatic proteome over the circadian phase is now warranted.

ACKNOWLEDGEMENTS

I would like to express my gratitude to my supervisors Dr Chris Goldring, Dr Jonathan Moggs and Prof. Kevin Park for their advice, support, guidance and understanding during my PhD studies. I could not have completed this work without them. Thank you.

A special thanks to Dr Cliff Rowe for his patience, expertise and assistance in the lab throughout my studies. I would like to thank Val Tilston for her expertise and help with FFPE preparations. I'd also like to thank Giovanni Pellegrini, Joanne Walsh, Jack Sharkey, Luke Palmer, and Rob Hornby for their positivity and willingness to help with animal studies. I would like to thank Viv Platt for her thoroughness and superb preparation during microRNA studies. I would like to mention Dr Daniel Antoine, Dr James Dear, Dr Neil French and Dr Dominic Williams for their scientific contribution and invaluable expertise in toxicology.

I would also like to thank the investigative toxicology team at Novartis for their kindness and scientific support to help me learn new techniques on my industrial placements. In particular I'd like to thank Dr Philippe Couttet, Dr Olivier Grenet, Dr Michael Kammuller, and Dr Valérie DuBost for their excellent coordination and providing a fascinating insight into the pharmaceutical industry. I'd also like to thank Caterina Vacchi Suzzi, Harri Laemäinen and Magdalena Westphal for their help in the laboratory and their friendship on those placements.

I'd like to express my thanks to my university colleagues for their friendship and laughter, namely James Firman, Jon Lea, Catherine Bell, Hannah Aucott, Kelly Robinson, Joanne Gamble, Mathieu Bangert, Micheal Heinrich and many more. They have made my post-graduate experience a thoroughly enjoyable one. Thanks for the memories.

I must mention my life-long friends Kevin Parr, Peter Kaiser and Christopher Howard who have provided me with kindness, love and laughter all my life. They have been through the ups and downs with me, and I am extremely lucky to call them friends.

Finally, I'd like to express a special thank you to my mum and dad who have supported me, and believed in me from the beginning. Thank you for your unwavering support, love, understanding and encouragement. This is yours as much as it is mine.

This thesis is dedicated to my Grandad, James Ainsworth (1917-2006).

PUBLICATIONS

Research articles

Starkey Lewis PJ, Dear J, Platt V, Simpson KJ, Craig DG, Antoine DJ, French NS, et al. Circulating microRNAs as potential markers of human drug-induced liver injury. Hepatology 2011; **54**(5): 1767-1776.

Antoine DJ, Dear J , **Starkey Lewis PJ**, Platt V, Coyle J, Masson M, Thanacoody R, et al Mechanistic biomarkers provide early and sensitive detection of paracetamol-induced acute liver injury at first presentation to hospital. Hepatology 2013, *in press*

Pellegrini G, Palmer, L, **Starkey Lewis PJ**, Goldring CE, Park BK, Kipar A, Williams DP Intraperitoneal administration of polyethylene glycol (PEG) causes low-grade peritonitis and hepatic subcapsular necrosis associated with a rise in hepatic biomarkers. *Manuscript in preparation*

Starkey Lewis PJ, Hornby R, Rowe C, Moggs J, Goldring C, Park BK. Exploring the hepatic proteome to investigate the chronotoxicity of acetaminophen and furosemide. *Manuscript in preparation*

Review articles

Starkey Lewis PJ, Merz M, Couttet P, Grenet O, Dear J, Antoine DJ, Goldring CE, Park BK, Moggs JG. Serum microRNA biomarkers for drug-induced liver injury. Clinical Pharmacology & Therapeutics

Correspondence articles

Starkey Lewis PJ, Dear J, Platt V, Moggs J, Goldring C, Park BK. Reply. Hepatology 2012; **55**(5): 1642-1643.

Abstracts

Investigation of circadian variation in the hepatic proteome in a mouse model of paracetamol-induced hepatotoxicity - BPS Winter meeting, London, U.K., December 2010.

ABBREVIATIONS

%CV	coefficient of variation
3'UTR	three prime untranslated region
5-FU	5-fluorouracil
ACE	angiotensin converting enzyme
ADR	adverse drug reaction
AFLP	acute fatty liver of pregnancy
AFP	alpha-fetoprotein
AGO2	argonaute 2
AIH	autoimmune hepatitis
ALAS1	aminolevulinic acid synthase 1
ALDH	aldehyde dehydrogenase
ALDOA	aldolase A
ALF	acute liver failure
ALI	acute liver injury
ALP	alkaline phosphatise
ALT	alanine aminotransferase
AMAP	N-acetyl-3-hydroxy-aminophenol
AMPK	AMP kinase
ANOVA	analysis of variance
APACHE II	acute physiology and chronic health evaluation II
APAP	acetaminophen
APAP ALI	acetaminophen-induced acute liver injury
APAP NO ALI	acetaminophen overdose without acute liver injury
APAP-induced ALI	acetaminophen-induced acute liver injury
APC	antigen presenting cell
ASK-1	apoptosis signal-regulating kinase-1
AST	aspartate aminotransferase
ATP	adenosine triphosphate
AUC	area under the curve
BCRP	breast cancer resistance protein
BD	bile duct
bHLH	basic helix loop helix
BMAL	aryl hydrocarbon receptor nuclear translocator-like
BMI	body mass index
BSEP	bile salt export pump
C/EBP	CCAAT/enhancer binding protein
CAR	constitutive androstane receptor
CCR2	C-C motif chemokine receptor 2
CCR4	C-C motif chemokine receptor 4
CDDO	2-cyano-3,12-dioxooleana-1,9,-dien-28-oic acid
CDDO-Im	1[2-Cyano-3,12-dioxooleana-1,9(11)-dien-28-oyl]imidazole
cDNA	copy DNA
CDSS	centre for drug safety science
cel	caenorhabditis elegans
CES	carboxylesterase

CI	confidence interval
CKD	chronic kidney disease
CLOCK	circadian locomotor output cycles kaput
CNS	central nervous system
CO2	carbon dioxide
COX	cyclooxygenase
CRM	chemically reactive metabolite
CRY	cryptochrome
CV	centrilobular vein
CVVH	continuous veno-venous hemofiltration
CYP450	cytochrome P450
DAMP	danger associated molecular pattern
DBP	D-site albumin promotor binding protein
DILI	drug-induced liver injury
DMSO	dimethyl sulfoxide
DNA	deoxyribonucleic acid
Dnd1	dead End 1
DPD	dehydropyrimidine dehydrogenase
DTNB	5,5'-dithiobis-(2-nitrobenzoic acid)
eIF4E	eukaryotic translation initiation factor 4E
ELISA	enzyme-linked immunosorbent assay
EPCAM	epithelial cell adhesion molecule
FDA	food and drug administration
FFPE	formalin-fixed paraffin embedded
FMO	flavin-containing monooxygenase
FS	furosemide
GAPDH	glyceraldehyde 3-phosphate dehydrogenase
GCL	glutamylcysteine synthetase
GCLC	glutamylcysteine synthetase catalytic domain
GCLM	glutamylcysteine synthetase modifying domain
GdCl3	galolinium chloride
GGT	gamma-glutamyltranspeptidase
GLDH	glutamate dehydrogenase
GSH	glutathione (reduced)
GSSG	glutathione (oxidised)
GST	glutathione-S-transferase
GW182	glycine-tryptophan repeat-containing protein
GYS1	glycogen synthase 1
H&E	hematoxylin and eosin
H20	water
H202	hydrogen peroxide
HA	hepatic artery
HBV	hepatitis B virus

HCC	hepatocellular carcinoma
HCV	hepatitis C virus
HE	hepatic encephalopathy
HLA	human leukocyte antigen
HLF	hepatic leukaemia factor
HMGB1	high-mobility group protein B1
HNF	hepatocyte nuclear factor
hsa	human
HuR	Human antigen R protein
i.p.	intraperitoneal
IFN	interferon
IGF2	insulin-like growth factor 2
IL	interleukin
IMI	innovative medicines initiative
INR	international normalised ratio
IQR	interquartile range
ISI	international sensitivity index
JNK2	c-Jun N-terminal protein kinase 2
KCC	king's college criteria
kDa	kilodalton
LD50	lethal dose at 50% mortality
LDH	lactate dehydrogenase
LKB	liver kinase B
LNA	locked nucleic acid
L-NAME	N-(G)nitro-L-arginine methyl ester
L-OHP	oxaliplatin
LT	liver transplant
LYS	lysine
m7G	7-methylguanosine
MELD	model for end-stage liver disease
MIF	macrophase migration inhibitory factor
miRISC	microRNA-induced silencing complex
miRNA	micro RNA
miRNA*	microRNA (passenger strand)
MnSOD	manganese superoxide dismutase
MPT	mitochondrial membrane permeability transition
mRNA	messenger RNA
MRP	multi-drug resistance protein
MTT	3-(4,5-dimethythiazol-2-yl)-2,5-diphenyl tetrazolium bromide

NAC	N-acetylcysteine
NADP+	nicotinamide adenine dinucleotide phosphate (oxidised)
NADPH	nicotinamide adenine dinucleotide phosphate (reduced)
NaF/Kox	sodium fluoride/potassium oxalate
NAPQI	n-acetyl-p-benzoquinoneimine
NBT	nitro blue tetrazolium
NCE	new chemical entity
NHS	national health service
nm	nanometers
NO	nitric oxide
NON-APAP ALI	acute liver injury not caused by acetaminophen
NonO	Non-POU domain-containing octamer-binding protein
NPM1	nucleophosmin1
NRF2	nuclear factor erythroid 2-related factor
nt	nucleotide
OAT	organic anion transporters
OCT	organic cation transporters
OLT	orthotopic liver transplant
ONOO-	peroxynitrite
P	probability
PAN	poly(A)specific ribonuclease
PAPS	3'phosphoadenosine-5-phosphosulphate
PAS	period arnt single-minded
PBS	phosphate buffered saline
PEG	polyethylene glycol
PER	period
pH	power of hydrogen
PMCA	plasma membrane calcium ATPase
POD	paracetamol overdose
pre-miRNA	precursor microRNA
pri-miRNA	primary miRNA
PROK-2	prokineticin 2
PROM1	prominin 1
PT	prothrombin time
PTIO	2-phenyl-4,5,5,5-tetramethylimidazoline-1-oxyl-3-oxide
PUF	pumilio protein
PV	portal vein
qPCR	quantitative polymerase chain reaction
R.E.M.	rapid eye movement
R2	correlation coefficient
REV-ERBα	nuclear receptor subfamily 1, group D, member 1
RNA	ribonucleic acid
RNU	small nuclear RNA
ROC	receiver operator curve

ROR	RAR-related orphan receptor
RRT	renal replacement therapy
SAFE-T	safer and faster evidence-based translation
SAM	S-adenosylmethionine
SCN	superchiasmatic nuclei
SENS	sensitivity
siRNA	small interfering RNA
SNP	single nucleotide polymorphisms
snRNA	small nuclear RNA
SRC	proto-oncogene tyrosine-protein kinase
SSA	sulfosalicylic acid
TBS	tris-buffered saline
TEF	thyrotroph embroyonic factor
TGFα	transforming growth factor alpha
THF	tetrahydrofolate
THY1	thymocyte differentiation antigen 1
TLR	toll like receptor
TNF	tumour necrosis factor
TRBP	transactivation response RNA binding protein
TS	thymidilate synthetase
U/L	international units per litre
UDP	uridine diphophaste
UDPGA	uridine diphophaste-glucuronic acid
ULN	upper limit of normal
US	United States
UV	ultraviolet
VEGF	vascular endothelial growth factor
VLDL	very low density lipoprotein
WDR5	WD repeat-containing protein 5
XRN	5-3 exoribonuclease 1
ZT	zeitgeber
ΔΔCt	delta delta cross threshold

FOREWORD

In chapter 3, parts of the text and figures are taken directly from a published article, namely:

Starkey Lewis PJ, Dear J, Platt V, Simpson KJ, Craig DG, Antoine DJ, French NS, et al. Circulating microRNAs as potential markers of human drug-induced liver injury. Hepatology 2011; 54(5): 1767-1776.

In chapter 4, parts of the text are taken directly from a published article in press, namely:

Antoine DJ, Dear J , Starkey Lewis PJ, Platt V, Coyle J, Masson M, Thanacoody R, et al Mechanistic biomarkers provide early and sensitive detection of paracetamol-induced acute liver injury at first presentation to hospital. Hepatology, 2013. *in press*

All work presented herein is my own. I am the sole author of the contents of this thesis.

P.J. Starkey Lewis

CHAPTER ONE

GENERAL INTRODUCTION

1.1 INTRODUCTION

Adverse drug reactions (ADRs) can be defined as any undesirable effect caused by a xenobiotic. ADRs can be broadly classified into two types, as follows: type A reactions are more common, often dose-dependent and can be described as an exaggeration of the known primary or secondary pharmacology. Type B reactions can be described as idiosyncratic reactions; they are unpredictable, rare but often severe. Several studies have shown that between 2.4-12 % of all hospital admissions are due to an ADR (Pirmohamed et al, 2004; Lazarou et al, 1998). Due to their prevalence, their impact on healthcare systems is significant, i.e. 4 out of 100 hospital bed days in the UK equating to an estimated cost of £400m per annum (Pirmohamed et al, 2004). They are a major cause of patient mortality, two studies found that between 0.13-0.15 % of all patients admitted to hospital died resulting from an ADRs, equating to approximately 5,700 deaths in England a year (Pirmohamed et al, 2004; Lazarou et al, 1998). Furthermore, ADRs represent one of the leading causes of drug attrition during pre-clinical drug development in an increasingly competitive and expensive drug discovery process (Kola & Landis, 2004). The cost of discovering, developing and marketing a new chemical entity is approximately $1bn and with increasing social and regulatory pressure to produce affordable drugs with exemplary safety profiles yet only one in three drugs that reach the market returns a profit (Grabowski et al, 2002).

Drug-induced liver injury (DILI) is one of the most common ADRs encountered in pre-clinical and clinical settings. Hepatotoxicity is the most cited reason a drug will be withdrawn or restricted by the FDA in the post-marketing phase (Giri et al, 2010). In the clinic, DILI is a major concern to physicians as 50% of ALF cases are attributed to drug-induced hepatotoxicity in the United States (Russo et al, 2004). The liver is susceptible to a drug-induced toxicity more than any other organ in the body and it has been estimated that over 900 drugs have been associated with hepatotoxicity (Giri et al, 2010). This can be explained from a physiological perspective as the liver is the major site of drug metabolism and drug biotransformation. Many drugs are hydrophobic and the drug metabolism systems

present in the liver will increase the hydrophilicity of these compounds, to facilitate clearance from the body. However, in many cases of DILI, these drug-metabolising systems inadvertently generate chemically-reactive metabolites (CRMs) which can in turn cause cell death. One of the major concerns for the pharmaceutical industry is the lack of predictive toxicity models available during pre-clinical drug testing, as many drugs have species-dependent drug metabolism, and species-dependent drug toxicities. In order for us to better understand the molecular mechanisms that underpin drug-induced liver toxicity, studies have identified archetypal hepatotoxins that can be utilised as models. Despite a rich literature of experimental evidence, the exact molecular pathways with which drugs elicit cell death remain poorly understood. Such model hepatotoxins provide a bridge between chemical structure, drug metabolism, cellular targets, and cell death pathways. Ideally, it would be possible to predict toxicity from the chemical structure to allow generation of safe, non-toxic drugs. In some cases, the toxicity cannot be 'designed out' of the molecule, as the pharmacophore (which provides drug efficacy) and the toxicophore (which provides drug toxicity) are the same.

Two well-defined hepatotoxins that cause predictable liver injury in rodent models are paracetamol (acetaminophen; APAP) and FS (frusemide; FS). APAP is a common, over-the-counter analgesic that has been used for 60 years. Despite an excellent safety profile at therapeutic doses (4g/day), in an overdose setting it can cause coagulative centrilobular liver necrosis and potentially fatal liver failure. In fact, a U.S. study found that APAP was the leading cause of acute liver failure (ALF) accounting for 50 % of cases (Lee, 2004). This equates to approximately 10,000 hospitalisations and 500 deaths per annum. APAP is an aminophenol compound that undergoes extensive phase II metabolism to yield non-toxic APAP-sulphates and APAP-glucuronides. A minor pathway involves phase I oxidation via cytochrome P450 (CYP) isoforms which generate a protein-reactive electrophile, n-acetyl-p-benzoquinoneimine (NAPQI). NAPQI binds to protein thiols and causes cell death due to centrilobular liver necrosis in rodents and in man (Mitchell et al, 1973; Gujral et al, 2002).

FS, a carboxylic acid diuretic used for the treatment of hypertension has been less well-studied. FS has been found to cause centrilobular liver necrosis in mice, but not in man, (Mitchell et al, 1974; Mitchell et al, 1976). It has been found that FS also generates a CYP-mediated, chemically reactive metabolite (Williams et al, 2007). Although both APAP and FS present a similar pattern of injury in mice, it is considered that they do so through distinct mechanisms.

Specific and sensitive biomarkers of DILI are essential to detect, diagnose, monitor and provide mechanistic insight into liver injury. Current biomarkers include protein-based markers, e.g. the aminotransferases, liver function markers such as albumin or prothombin time and novel mechanistic markers such as HMGB1 and cytokeratin-18 (Amacher, 1998; Ozer et al, 2008; Antoine et al, 2009). However, several limitations exist which confound the reliability of these markers in clinical and pre-clinical settings. Such limitations include unacceptable false-positive / false-negative rates, poor tissue specificity, poor biological or technical sensitivity and an excessive latent phase between injury and circulatory signal. An ideal biomarker would be accurate (i.e. reflects the physiological/pathophysiological status of the liver), sensitive, liver-specific, abundant in a non-invasive biofluid such as blood or urine, stable, translatable (i.e. across *in vitro*, *in vivo* and in clinical settings), able to be assayed quickly and cheaply, and detectable soon after (or even before) injury has occurred.

MicroRNAs (miRNAs) are short, non-coding RNA species, between 19-25 nucleotides in length. They function to repress a distinct set of cognate mRNAs which they do so through a variety of mechanisms. miRNAs thereby regulate protein output and the phenotype of the cell. To date, over 1500 miRNAs have been described in man (approximately 750 in mice) some of which are highly conserved between species (Altuvia *et al*, 2005). Despite their ribonucleic acid make-up, their abundance in RNase-rich matrices including blood and urine is surprisingly high suggesting that protection is afforded by auxiliary molecules. The potential of circulating miRNAs to inform on a number of pathologies has been reported in a number of publications, including cancer, myocardial infarction and hepatitis (Mitchell et al,

2008; D'Alessandra et al, 2010; Zhang et al, 2010). Recently, it was reported that miR-122 and other liver-specific miRNAs were found to be raised in the serum of mice treated with APAP (Wang et al, 2009). Furthermore, this study found that miR-122 was detected earlier and at lower doses of APAP than serum alanine aminotransferase (ALT) activity, the current gold-standard biomarker of liver injury. Liver specific miRNAs have the potential to complement existing biomarkers of DILI in clinical and pre-clinical settings, but need further work to assess their utility. Therefore, this represents a key focus for the work presented in this thesis.

Another smaller but significant aim of the work in this thesis has focussed on a relatively under-researched are in the field of drug toxicity, that of the role of circadian rhythms in DILI. Circadian rhythms can be defined as 24 hour rhythms in a biological system. They have been found to exist in diverse life forms from cyanobacteria to higher mammals. The role of the biological clock is to enable anticipatory behaviour, rather than a reactionary activity, to stimuli e.g. food availability. Many physiological processes are known to express a degree of circadian variation, including heart rate, blood pressure, body temperature, rest-activity cycles, hepatic blood flow, bile production, endocrine function and metabolism. The discovery of clock genes provided mechanistic insight into the generation and autonomy of circadian rhythms (Vitaterna et al, 1994). Initially, it was thought that main site of circadian regulation was in the superchaismatic nuclei (SCN) of the central nervous system (CNS). However, since then, it has been found that functional clocks exist in almost all cell types in the body, including hepatocytes and keratinocytes (Panda et al, 2002; Zanello et al, 2000). The association between drug effect and time of day has been appreciated for centuries; a concept more recently termed 'chronopharmacology'. Pharmacokinetics, pharmacodynamics and drug toxicities have all been shown to display circadian variation in both animal models and in man for a number of drugs. With the current burden of ADRs and lack of understanding behind the causal mechanisms, new concepts and tools are needed to improve drug safety. Understanding the molecular basis of

chronopharmacology represents a potential area to provide a better understanding behind the causality of drug toxicities.

1.2 ADVERSE DRUG REACTIONS

ADRs are a major clinical problem in terms of prevalence, patient morbidity, patient mortality and cost to healthcare systems. A 2004 UK study found that 1225 (6.5%) of 18,820 inpatients were admitted between two hospitals were due to an ADR (Pirmohamed et al, 2004). The median hospital stay was 8 days (4% of hospital bed capacity), a significant amount of clinical resource. This was estimated to equate to an annual cost of £466m to the NHS. The overall mortality rate in this study was 0.15%, a figure which is similar to that stated in other reports (Lazarou et al, 1998). ADRs were responsible for the withdrawal of 16 out of 548 new chemical entities (NCEs) from the US market between 1975 and 1999. Moreover, 56 out of 548 were labelled with a black box warning which may severely reduce the confidence in the utility of a NCE (Lasser *et al*, 2002). The majority of ADRs that are presented in the clinic are type A reactions, which are distinct from rarer type B idiosyncratic ADRs. Type A reactions (also known as "on target" reactions) are common, predictable, and are considered exaggerations of the known primary and secondary pharmacology. Due to the drug-related causality of type A ADRs, reactions usually respond well to dose-reduction, and are only in some cases life-threatening. Typical examples of type A reactions include bleeding with the anticoagulant warfarin, hypotension caused by angiotensin converting enzyme (ACE) inhibitors and bradycardia due to atenolol administration.

Type B (idiosyncratic) ADRs are unpredictable and not necessarily dose-dependent. Although they are much rarer than type A reactions, they are often more severe and life-threatening. Idiosyncratic ADRs typically occur at a rate between 1 in 10,000 to 1 in 100,000 individuals and are often not detected in preclinical safety studies or even in the early clinical trials when NCEs are evaluated on their safety profile in man (Giri et al, 2010). Therefore idiosyncratic ADRs may only be observed in the post-marketing phase of a NCE leading to significant patient morbidity and patient mortality. Often idiosyncratic ADRs can be linked to host factors in the patient, such as genetic variation or an underlying disease

which may predispose that patient to the ADR. One example includes the genetic variant of human leukocyte antigen (HLA), HLA-B*5701, an allelic variant of the major histocompatibility class I complex (Mallal et al, 2002). This allele occurs at a rate of approximately 5% in the general population and was found to predispose patients to hypersensitivity reactions with Abacavir (Mallal et al, 2008). However, not all patients with this allele, develops toxicity. There is cause for optimism as a 2008 clinical study confirmed that prior pharmacogenetic testing for this allelic variant could reduce the risk of hypsersensitivity reactions in patients taking abacavir (Mallal et al, 2008).

1.3 DRUG-INDUCED LIVER INJURY (DILI)

Of all the different forms of ADRs, the liver is one of the most susceptible organs in which a drug can evoke toxicity. The majority of cases (80%) of drug-induced liver failure cases are due to APAP intoxication. To date, over 900 different drugs have been associated with liver injury which are independent of drug class or disease type (Etxagibel *et al*, 2008). These drugs include prescribed medicines such as antiretrovirals or statins but also widely-available, over-the-counter medications, e.g. analgesics and NSAIDs. DILI is a multi-factorial disease that can be influenced by host factors including age, sex, nutrition, other drugs (including alcohol), underlying illness, and genetics. The manifestation of DILI in the clinic is diverse, even for the same drug. Drugs can cause a variety of pathologies including subtle asymptomatic rises in circulating aminotransferase levels, acute fatty liver, cirrhosis and in rare cases fulminent liver failure (Tujios et al, 2011). Despite a rich literature of evidence, the causal mechanisms behind which drugs cause DILI are poorly defined. Even for model hepatotoxins, such as APAP, which encompasses a huge body of work, the proposed mechanisms of toxicity are controversial and remain poorly understood. This paradox has been attributed to the lack of diagnostic biomarkers, poor translational ability in pre-clinical models and unsuitable *in vitro* models that poorly reflect *in vivo* conditions. Nevertheless, one of the major advances in molecular toxicology was the establishing the

association between drug metabolism, chemically reactive metabolites and the initiation of hepatotoxicity (for review, see Kaplowitz, 2005; Park et al, 2005).

1.3.1 The role of drug metabolism in DILI

The liver is a multicellular and multifunctional organ, as well as being the major site of drug metabolism in the body. The liver receives 30 % of the resting cardiac output, 75 % of which reaches the liver direct from the gastrointestinal organs providing the liver with a substantial exposure to potentially toxic species ingested through the diet. Regardless of the dosing route, the liver is responsible for the biotransformation of most xenobiotics. The liver probably gained its repertoire of drug-metabolism pathways throughout evolution as a means to detoxify noxious components in the diet (Gonzalez and Gelboin, 1993). Broadly speaking, the physiological role of the liver is to convert lipophilic compounds into more hydrophilic species in order to facilitate drug clearance from the body, and expunge pharmacological activity. The drug metabolism systems between mammals are relatively well conserved which allows many drugs to be investigated in clinically-relevant animal models. The mammalian drug metabolism system is comprised, traditionally, of three phases; phase I, phase II and phase III drug metabolism. The role of each phase is briefly explained in table 1 below. N.B. Phase I metabolism does not necessarily always preclude phase II metabolism; however both of these phases are often required for the conjugation of large polar groups to a xenobiotic.

Table 1: The basic role of phase I, phase II and phase III drug metabolism

Drug Metabolism Phase	Role
Phase I	Small chemical modifications, reveals functional groups
Phase II	Conjugation reactions, vastly increases hydrophilicity
Phase III	Transportation of suitable substrates, e.g. at cell membranes

1.3.2. Phase I drug metabolism

Phase I drug metabolism encompasses oxidation, reduction and hydrolysis reactions to substrates which reveal functional groups, usually a hydroxide, an amine or a carboxylic acid. These relatively reactive functional groups allow the conjugation of large polar moieties to a drug by phase II drug metabolising systems (for review, see Gibson & Skett, 2001). The major components of the phase I drug metabolising system include the cytochrome P450 (CYP450) enzymes, flavin-containing monooxygenases (FMOs), alcohol dehyrogenases and epoxide hydrolases, amongst others (Testa et al, 2012). The most functionally- and clinically-important group are the CYP450 enzymes, which contribute approximately 75% of phase I metabolism to drugs (Ingelman-Sundberg, 2002). The CYP450 superfamily (so called, because of the unique spectral absorbance peak of 450 nm when bound to carbon monoxide) are a diverse class of metabolising enzymes found throughout nature. Humans have approximately 59 active CYP genes, many of which are important in the metabolism of endogenous sterols, vitamins and fatty acids (Guengerich, 2006). However, in man, the majority of xenobiotics are metabolised by eight genes; CYP1A2, CYP2B6, CYP2C9, CYP2C19, CYP2D6, CYP2E1, CYP3A4 and CYP3A5 which exhibit different substrate specificities, tissue localisation, zonal expression, and abundance in the liver. The characteristics of clinically-important CYP enzymes are summarised in table 2. The activity of CYP isoenzymes can differ between individuals, either due to different basal levels of expression, or the presence of single nucleotide polymorphisms (SNPs) within certain CYP genes which can affect CYP function. This variation explains how individuals may respond differently to drugs, as metabolism can affect pharmacokinetics, pharmacodynamics and drug-related toxicity.

The role of phase I metabolism is to reveal functional groups on a xenobiotic for further biotransformation and detoxication. However, in some cases, this metabolic process generates a more chemically-reactive species. These chemically-reactive metabolites (CRMs) may be reactive to nucleophilic intracellular targets such as proteins, RNA and

DNA, which may induce toxicity. Covalent binding to cellular proteins is considered an important step in the progression of liver injury for many drugs. The individual target proteins which CRMs can bind may influence the outcome of toxicity, i.e. the balance between critical protein vs non-critical protein modification may be a predictor for the outcome of DILI (Park et al, 2005). Carbon tetrachloride, an industrial solvent and potent

Table 2: Characteristics of eight human CYP genes involved in phase I drug metabolism (adapted from Danielson et al, 2002)

CYP Gene	Substrate type	Tissue Localisation	Typical Drug Substrates
CYP1A2	Aromatics, Amines, Pre-carcinogens	Hepatic	caffeine, naproxen
CYP2B6	Xenobiotics	Hepatic	bupropion
CYP2C9	Xenobiotics	Hepatic	ibuprofen, fluoxetine
CYP2C19	Xenobiotics	Hepatic	lansoprazole, diazepam
CYP2D6	Xenobiotics	Hepatic	alprenolol, codeine
CYP2E1	Solvents, xenobiotics, pre-carcinogens	Hepatic	ethanol, APAP
CYP3A4	Xenobiotics, hormones, dietary components	Hepatic, intestinal	lidocaine, hydrocortisone, codeine,
CYP 3A5	Xenobiotics, hormones, dietary components	Hepatic, intestinal	lidocaine, hydrocortisone, codeine,

hepatotoxin, has been shown to form free radicals mediated by CYP2E1 metabolism (Guengerich et al, 1991). Free radicals are recognized cellular stressors that can induce oxidative stress and mediate cell death. However, CRMs can induce cell death via several different mechanisms including oxidative/nitrative stress, apoptosis, necrosis and carcinogenesis and activation of the innate/adaptive immune system. The likelihood of a compound to generate a reactive metabolite is a function of its chemistry. Structural alerts

are now recognised as potential toxicophores, such as quinones, epoxides and thiophenes, which can inform the medicinal chemist to design safer NCEs in an iterative process. CRMs are short-lived species, and difficult to detect in the circulation, and therefore difficult to quantify in man. CRMs, usually electrophiles, remain in the cell where they react to cellular components, typically electron-rich moieties such as thiol groups on cysteine residues. Xenobiotics that are associated with the production of chemically reactive metabolites include APAP (Hinson et al, 1981), FS (Mitchell et al, 1976) and bromobenzene (Jollow et al, 1974). These compounds can be used as training compounds to understand the role of phase I bioactivation in hepatotoxicity in animal models through enzyme induction, enzyme inhibition or gene manipulation studies. Therefore, phase I metabolism can be considered, for many compounds, an integral step in the detoxication and inadvertent initiation of DILI.

1.3.2. Phase II drug metabolism

The phase II drug metabolising systems involve conjugation of large molecular weight species, to increase the polarity and hydrophilicity of xenobiotics. Phase II drug metabolism can be extremely cytoprotective, and can nullify the toxic capacity of a hepatotoxin and a CRM. Phase I and Phase II drug metabolising systems can work in isolation but can also provide tightly coupled detoxication pathways for drugs. This explains why not all drugs that form reactive metabolites cause hepatotoxicity. At therapeutic doses of APAP, the major clearance pathways involve phase II glucuronidation (the addition of glucuronic acid to a substrate) and sulfation (the addition of a sulphate residue to a substrate) mechanisms, which yield non-toxic metabolites. However, a minor proportion of the dose is bioactivated by phase I metabolism (via CYP2E1) to form small quantities of n-acetyl-p-benzoquinoneimine (NAPQI), a protein-reactive electrophile. This potentially toxic species is rapidly bioinactivated by glutathione (GSH) conjugation, mediated in part by glutathione-S-transfereases (GSTs), thereby inhibiting the toxic capacity of NAPQI (Henderson et al, 2000). Due to the large intracellular stores of GSH in the hepatocyte, APAP is an extremely

safe drug when administered at therapeutic doses. Phase II drug metabolism involves a diverse panel of enzymes and substrates which have been summarised in table 3.

With respect to DILI, one of the most important detoxication processes against hepatotoxins, CRMs, and oxidative stress in general is GSH conjugation. GSH is a ubiquitous tripeptide

Table 3: Characteristics of common phase II drug metabolism reactions

Reaction	Enzyme	Substrate
Glucuronidation	UDP-glucuronosyltransfereases	UDP-glucuronic acid (UDPGA)
Sulfation	Sulphotransferase	3'phosphoadenosine-5-phosphosulphase (PAPS)
Methylation	Methyltransferase	S-adenosylmethionine (SAM)
Acetylation	Acetyltransferase	acetyl coenzymeA
Amino acid conjugation	CoA ligase	glycine, glutamine, ornithine, arginine, taurine
Glutathione conjugation	Glutathione-S-transferase / sponteaneous	glutathione
Fatty acid conjugation		stearic acid, palmitic acid

comprising glycine, cysteine and glutamate residues, and is the most abundant non-protein thiol in the hepatocyte (approximately 5-10 mM) (Lu, 1999). GSH is mainly cytosolic, but high concentrations are also found in the mitochondria. GSH is an essential antioxidant in its own right, maintaining cytocellular redox homeostasis and scavenging free radicals generated from endogenous metabolic processes. However, due to the thiol moiety on the

cysteine residue, it exhibits substantial nucleophilic potential, which afford GSH its protective capacity against reactive species formed during drug metabolism. GSH can form conjugates spontaneously, or can be mediated by the GSTs (Meister et al, 1988). Many glutathione conjugates are cleaved by ɣ-glutamyltranspeptidase (GGT) and then dipeptidase to generate a cysteinyl conjugate (Lu, 1999). The cysteinyl conjugate can then be *N*-acetylated to form the resultant non-toxic mercapturic acid for urinary or biliary excretion.

GSH synthesis is a two-step active process involving the conjugation of its constituent amino acids. An absolute prerequisite for GSH synthesis is the conversion of the essential amino acid methionine to cysteine via the transsulfuration pathway. In clinical situations, the hepatic pool of glutathione can be repleted by administering methionine, or more commonly *N*-acetylcysteine (NAC), which both provide the requisite donor amino acids for rapid GSH synthesis. The first synthetic, rate-limiting step involves the active conjugation of L-glutamate and L-cysteine to form ɣ-glutamylcysteine via the enzyme, glutamate-cysteine ligase (GCL; glutamylcysteine synthetase, GCS). This heterodimeric enzyme consists of a heavy catalytic unit (GCLC; 73,000 kDa) and a lighter modifying unit (GCLM; 30,000 kDa) which are encoded by separate genes in rodents and humans (Yan & Meister, 1990, Gipp et al, 1992). The second active step involves the rapid conversion of ɣ-glutamylcysteine with L-glycine by GSH synthetase to form the mature GSH tripeptide. Reduced GSH is the predominant form in the cell which when oxidised, forms a disulphide bond with another GSH molecule to form GSSG. The ratio of GSH to GSSG has been estimated to be approximately 10:1 in the cytosol and mitochondria (Meredith & Reed, 1982; Meister et al, 1988).

GSH depletion is considered a hallmark of DILI as many hepatotoxins, but not all, have been associated with substantial loss of hepatocellular GSH during injury (APAP: Davis et al, 1974, 1,-dichloroethylene: Dowsley et al, 1995, ethanol: Guerri et al, 1980, Randle et al, 2008). The hepatic capacity to conjugate GSH to hepatotoxins can reflect the detoxication potential of the liver. Mice are much more resistant to aflatoxin B1 compared to rats and

humans which is associated with the enhanced ability to detoxify the epoxide metabolite by GST-mediated GSH conjugation (Hengstler et al, 1999). GSH has been shown to be induced after APAP (Goldring et al, 2004) and methapyriline (Mercer et al, 2009) exposure. This induction, associated with increased cell defence protects against subsequent exposure to the drug (Shayiq,et al, 1999; Aleksunes et al, 2008,). More recently, this adaptive protection can be afforded by treatment with novel semi-synthetic triterpenoids (2-cyano-3,12 dioxooleana-1,9 diene-28-imidazolide, CDDO-Im) at relatively low doses (1 mg/kg) against toxic doses of APAP in mice (Reisman et al, 2009). This is a classic example of cellular adaptation to drug-induced stress.

1.3.2. Phase III drug metabolism

As discussed, the role of the liver is to detoxify noxious species, including drugs, from active lipophilic molecules into more hydrophilic, non-toxic species, whilst concomitantly expunging pharmacological activity. This process will ultimately facilitate the clearance of the drug. Glucuronides, sulphates and glutathione conjugate metabolites are often substrates for transporters, a class of membrane bound proteins that represent members of the phase III drug metabolising system. Although phase III drug metabolism doesn't account for a chemical modification to the drug itself, it has an important role in the ultimate disposition and clearance of the drug. Phase III transporters can be broadly classified into two groups; solute carriers and ABC transporter superfamilies. These are summarised in table 4.

Table 4: Members of two classes of phase III transporter proteins

Solute Carriers	ABC transporters
Organic anion transporters (OATs)	Multi-drug resistance protein (MRP)
Organic cation transporters (OCTs)	Breast cancer resistance protein (BCRP)
	Bile salt export pump (BSEP)

The MRP class of transporters are important during APAP metabolism in toxicity. It has been shown that MRP3 and MRP4 are implicated in the efflux of APAP metabolites including the glutathione-conjugate from hepatocytes (Zamek-Gliszczynski et al, 2006, Aleksunes et al, 2008). Furthermore, in mice, MRP3 and MRP 4 are upregulated after a toxic dose of APAP by the nrf2-keap1 cell defence system (Aleksunes et al, 2008). Drug-induced cholestasis is a feature of perturbed phase III drug metabolism, in which cytotoxic bile acids are retained in the liver which can cause both acute and chronic liver injury. Clinical markers of drug-induced cholestasis include elevations in circulating bilirubin and alkaline phosphatase (ALP) (Stapelbroek et al, 2010). Many drugs that are associated with drug-induced cholestasis are substrates for transporters, examples include rifampicin-mediated BSEP inhibition. Transporters are also subject to genetic variation which might predispose individuals to drug-induced cholestasis or liver disease in general (Lang et al, 2007). Clearly, phase III metabolism is an important contributing factor in both the detoxication and the potential pathophysiology of DILI.

1.4. APAP-INDUCED ACUTE LIVER INJURY (APAP-induced ALI)

APAP is a widely-available, over the counter analgesic that has provided effective pain relief for six decades. APAP is available in single formulation or coformulation with other drugs, e.g. codeine or phenylephrine. APAP is well tolerated at therapeutic doses (4g/day) in the general population, despite reports of subtle asymptomatic rises in circulating ALTs (Watkins et al, 2006) at this dose. However, when the therapeutic dose is exceeded, APAP can cause severe centrilobular liver necrosis and potentially fatal liver failure. APAP is the leading cause of liver failure in the United States, accounting for 56,000 emergency room visits, 2,600 hospitalisations and approximately 500 deaths per annum (Lee, 2004). This equates to almost 50 % of the annual cases of liver failure in the United States (Lee, 2008). Despite a UK legislation to restrict pack sizes of APAP, from 16 g to 8 g per pack, the rate

of APAP-related deaths remain unchanged (Bateman, 2009). Most APAP overdose patients survive, due to rapid antidotal treatment in hospital with *N*-acetylcystine. However, a small percentage (usually < 10 %) of patients will succumb to their illness. Two major factors dictate the severity of liver injury; the ingested dose of APAP, and time from ingestion to treatment. APAP overdose patients can be stratified into two groups; those who intentionally overdose (i.e. suicide attempt) and those who unintentionally overdose (Larson et al, 2005). Paradoxically, patients who intentionally overdose are usually at lower risk, and have a good prognosis. This can be attributed to the fact that most intentional overdose patients ingest one large single dose of APAP and are treated within 4 hours of ingestion (Schiødt et al, 1997). In the same study, it was found that only 20% of patients who intentionally overdose ever exhibited an ALT activity over 1,000 U/L. Conversely, unintentional overdose patients are associated with high risk and poor prognosis (Shayiq et al, 1999). This group of patients usually present with staggered APAP ingestion that has occurred over several days, when the process of liver injury may have already initiated. Other factors can affect patient susceptibility, including serious cases of hepatotoxicity from therapeutic doses of APAP in chronic alcoholics (Rex & Kumar, 1992). Patients who have recently fasted or who are malnurished, e.g. due to dental pain, are also at higher risk of developing APAP-induced ALI (Whitcomb et al, 1994). Drug-drug interactions have also been reported to influence the risk of APAP-induced ALI in patients who are concomitantly taking isoniazid or rifampacin (Murphy et al, 1990; Nolan et al, 1994).

1.4.1. Molecular toxicology of APAP-induced ALI

APAP has a superb safety profile at therapeutic doses. However, at supratherapeutic doses, APAP has the propensity to elicit liver injury which could lead to potentially fatal liver failure. The pathophysiology of APAP-induced hepatotoxicity is strikingly similar between man and rodent. This has led to a substantial body of work which has set about

characterising the molecular events that lead to APAP-induced hepatotoxicity. Despite significant progress over the past four decades in the understanding of APAP-induced ALI, many aspects remain controversial or unknown. At therapeutic doses of APAP, the large majority of the dose is directly modified by phase II metabolising systems. Approximately 50% of the dose is glucuronidated by several members of UGTs to form a stable non-toxic metabolite whilst a smaller proportion, approximately 30%, is sulphated by members of the SULT enzymes (Schenker et al, 2001). These metabolites can be detected in serum and are excreted in the urine alongside a small proportion of parent drug and other minor metabolites. A small but significant proportion of the therapeutic dose (5-15%) undergoes oxidative metabolism via CYP2E1 (and to a lesser extent by CYP1A2 and CYP3A4) (Patten et al, 1993; Thummel et al, 1993; Chen at al 1998). This oxidative metabolism yields a reactive electrophilic intermediate, NAPQI, which has the propensity to bind macromolecular components of the cell and elicit toxicity. However, due to the relatively low abundance of NAPQI at therapeutic doses of APAP and the vast intracellular stores of GSH, this potentially toxic metabolite is rapidly bioinactivated by GSH. NAPQI, an electrophile, can independently bind to the nucleophilic thiol group on the cysteine residue of GSH, however GST π has been shown to catalyse this reaction *in vitro* (Coles et al, 1988). GSH conjugates are then biotransformed into stable non-toxic cysteinyl conjugates or mercapturic acids which are then eliminated in the urine.

In an overdose setting, the two major routes of metabolism, glucuronidation and sulfation, become overwhelmed. In particular, the sulfation pathway is a low capacity system and the maximal rate of sulfation is exceeded in APAP overdose. In this case, oxidative metabolism bioactivates a greater proportion of the dose and relatively large quantities of NAPQI can be formed. CYP2E1 has been shown to be the predominant CYP isoform responsible for NAPQI formation and is certainly the most clinically relevant in APAP-induced ALI. The CYP2E1 enzyme has a wide but unique substrate specificity, as it is responsible for the metabolism of flat planar molecules, including many solvents and industrial chemicals such

as benzene, ethylene glycol, and vinyl chloride. CYP2E1 also catalyses the turnover of many endogenous metabolic by-products, such as acetone. It is also primarily responsible for the conversion of ethanol to acetaldehyde. Coadministration of ethanol with APAP is common and can cause increased uncertainty as to the prognosis of overdosed patients. The relationship between ethanol and APAP coadministration is complex; acute and chronic alcohol ingestion may have opposing effects. A large single dose of ethanol may paradoxically protect the liver from APAP-induced ALI by competing for the CYP2E1 active site. However, chronic administration of ethanol causes CYP2E1 induction as has been shown in rodent models (Roberts et al, 1995) which increases the capacity for NAPQI formation. Alcoholics are also considered to be particularly sensitive to APAP-induced ALI where cases of liver injury have been reported even at therapeutic doses of APAP. Work from the Gonzalez lab showed the importance of CYP2E1 in APAP-induced ALI when CYP2E1-deficient mice were found to be more resistant after APAP exposure (Lee et al, 1996). This study found that at a dose of 400 mg/kg of APAP, 50% of wild-type mice died (LD50) whereas all CYP2E1-deficient mice survived an exhibited normal circulating transaminase activity. However, CYP2E1-deficient mice were not entirely resistant as the highest dose caused aminotransferase elevations suggesting other enzymes may be implicated in NAPQI formation. In accordance with the mechanism of bioactivation, several studies have shown the importance of CYP2E1 in APAP-induced liver injury by using a panel of CYP2E1 inducers and inhibitors. The susceptibility of animals to APAP-induced ALI was increased by prior administration of CYP2E1 inducers such as phenobarbitone and 3-methylcholanthrene. Furthermore, protection to APAP-induced ALI is afforded after pre-dosing with CYP2E1 inhibitors such as piperonyl butoxide, 4-methylpyrazole and acute ethanol exposure (Mitchell et al, 1974; Jollow et al, 1974; Thummel et al, 1989). Even after large doses, the intracellular pools of GSH prevent toxicity by sequestering large quantities of NAPQI for elimination. However, intracellular GSH stores are finite and if the dose of APAP is sufficiently large, GSH can be depleted and NAPQI can target alternative intracellular proteins. It is estimated that > 90% GSH depletion

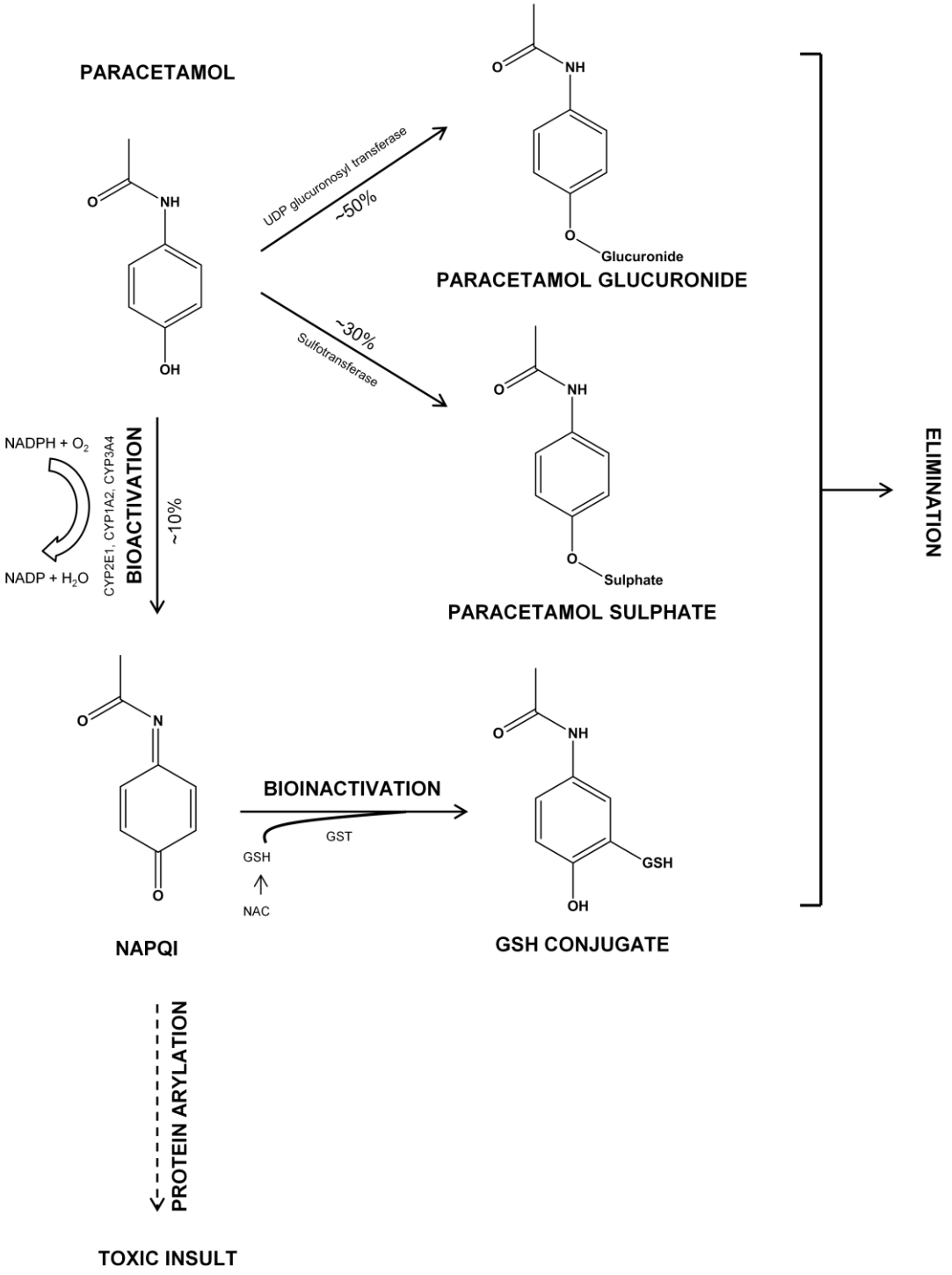

Figure 1: Metabolism and bioactivation of APAP.
The major pathways of activation include glucuronidation (~50%) and sulphation (~30%) pathways. These non-toxic metabolites are elimatied in the urine. However, a small proportion of the overall dose is bioactivated through oxidative metabolism by several CYP enzymes to yield an electrophilic protein-reactive metabolite. Large intracellular stores of GSH sequester and bioinactative the potentially toxic metabolite. In overdose settings, the GSH pool is exhausted and toxicity results via protein arylation and oxidative stress.

is required before APAP can form protein adducts and initiate toxicity (Mitchell et al, 1974). The mechanism of APAP metabolism and bioactivation is summarised in Fig 1.

The causal molecular mechanisms which bring about hepatocyte death after a toxic exposure to APAP remain controversial and poorly understood. Two theories that themselves are not mutually exclusive include protein binding and generation of secondary reactive oxygen species. After GSH depletion, which is a prerequisite step in the progression of APAP-induced ALI, the first contact between the molecule and the cell occurs during protein binding. NAPQI, an electrophile, can covalently bind to nucleophilic components in the cell, particularly lysine or cysteine residues on proteins. The propensity of a compound to covalently bind to proteins does not always determine toxic outcome. Rather, it is the specific spectrum of proteins that are irreversibly modified which induces a series of molecular events that results in cell death, i.e. the critical protein hypothesis. Several studies have identified a list of proteins which become modified during APAP-induced ALI providing a chemical 'fingerprint' of adducts.

1.4.2. NAPQI and critical protein modification

One postulated mechanism of cell death is NAPQI-mediated covalent modification of key proteins in the hepatocyte. Upon forming the NAPQI-protein complex, the target protein function is irreversibly corrupted thereby shifting cell homeostasis and impairing cell defence systems. Work in the Mitchell lab first identified an APAP-modified cell membrane protein, plasma membrane Ca^{2+} ATPase (PMCA) (Tsokos-Kuhn et al, 1985). They reported a 76% reduction in vesicular Ca^{2+} accumulation caused after a toxic APAP dose in rats. Ca^{2+} dysregulation is considered a hallmark of APAP-induced ALI. Nelson and colleagues identified that mitochondrial proteins form a disproportionate amount of covalent adducts with APAP compared to the regioisomer AMAP (N-acetyl-3-hydroxy-aminophenol), which is approximately 10-fold less toxic (Holme et al, 1991; Tirmenstein & Nelson, 1991).

Corcoran and colleagues also reported early inhibition of Na+/K+ ATP ion pump 3 hours after APAP exposure in the rat (Corcoran et al, 1987) which they concluded may contribute to the pathogenesis of APAP-induced ALI. Cohen and Khairallah stated that APAP-modified proteins appear to be specific and not necessarily the most abundant hepatocellular proteins (Cohen & Khairallah, 1997). Their group published a number of papers isolating and identifying individual APAP-modified proteins including cytosolic targets such as selenium binding protein and N-10-THF-formyl dehydrogenase (Bartolone et al, 1992), microsomal glutamine synthetase (Bulera et al, 1995) and mitochondrial aldehyde dehyrogenase (Landin et al, 1996). Subsequently, Qiu and colleagues used a more global approach to identify APAP-modified proteins using two-dimensional electrophoresis coupled with mass spectrometric identification (Qiu et al, 1998). This method complemented previous work by confirming previously-identified adducts whilst revealing novel adducts such as GSH peroxidise, GSTπ and ATP synthetase (α subunit); important cell-defence enzymes. Overall thirty modified proteins were identified, six of which were mitochondrial. Abrogation of GSH peroxidase and ATP synthetase has functional consequences; GSH peroxidise provides antioxidant activity by sequestering hydrogen peroxide (H_2O_2), a potent oxidative stressor. ATP synthetase is critical in maintaining energy homeostasis which is known to be dysregulated in APAP-induced ALI. Substantial protein modification in the mitochondria suggests that APAP-induced hepatotoxicity is mediated, at least in part, through abrogation of mitochondrial function and therefore disruption to ATP homeostasis, increased oxidative stress and enhanced Ca^{2+} dysregulation.

1.4.3. APAP and oxidative/nitrative stress: propagation of liver injury

A competing hypothesis to the critical protein hypothesis was that APAP triggered substantial oxidative stress in the hepatocyte (Wendel et al, 1979). Whilst protein modification is an obligatory event for toxicity to occur, alone it is not sufficient to provoke cell death directly (Jaeschke et al, 2012). There is also a poor correlation with protein binding and provocation of liver injury as has been demonstrated with AMAP. Despite that,

protein binding with APAP appears to be a targeted phenomenon. It was reported that modified mitochondrial proteins associate with increased oxidative stress and enhanced toxicity in APAP-induced ALI (Jaeschke et al, 2003). The mitochondrion is a vital organelle responsible for ATP production, cell signalling and cellular metabolism. Many drugs, including APAP, are known to interfere with mitochondrial signalling and induce toxicity through a number of mechanisms (Labbe et al, 2008). In the mitochondria, superoxide can react with nitric oxide (NO) to form peroxynitrite ($ONOO^-$), a potent oxidative and oxidative species (Denicola & Radi, 2005). Normally, peroxynitrite is scavenged by GSH via GSH peroxidise, however NAPQI has not only been found to modify GSH peroxidise directly, but also deplete cellular GSH (including mitochondrial GSH). In an oxidative environment, such as that found in APAP-induced ALI, peroxynitrite is highly toxic. Peroxynitrite can induce oxidative stress and can oxidise a wide range of intracellular targets, including lipids (Rubbo, 1998), proteins and DNA bases (Pryor & Squadrito, 1995). Furthermore, a hallmark of APAP-induced liver injury is the formation of nitrotyrosine protein adducts, which disproportionately occur in the mitochondria. Nitrotyrosine modification occurs through the reaction of peroxynitrite ($ONOO^-$) and tyrosine residues on target proteins. One such protein that becomes nitrated is manganese superoxide dismutase (MnSOD) which is actually involved in clearing superoxide and therefore prevents peroxynitrite formation (Agarwal et al, 2011). Heterozygous MnSOD (+/-) mice were more susceptible to APAP-induced ALI highlighting the importance of this enzyme in APAP hepatotoxicity (Fujimoto et al, 2009, Ramachandran et al, 2011). Upon nitration, MnSOD loses activity which thus potentiates the oxidative/nitrative burden in the mitochondria and exaggerates dysfunction. The important role of nitrative stress in APAP-induced ALI was exemplified by Ishida and colleagues who reduced serum ALT activity 8-fold in mice by administering a nitric oxide synthetase inhibitor, N-(G)-nitro-L-arginine methyl ester (L-NAME) or almost 70-fold using a nitric oxide scavenger 2-phenyl-4,4,5,5,-tetramethylimidazoline-1-oxyl-3-oxide (PTIO) (Ishida et al, 2002).

The consequences of prolonged oxidative/nitrative stress in the mitochondria lead to increased dysfunction culminating in opening of the mitochondrial membrane permeability transition MPT which causes collapse of the mitochondrial membrane potential and therefore abolition of ATP generation. Furthermore, Ca^{2+} homeostasis is perturbed and the mitochondria release injurious factors which can promote apoptosis or necrosis. MPT occurs after GSH depletion and oxidative/nitrative stress but before necrotic cell death (Bajt et al, 2004). Although many pro-apoptotic species are released from the mitochondria during APAP-induced ALI, such as cytochrome c, the massive bioenergetic catastrophe and oxidative environment results in a muted apoptotic response *in vivo* (Lawson et al, 1999). Furthermore, inhibition of caspases, the 'executioners' of apoptotic cell death, do not protect against APAP-induced ALI (Gujral et al, 2002). One report did show that protection could be afforded by a pan-caspase inhibitor (El-Hassan et al, 2003), however, Jaeschke and colleagues refuted this finding by suggesting the vehicle used (dimethylsulphoxide, DMSO) had inhibited APAP bioactivation (Jaeschke et al, 2006). It is generally accepted that the final form of cell death is via necrosis in animals and in man. Nevertheless, Antoine and colleagues in the CDSS showed that circulated caspase-cleaved cytokeratin-18 is evident in mouse models of APAP-induced ALI (Antoine et al, 2009). Although a caspase inhibitor prevented the cleaved metabolite being formed, it did not protect against overall injury. This suggests that the hepatocyte becomes primed for apoptosis during APAP-induced ALI, but cannot perform the energy-dependent process of apoptosis. Therefore, cell death occurs via necrosis due to massive oxidative and nitrative stress and ATP depletion.

1.4.4. APAP-induced ALI modulatory factors

As discussed, APAP bioactivation, GSH reduction, protein binding and mitochondrial dysfunction are all pre-requisite steps in the evolution of APAP-induced ALI. However, APAP toxicity is not a disease limited to the hepatocyte. The liver is largely comprised of hepatocytes, which make up approximately 80% of the cells. However, other cell types are found in the liver which have been shown to contribute to the progression of APAP induced

ALI. Kupffer cells, around 5% of liver cells, are specialised hepatic macrophages which are important in the innate immune response. Kupffer cell activation is associated with cytokine and chemokine release, which can provide both anti-inflammatory (protective) and pro-inflammatory signals (injurious) to dying hepatocytes. The injurious role of Kupffer cells was first identified by Laskin and colleagues when they reported that pre-treatment with gadolinium chloride ($GdCl_3$), a Kupffer cell inactivator, protected against APAP-induced ALI in rats (Laskin et al, 1995) and mice (Michael et al, 1999). Conversely, it was later shown that using clodronate-conjugated liposomes, which deplete Kupffer cells more efficiently than $GdCl_3$, caused increased injury after APAP exposure (Ju et al, 2002) due to removal of IL-10 and other protective factors. Conflicting studies like this highlight the difficulty in examining the roles of inflammatory mediators in toxicity studies. Nevertheless, Kupffer cells and other immune cells are recognised as cellular reservoirs of inflammatory signalling molecules which may be implicated in the progression of DILI. Clearly there is an important balance between pro- and anti-inflammatory signals has been shown in a variety of rodent models of APAP-induced ALI . Table 5 summarises various models that have been utilised to gain mechanistic understanding and to highlight the significance of different factors in the progression of APAP-induced ALI.

Clearly, the roles of inflammatory mediators are important in the late stages of liver injury. The anti-inflammatory interleukin factor, IL-10 appears to be very important in reducing the progression of liver damage, and allowing healing and regeneration of hepatocytes (Bourdi et al, 2002). However, TNFα and IFNɣ promote inflammation and provoke leukocyte infiltration to the damaged area, most notably neutrophils and macrophages. Ishida noted that hepatic IFNɣ levels correlated with severity of APAP-induced ALI in mice (Ishida et al, 2002). Administration of an anti-IFNɣ antibody could reduce both circulating transaminase levels and histological changes. The same group reported similar findings with TNFα, with TNF receptor deficient mice more resistant to APAP-induced ALI than wild type mice (Ishida et al, 2004). In parallel with IFNɣ, protection could be afforded with post-

administration of an anti-TNF antibody. These studies not only provide mechanistic insight but also highlight potential candidate species in order to develop new medicines to protect

Table 5: A summary of genetic manipulation or targeted cell depletion studies to gain better understanding of the role of different factors which influence APAP hepatotoxicity. Abbreviations: IL, interleukin; TNF, tumour necrosis factor; MIF, macrophage migration inhibitory factor; ASK-1, apoptosis signal-regulating kinase-1; nrf-2, nuclear factor erythroid 2-related factor; COX-2, cyclooxygenase 2, CCR2, C-C motif chemokine receptor 2.

Protective models		**Enhanced injury models**	
Experimental model	*Reference*	*Experimental model*	*Reference*
Cyp2e1 $^{(-/-)}$	Lee *et al*, 1996	GSH depletion	Jollow et al, 1973
Gstπ $^{(-/-)}$	Henderson *et al*, 2000	nrf2 $^{(-/-)}$	Enomoto et al, 2001
IL-1 $^{(-/-)}$	Blazka *et al*, 1996	IL-6 $^{(-/-)}$	Masubuchi et al, 2003
IL-6 administration	Masubuchi *et al*, 2003	IL-10 $^{(-/-)}$	Bourdi et al, 2002a
IL-10 and MIP2 administration	Bone-Larson *et al*, 2001, Hogaboam *et al*, 1999a, Hogaboam *et al*, 1999b	COX-2 $^{(-/-)}$	Reilly et al, 2001
anti-TNF-α ab, TNF-R $^{(-/-)}$	Ishida *et al*, 2004	CCR2 $^{(-/-)}$	Hogaboam et al 2000
anti-IFN ɣ ab IFN-ɣ $^{(-/-)}$	Ishida *et al*, 2002	JNK2 $^{(-/-)}$	Bourdi et al, 2008
MIF $^{(-/-)}$	Bourdi et al , 2002b	Kupffer Cell depletion (liposome/clodronate)	Ju et al, 2002
ASK-1 $^{(-/-)}$	Nakagawa *et al*, 2008		
NO inhibition	Ishida *et al*, 2002		
VEGF administration	Donahower *et al*, 2010		
TLR4 $^{(-/-)}$	Yohe *et al*, 2006		
CAR $^{(-/-)}$	Zhang, 2002		
Kupffer Cell depletion, (gadolinium chloride)	Laskin, 1995		

against the progression of APAP-induced ALI in the clinic, which has extremely limited therapeutic options. The key point here is that the balance between pro- and anti-inflammatory signals from outside the hepatocyte may influence the progression and outcome of APAP-induced ALI.

1.4.4. Clinical manifestation of APAP-induced ALI

APAP-induced ALI is a short intense illness which can provoke ALF and death if the appropriate therapy is not provided at the appropriate time. As discussed, APAP is responsible for the majority of ALF cases in the western world resulting in approximately 500 deaths a year in the United States (Lee, 2004). Whilst APAP causes severe hepatotoxicity, less common cases of acute renal failure have also been reported (Jeffery & Lafferty, 1981). Early recognition of APAP overdose and liver injury by the physician are essential to reduce the risk of morbidity or mortality. The clinical manifestations of APAP-induced ALI can be grouped into four stages (Rumack et al, 1981). Stage I APAP toxicity describes the events before liver injury has occurred; typically in the first 12 hours after drug ingestion. Usually, patients may present non-specific symptoms typified by vomiting, nausea, and general malaise. Even in patients who have taken huge doses of APAP, there may be an absence of direct liver-related symptoms and clinical chemistry markers provide normal readings at this stage. In stage II toxicity, between 12-36 hours, the onset of early liver injury has occurred. APAP-induced ALI usually mimics hepatocellular diseases such as hepatitis. The symptoms of APAP-induced ALI will vary depending on the severity of injury but are typified by upper-right quadrant pain with continued general malaise. During this stage, the earliest biochemical indices can identify the occurrence of liver injury. Alanine aminotransferase (ALT) and aspartate aminotransferase (AST) are the current gold standard biomarkers of liver injury that are currently widely employed in the clinic. They are relatively sensitive and specific markers for liver injury that precede the liver function abnormality markers, such as bilirubin or prothrombin time. Stage III toxicity (48-72 hours after drug ingestion) includes time of peak hepatotoxicity. At this stage, the liver degenerates further from an injured state into late-stage liver failure. Whilst ALT and AST are useful biomarkers to detect injury, they are poor at correlating outcome. Even very high ALT and AST readings (>10,000 U/L) do not always associate with liver failure. The best clinical markers of liver function at this stage are serum albumin levels, prothrombin time (clotting

tendency), bilirubin, glucose, lactate and phosphate concentrations, which are all useful determinants of liver failure and prognosis. Extra-hepatic toxic manifestations such as coma (encephalopathy), haemorrhage, hypotension and tachycardia also occur at this stage. Death is most likely to occur at this point, around 4 days after initial drug ingestion, most commonly due to complications arising from multi-organ failure which is commonly manifested by respiratory stress, sepsis or cerebral edema. Patients who spontaneously survive, enter phase IV recovery. The liver has the unique ability to regenerate and whilst recovery rates vary, most patients recover 5-7 days after initial overdose. Remarkably, survivors are unlikely to suffer any chronic hepatic dysfunction despite the massive chemical insult to the organ.

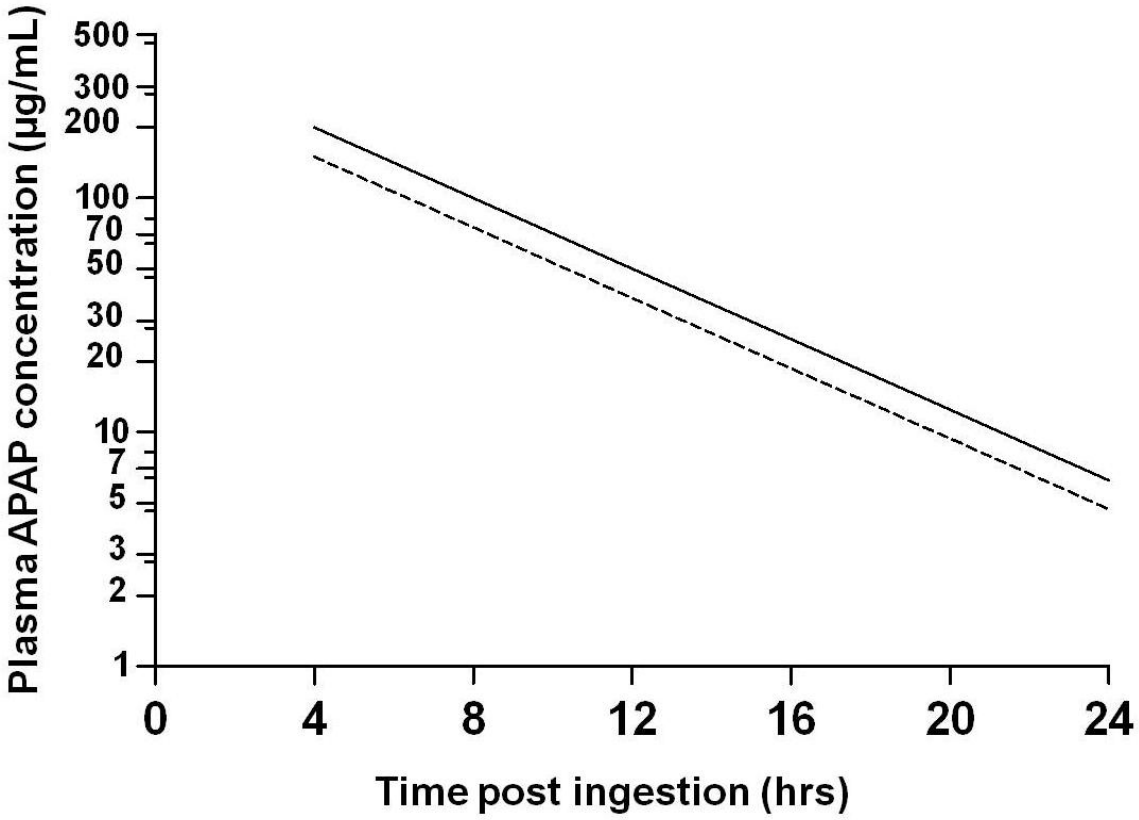

Figure 2: The Rumack-Matthew nomogram (reconstructed) used to determine risk in APAP poisoned patients from a single drug ingestion. Plasma APAP concentration is plotted against time from drug ingestion. The bold line is the "200 line" which was first used (Rumack & Matthew, 1975). The dashed line represents the "150" line and may be used in patients who may exhibit risk factors (e.g. alcoholism). Readings that fall above the line are to be considered high-risk where NAC therapy should be initiated at once.

1.4.4. Assessing risk and clinical triage

With such a rapid progression of toxicity, it is essential that the physician can provide therapy as soon as possible to 'at risk' patients. Whilst deaths due to overdoses of APAP do occur, in many cases they can be prevented by antidotal NAC therapy. However, many APAP overdose patients are not at risk of developing liver injury at any time. Therefore an approach is necessary to avoid the huge cost and strain on clinical resource of unnecessary treatment. Furthermore, whilst NAC therapy is efficient at providing antidotal therapy to APAP poisoned patients, treatment itself requires > 20 hours of intravenous administration. Oral NAC has been utilised in the United States to protect against APAP toxicity (Rumack

& Peterson, 1978), however it appears to be less effective than intravenous administration (Jones, 1998). Furthermore, NAC treatment has been associated with several ADRs of its own, from minor complications such us pruritis and nausea to rare anaphylactoid reactions that can be fatal (Elms et al, 2011). Nevertheless, NAC appears to be less toxic than other cysteine-based antidotes such as methionine or cysteamine (Prescott et al, 1974, Prescott et al, 1976, Meredith et al, 1978). One of the most common methods to assess risk in APAP overdose patients is through use of the Rumack-Matthew nomogram. The nomogram was devised based on the observation that patients who develop transaminase rises > 1000 U/L could be separated from patients who did not, based on their admittance plasma APAP concentration. The nomogram itself is based on a plasma half-life of 4 hours for APAP, which is extrapolated to 24 hours whilst readings before 4 hours are unreliable due to continuing APAP absorption. The original cut-off line devised by Rumack & Matthew which read 200 ug/mL APAP at 4 hours and 50 ug/mL at 12 hours was lowered to 150 ug/mL at 4 hours and 37.5 ug/mL at 12 hours by the FDA. This was done to provide a 25% safety margin during the clinical trial to demonstrate efficacy of NAC (Rumack et al, 1981) which had hitherto been unlicensed in clinical practice. Despite very rare 'idiosyncratic' cases where patients below the "150 line" still develop hepatotoxicity, the nomogram continues to serve reasonably well for the majority (Rumack & Bateman, 2012). In the UK, the "150" line was dropped further to "100" to provide enhanced safety for 'at risk' patients (Ferner et al, 2011). From a blood sample that is taken upon arrival in hospital, the plasma concentration of APAP is ascertained. This can be plotted against time from ingestion to determine the risk of serious liver toxicity developing in patients. If the patient exhibits a risk factor such as malnourishment, alcoholism or underlying hepatic or renal complications, the patient is deemed 'high risk' and the '100 line' should be utilised to assess risk. Only when all risk factors can be satisfactorily excluded can a physician use the '200 line' (Ferner et al, 2011). The clinician must also rely on an accurate time of ingestion from the patient or otherwise, which is often unreliable. Whilst the use of the nomogram has several drawbacks,

it does however provide the clinician with a relatively rapid and sensitive method to determine overall risk of liver damage.

1.4.5. Antidotal therapy with NAC

The treatment of APAP-induced ALI will depend upon two factors; the dose of APAP and the time since APAP ingestion. If the patient presents very early, i.e. within 1 hour of overdose, the patient can be administered activated charcoal or undergo stomach lavage to reduce APAP absorption. However, few cases will present this early and in patients that present more than 1 hour after APAP ingestion, preventive measures against APAP absorption are no longer effective (Chyka & Segar, 2005). The mainstay of APAP-induced ALI treatment is through NAC administration. Several NAC dosing regimens have been utilised, including oral and intravenous administration, both of which appear safe and effective. NAC therapy should be initiated if there is evidence of liver injury (raised ALT) or if the nomogram provides a 'high risk' reading once the plasma APAP concentration has been measured. It is accepted that NAC therapy should be continued past the recommended dosing time of 20 hours if there is still evidence of either raised ALT (>100 U/L) or detectable plasma APAP concentrations (10 μg/mL) (Goldfrank et al, 2006). NAC, a sulfhydryl donor, affords therapy by providing cysteine, a precursor amino acid of GSH, to hepatocytes to boost GSH levels. As discussed, GSH levels become depleted after an APAP overdose, therefore repletion of GSH boosts NAPQI detoxication and protection against oxidative stress. An additional benefit of NAC administration, is that the thiol residue on cysteine can react with NAPQI directly, therefore providing direct chemical detoxication against NAPQI and indirect biological protection via GSH repletion. NAC-based therapy is considered most effective within 10 hours (within stage I of APAP-induced ALI) of drug ingestion, i.e. during drug absorption and bioactivation when pronounced liver injury has not yet occurred Even after 10 hours post drug ingestion, NAC may not completely protect against liver injury, but can reduce the severity of injury. Prescott and colleagues reported that administering NAC within 10 hours of APAP ingestion provides almost complete

protection against APAP-induced ALI (Prescott et al, 1979). However, the same study showed that when NAC treatment was administered 10-24 hours after drug ingestion, it provided little benefit to the patients. Clearly, timing is crucial for this antidote to be most effective. It was later shown that late-administration of NAC beyond 15 hours (in stage III of APAP-induced ALI) had no ameliorative effects against liver damage *per se* (with respect to prothrombin time) but significantly more patients survived on NAC therapy compared to controls which was associated with less cerebral edema. It is known that NAC administration also protects against forms of kidney injury (Fishbane et al, 2004) therefore it is entirely possible that extra-hepatic protection is afforded by NAC in late-stage liver failure.

1.4.6. APAP-induced ALI: assessing prognosis

If a patient presents within 8-10 hours of taking an acute APAP overdose, the physician can administer NAC to prevent serious hepatic injury from occurring. However, if the patient presents later than 10 hours, or if the overdose is staggered, which may occur over hours or even days, it is more challenging to assess risk and provide an accurate prognosis. However, patients who present late and those who have had staggered ingestions are considered to be at higher risk of developing serious liver injury or ALF. If patients do develop serious liver injury, intensive care is provided alongside NAC therapy. In patients who have late-stage liver failure, NAC therapy is no longer a viable treatment option, and orthotopic liver transplantation may become a drastic but absolutely necessary measure to save a patient's life. Before liver transplantation became an established treatment option, prognosis of end-stage liver disease was very poor, with less than 20% survival (Riordan & Williams, 2008). However, in the era of liver transplantation, survival rates now exceed 65% in the US (Lee, 2003). ALF is defined as an abrupt loss of hepatocellular function in a patient with previously normal liver function, the expression of which includes coagulopathy and encephalopathy. A healthy liver secretes a range of clotting factors including fibrinogen (coagulation factor I) and prothrombin (coagulation factor II) in the peripheral circulation. If

liver degeneration is sufficient, the generation and secretion of these hemodynamic proteins ceases which causes circulating levels to fall. Sufficient levels of circulating coagulation factors are required to provide adequate hemostasis (cessation of blood loss from damaged vessels) and maintenance of hemodynamics. Therefore, bleeding tendency and risk of haemorrhage is increased in patients with ALF. Coagulopathy can be quantified using the prothrombin time measurement assay on citrated plasma samples. The prothrombin time is simply the length of time for a plasma sample to clot after addition of a coagulation activator, usually CaCl or thromboplastin (tissue factor), which can be measured optically or mechanically. The normal healthy reference range for prothrombin time is considered 8.8-11.6 seconds (Jordan et al, 1992). Prothrombin times exceeding 2 minutes are not uncommon in APAP-induced ALF patients. In the 1980's the World Health Organisation introduced the International Normalised Ratio INR which aimed to reduce variation in the prothrombin time assay between laboratories. The INR is a ratio of a test sample to the mean normal prothrombin time (prothrombin ratio), which is then raised to the power of the International Sensitivity Index (ISI), a pre-defined value reflecting the relative activity of the manufacturer's tissue factor.

$$\mathbf{INR} = \left(\frac{\textbf{Prothrombin Time (Test)}}{\textbf{(Prothrombin Time (Normal)}} \right)^{ISI}$$

Clearly the onset of ALF is an immediate concern for the physician when treating a patient with severe liver injury. Firstly, it is essential that ALF is recognised as early as possible in the clinic, due to the speed of deterioration and risk of death. Well-defined biological parameters such as INR can help detect and diagnose ALF. Secondly, it is necessary for the physician to decide whether to administer NAC treatment. Thirdly, it is the responsibility of the physician to determine if the patient needs to be transferred to a liver transplantation unit. Due to a lack of healthy liver donors and limited clinical resources, this expert decision

needs to be based on patient prognosis coupled with psychosocial factors such as age, mental status and history of substance abuse. Only 25% of ALF patients in the US undergo liver transplantations, therefore strict patient candidate criteria is unfortunately a factor (Lee et al, 2008).

In the setting of ALF, the INR is used as a strong predictor of patient outcome; in fact, coagulapathy itself is defined biologically as an INR > 1.5 (Fontana et al, 2008). However, the most accepted prognostic method for ALF is through use of the Kings College Criteria (KCC) (Stravitz & Kramer, 2009). The Kings College Criteria was introduced in 1989 when a retrospective study associated spontaneous survival from ALF with arterial blood pH, prothrombin time and serum creatinine. The Kings College Criteria for APAP-induced ALF is summarised in table 6.

Table 6: Kings College Criteria for poor prognosis in APAP-induced ALF.

Biomarker	Value
Arterial pH (after fluid resuscitation)	< 7.3
OR ALL OF THE FOLLOWING FEATURES	
Prothrombin Time	> 100 seconds (INR > 6.5)
Serum Creatinine Concentration	> 259 µmol/L (3.4 mg/dL)
Encephalopathy Grade	> Grade 2

Validation studies have showed that patients who meet the KCC and do not receive liver transplantation, survival rates are less than 15% (Shakil et al 2000; Makin et al, 1995; Mitchell et al, 1998; Bernal et al, 1998). Whilst KCC criteria is relatively accurate in identifying patients who are at most risk of death, it was found that 26% of patients were too unwell to receive liver transplantation by the time they met KCC (Simpson et al, 2009). Moreover, whilst KCC is reasonably specific in identifying 'at risk' patients, KCC sensitivity is less impressive as many patients who do not meet KCC still die (Shakil et al,

2000, Bernal et al, 1998, Anand et al, 1997). Other strategies have been sought to improve upon KCC performance to predict clinical outcome in APAP-induced ALF including measurement of blood lactate, alpha-fetoprotein, APACHE II score, MELD score, interleukin-6 levels and HMGB1 levels. Nevertheless, these novel markers have not been well validated in multi-centre prospective studies. Therefore, KCC remains the most widely used and robust method to determine prognosis in ALF patients (Craig et al, 2010).

1.4.6. Novel Biomarkers for APAP-induced ALI

In the wider context of DILI, novel biomarkers are urgently sought to facilitate pre-clinical and clinical research. In drug development, identification of high-performance translational biomarkers could potentially detect organ toxicities earlier, reduce costs, reduce drug attrition and accelerate drug development. Such is the pressing need for novel disease biomarkers that the National Institute of Health awarded over $2.5 bn in grants between 2008 and 2009 for biomarker research (Ptolemy & Rifai, 2010). In order to screen for novel biomarkers of organ toxicity, it is important to have a clear definition of a biomarker. The official FDA definition of a biomarker is "a characteristic that is objectively measured and evaluated as an indicator of normal biologic processes, pathogenic processes, or pharmacologic responses to a therapeutic intervention" (Woodcock et al, 2011). Some required characteristics of a clinical biomarker are separate from that required in the pre-clinical field. However, many of these 'ideal' characteristics are shared between the two settings. In 2010, Dear described 8 desirable qualities of a high-performance clinical biomarker of APAP-induced ALI, which are summarised in Table 7 (Dear, 2010). Further to these clinical requirements, more general qualities of a novel biomarker include ease of access (non-invasiveness), have a high dynamic range, have a high signal to noise ratio, translational capability between species, translational capability between test systems, i.e. *in vivo* and *in vitro*, and provide mechanistic information, i.e. mode of cell death.

A catalogue of biomarkers for the detection of DILI now exist. However, four individual biomarkers deserve mention; ALT, AST, alkaline phosphate (ALP) and total bilirubin concentration which together form the markers which are recognised by the FDA to define DILI (Shi et al, 2010). Hy's law describes ALT elevations three times the upper limit of normal (3x ULN) and bilirubin concentrations 2x ULN to define severe hepatotoxicity, which when used in combination is considered more specific than any single marker on its own (Senior, 2006). During hepatocellular necrosis, the cell membrane ruptures allowing intracellular contents to leak into the extracellular space and then into the circulation. Due to the stability of the enzyme in the blood (half life = approximately 42 hours), a correlation exists between serum ALT activity and amount of hepatocellular damage (Ozer, 2008). A

Number	Characteristic
1	The biomarker assay should be easy to measure in the standard hospital laboratory without the need of specialist equipment or technology.
2	There should be a rapid turnaround from blood sampling to test result
3	The assay should be robust and reproducible between different laboratories
4	An accurate time of drug ingestion should not be required
5	The assay should be informative in cases of delayed or staggered APAP overdose
6	The biomarker should identify liver injury early, with high sensitivity and specificity
7	The biomarker should exclude liver injury early, with high sensitivity and specificity
8	The biomarker should predict hard clinical end-points such as the need for hepatic transplantation or need for renal replacement therapy

Table 7: Ideal characteristics of novel clinical biomarkers for APAP-induced ALI. Adapted from Dear, 2010.

common misconception of ALT is that the enzyme is liver specific. ALT consists of two isoforms, ALT1 and ALT2 both of which are found in rat liver and extrahepatic tissues

(Yang et al, 2009). The standard laboratory optical assay cannot discriminate between the two isoforms, therefore both isoenzymes contribute to the serum ALT activity reading. Whilst it is certainly an abundant enzyme in the liver, both isoforms are also expressed in lower levels in other tissues; indeed, transamination reactions occur in many cell types. In fact, the first use of serum ALT activity was to confirm diagnosis of acute myocardial infarction highlighting the modest levels of the enzyme in myocardial tissue (Agress et al, 1955). AST has similar characteristics to ALT but is less liver-enriched therefore less specific in detecting DILI (Ozer et al, 2008). De Ritis and colleague noted that the ratio between AST and ALT can differentiate different forms of liver injury (normal = 1.33, acute viral hepatitis = 0.6, liver cirrhosis = 1.34) (De Ritis et al, 1956).

ALP is a useful biomarker recognised in the FDA guidelines. ALP offers mechanistic insight into the aetiology of DILI due to the specific tissular expression in the hepatic biliary ducts. ALP can therefore be used as a marker of cholestatic DILI, a sub-type of DILI where toxic biliary components exert a local toxic effect, which, in part, may be caused by inhibition of phase III metabolism. It is important to note that whilst elevations in circulating transaminases indicate hepatocellular injury has occurred, functionally, the liver may not be affected. Watkins reported in a prospective study that some patients exhibit transient rises in circulating ALTs whilst taking therapeutic doses of APAP (4 g/day) (Watkins et al, 2006). Such rises were mild, asymptomatic, and although concerning, are assumed to clinically irrelevant. A subset of DILI biomarkers include the functional markers which reflect the effect of liver in jury that has occurred. These liver function tests include prothrombin time, discussed earlier, and total bilirubin concentration. Bilirubin is a product of heme catabolism, a liver-specific process. If hepatocellular function is perturbed, hepatic bilirubin levels cannot be cleared and lead to elevations of circulating bilirubin (hyperbilirubinaemia; jaundice). Bilirubin is an accurate marker of liver function, but for APAP-induced ALI, rises occur late when the patient becomes sick. Furthermore, false positive readings in total bilirubin have been attributed to red blood cell lysis, which may be a confounding factor in

patients with haematological diseases. liver function have been validated which reflect more accurately the effect of the injury on the liver. When these functional markers are assessed in combination with liver injury biomarkers, it provides the toxicologist with a more accurate reflection of the degree of hepatotoxicity. The current set of FDA-endorsed biomarkers lack sensitivity and specificity. Novel biomarkers are needed to complement or supersede the existing catalogue of DILI biomarkers to help detect, diagnose, monitor and predict APAP-induced ALI in the clinic. More generally however, the validation and qualification of novel DILI biomarkers can aid drug development to detect potential hepatotoxins earlier whilst also possibly providing better mechanistic understanding that can generate safer medicines of the future.

1.5 MICRORNAs

In recent years, microRNAs (miRNAs) have shown great promise for their use as stable blood-based biomarkers of a range of pathologies. MiRNAs are small (approximately 22 nucleotides in length) non-coding RNA species found to modulate the protein output, and therefore the phenotype of the cell. The discovery of this vast family of small RNAs was only made relatively recently by the inspiring work of Ambros and Ruvkun (Wightman et al, 1993, Arasu et al, 1991, Lee et al, 1993). The discovery of the first miRNA, lin-4, in *caenorhabditis elegans* (c.elegans) was initially thought to be an isolated finding only applicable to nematodes. However, almost a decade later, let-7 was discovered in c.elegans and then homologues were found in drosophila and human (Reinhart, et al, 2000; Slack et al, 2000; Pasquinelli et al, 2000). This created an explosion of research in the field. To date, 25,141 mature sequences have been catalogued in 193 different species encompassing viruses to higher mammals (www.mirbase.org). The number of human sequences stands at approximately 1600, whilst 855 and 446 species have been identified in mouse and rat respectively. Many miRNA species are highly conserved; some are annotated as “vertebrate-

specific" such as miR-194 and miR-130. This level of conservation between species hints at the evolutionary importance of these modulatory factors.

1.5.1 MiRNA nomenclature

MiRNAs are usually identified by species, number, genome location (for identical transcripts in the same organism), and their relationship with other closely-related sequences. However, there are some exceptions such as let-7 and lin-4 which retain their unique identification for historical reasons, being some of the first miRNAs discovered. A prefix to the miRNA identifier indicates the relevant species, e.g. human (hsa-), rat (rno-), mouse (mmu-), etc). The miRNA identification (ID) number itself is simply the sequence number in which the miRNA was discovered (therefore miR-1 does not necessarily share any functional or structural similarity with miR-2). However, closely related microRNAs (i.e., in genomic location/nucleotide sequence) are given a suffix of a letter after the miRNA ID, e.g. miR-302a, miR-302b, miR-302c, miR-302d. MiRNA cloning studies can discover two sequences from an initial hairpin precursor. If the relative abundances show that one sequence is predominantly expressed, it will be annotated in the conventional way, with the

Figure 3: Examples of miRNA annotation

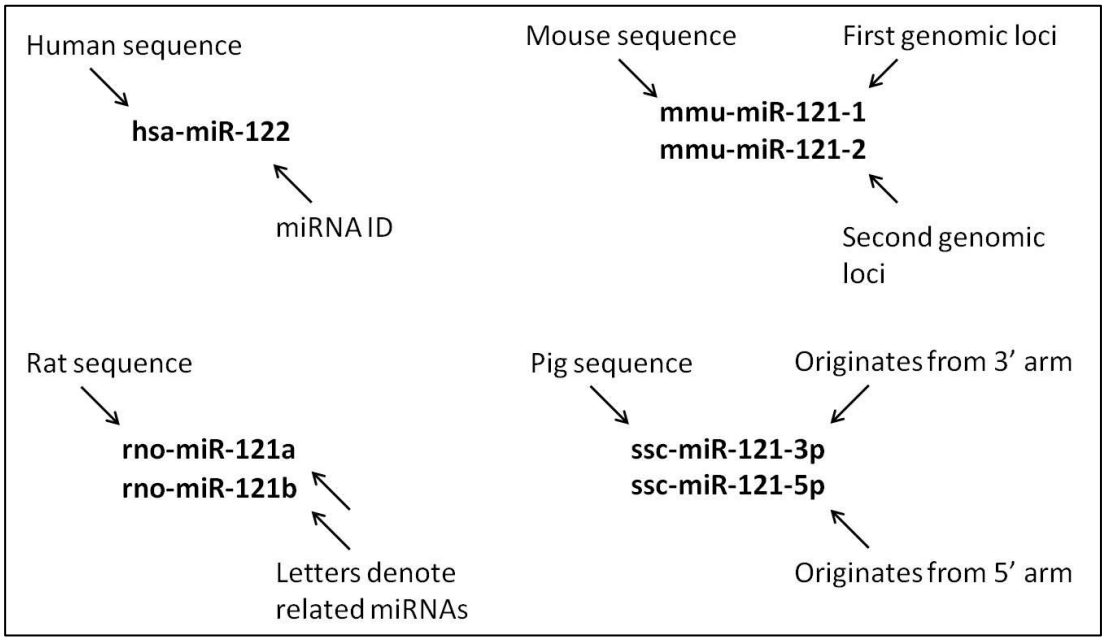

less dominant 'passenger' sequence given an asterisk following the miRNA ID (e.g. miR-122*). When the relative abundances are similar, they can be distinguished by whether they originate from the 3' or 5' strand (e.g. miR-302d-3p and miR-302d-5p). Some examples of miRNA annotation are shown in figure 3.

1.5.2 MiRNA biogenesis and maturation

MiRNA loci occur throughout the genome. Some related miRNAs can occur in close proximity such as miR-302 family; all four members (a-d) occur within 553 bases on chromosome 4. Many miRNAs are coded in introns of host genes, where miRNA transcription occurs before mRNA splicing (Kim & Kim, 2007). Nascent miRNA sequences are found in stem-loop structures in the genome. Transcription of these "hair-pin" structures, in most cases, is mediated by RNA polymerase II in the nucleus to yield long sequences (approx 100-100000 bp in length) which are termed primary transcripts and denoted pri-miRNAs. RNA polymerase II and RNA polymerase III also transcribe other members of the small RNA family including small nuclear and small nucleolar RNAs. Pri-miRNA transcripts can harbour more than one stem loop, and therefore more than one mature miRNA sequence (Lagos-Quintana et al, 2002).

Once the pri-miRNA is generated, it undergoes a maturation step involving a multiprotein complex containing Drosha (RNase III endonuclease) which recognise, bind, and cleave both strands at the base of the hair-pin structures away from their flanking regions. This liberates a ~70 nt hairpin precursor (pre-miRNA) with 5' phosphate and a 2-nt 3' overhang, which is characteristic of RNase III enzymatic cleavage (Basyuk et al, 2003; Lee et al, 2003). The pre-miRNA is then actively transported by Ran-GTP and Exportin-5 from the nucleus into the cytoplasm. Once the pre-miRNA enters the cytoplasm, the hair-pin structure is cleaved further by Dicer (RNase III endonuclease) complexed with TRBP (the human immunodeficiency virus transactivating response RNA-binding protein). The mature sequence of around 22nt is then liberated (Chendrimada et al, 2005). In each hairpin, the

miRNA sequence is usually encoded on the 5' arm, which is then incorporated into the miRNA-induced silencing complex (miRISC) with argonaute 2 (Ago2), TRBP and glycine-tryptophan repeat-containing protein of 182kDa (GW182). The 3' complementary strand from the pre-miRNA sequence, often termed the passenger strand (denoted miRNA*), is selectively degraded. It has been generally considered that miRNA passenger strands afford no regulatory activity; however, this concept is currently being challenged (reviewed by Mah et al, 2010).

1.5.3 MiRNA function

Once the single-stranded mature miRNA has been generated and associated within the RISC complex, it is able to guide the complex to cognate messenger RNA targets. Numerous mechanisms have been proposed for miRNA-mediated mRNA destabilisation but our complete understanding of the molecular mechaniams behind target mRNA silencing is not fully understood. The degree of complementarily between miRNA and mRNA is thought, in part, to govern the mechanism. A perfect or near-perfect degree of complementarity confers Ago2-mediated cleavage and degradation of target mRNAs. This miRNA-mediated cleavage has been found to be consistent between the nucleotide complementary to the 11^{th} and 12^{th} nucleotide of the miRNA. Upon cleavage, the miRNA remains intact and active for further regulatory action. However, this cleavage mechanism is thought to play a minor role in mammalian miRNA function, yet being surprisingly well conserved (Bartel, 2004). More commonly in mammals, the degree of complementarily is less perfect with only a small number of cognate base pairs. The 'seed sequence' in the miRNA is described as the first 6-8 nucleotides at the 5' end of the miRNA. The seed sequence was found to be overrepresented of conservation of matches between miRNA and target, i.e. the seed sequence is the key determinant that defines target specificity. miRNA targets usually occur in the 3'UTR region of mRNAs in AU-rich sequences. One mRNA may contain numerous

miRNA binding sites for one or more miRNAs and it has been estimated that 30% of mammalian genes contain at least one miRNA target motif. The major mechanism of mammalian miRNA-mediated silencing is through interference with mRNA translation. Mammalian mRNAs contain a 5'GpppN motif known as the 5' cap, which interacts with eIF4E (eukaryotic translation initiation factor 4E). This interaction is thought to be important in ribosomal recruitment and the initiation of mRNA translation. The miRISC is known to inhibit cap dependent translation which can occur at the initiation of translation, or during protein elongation.

An alternative mechanism for miRNA-induced silencing is through mRNA denadenylation. The miRISC is known to associate with CCR4-NOT complex and PAN2-PAN3 deadenylation complex to augment deadenylation from the 3' end of the target mRNA. Following this, m^7G decapping and Xrn-1 5'-3' exonuclease-mediated mRNA cleavage occurs resulting in mRNA degradation. Furthermore, the extent of miRNA-mediated silencing can be modulated further by auxiliary RNA-binding proteins such as PUF proteins, HuR proteins and other 3'UTR binding proteins such as Dead end 1 (Dnd1). These auxiliary factors have been shown to positively and negatively regulate miRISC binding by altering local 3'UTR secondary structures which affect the efficiency of miRNA binding.

1.5.4 Extracellular miRNAs: stability and circulatory form

The apparent stability of miRNAs in formalin-fixed tissue preparations lead Mitchell and colleagues to investigate their stability in plasma and serum (Mitchell, 2008). Coupled with the fact that miRNAs can be highly abundant, exhibit remarkable tissue specificity, and show altered expression in pathophysiological conditions they were identified as being a potentially valuable class of blood-based biomarkers. Mitchell and colleagues identified a total of 98 miRNAs, three of which (miR-15b, miR-16 and miR-24) were measured by absolute quantification and found to be abundant in plasma (10,000-100,000 copies/µL)

despite high blood nuclease activity. Furthermore, all three miRNAs showed impressive plasma stability at room temperature for at least 24 hours, and after 8 freeze-thaw cycles. Intriguingly, spiked-in (exogenous) miRNAs were undetectable unless the plasma was previously denatured, indicative of RNase-mediated degradation, which led the authors to conclude that the endogenous miRNAs studied were protected from RNase activity by an unknown mechanism. MiRNAs have also been detected at appreciable concentrations in many biofluids such as urine, saliva, cerebro-spinal fluid and breast milk. The form of extracellular protection was investigated by Wang and colleagues who found that miRNAs were contained within cell-derived vesicles (up to 1μm in size) and exosomes (50-100 nm), however, substantial amounts were also detected in the vesicle-poor supernatant during centrifugation studies (Wang et al, 2010). The same study found that exogenous miR-122 could be protected by nucleophosmin 1 (NPM1), an RNA-binding protein, in cell-free supernatant during RNase challenge. It was later found in differential centrifugation studies that vesicle-enveloped miRNAs account for a minor proportion of circulating miRNAs (Arroyo et al, 2011). This study found that miRNA species existed in three predominant populations; vesicle-enveloped miRNAs (miR-142, let7a), protein-bound miRNAs (miR-122, let-7d) or miRNAs split equally amongst vesicles and proteins (miR-126, miR-720). Immunoprecipitation experiments revealed that Ago2 proteins co-fractionate with protein-bound miRNAs, but not vesicle-enveloped miRNAs. Furthermore, protein-bound miRNAs were resistant to RNase challenge but not resistant after pre-treatment with proteinase K suggesting argonaute proteins play an important role in extracellular protection of miRNAs.

The role of these extracellular miRNAs is unclear, however it has been shown that exosomes containing mRNA and miRNA can be exchanged between mast cells, a vesicle-rich cell type (Valadi et al, 2007). The ectopic mRNA in the recipient cell was found to be active, i.e. capable of translating protein in. At the time of publication, this represented a novel mechanism of genetic exchange between cells. The spectrum of exosomal miRNAs did not reflect the host cell abundance of cellular miRNAs suggesting that exosomal loading

of miRNAs was targeted and regulated by an unknown mechanism. A later study showed that transfer of miRNA can also occur at the immune synapse between T-cells and antigen-presenting cells (APCs) during antigen recognition. Not only was this exchange unidirectional and exosome-mediated, (i.e. only from T-cell to APC), but that exchanged miRNAs were active in recipient APCs (Mittelbruun et al, 2011). These findings have prompted groups to speculate on the potential therapeutic potential of circulating exosomal miRNAs, both for their diagnostic promise and as a possible vector for therapeutic siRNA delivery (reviewed in Ramachandran & Palanisamy, 2012).

1.5.5 Liver-enriched miRNAs as potential markers of liver injury

The liver is host to a spectrum of miRNAs, some of which exhibit remarkable liver-enrichment. Liver-enriched miRNAs include miR-192 and miR-29a, however the most abundant and liver-specific miRNA is the vertebrate-conserved species, miR-122. The sheer abundance and liver-specificity was exemplified in Chang et al who reported that primary human hepatocytes contained approximately 135,000 copies per average cell (Chang et al, 2004). Adult mouse liver contained 66,000 copies/average cell, which shows great enrichment when compared to lung, kidney, spleen and skeletal muscle, which all contained less than 50 transcripts. The promise of miRNAs as potential biomarkers of cancer detection led Wang and colleagues to test whether circulating liver-enriched miRNAs could inform on DILI in a rodent model. This landmark paper reported that liver enriched miRNAs (especially miR-122 and miR-192) exhibited massive elevations in mouse plasma (with a concomitant decrease in liver) after a toxic dose of APAP, therefore confirming detection of APAP-induced ALI. Furthermore, this study found that elevations in liver-enriched miRNAs (miR-122 and miR-192) occurred as early as 1h, before detectable rises in ALT in APAP-treated mice suggesting that these have potential as earlier markers of APAP-induced ALI. It was also found that small rises in miR-122 and miR-192 could be detected at APAP levels of 150mg/kg whereas ALT elevations only occurred at 300 mg/kg, which also suggest liver-enriched miRNA could be more sensitive markers than currently used clinical biomarkers.

Laterza and colleagues also reported that plasma miR-122 levels were raised in rats after treatment with carbon tetrachloride and trichlorobromomethane, confirming that elevations of liver-enriched miRNAs were not compound- or species-specific (Laterza et al, 2009).

Many liver-enriched miRNAs (including miR-122 and miR-192) are perfectly conserved between rodents and humans which further highlights the translational potential between preclinical and clinical models of DILI. Zhang and colleagues reported that plasma miR-122 significantly correlated with serum ALT levels in patients with hepatitis B virus (HBV) induced liver disease (Zhang et al, 2010). Furthermore, in patients with muscle injury, induced by either intense endurance exercise or polymyositis, plasma miR-122 levels did not increase, unlike serum ALT activity which exhibited a 7.8-fold increase in these patients. This finding highlights the higher liver-specificity of miR-122 compared to ALT, which is expressed in muscle tissue at modest levels. Together with an enhanced liver-specificity, earlier time of release and increased sensitivity compared to currently used clinical markers, circulating liver-enriched miRNAs may lend themselves well to be useful clinical biomarkers for APAP-induced ALI and other potential liver toxicants.

1.5.6 Hepatic function of miR-122

A growing body of evidence shows that miRNAs play a significant role in development with regard to cell lineage determination and tissue specification. miR-122 plays an important role in liver homeostasis, cell proliferation and cellular metabolism. Several internet-based miRNA target prediction algorithms, based on nucleotide recognition suggest that miR-122 may target over 4,000 genes in humans. However, relatively few genes have been experimentally verified. Several methods have evolved to knockdown miRNAs *in vivo* using antisense oligonucleotides, either with cholesterol-conjugated "antagomiRs" or hybrid locked nucleic acid (LNA)/DNA "antimiRs". It was shown in mice that plasma cholesterol and plasma triglycerides were significantly reduced after 4 weeks of antisense oligonucleotide administration (Esau et al, 2006). Furthermore, this study identified

glycogen synthase (GYS1) and aldolase A (ALDOA) as miR-122 targets using complementary *in vitro* and *in vivo* approaches. An earlier study had also found that the expression of several genes involved in cholesterol metabolism was reduced after miR-122 inhibition in mice (Krutztfeldt et al, 2005). More recently, a miR-122 deficient mouse was generated which lacks the MiR-122a gene (Tsai *et al*, 2012). These mice also exhibit significantly reduced serum cholesterol and serum triglycerides throughout the first 12 months of life which reflects reduced expression of genes responsible for lipogenesis, bile metabolism, very low density lipoprotein (VLDL) export and lipid transcriptional regulation. It is clear from these studies that miR-122 plays a pivotal role in lipid metabolism and cholesterol homeostasis.

Another important role of miR-122 is the maintenance of the hepatic phenotype and control over cell proliferation. It was found that cyclin G1 is a target of miR-122 that shows an inverse correlation in HCC cell lines. Kutay and colleagues found that miR-122 was significantly decreased in hepatocellular carcinomas (HCCs) induced in rats by folic-acid-, methionine- and choline-deficient diet (Kutay et al, 2006). Similarly, analysis of human primary found significantly reduced levels of miR-122 when compared to surrounding healthy tissue. The authors suggest that miR-122 may have a causal role in hepatocarcinogenesis. In miR-122-deficient mice, liver lesions and spontaneous HCC developed in early stages of growth. However, older mice developed larger tumours with an invasive morphology. Genetic analysis of these tumours indicated an upregulated panel of oncofetal genes including *Afp*, *Igf2*, *Src*, *Prom1*, *Thy1* and *Epcam* (*prom1* is a miR-122 target). Tumour size and rate of tumour incidence could be reduced by rescuing mice with miR-122 injection providing a direct link between miR-122 status and hepatocarcinogensis.

1.5.7 Regulation of miR-122

Like many miRNAs, miR-122 plays a pivotal role in development. miR-122 is strongly upregulated during mouse liver embryonic development reaching maximal expression just

before birth (Chang et al, 2004). Therefore, it is likely that miR-122 is involved directly in the differentiation of the hepatocyte (Xu et al, 2010). The expression of miR-122 is closely correlated with a group of liver-enriched transcription factors including hepatocyte nuclear factor (HNF) 1α, HNF3β, HNF4α and CCAAT/enhancer binding protein (C/EBP) during mouse embryogenesis. Li and colleagues found that HNF4α binds to the miR-122 promoter directly via a conserved DR-I element and HNF4α positively regulates miR-122 in Huh7 cells and in mouse liver (Li et al, 2010). The expression of miR-122 is also under circadian control via positive regulation by REV-ERBα, a *bona fide* clock gene (Gatfield *et al*, 2009). Whilst the transcription of miR-122 (pri-miR-122) is highly dynamic over the course of the day, the absolute levels of mature miR-122 remain constant over the circadian phase due to the long intracellular half-life of miR-122. However, it was also found that many circadian genes are miR-122 targets themselves providing a clear link between miR-122 and circadian regulation.

1.6 The role of circadian rhythms in DILI

The pipeline of NCEs represents an essential asset to improve the quality of life and reduce morbidity and mortality in man. However, adopting novel tools and approaches to improve the safety and efficacy of existing drugs may also substantially improve human health (Kola & Landis, 2004). There is a growing body of evidence which suggests that the intrinsic biological clock has an important role in the coordination of drug metabolism, and therefore drug efficacy and drug detoxification. A better understanding in the link between circadian physiology and its effects on drug response may lead to safer and/or more efficacious drug regimens in the clinic (Levi &Schibler, 2007).

1.6.1 Cellular coordination of circadian physiology

The biological clock has been found to regulate daily physiological changes in a plethora of different ways; from diurnal effects on heart rate and blood pressure to behavioural sleep-

wake cycles. Circadian (derived from latin *circa-diem*, 'about a day') rhythms are thought have developed in virtually all light-sensitive organisms, including cyanobacteria, simple eukaryotes and higher mammals. Rosbash and Gehring explained how circadian rhythms may have evolved in primitive organisms to confer a selective advantage in anticipating daily cycles of UV light (Gehring & Rosbash, 2003). Indeed, a light sensitive family of proteins, the cryptochromes, are integral in the coordination of the mammalian biological clock. The generalised role of the biological clock is to optimise metabolism and energy utilisation by conferring an anticipatory response, rather than reactionary response, to the availability of nutrition or energy in an organism. Therefore, it is not surprising that circadian coordination affects mammalian physiology in such a marked way.

The mammalian circadian system is organised in a hierarchical structure. The circadian axis is orchestrated by the 'master' clock which is present in the suprachiasmatic nuclei (SCN), a 10,000 neuron paired structure in the anterior hypothalamus of the brain (Reppert & Weaver, 2002). Light is transduced by photopigments in the retina, which produce long-lasting non-image forming signals (as opposed to image-forming rods and cones) which are relayed to the suprachiasmatic nuclei (SCN) via the retinohypothalmic tract completing the sensory limb of the circadian system. However it should be noted that light-dark cycles only *entrain* the clock, i.e. the biological clock will oscillate regardless of external light cues. The actual dynamics of the biological clock is achieved through the temporal interplay between proteins in a transcriptional/post-transcriptional negative feedback loop (Freedman et al, 1999). When one considers that that the period of expression of these clock genes is approximately twenty four hours, then the basis of diurnal control on downstream pathways can be appreciated. The components of the molecular oscillator in the SCN are very similar in make-up to those in peripheral tissues. The master clock can synchronise peripheral clocks which are known to exist in many cell types, including hepatocytes, fibroblasts and keratinocytes (Balsalobre et al, 1998, Panda et al, 2002, Zanello et al, 2000). However, clocks in peripheral organs are not tightly coupled like those in the

SCN, which communicate locally via paracrine and synaptic signalling (Liu et al, 2007, Maywood et al, 2006). Although cellular clocks will continue to free-run in peripheral cells, they become gradually desynchronised if the entrainment by the SCN is lost, i.e. in SCN-lesioned animals or cells in culture (Guo et al 2006, Nagoshi et al, 2004). Such SCN ablation experiments lead to perturbations in hormonal production, sleep patterns and locomotor activity (Ralph et al, 1990). The exact mechanisms governing this remote signalling of peripheral clocks is not fully understood, but is thought to be regulated through both synaptic and humoral signalling. Candidate circulating peripheral synchronisers include prokineticin-2 (PROK-2, PK2), a light-sensitive protein secreted by the SCN, and transforming growth factor α (TGFα), both of which have been implicated in controlling behaviour and locomotor activity and exhibit circadian expression. Glucocorticoids are also likely to be implicated. Hence, each organ in the body can be synchronised in coordination but as independent entities.

1.6.2 Molecular architecture of the biological clock

The molecular architecture behind the generation of self-sustained, autonomous circadian rhythms is complex involving multiple regulatory loops. However, advances have been made in the last decade to improve the understanding behind the dynamics and interactions of the clock components. At the heart of the mammalian clock are two classes of genes, the cryptochromes (CRY1 and CRY2) and period genes (PER1 and PER2). A third member of the period genes was discovered but is thought not to play an important role in the regulation of the molecular clock (Im *et al*, 2010). The expression of these two clock gene classes are under positive regulation by two heterodimeric transcription factors, CLOCK and BMAL1 which are members of the basic helix-loop-helix (bHLH)-PAS (Period-Arnt_Single-minded) transcription factor family. Clock acetylates Bmal1 at a conserved lysine residue (Lys 537) to bind and form the active heterodimer. The active Clock:Bmal1 complex can then bind to cognate E-box or G-box motifs within *cis*-acting promoter or enhancer regions of the PER1/2 and CRY1/2 genes and promote transcription. PER and CRY proteins then

accumulate in the cytoplasm and themselves form heterodimers with a number of auxiliary proteins such as casein kinase 1δ, casein kinase 1ε (Lee et al, 2009), NonO, and WDR5 (Brown et al, 2005). When these factors reach a threshold concentration, they actively repress their own transcription by affecting the binding affinity of CLOCK:BMAL1 thereby attenuating CRY and PER expression. The half-life of CRY and PER proteins is a factor of the time of this repression, i.e. once the levels of these proteins fall, the expression of CRY and PER can then resume, completing the rhythm. A working model for the molecular mechanism governing circadian regulation is shown in figure 3. Another regulatory loop that is very important in circadian regulation involves two members of the nuclear orphan receptor family, REV-ERBα (Nr1d1) and REV-ERBβ (Nr1d2). The CLOCK-Bmal1 heterodimer can transactivate expression of both REV-ERB isoforms in a strong circadian manner (>100-fold increase in expression within 6 hours). REV-ERBα and REV-ERBβ compete then bind to RORE elements of Bmal1 and strongly repress with members of the RAR-related orphan nuclear receptors (RORs), mainly RORα and RORɣ, which counteract Bmal1 repression by promoting expression at the same RORE elements. Therefore, the status of Bmal1 expression depends on a balance between REV-ERB-mediated repression and ROR-mediated activation. Whilst these two regulatory systems are important in the regulation of circadian regulation, they peak at different times allowing downstream E-box driven regulation and RORE-driven regulation to occur at different phases.

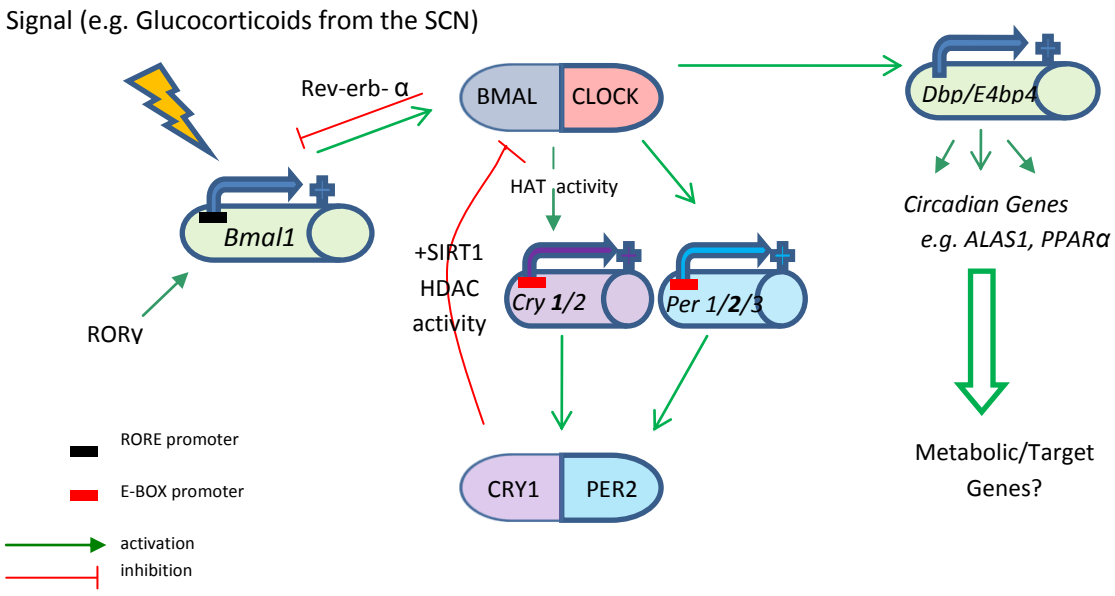

Figure 3. Schematic mechanism (adapted from Lim et al, 2006) showing the molecular oscillator model. The model is based on a cyclic transcriptional/post-transcriptional negative feedback mechanism where Bmal1 and Cry isoform expression is in anti-phase. This molecular oscillator drives daily fluctuations in output 'circadian' genes (e.g. D-site albumin binding promoter) which, in turn, will positively regulate various endogenous signalling/enzymatic pathways with a 24 hour period.

Remarkably, it has been found that at least 10% of transcripts in many tissues oscillate with circadian rhythmicity (Akhtar et al, 2002). Several key circadian regulators have been described that provide a link between the molecular oscillator and the circadian expression of hundreds of genes, some of which are important in drug detoxification. Members of the proline and acidic amino acid rich-domain basic leucine zipper (PAR bZip) transcription factors, including D-site albumin promoter binding protein (DBP), thyrotroph embryonic factor (TEF) and hepatic leukaemia factor (HLF), are directly regulated by key clock components and are expressed with strong circadian rhythmicity (Ripperger & Schibler, 2006). They are not clock genes *per se*, as they are not involved in clock entrainment but act immediately downstream and can be considered molecular adapters between core clock components and downstream circadian regulation. Identification of targets for the PAR bZIP transcription factors was achieved through the generation of a triple knockout mouse, i.e. DBP $^{(-/-)}$, TEF $^{(-/-)}$, HLF $^{(-/-)}$ (Gachon et al, 2006). Many genes

involved in xenobiotics metabolism were found to be significantly underexpressed in PAR bZIP deficient mice including members of the CYP450 superfamily (Cyp2a4/5, Cyp2b9, Cyp2b10, Cyp2c37, Cyp2c50), carboxylesterases (Ces1, Ces3), UGTs (UGT2b37) GSTs (Gstα3, Gstθ1), aldehyde dehydrogenases (Aldh1a1, Aldh1a7) and drug transporters (MRP4, BCRP1). Other genes thought to be implicated with drug detoxification were also altered, such as aminolevulinic acid synthase (Alas1), which provides a rate-limiting step to heme biosysnthesis and constitutive androstane receptor (CAR) which is responsible for induction of genes implicated in drug detoxification. Strikingly, in PAR bZIP deficient mice, genes involved in all three phases of drug metabolism were underexpressed. This shows the high level of significance that circadian regulation may have over drug detoxification systems.

A transgenic mouse model with a system-driven conditionally active liver clock has been developed (Kornmann et al, 2007). This model was produced in an attempt to avoid the severe phenotypic observations that complicate other whole-genome clock deficient models (Gachon et al, 2006). Importantly, this conditionally active model offers clock disruption in a liver-specific manner through exogenous constitutive REV-ERBα over-expression, under the control of an albumin promoter. When the liver clock was "switched off", the robust circadian expression of many genes involved in drug disposition was lost including Cyp2b9, Cyp2b10, Fmo5 and P450 oxidoreductase. In total 351 transcripts with circadian expression was identified, 90% of which lost rhythmicity when the local liver clock was perturbed. A small subset of genes retained circadian rhythmicity during liver clock perturbation suggesting some genes are influenced by remote zeitgebers, such as temperature. Together, these studies confirm that the biological clock plays an important role in the expression of many genes important in the detoxification and disposition of drugs.

1.6.3 The role of the biological clock: clinical significance

The fixed-dose lethality of many drugs in laboratory rodent models is dependent on the time of administration. This is particularly marked in halothane and APAP toxicity

(Chassard & Brugerolle, 2004; Matsunaga et al, 2004). These findings have led to investigative studies on the time-of-day dependence on the efficacy or toxicity of medicines in humans, studies which have been termed "chronopharmacology" studies. As predicted, drug chronopharmacology often displays reciprocal circadian patterns in humans relative to rodent models reflecting the diurnal human system and the nocturnal rodent system. As discussed, circadian rhythms are displayed in many physiological systems such as gastric acid secretion, intestinal motility and hepatic blood flow, all of which can play an important role in drug disposition (Moore & Halberg, 1986; Kumar et al, 1986; Lemmer & Nold 1991). Substantially reduced pharmacokinetics have been observed in asthmatic children when administered sustained-release theophylline in the morning when compared to evening dosing (Smolensky et al, 1987). Moreover, in cancer patients, a pronounced circadian rhythm in plasma 5-fluorouracil (5-FU) concentration exists despite constant rate intravenous infusion (Petit et al, 1988; Metzger et al, 1994).

Further to time-of-day differences in pharmacokinetics, the pharmacodynamics of some drugs also follow a 24-hour rhythm. For example, the anticoagulation potency of heparin was almost doubled in the mid-dark phase (early morning) in patients with venous thromboembolic disease during constant rate infusion. However, the most striking circadian differences in efficacy and toxicity of drugs exist in the cancer field. Two anti-cancer agents that when combined are effective in the treatment of gastrointestinal cancers including colorectal cancer are 5-FU and oxaliplatin (L-OHP). Despite being efficacious, both agents exhibit serious ADRs due to their non-specific cytotoxic action. The main metabolising enzyme of 5-FU is dehydropyrimidine dehydrogenase (DPD) which exhibits strong circadian expression. Furthermore, the target enzyme of 5-FU thymidilate synthetase (TS) also displays circadian variation. Likewise, L-OHP is better tolerated in rodents when GSH levels are highest, thereby providing greater cytoprotection. These findings guided the development of a modified chronopharmacological-based regimen in an attempt to both improve efficacy and reduce ADRs with these cytotoxic agents. Therefore, a multi-channel

programmable pump was devised to automatically change the dosing rate of each drug individually according to the time of day. This administered 5-FU (supplemented with folinic acid; a chemotherapy adjuvant) to peak at 04:00 to coincide with high DPD levels and low TS levels thus providing maximal enzyme inhibition without producing toxic levels of the drug (Levi et al, 1992). Alongside this, L-OHP was administered with a peak infusion rate at 16:00 to coincide with higher GSH levels in bone marrow to attempt to reduce the risk of L-OHP-induced haematological complications. The tolerability and efficacy of these modified regimens have been assessed in phase I, phase II and phase III clinical trials involving over 2000 patients (Mormont & Levi, 2003, Levi et al, 1997). It was found that the chronomodulated regimen achieved 51% objective tumour responses compared to 30% who received constant rate infusion. Furthermore, the incidence of serious toxicities related to severe mucositis, peripheral sensory neuropathy and toxicity requiring hospitalisation all fell by at least two-fold.

These studies show how understanding the daily variations in target or metabolising proteins that ultimately effect drug response can help improve drug effectiveness and reduce the risk of ADRs in the clinic. Similar methodologies could be applied to other drugs currently used in the clinic that are associated with poor efficacy or ADRs that may be avoidable. Chronopharmacology studies may also become standard practice in the development of NCEs to identify the optimal time for drug administration to gain the most efficacy with the lowest possible risk of an ADR. Essentially, a better understanding in the dynamics of the molecular clock and how it affects drug response may improve the risk:benefit ratio of drugs in clinical and pre-clinical settings.

1.7 AIMS OF THESIS

New biomarkers of DILI are urgently required in the clinic and in pre-clinical settings during pharmaceutical evaluation. Circulating miRNAs represent a promising class of biomarkers that have been successfully utilised in a range of pathologies from cancer detection to cardiovascular dysfunction. Recently, two liver-enriched miRNAs (miR-122 and miR-192) were found to be superior biomarkers of liver injury compared to the current gold-standard biomarker, ALT, in a murine model of APAP-induced ALI. However, these markers have not yet been tested in a real-life clinical setting in a heterogeneous cohort of APAP-overdosed patients. If these potential biomarkers of liver injury can provide earlier detection with enhanced liver-specificity and/or correlate to real clinical outcomes, they may provide the physician with a more accurate and prognostic marker of liver injury. Furthermore, little is known about the release mechanism or site of loss of miRNAs during liver injury. It is also not known if miRNAs can serve as biomarkers of DILI during different mechanisms of DILI.

This thesis will set about addressing the following hypotheses:

- Circulating liver-enriched miRNAs can be used as biomarkers of liver injury in a rodent APAP model of DILI and a FS model of DILI.
    - Can circulating liver-enriched miRNAs inform on two models of DILI that injure through two separate mechanisms?
    - Can we corroborate previous studies to show that miR-122 and miR-192 can be released earlier and at lower toxic doses of APAP?

- Circulating liver-enriched miRNAs can be used as sensitive, non-invasive biomarkers to detect DILI in a heterogeneous cohort of APAP-overdose patients.

  - Do circulating, liver-enriched, miRNAs correlate with ALTs or any functional marker of liver or kidney damage, such as serum bilirubin, prothrombin time or serum creatinine?
  - Do circulating, liver-enriched, miRNAs inform on non-APAP-induced liver injury such as liver damage associated with hepatitis?
  - Is the half-life of circulating miRNAs shorter than that of ALT, i.e. do miRNAs reflect the actual status of the liver more accurately during liver recovery?

- A rise in circulating liver-enriched miRNAs can detect APAP-induced ALI before a rise in ALT and can predict patients who will develop ALF.
  - Do circulating liver-enriched miRNAs increase within 8 hours of APAP ingestion in cohort of APAP overdose patients?
  - Do circulating liver-enriched miRNAs correlate with peak ALT or peak INR levels which are accurate markers of liver failure?

- APAP and FS murine models of DILI show distinct time-of-day dependence on severity of toxicity.
  - Is it possible to associate any differences in toxicological outcome with endogenous variations in circadian physiology?
  - Do circadian rhythms exist in the expression of important genes involved in drug disposition, how can they be implicated in the circadian variation in APAP- or FS- induced liver injury

The work in this thesis has been undertaken in an attempt to better understand the utility of a promising marker of DILI by bridging between pre-clinical models and clinical settings. This may ultimately add to the catalogue of available biomarkers that can be used either by

the physician to better direct the most appropriate treatment to patients and/or by pre-clinical scientists to detect liver injury sensitively during NCE evaluation. This work will also aim to characterise the circadian variation in two archetypal hepatotoxins, which may reveal a better mechanistic understanding behind drug disposition and toxic outcome.

CHAPTER TWO

MICRORNAS AS POTENTIAL BIOMARKERS OF DILI USING *IN VIVO* MODELS

2.1 Introduction

The identification and development of novel biomarkers of DILI is a pressing need in clinical and pre-clinical settings. In drug development, NCEs require rigorous pre-clinical testing to ensure efficacy is achieved whilst providing an excellent safety profile. However, many NCEs fail due to the development of organ-related toxicity either in pre-clinical species or in late-stage drug development during clinical trials. One of the most common organ-targeted toxicological outcomes encountered during drug development is hepatotoxicity (Mandenius *et al*, 2011). Ideally, NCEs that contain a chemical liability to provoke DILI in man would be identified early in pre-clinical testing. However, this is often not the case. The current models for NCE hepatotoxicity testing include the use of *in vivo* methods with non-human pre-clinical species such as rodents, dogs and cynomolgus monkeys. Although these can predict human hepatotoxicity in most cases, drug metabolism can be species-specific which may be critical if toxicity is mediated through the generation of a chemically reactive metabolite. Other models to test for potential hepatotoxicity include *in vitro* methods. The advantage of *in vitro* methods is the utilisation of human cells and tissues. However, there is a general consensus among pharmaceutical companies that the current *in vitro* models for safety testing need to be improved upon. For example, the popular use of immortalised hepatocellular cell lines is a poor translational tool for modelling various types of DILI as these cell lines do not express important proteins implicated in drug disposition, e.g. specific CYP450s isoforms A great effort is currently underway to develop more physiologically-relevant, *in vivo*-like *in vitro* systems such as 3-D cell bioreactors or human hepatocytes derived from pluripotent stem cells.

The identification and development of novel sensitive biomarkers are also urgently required. The current gold-standard laboratory biomarker of DILI is ALT (Amacher, 1998). This liver-enriched enzyme is highly sensitive and reasonably specific for liver injury. The photo-optical activity assay is also translational between pre-clinical species and man. Despite these advantages, several limitations are also recognised. The ALT enzyme exists in two

isoforms; ALT1 is highly liver-enriched and ALT2 is expressed at lower levels in muscle. The photo-optical assay does not discriminate between the two isoenzymes; therefore, ALT is prone to producing false-positive results in animals. Furthermore, O'Brien and colleagues found that ALT could be inhibited by isoniazid and lead nitrate induced by cyproterone and dexomethosome in rats, which lead to hepatic and serum increases in ALT levels (O'Brien et al, 2002). These findings suggest that under specific toxic conditions, serum ALT activity had the potential to over-estimate or under-estimate the true degree of liver injury. Ideal characteristics of novel DILI biomarkers for use in pre-clinical settings include: ability to detect liver injury with a high degree of sensitivity and specificity, translational capability between pre-clinical species and man, good stability in an easily accessible biofluid (blood or urine), rise early during hepatotoxicity, good analytical sensitivity with a large dynamic range, and provides strong correlation between readouts and the true degree of injury present in the liver.

Circulating miRNAs from host tissues/cells have been found to exist in a remarkably stable form in various biofluids including blood, urine, cerebrospinal fluid and breast milk. This has prompted an intense world-wide effort to evaluate miRNAs for their potential in various disease states, tissue injury and to report on drug efficacy. Recently, Wang and colleagues discovered a panel of liver-enriched miRNAs (notably miR-122 and miR-192) that rise in blood in a mouse model of APAP-induced ALI (Wang et al, 2009). Most striking was the observations that a) liver-enriched miRNAs were increased earlier than ALT in blood and b) liver-enriched miRNAs were elevated at lower toxic doses of APAP than ALT. These findings suggest that liver-enriched miRNAs could serve to be informative biomarkers of liver injury with an earlier time of release and increased sensitivity over ALT. Furthermore, miRNA screening across approximately 40 human tissue types found that miR-122, a highly-abundant liver miRNA, exhibited extremely high enrichment in liver tissue (Liang *et al*, 2007). Coupled with the fact that miR-122 is highly conserved throughout most

mammalian species, this growing body of evidence increasingly suggests miR-122, and other liver-specific miRNAs, have the potential to serve as powerful biomarkers of DILI.

In this chapter, the utility of liver-enriched miRNAs (miR-122 and miR-192) is assessed in an established mouse model of APAP-induced ALI. Specifically, miR-122 is measured alongside ALT in time-response and dose-response studies to ascertain the relative earliness and sensitivity of liver-enriched miRNAs. Furthermore, the loss of miR-122 from liver during APAP-induced injury is examined through miR-122 in situ hybridisation studies.

2.2 EXPERIMENTAL ANIMALS AND METHODS

2.2.1 Materials

Purified reduced GSH, acetaminophen, beta-nicotinamide adenine dinucleotide phosphate tetrasodsium salt (NADPH), sulfosalicylic acid (SSA), 5,5-dithiobis(2-nitrobenzoic acid) (DTNB), GSH reductase and neutral buffered 10% formalin were all purchased from Sigma Aldrich (St Louis, MO). miRNeasy kits and minElute kits were purchased from Qiagen (Venlo, Netherlands). Stem-loop reverse transcription primers and Taqman stem-loop reverse transcription primers/reporter (miRNA assays) were purchased from Applied Biosystems (Foster City, CA). Thermo Infinity ALT Liquid stable reagent was purchased from Thermo (Waltham, MA). miRCURY LNA detection probes (miR-122, U6 snRNA and scramble control) were purchased from Exiqon (Vedbaek, Denmark).

2.2.2 Experimental animals

The protocols described were performed according to the regulations defined in the project licence granted under the Animals (Scientific Procedures) Act 1986 and approved by the University of Liverpool Animal ethics committee. All animals were purchased from Charles River (Manston, UK) and housed at constant temperature and humidity with free access to food and water. All animals were allowed to acclimatise to a 12-hour light-dark cycle (lights on: 08:00/lights off: 20:00) for at least 14 days prior to experimentation. Mice were humanely culled via rising concentration of CO2 before exsanguinations according to the Humane Killing of Animals Under Schedule 1 to the Animals (Scientific Procedures) 1 Act 1986.

2.2.3 Animal dosing schedule

Male CD-1 mice (5-7 weeks old / ~ 30g) were used in all studies. For time-response studies, mice were administered a single *i.p.* injection of APAP (530 mg/kg) in warm 0.9% saline for 1-8 hours. For dose response studies, mice were administered APAP (*i.p.*) (30-530 mg/kg) in warm 0.9% saline for 5 hours. Control animals received a single *i.p.* injection of warm saline equivalent to a 530 mg/kg dose. Treatment groups consisted of four mice each.

2.2.4 Serum ALT Activity Determination

Complete exsanguination was performed via cardiac puncture using a 25 gauge needle. Blood was collected in microtubes and allowed to clot overnight at 4°C. The blood clot was initially separated and serum removed by centrifugation (1500g, 5 mins, 4 °C). Residual red blood cells were pelleted by centrifugation (10,000g, 5 mins, 4 °C) to yield cell-free supernatant. Serum ALT levels were determined immediately (to prevent freeze-thawing) using a Thermo Infinity ALT Liquid stable reagent-based (Thermo, Waltham, MA) kinetic assay, at 37°C, according to the manufacturer's instructions.

2.2.5 miRNA extraction

miRNA was extracted using an miRNeasy kit (Qiagen, Venlo, Netherlands), following the manufacturer's instructions, with minor modifications. Briefly, 40 µL of biofluid was made up to 200 µL with nuclease-free water, then combined with 700 µL of QIAzol. The sample was mixed and left for 5 minutes before the addition of 140 µL of chloroform. In some experiments, 10µL of cel-lin-4 (5fM) was added to denatured serum before the addition of chloroform (to serve as exogenous control). Samples were then mixed vigorously for 15 seconds and centrifuged at 12,000 g for 15 minutes at 4 °C. Equal volumes (350 µL) of the upper aqueous phase and 70% ethanol were mixed in a fresh microtube before adding the total volume to an miRNeasy minispin column. The column was centrifuged at 8,000g for 15 seconds at room temperature. The flow-through, containing the small RNA fraction,

including the miRNA complement, was mixed with 450 µL of 100% ethanol. The elute was then purified using a MinElute kit (Qiagen, Venlo, Netherlands).

2.2.6 miRNA purification

The small RNA elution mixture was applied to a MinElute column, 700 µL at a time. The immobilized RNA was then washed with various buffers before a final 80 % ethanol wash. The column was then dried by centrifugation. The small RNA fraction was eluted in 14 µL of nuclease-free water and stored at -80 °C.

2.2.7 Quantitative Polymerase Chain Reaction Analysis.

miRNA levels were measured using Taqman-based quantitative polymerase chain reaction (qPCR). The small RNA elute was reverse transcribed using specific stem-loop reverse-transcription RT primers (Applied Biosystems, Foster City, CA) for each target miRNA species, following the manufacturer's instructions. Next, 2 µL of RNA was used to produce the complementary DNA (cDNA) template in a total volume of 15 µL. Then, 1.33 µL of cDNA was used in the PCR mixture with specific stem-loop PCR primers (Applied Biosystems, Foster City, CA) in a total volume of 20 µL. Levels of miRNA were measured by the fluorescent signal produced from the Taqman probes on an ABI Prism 7000 (Applied Biosystems). All samples were assayed in duplicate. miRNA levels were normalized to levels of U6 snRNA, a ubiquitous small nuclear RNA (snRNA) species used as an endogenous control, as described elsewhere (Zhang et al, 2010).

2.2.9 FFPE tissue preparation

In a separate experiment, a time-course study was performed in mice receiving APAP (530 mg/kg) dissolved in warm saline for 1-8 hours (n=4). Time-matched controls received warm saline equivalent to a 530 mg/kg APAP dose (n=4). Mice were culled as described. The right

lobe of the liver was fixed in neutral buffered 10% formalin for 24 hours, the remaining liver was snap frozen. The liver tissue was then dehydrated with increasing concentrations of ethanol before a xylene wash. Cassettes containing dehydrated liver tissue were infiltrated with molten paraffin wax and allowed to cool to create FFPE blocks.

2.2.10 miRNA *in situ* hybridisation

miRNAs (miR-122, U6 snRNA and scrambled control) were visualised using miRCURY LNA anti-sense DIG-labelled probes. First, 4 µm sections were cut from the FFPE blocks and mounted on Superfrost Plus slides (Thermo Scientific, Waltham, MA). Method optimisation experiments determined that an annealing temperature of 54 °C (miR-122) and 55 °C (U6 snRNA) provided the best sensitivity and specificity for each probe. Briefly, the slides were baked at 60 °C for 8 minutes before deparaffinisation at 62 °C for 12 minutes. For partial digestion, proteinase K was added to each slide and incubated at 37 °C for 8 minutes (U6 snRNA) or 24 minutes (miR-122). After denaturisation of the enzyme, the antisense DIG-labelled probes (miR-122, 12.5 mM; U6 snRNA 10 mM) were incubated for 1 hour (U6 snRNA) or 3 hours (miR-122). Each slide was washed with increasing stringency (2.0 X SSC - 0.5 X SSC) at 55 °C (U6 snRNA) or 37 ° C (miR-122). One drop of alkaline phosphate-conjugated antibody was applied to each slide and incubated at 37 °C for 32 minutes. Next, one drop of NBT was added to each slide before counterstaining. The miR-122 is visualised by alkaline phosphate mediated reduction of NBT to the NBT formazan precipitate. The slides were cleaned and mounted with cover slides using lab-grade gelatine.

2.2.11 Statistical analysis

Each data group was tested for normality using the Shapiro-Wilk normality test. Descriptive statistical analysis was performed on each data group. For normal data sets, the mean and standard deviation was determined for each group. For non-normal data sets, the median and interquartile range was determined for each group. To determine statistical significance,

comparisons were made using the Student's t-test (for two parametric groups), the Mann-Whitney U test (for two nonparametric groups), the ANOVA (for more than two parametric groups) and the Kruskall-Wallis test (for more than two nonparametric groups) (StatsDirect, Cheshire, UK). For graphical interpretation GraphPad Prism 5 software was used (GraphPad Software, La Jolla, CA). Statistical significance was set at $P < 0.05$.

2.3 Results

2.3.1 Serum miR-122 is increased earlier than serum ALT activity in a murine model of APAP-induced ALI

CD-1 male mice (5-7 weeks old, fed *ad libitum*) were administered a single toxic dose (530 mg/kg, i.p.) as described for 1-8 hours. Hepatic GSH levels were significantly decreased early after APAP exposure (figure 2.1). Mean hepatic GSH levels (SD) for control animals (saline-injected) were 59.4 µmol/g protein. However, in APAP-exposed mice, mean hepatic GSH levels (SD) were 10.6 (4.2), 8.1 (4.9) 37.0 (21.3) and 63.2 (0.5) at 1h, 2h, 4h and 8h respectively. Hepatic GSH levels were significantly lower at 1h and 2h after APAP exposure compared to the control group, showing a 82.2% ($P = 0.0007$) and 86.4% ($P < 0.0001$) drop respectively.

Small RNA was extracted from serum where four separate miRNAs were measured including liver-enriched miRNAs (miR-122 and miR-192), a muscle-enriched miRNA (miR-1), and a brain-enriched miRNA (miR-218). Serum miRNAs were quantified against a reference species (U6 snRNA) using 2 ^ - (ΔCt) method. In the same samples, serum ALT activity was measured as described. Serum ALTs exhibited a time-dependent increase after APAP administration (figure 2.2A). Median serum ALTs (IQR; interquartile range) are shown in table 1. Serum ALTs were significantly raised at 4h (P=0.007) compared to control mice. Liver enriched miRNAs (miR-122 and miR-192) in serum also showed a time-dependent increase (figures 2.2 B-C; table 1). Serum miR-122 levels were significantly higher at 2 hours (P=0.02) compared to control mice. Serum miR-192 levels were significantly higher at 4 hours (P=0.001) compared to control mice.

Serum levels of non-liver enriched miRNAs (miR-1, muscle-enriched; miR-218, brain-enriched) were relatively unchanged throughout APAP-induced ALI compared to liver-enriched miRNAs (figures 2.2 D-E; table 1). Serum miR-1 levels were significantly higher

at 4 hours (*P*=0.03) compared to control mice. Serum miR-218 levels were not significantly higher at any time in APAP-treated mice compared to control mice.

Table 1: Serum ALT activity and miRNA values during APAP exposure in mice

	Control	**1h**	**2h**	**4h**	**8h**
ALT **U/L** (± SD)	**12.5** (3.5, 25)	**14.5** (11.5, 16.8)	**21.0** (11.5, 54.5)	**856** (732, 2405)	**299** (278, 320)
miR-122 **ΔCt** (± SD)	**4.1** (1.1, 8.0)	**87.2** (12.2, 153.4)	**75** (37.5, 441.1)	**4096** (910.2. 15393)	**8984** (709.2, 17258)
miR-192 **ΔCt** (± SD)	**4.83** (1.7, 33.6)	**30.0** (12.5, 68.2)	**23.6** (12.8, 90.7)	**1448** (105.1, 3180)	**1332** (167.8, 2495)
miR-1 **ΔCt** (± SD)	**2.1** (1.3, 3.7)	**9.8** (6.9, 26.3)	**10.1** (4.6, 12.3)	**28.4** (5.3, 53.4)	**37.0** (0.01, 74.0)
miR-218 **ΔCt** (± SD)	**0.2** (0.1, 1.6)	**2.3** (1.1, 3.6),	**1.0** (0.4, 1.5),	**1.6** (0.2, 3.1)	**9.1** (0.9, 17.3)

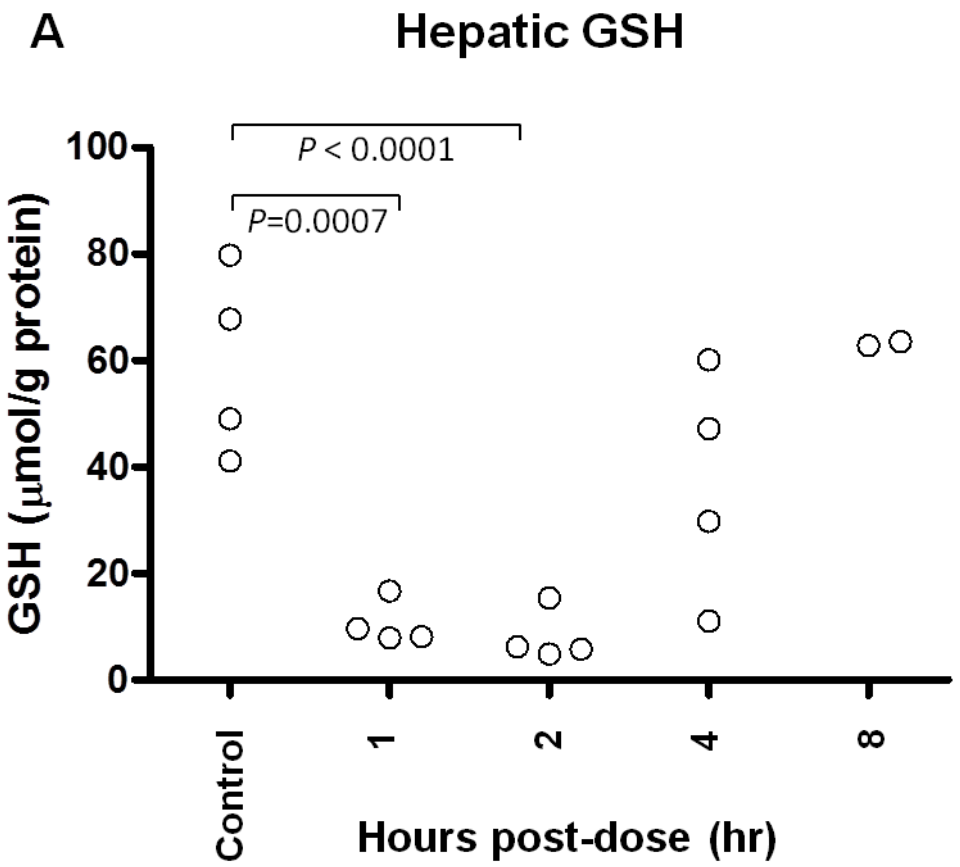

Figure 2.1: Hepatic GSH levels fall dramatically early after exposure to a toxic APAP dose. Hepatic GSH levels were measured from whole liver homogenates generated from flash-frozen liver sections taken at the time points indicated on the x-axis. Control mice received saline (i.p.) equivalent to a 530 mg/kg APAP dose for 8 hours. Each open circle represents a protein-corrected GSH level from individual mice. Hepatic GSH levels were significantly lower 1h (P=0.0007) and 2h (P<0.0001) after APAP administration (Kruskall-Wallis test).

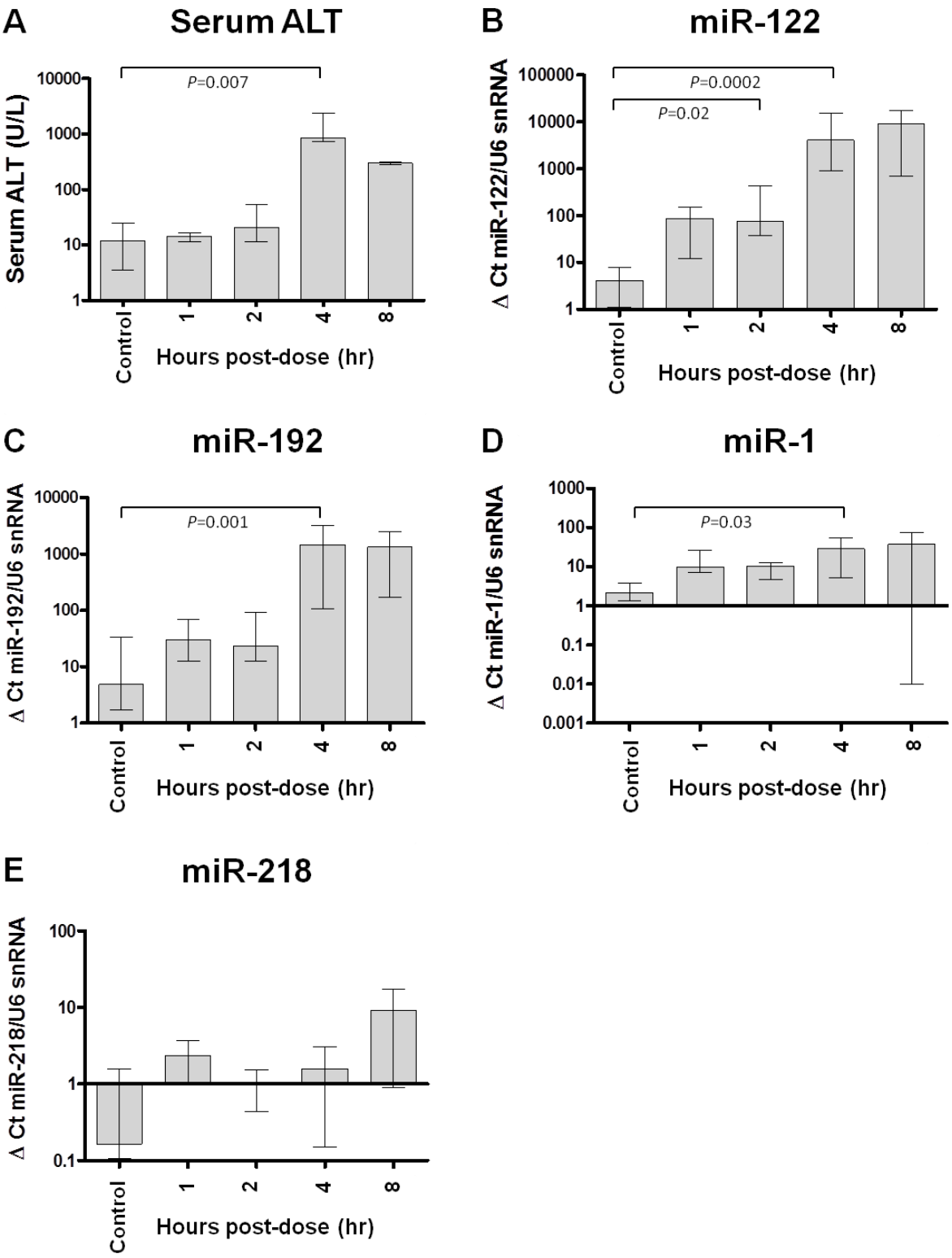

Figure 2.2: Serum miR-122 levels are significantly raised 2 hours after APAP exposure unlike serum ALT activity. Serum ALT activity and serum miRNAs were measured in serum taken from individual mice. Each panel shows the median (grey bar) and the whiskers represent the IQR for each group (n=4; 8h: n=2 due to mortalities). Panels show serum ALT activity (A), miR-122 (B), miR-192 (C), miR-1 (D), and miR-218 (E). Statistically significant differences are shown in panels (Kruskall-Wallis test)

2.3.2 Serum ALT and serum miR-122 provide similar sensitivity in a murine model of APAP-induced liver injury.

CD-1 male mice (5-7 weeks old, fed *ad libitum*) were administered a single dose of APAP ranging from 30-530 mg/kg, *i.p.* as described for 5 hours, to test the sensitivity of serum miRNAs against the serum ALT activity (figures 2.3 A-E). Small RNA was extracted from serum where four separate miRNAs were measured including liver-enriched miRNAs (miR-122 and miR-192), a muscle-enriched miRNA (miR-1), and a brain-enriched miRNA (miR-218). Serum miRNAs were quantified against a reference species (U6 snRNA) using 2 ^ - (ΔCt) method. Median (IQR) Serum Serum ALT activity was significantly higher at 4 hours (P = 0.003; figure 2.3A; table 2). Serum miR-122 levels were not significantly different between 300 mg/kg *vs* 0 mg/kg (and 530 mg/kg *vs* 0 mg/kg) due to variation in the 0 mg/kg group (P=0.27) (figure 2.3B, table 2). However, they were significantly raised when compared to low-dose APAP groups; either 30 mg/kg (P=0.013) or 75 mg/kg (P=0.017) which showed no hepatotoxicity. For miR-192, a statistically significant difference was observed between 530 mg/kg and 0 mg/kg group (P=0.02) and also between 530 mg/kg and 30 mg/kg APAP group (P=0.046) (figure 2.3C, table 2). For miR-1, statistical significance was observed between 0 mg/kg and 150 mg/kg (P=0.01), and between 0mg/kg and 300 mg/kg (P=0.048) (figure 2.3D; table 2). For miR-218, statistical significance was not observed between differences in any groups (figure 2.3E; table 2).

Table 2: Serum ALT activity and miRNA values in an APAP dose-response study in mice

	0 mg/kg	**30 mg/kg**	**75 mg/kg**	**150 mg/kg**	**300 mg/kg**	**530 mg/kg**
ALT **U/L** (± SD)	**38.1** (27.5, 79.3)	**38.7** (23.5, 79.3)	**29.6** (26.9, 43.1)	**36.4** (14.6, 91.8)	**490.4** (293.7, 5699)	**4251** (170.4, 13069)
miR-122 ΔCt (± SD)	**282.9** (124.1, 437.6)	**109.3** (88.9, 186.0)	**131.3** (71.5, 163.1),	**282.9** (124.1, 437.6)	**572.9** (214.9, 3150)	**2069** (598.4, 2628)
miR-192 ΔCt (± SD)	**29.5** (8.1, 34.9)	**23.3** (9.0, 39)	**9.38** (8.5, 16.0)	**8.4** (7.4, 21.9)	**224** (33.9, 1060)	**106** (47.6, 464)
miR-1 ΔCt (± SD)	**1.8** (0.9, 2.2)	**1.8** (0.7, 2.7)	**2.3** (0.1, 3.5),	**5.7** (3.2, 6.7),	**3.2** (2.1, 15.0)	**2.8** (1.6, 3.5)
miR-218 ΔCt (± SD)	**0.17** (0.10, 0.32)	**0.17** (0.09, 0.22)	**0.12** (0.10, 0.14)	**0.16** (0.01, 0.22),	**0.17** (0.01, 0.23)	**0.12** (0.06, 0.20)

,

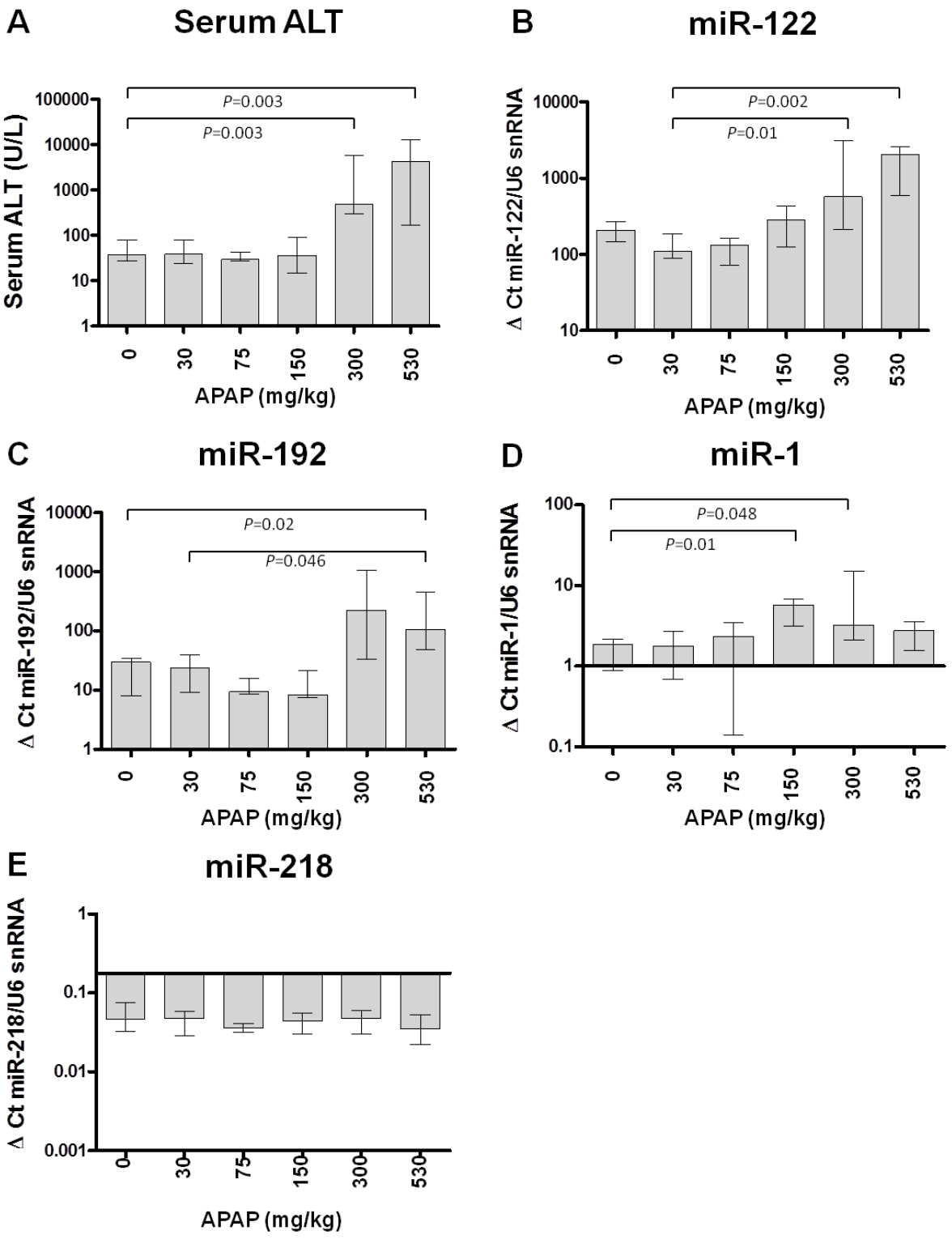

Figure 2.3: Serum ALT activity and serum miR-122 levels provide similar sensitivity to inform on APAP-induced liver injury. Serum ALT activity and serum miRNAs were measured in serum taken from individual mice. Each panel shows the median (grey bar) and the whiskers represent the IQR for each group (n=4). Panels show serum ALT activity (A), miR-122 (B), miR-192 (C), miR-1 (D), and miR-218 (E). Statistically significant differences are shown in panels (Kruskall-Wallis test).

2.3.4 miR-122 is lost progressively from centrilobular zones in mouse liver during APAP-induced ALI

In a separate time-course study, CD-1 male mice (5-7 weeks old, fed *ad libitum*) were administered APAP (530 mg/kg, i.p.) for 1h, 2h, 4h and 8h with time-matched controls which received 0.9% saline vehicle equivalent to a 530 mg/kg APAP administration. Livers were removed at the indicated time-points and fixed in formalin for 24 hours. From FFPE preparations, miR-122 and U6 snRNA were stained using specific riboprobes as described. In saline administered mice, miR-122 is visible as a blue stain due to presence of the nitroblue tetrazolium formazan precipitate, against a pink counter-stain. miR-122 staining in control mice exhibited mild zonal variation with strongest staining in peri-portal hepatocytes and slightly milder staining in centrilobular hepatocytes. However, miR-122 was present in all hepatocytes with no observable evidence of miR-122 loss in control mice (figure 2.4 A-D). In liver sections generated from APAP-treated mice, miR-122 staining appears normal 1 hour after APAP administration (figure 2.4E), with no observable changes compared to saline-treated mice. However, noticeably less staining is observed around centrilobular and midzonal regions 2 hours after APAP dosing (black arrows, figure 2.4F) when the pink counterstain becomes visible. This loss of miR-122 staining becomes increasingly evident at 4 hours (figure 2.4G) and 8 hours (figure 2.4H) after APAP dosing.

To investigate the mechanism of cell release at early time points, one single mouse was selected from the two hour time point which showed miR-122 loss around centrilobular and midzonal regions. A higher-magnification image (10x) was focussed on one central vein showing typical miR-122 loss, indicated by black arrows (figure 2.5A). From the same section of liver, a H&E stain was performed to visualise necrotic cells. H&E staining showed no visual signs of necrotic cells with intact parenchyma (figure 2.5B). Furthermore, a riboprobe against U6 snRNA, a small nuclear RNA (and popular choice of reference species in miRNA studies) was also stained in the same centrilobular region. The central

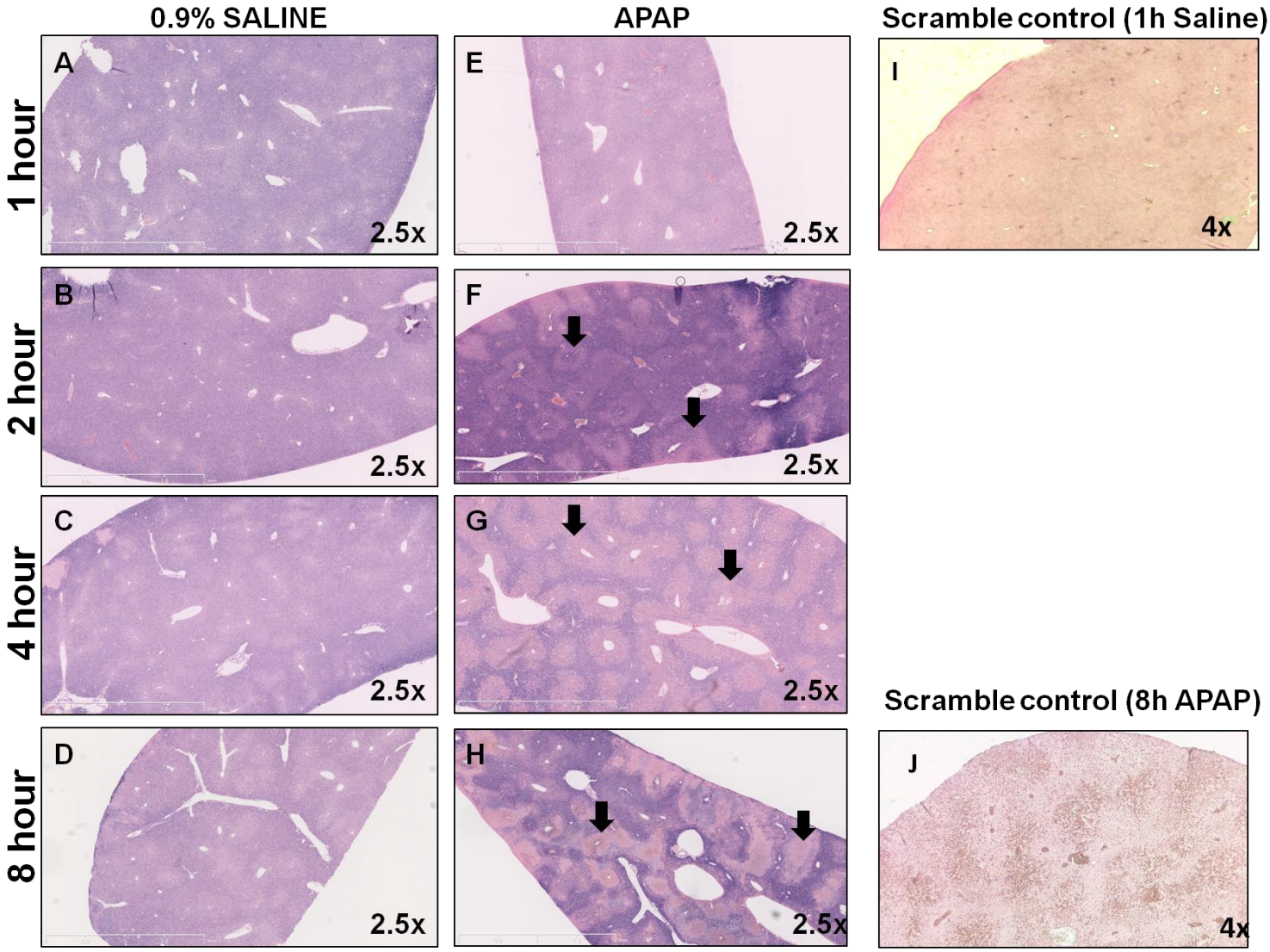

Figure 2.4: miR-122 is lost progressively from centrilobular hepatic regions during APAP-induced ALI. Panels show staining images (2.5x magnification) from individual mice taken at the indicated time (left-hand side). Left-hand panels show liver sections stained for miR-122 in mice who received saline injections for 1 hour (A), 2 hours (B), 4 hours (C) and 8 hours (D). No loss of miR-122 is apparent. Right hand columns show liver sections stained for miR-122 in mice who received APAP (530 mg/kg, i.p.) for 1 hour (E), 2 hours (F), 4 hours (G) and 8 hours (H). Black arrows indicate centrilobular regions where miR-122 staining appears less intense (pink counterstain) noticeable at 2 hours, becoming more pronounced at 4 hours and 8 hours. Scramble control showing pink counterstain only is shown in control mice administered saline for 1h (I) and mice administered APAP for 8h (J).

vein is less obvious in this tissue slice due to the variable three-dimensional architecture of the liver, however U6 snRNA staining in intact nuclei in cells is clear (figure 2.5C).

2.3.5 miR-122 is a hepatocyte-specific miRNA expressed in cytosolic and nuclear intracellular compartments.

To ascertain the specificity of cell expression of miR-122 in the liver, liver slices were generated from control mice from the time-course study. The image was focussed on a portal triad (PT) (hepatic artery, hepatic portal vein and bile duct) which contains substantial amounts of cells other than hepatocytes including endothelial cells and connective tissue. From this image, miR-122 staining (blue) is specific to the surrounding parenchyma tissue made up of hepatocytes (black arrows, figure 2.6A). Endothelial cells and connective tissue comprising the vessels of the portal triad are clearly not stained (pink counterstain). Red blood cells can be visualised within the hepatic portal vein.

In the same mouse, a high-magnification (40x) image was focussed on the hepatic parenchyma to resolve the intracellular location of the miR-122 staining. Localised miR-122 staining (blue) is visible in both cytosolic (white arrow, figure 2.7A) and nuclear (black arrow, figure 2.7B) compartments. Hepatic sinusoids are unstained (white).

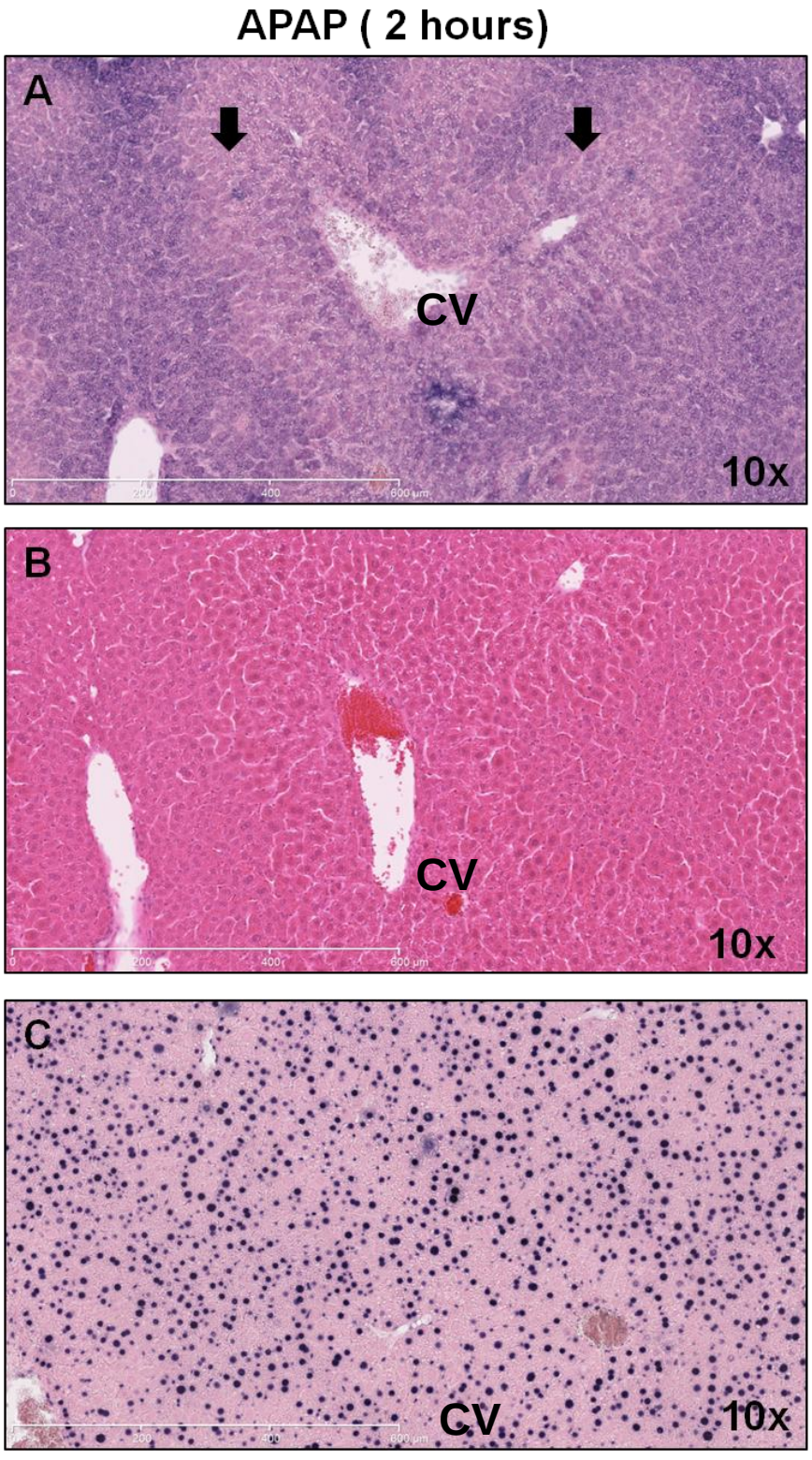

Figure 2.5: miR-122 is lost from hepatocytes which are not yet necrotic 2 hours post APAP administration. Panels show staining and histology images (10x magnification). Centrilobular and midzonal *in situ* hybridisation of miR-122 appears considerably lighter suggesting loss of miR-122 (A). Histological (H&E) analysis of the same region shows no signs of necrosis (B). *In situ* hybridisation against U6 snRNA shows strong nuclear staining in intact cells (C).

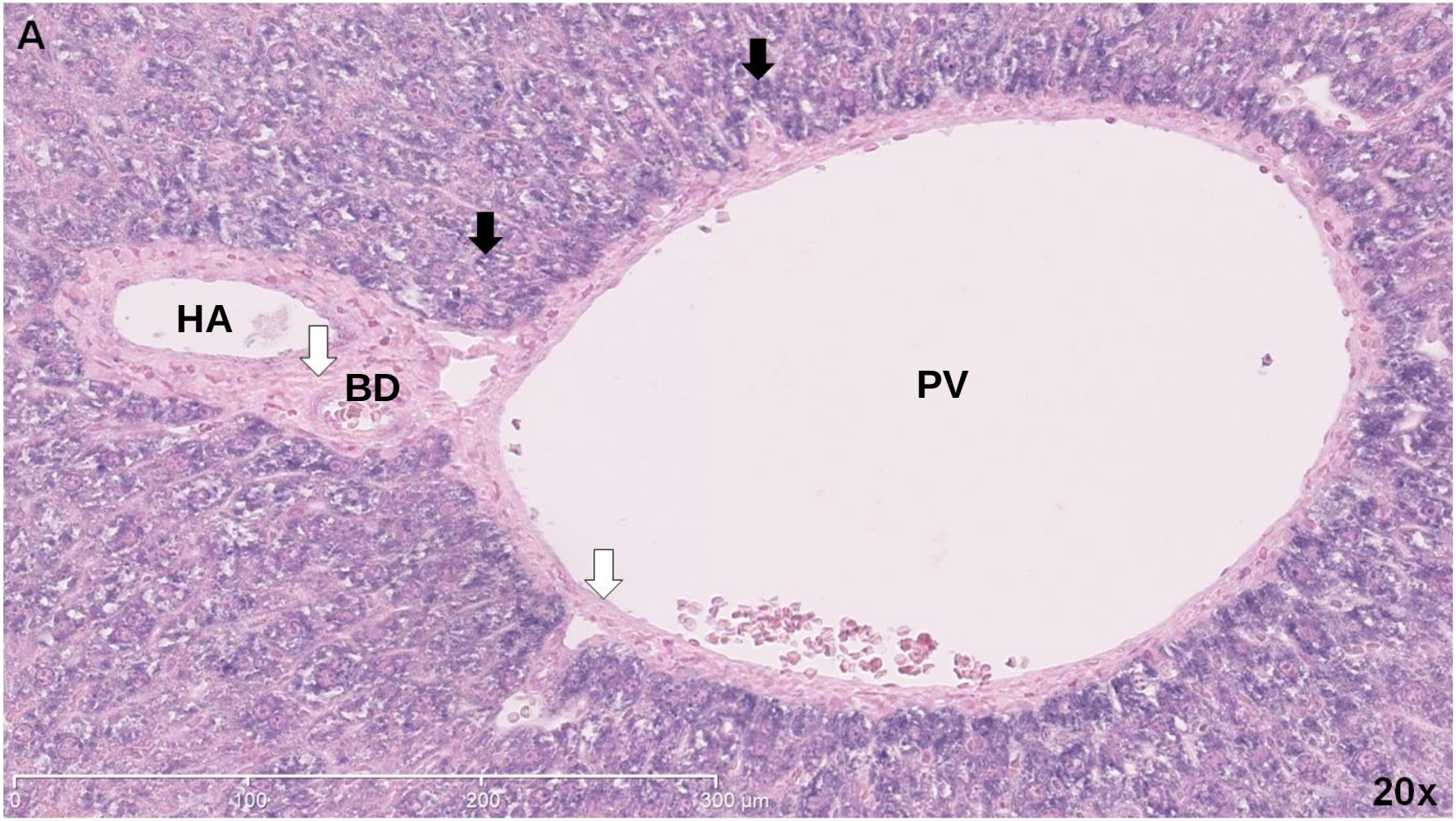

Figure 2.6: miR-122 is expressed specifically in hepatocytes. Panel shows *in situ* hybridisation against miR-122 at a portal triad junction (20x magnification) in a saline-treated mouse. The three main vessels are visible; branch of hepatic portal vein (PV), branch of hepatic artery (HA), branch of bile duct (BD). *In situ* hybridisation against miR-122 reveals hepatocyte-specific staining (black arrows). Endothelial cells and connective tissue are visible in light pink (counterstain, white arrows). Red blood cells are visible in the hepatic portal vein.

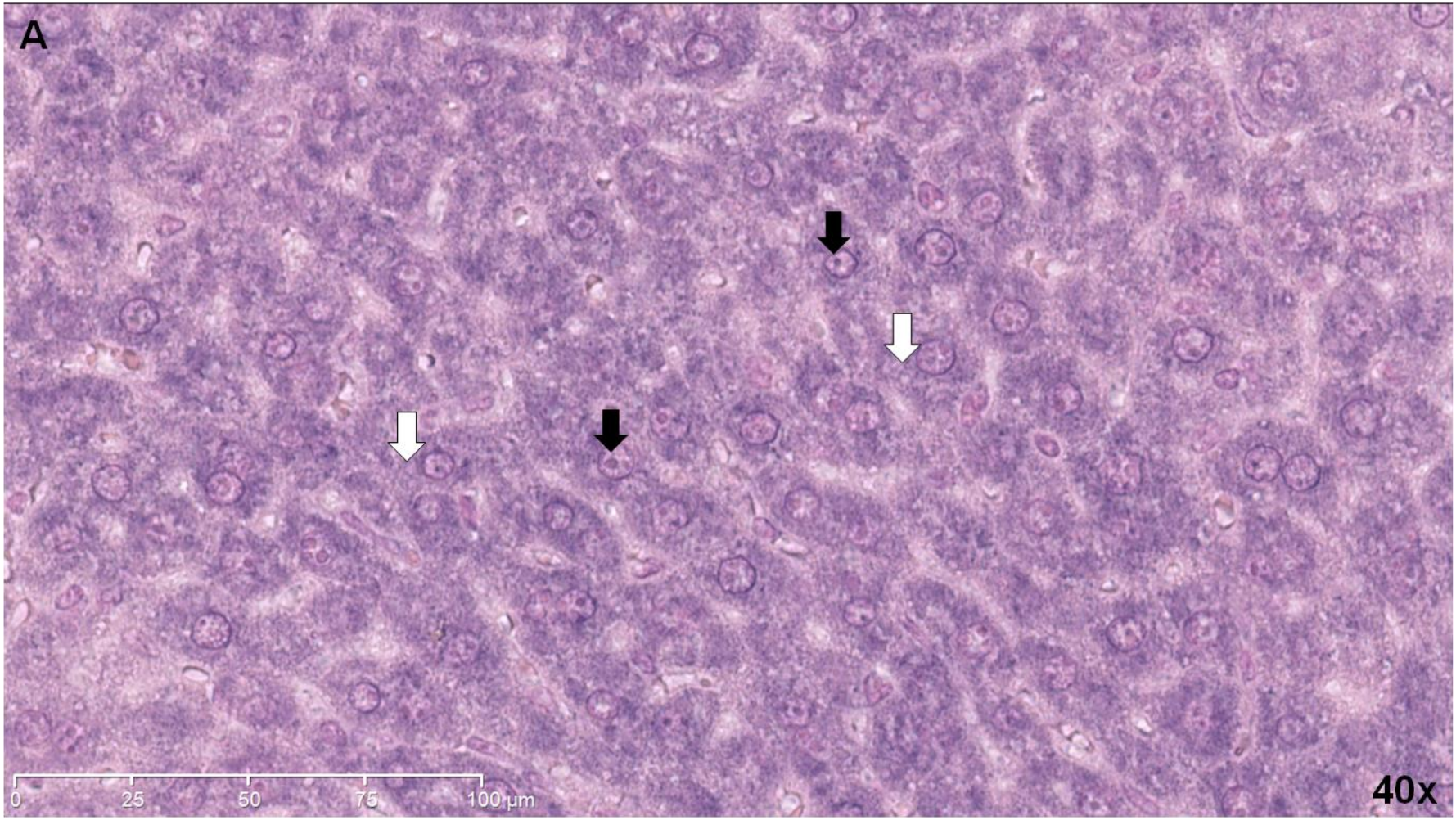

Figure 2.7: miR-122 staining in the hepatic parenchyma is localised to cytosolic and nuclear compartments. Panel shows *in situ* hybridisation against miR-122 in the parenchyma (40x magnification) in a saline-treated mouse. Cords of hepatocytes are visible punctuated with sinusoids (white areas between cells). *In situ* hybridisation against miR-122 reveals strong cytosolic (white arrow) and nuclear (black arrow) intracellular staining.

2.4 Discussion

There is an urgent requirement for the identification and development of novel biomarkers of DILI in pre-clinical and clinical settings. In recent years, miRNAs have emerged as a class of molecules that have the potential to serve as biomarkers of various disease states, pathophysiological conditions and drug response. MiRNAs are small (~22nt in length) non-coding RNA molecules that function to repress a set of target mRNAs through cognate nucleotide binding thereby regulating protein output and the phenotype of the cell. MiRNAs exist in a remarkably stable form in various biofluids including blood and urine. Although species-specific miRNAs exist, as a class they confer true translational potential as many miRNAs show high conservation between mammalian species, including pre-clinical species. Furthermore, the expression of miRNAs can exhibit high tissue specificity combined within high abundance in tissues. These characteristics together provide promise for the identification and development of miRNAs as novel biomarkers of DILI.

In this chapter, the earliness and sensitivity of two liver-enriched miRNAs (miR-122 and miR-192) were tested in a 6 week old male CD-1 model of APAP-induced hepatotoxicity. These two miRNA species were previously reported to be earlier and more sensitive markers of APAP-induced liver-injury in 6-month old male Balb/C mice that were overnight fasted (Wang et al, 2009). Hepatic GSH depletion occurs very early in the evolution of APAP-induced ALI, confirming early biochemical stress in the mouse model (figure 2.1A). In our non-fasted model, miR-122 was raised in some animals at 1 hour, but as a group, this did not reach statistical significance. However, miR-122 was significantly raised at 2 hours (P=0.02) in our model, while serum ALT activity was still not raised indicating earlier release of miR-122 into the circulation (figure 2.2A-B). Serum miR-192 levels were not as abundant as miR-122 and did not show a significant rise until 4 hours after APAP administration (P=0.001, figure 2.2C), although this may be due to the low power of the experiment (n=4). The main finding that miR-122 is raised earlier than ALT in the CD-1 male model corroborates previously published findings by Wang *et al*. Furthermore, miR-1 showed

modest changes in serum after APAP with a statistical significant rise occuring after 4 hours (*P*=0.03, figure 2.2D). Brain-specific miR-218 was not different at any time (figure 2.2E) confirming that non-specific rises in global miRNAs after APAP-overdose occuresd. The finding that miR-122 is released earlier than ALT suggests that these markers do not share the same release mechanism from injured hepatocytes. ALT is believed to be leaked passively from necrotic hepatocytes into the circulation. The mechanism of miR-122 release from hepatocytes is unknown, however, it has been shown that miR-122 exists in various forms in the circulation; coupled with auxiliary proteins such as Argonaut 2 or encapsulated within exosomes and cell-derived vesicles (Arroyo et al, 2011, Bala et al, 2012). It is possible that miR-122 release may provide a specific signal to stressed hepatocytes to promote cell defence and cell proliferation. Indeed, loss of miR-122 is known to be associated with hepatogenesis and cell proliferation (Tsai *et al* 2012, Hsu *et al* 2012). However, this hypothesis requires testing.

In another mouse study, the sensitivity of liver-enriched miRNAs was tested alongside the "gold-standard" sensitive marker for DILI, serum ALT activity. The data showed that miR-122 was not more sensitive than ALT in this CD-1 mouse model. From this study, statistical significance was not reached for miR-122 at any time when compared to control animals (figure 2.3 B). However, this can be accounted for by the unexpected greater variation of miR-122 in control animals compared to other non-toxic groups. Indeed, if the comparison was made against low-dose (non-toxic) APAP groups (30 mg/kg and 75 mg/kg), a strong significant increase was observed at 300 mg/kg (*P*=0.01) and 530 mg/kg (*P*=0.002), similar to serum ALT activity (figure 2.3A). Nevertheless, this finding is contrary to the findings by Wang *et al*, who found rises in miR-122 and miR-192 at 150 mg/kg APAP doses after 3 hours in Balb/C mice (Wang et al, 2009). This may be explained by differences in experimental design and quantification technique used in the two studies. The mice in this study were exposed to APAP for 5 hours at each dose whereas Wang *et al* used 3 hours exposure, which is an early point during APAP-induced hepatotoxicity in rodent models.

Increases in circulating miRNAs at 3 hours are evident, however serum ALTs typically peak at a point beyond 4 hours, suggesting that the difference in sensitivity observed by Wang and colleagues may be due to, in part, different times of biomarker release. Nevertheless, we cannot discount fundamental biological differences between the two mouse strains that may also account for this. Further work is required with high-powered toxicity studies to elucidate the true sensitivity of liver-enriched miRNAs versus other biomarkers.

To better understand the origins of miR-122 release into the circulation, an APAP time-course study was performed in the CD-1 mouse model. From mice treated with and without APAP, hepatic miR-122 content was analysed via *in situ* hybridisation. A progressive loss of miR-122 staining was observed as early as two hours from centrilobular and midzonal areas in liver treated with a toxic dose of APAP (figures 2.4E-H). Importantly, comparator time-matched controls treated with vehicle showed consistent miR-122 staining at all time points (figures 2.4A-D). Zonal toxicity with APAP is well recognised (Mitchell et al, 1973, James et al, 2003) with necrosis occurring most predominantly around centrilobular areas. This can be explained in part due to the relatively high levels of CYP2E1 that are expressed in centrilobular hepatocytes (Forkert et al, 1995) which generates the toxic metabolite. These morphological changes are consistent between rodent models and man (Mitchell et al, 1973). This study confirms that miR-122 release at early and late time points occurs from the same areas of liver where toxicity is manifested.

At two hours, hepatic miR-122 depletion is visible (figure 2.4F) which coincides with a concomitant rise in the serum at this time (figure 2.2B). To gain insight into the release mechanism, a H&E stain was performed in the same histology samples. In the same APAP-treated mouse (2 hours), a high-magnification image shows centrilobular miR-122 depletion in individual hepatocytes (black arrow, figure 2.5A). H&E staining from sections taken from the same central vein branch indicate that the hepatocytes are not yet necrotic in nature (figure 2.5B). Viable hepatocytes can clearly be defined with sinusoids providing obvious borders between cells. Furthermore, a stain directed against a small nuclear RNA species

(U6 snRNA), shows clear nuclear staining in cells around the same central vein branch. This provides further confirmation that cells are not severely necrotic and that not all small RNA species are lost at the same rate as miR-122 (figure 2.5C). The fact that miR-122 depletion occurs in cells which appear still viable provides insight into the release mechanism. It is likely that during APAP-induced ALI, miR-122 release is associated with necrosis at later times; however this work suggests that a proportion of intracellular miR-122 appears to be released at times before substantial necrosis occurs. Clearly more work is required to identify the exact biological mechanism that governs early release. These findings allow one to speculate that miR-122 release may be bi-phasic, with an early energy-dependent step occurring before massive miRNA loss during necrosis. However, this concept has yet to be examined specifically in the context of DILI.

This histology data also provides further insight into the hepatocellular expression of miR-122. Although miR-122 is liver-enriched, the liver is a heterogenous organ comprising multiple cell types. From this data, we focussed on a portal triad which defines the borders of the hepatic lobule (figure 2.6A) and contains hepatocytes, endothelial cells and connective tissue. Analysing such data should inform on whether miR-122 is expressed equally among all hepatic cell types or whether there is cellular specificity. The cellular expression of miR-122 is striking; strong expression in periportal hepatocytes with no visible staining in the vessels of either the hepatic portal vein or the hepatic artery. This specificity is likely to provide added confidence in the utility of miR-122 as a biomarker of DILI by indicating stress/injury strictly to cells in the liver-parenchyma. Furthermore, analysis of high-magnification images of the liver parenchyma allows one to determine miR-122 localisation within individual hepatocytes. Strong staining occurs within the cytosolic and nuclear regions providing evidence that miR-122 is localised to multiple cellular compartments (figure 2.7A).

In summary, this chapter tests miR-122 as a potential marker of DILI in various models, including *in vivo* and *in vitro* approaches. This data shows that miR-122 can inform on

APAP-induced ALI in a young murine model, with good sensitivity and early detectability. Amongst the miRNA tested, miR-122 appears to the most promising biomarker of DILI with high circulating abundance, coupled with a high dynamic range and high liver-enrichment. miR-122 also holds promise as an *in vitro* marker of DILI using human cells, further highlighting the translational potential of this marker. However, obviously more work is needed to study the kinetics and extra-cellular form of miR-122 after treatment with APAP and other drugs. Finally, the release of miR-122 occurs at hepatocytes surrounding the central vein, cells which become necrotic during APAP-induced ALI. More information can be taken from the fact that miR-122 is expressed exclusively within hepatocytes and is localised within cytosolic and nuclear compartments. Further work is now required to define miR-122 baselines in different species, study the biological form in early and late phases of APAP-induced ALI, optimise assays to study miRNA release *in vitro*, examine the biological fate/turnover of circulating miRNA species and evaluate the possible clinical role of miR-122 in DILI.

CHAPTER THREE

CIRCULATING MICRORNAS AS POTENTIAL CLINICAL BIOMARKERS OF DILI

3.1 INTRODUCTION

The development of informative biomarkers of DILI is a primary goal for the clinic and for pre-clinical pharmaceutical evaluation. The challenge for the development of useful clinical markers includes identification and development of biomarkers that are ideally stable, non-invasive (i.e. can be sampled easily from patients), reflect accurately the (patho)physiological state of the liver (Adler et al, 2010), detect injury early with high sensitivity and high specificity without the need of specific patient information (i.e. an accurate time of ingestion) and be able to predict hard clinical end-points (reviewed by Dear, 2010) . The current set of clinical markers includes the aminotransfereases (ALT/AST), functional markers of liver impairment such as prothrombin time or total bilirubin levels. More recently, novel mechanistic markers have emerged such as HMGB1 and cytokeratin-18 have been discovered, however these have yet to be validated in multi-centre prospective clinical studies (Antoine et al, 2009). Limitations exist within the current set of established markers such as an unacceptable rate of false positive/negatives, poor sensitivity and lack of liver-specificity which together reduce the reliability of such biomarkers in the clinic. Due to the burden of DILI in the clinic and in drug development, novel markers that can complement or supersede the existing catalogue of biomarkers are urgently sought. (Amacher, 2010)

APAP is a well characterised hepatotoxin that has been used clinically as a mild analgesic and antipyretic for six decades. Despite an excellent safety profile at therapeutic doses, in an overdose setting APAP can cause centrilobular coagulative liver necrosis and possibly fatal fulminant hepatic liver failure. APAP is the leading cause of liver failure in the United States, reported to be responsible for 10,000 hospitilisations and 500 deaths per annum due to intentional or unintentional overdose (Lee, 2004; Larson et al, 2005; Ostapowicz et al, 2002). Although NAC therapy can provide effective antidotal therapy, in some cases (e.g. in patients who present late after drug ingestion) this treatment is not an option and orthoptopic liver transplantation may be required to save lives. New biomarkers of DILI (in this case,

APAP-induced ALI) are required to identify injury at the earliest possible stage to help the physician better manage patient therapy. Novel markers with enhanced liver-specificity would also provide added confidence in the utilisation of the marker in the clinic by potentially reducing the risk of false positives.

The promise of liver-enriched miRNAs serving as sensitive and specific biomarkers in the mouse model of liver injury needs to be evaluated in a patient population. In this chapter, the translational ability (i.e. from mouse to man) of these biomarkers to detect liver injury was tested in a cohort of patients who have overdosed on APAP and developed severe liver injury. miRNAs are measured in four patient cohorts (APAP-overdosed patients who develop injury, ***APAP ALI***); APAP-overdosed patients who do not develop injury, ***APAP NO ALI***; patients who develop liver injury not caused by APAP e.g. through hepatitis infection, ***NON-APAP ALI***; and patients who have chronic kidney disease, ***CKD***, in order to test organ injury specificity) versus a group of healthy volunteers. We measured four miRNAs; miR-122 (liver-enriched), miR-192 (liver/kidney-enriched) miR-1 (heart/muscle enriched) and miR-218 (brain-enriched) alongside U6 snRNA which was used as a reference species. In the same samples, we correlated our miRNA data with retrospective clinical chemistry data. Moreover, we tested whether miRNAs returned to baseline earlier than ALT in serial samples obtained from selected patients. Finally, we tested the performance of different normalisers (hsa-miR-376, U6 snRNA hsa-let-7d and cel-lin-4) between healthy volunteers and test APAP ALI patients.

3.2 PATIENTS AND METHODS

3.2.1 APAP-ALI patients

This study was prospectively approved by the local research ethics committee, and informed consent was obtained from all patients, or the patient's next of kin, before entry into the study. A total of 53 adult patients (age >16 years) admitted to the Royal Infirmary of Edinburgh with acute liver injury (ALI) secondary to APAP ingestion were entered into the study. ALI was defined as a sudden deterioration in liver function with associated coagulopathy in the absence of a history of chronic liver disease.13 Clinical parameters were recorded and are summarized in Table 1. Day 1 was defined as the day of entry into the study, and on this, and subsequent days, peripheral blood samples were collected. Patients were monitored up to day 30, whereupon the outcome of each patient was recorded as either poor (died/required liver transplantation) or survived. All serum and plasma samples used in this study were obtained by centrifugation, separated into aliquots, and stored at 80 °C until analysis.

3.2.2. Healthy controls

Blood was collected from a cohort of 25 selected healthy volunteers with ethical approval (National Research Ethics Service, Bristol, UK). Median age was 38, and the female-to-male ratio was 6:4 to reflect the age and sex bias in the poisoned-patient cohort. Analysis was performed in a single-blinded fashion.

3.2.3. Non-toxic APAP overdosed patients (APAP NO ALI)

Six patients were recruited from the Royal Infirmary of Edinburgh. Consent was obtained from all patients before recruitment, and the study received appropriate local ethical approval. The entry criterion was a history of a single APAP ingestion in overdose that required treatment with N-acetylcysteine (NAC). Blood was collected at the end of intravenous acetylcysteine infusion for measurement of ALT and other biomarkers. Absence

of liver injury was confirmed by a normal serum ALT activity (defined as ≤ 3 x upper limit of normal [ULN]).

3.2.4 Non-APAP induced ALI patients (NON-APAP ALI)

Eleven patients were recruited from the Royal Infirmary of Edinburgh. Informed consent was obtained from all patients, or the patient's next of kin, before entry into the study. The entry criterion was presentation of ALI independent of APAP ingestion. Clinical characteristics of these patients, including etiology of ALI, are summarized in table 1.

3.2.5 Chronic kidney disease patients

Twenty-two patients (mean age, 46 ± 3 years) were recruited from the Royal Infirmary of Edinburgh. Informed consent was obtained from all patients, or the patient's next of kin, before entry into the study. All patients had been diagnosed with chronic proteinuric kidney disease (CKD). The mean urinary protein excretion rate was 1,570 ± 371 µg/min, with a mean glomerular filtration rate of 43 ± 5 mL/min/1.73 m^2.

3.2.7 miRNA extraction

miRNA was extracted using an miRNeasy kit (Qiagen, Venlo, Netherlands), following the manufacturer's instructions, with minor modifications. Briefly, 40 µL of biofluid was made up to 200 µL with nuclease-free water, then combined with 700 µL of QIAzol. The sample was mixed and left for 5 minutes before the addition of 140 µL of chloroform. In some experiments, 10µL of cel-lin-4 (5fM) was added to denatured serum before the addition of chloroform (to serve as exogenous control). Samples were then mixed vigorously for 15 seconds and centrifuged at 12,000 g for 15 minutes at 4 °C. Equal volumes (350 µL) of the upper aqueous phase and 70% ethanol were mixed in a fresh microtube before adding the total volume to an miRNeasy minispin column. The column was centrifuged at 8,000g for 15 seconds at room temperature. The flow-through, containing the small RNA fraction,

including the miRNA complement, was mixed with 450 µL of 100% ethanol. The elute was then purified using a MinElute kit (Qiagen, Venlo, Netherlands).

3.2.8 miRNA purification

The small RNA elution mixture was applied to a MinElute column, 700 µL at a time. The immobilized RNA was then washed with various buffers before a final 80 % ethanol wash. The column was then dried by centrifugation. The small RNA fraction was eluted in 14 µL of nuclease-free water and stored at -80 °C.

3.2.9 Quantitative Polymerase Chain Reaction Analysis.

miRNA levels were measured using Taqman-based quantitative polymerase chain reaction (qPCR). The small RNA elute was reverse transcribed using specific stem-loop reverse-transcription RT primers (Applied Biosystems, Foster City, CA) for each target miRNA species, following the manufacturer's instructions. Next, 2 µL of RNA was used to produce the complementary DNA (cDNA) template in a total volume of 15 µL. Then, 1.33 µL of cDNA was used in the PCR mixture with specific stem-loop PCR primers (Applied Biosystems, Foster City, CA) in a total volume of 20 µL. Levels of miRNA were measured by the fluorescent signal produced from the Taqman probes on an ABI Prism 7000 (Applied Biosystems). All samples were assayed in duplicate. Assay performance was assessed (figure 3.3.94), providing acceptable variation and reproducibility. miRNA levels were normalized to levels of U6 snRNA, a ubiquitous small nuclear RNA (snRNA) species used as an endogenous control, as described elsewhere.

3.2.10 Statistical analysis

Descriptive statistical analysis was performed on each data group, including medians and interquartile ranges. Each data group was tested for normality using the Shapiro-Wilk normality test. To determine statistical significance, comparisons were made using the Student's t-test (for two parametric groups), the Mann-Whitney U test (for two

nonparametric groups), and the Kruskall-Wallis test (for more than two nonparametric groups) (StatsDirect, Cheshire, UK). For correlative analysis, a Pearson's correlation test was used, employing GraphPad Prism software (GraphPad Software, La Jolla, CA). Statistical significance was set at $P < 0.05$.

3.3 RESULTS

3.3.1 Liver-Enriched miRNAs Are Higher in APAP ALI Patients

Serum ALT activity (figure 3.1) was measured alongside two liver-enriched miRNAs (miR-122 and miR-192; figure 3.2) and two non-liver-enriched miRNA species (miR-1 and miR-218; figure 3.3) in serum or plasma obtained from four patient cohorts and one healthy cohort. Two cohorts comprised patients with ALI: APAP ALI (n = 53) and non-APAP ALI (n = 11). Two control cohorts comprised healthy controls (n = 25) and APAP no ALI overdosed patients (n = 6). A control disease cohort comprised patients diagnosed with CKD (n = 22). The characteristics of the cohort of patients with APAP ALI and non-APAP ALI are presented in Table 3.1 and Table 3.2, respectively. No underlying pathologies were recorded in the control cohorts. Serum ALTs were raised in APAP ALI patients ($P < 0.0001$) and non-APAP ALI patients ($P < 0.0001$) relative to healthy controls (figure 3.1; table 3.3). Moreover, these data also show that liver-enriched miRNAs are significantly higher in the serum of APAP ALI patients, compared to healthy controls (miR-122: $P < 0.0001$; miR-192: $P < 0.0001$) (figure 3.2 A,B). Also, miR-122, but not miR-192, was significantly higher in non-APAP ALI patients, compared to healthy controls (miR-122: $P < 0.001$; miR-192: $P = 0.3$) (figure 3.2 A,B). The heart-enriched miRNA, miR-1, was not statistically different between both ALI (APAP and non-APAP) groups and healthy controls (figure 3.3A). The brain-enriched miRNA, miR-218, was significantly higher in the APAP ALI patients, compared to healthy controls ($P = 0.015$), but only over a small dynamic range (figure 3.3B). In CKD patients, liver-enriched miRNAs showed a modest elevation, when compared to the healthy controls (figure 3.2 A,B). Nevertheless, levels of liver-enriched miRNAs in APAP ALI patients were substantially higher, compared to CKD patients (miR-122: $P < 0.0001$; miR-192: $P = 0.0004$) (figure 3.2A,B). Levels of miR-1 were not different between CKD patients and healthy controls (figure 3.3A). Circulating levels of miR-218 were substantially higher in CKD patients, when compared to healthy controls ($P < 0.0001$) (figure 3.3B).

	No. of cases (POD)
Gender	
Male (%)	22 (42%)
Female (%)	31 (58%)
Age (years)	
Median (range)	37 (16-66)
<50	47
≥50	6
KCC met	
Yes	19
No	34
Required CVVH	
Yes	17
No	33
Data not available	3
OLT performed	
Yes	5
No	48
Day One Encephalopathy Score	
Grade 0	25
Grade 1	9
Grade 2	4
Grade 3	2
Grade 4	13
Max Encephalopathy Score	
Grade 0	21
Grade 1	7
Grade 2	2
Grade 3	3
Grade 4	20
Died	
Yes	10
No	43
Poor Outcome (OLT/Died)	
Yes	15
No	38

Table 3.1: Clinical parameters of the APAP ALI patient cohort. Various parameters from the patient cohort. Abbreviations: POD, acetaminophen overdose; KCC, Kings College criteria for transplantation; OLT, orthotopic liver transplant; CVVH, continuous veno-venous hemofiltration; ALT, alanine aminotransferase; n, number; s, seconds.

Four patients presented with miR-122 levels within the normal range (figure 3.2A). The clinical data for these patients were analysed in more detail (table 3.4). All four patients presented with coagulopathy (INR> 1.3) and three out of four patients presented with advanced encephalopathy (HE grade >2) and high serum creatitine levels indicating perturbed kidney function. These data taken together suggest that this small group of patients presented late after drug ingestion, although clinical data is limited for subject 68 so these assumptions should be taken with caution. In this small group, one patient (subject 61) died on day 2 of the study - this patient is likely to have presented very late after drug ingestion when intensive care therapy was futile.

Patient	Aetiology	Age (yrs)	Sex	ALT (U/L) Day 1	Creatinine (µmol/L) Day 1	PT (sec) Day 1	Bilirubin (µmol/L) Day 1	KCC	RRT	OLT	Day 1 Encephalopathy grade (0-4)	Max Encephalopathy grade (0-4)	Died	Poor outcome (died / OLT)	miR-122 / U6
1	Acute HBV	44	M	2665	77	19	319	No	No	No	0	0	No	No	329.698
2	Acute HCV	41	M	1676	61	15	256	No	No	No	0	0	No	No	1108.966
3	AFLP	32	F	73	299	17	72	No	Yes	No	1	4	No	No	238.03
4	AIH	71	F	854	55	56	478	Yes	No	Yes	2	4	No	Yes	205.074
5	AIH	64	M	3393	83	12	199	No	No	No	0	0	No	No	349.706
6	AIH	69	F	145	105	16	199	Yes	Yes	Yes	0	4	No	Yes	279.17
7	DILI	58	F	2773	91	15	138	No	No	No	0	1	No	No	831.746
8	HBV	41	M	794	482	82	375	Yes	Yes	No	0	4	Yes	Yes	922.88
9	HBV	26	M	2966	89	16	279	No	No	No	0	0	No	No	82.998
10	Ischaemia	42	F	5192	102	18	84	Yes	No	0	4	4	No	No	28.345
11	Malignancy	59	F	310	368	27	121	No	Yes	0	3	3	Yes	Yes	1172.198

Table 3.2. Clinical characteristics of non-APAP acute liver injury patients. HBV – hepatitis B virus; HCV – hepatitis C virus; AFLP – acute fatty liver of pregnancy; AIH – autoimmune hepatitis; DILI – drug-induced liver injury (clarithromycin); Malignancy – breast cancer hepatic infiltration; Day 1 – entry into study; KCC – King's College Criteria; RRT – renal replacement therapy; OLT – orthotopic liver transplantation.

Cohorts	***ALT (U/L)***	***miR-122 (ΔCt)***	***miR-192 (ΔCt)***	***miR-1 (ΔCt)***	***miR-218 (ΔCt)***
	Range				
Healthy Controls	Und-26.5	2.98 – 65.8	0.119 – 1.80	0.007 – 0.61	0.022 – 0.313
APAP no ALI	9-24	2.14 – 54.0	0.120 – 2.20	0.01- 2.39	0.01 – 0.132
CKD	Und-35.6	11.9 – 54.4	0.142 – 6.06	0.008 – 0.502	0.586 – 3.76
Non APAP ALI	73-5192	8.57-1172	0.006-27.7	Und -1.93	0.014 -0.396
APAP-induced ALI	452-18040	11.4 - 53231	0.13 - 406	Und – 1.15	0.002 – 1.44
	Median (25th percentile, 75th percentile)				
Healthy Controls	5.948 (3.618, 14.19)	12.13 (6.99, 26.91)	0.4350 (0.295, 0.694)	0.0580 (0.021, 0.089)	0.07 (0.04, 0.1215)
APAP no ALI	19.0 (14.25, 23.25)	23.21 (3.192, 45.95)	0.941 (0.359, 1.784)	0.0575 (0.00875, 1.423)	0.0280 (0.009. 0.09075)
CKD	6.13 (4.044, 10.37)	32.03 (21.14, 40.86)	1.230 (0.741, 1.912)	0.0580 (0.0365, 0.1058)	1.714 (1.087, 2.271)
Non APAP ALI	2665 (794, 2966)	279.2 (194.7, 922.9)	2.420 (0.196, 8.225)	0.0130 (0.00325, 0.06925	0.0950 (0.017, 0.269)
APAP-induced ALI	5199 (2966, 7984)	1265 (491.3, 4270)	6.940 (1.96, 29.16)	0.0270 (0.006, 0.129)	0.170 (0.0675, 0.504)
	Fold change (Mean)				
APAP ALI vs Healthy controls	665	252	65.5	1.02	3.5
APAP ALI vs APAP no ALI	313	189	35.2	1.12	6.67
CKD vs Healthy Controls	1.03	1.73	2.93	0.931	20.3
Non-APAP ALI vs Healthy controls	245	26.4	11.7	2.72	1.57
APAP ALI vs CKD	647	146	22.3	1.1	0.17
	P value				
APAP ALI vs Healthy controls	< 0.0001	< 0.0001	< 0.0001	0.7093	0.0147
APAP ALI vs APAP no ALI	0.0009	0.0031	0.056	0.9383	0.06
Healthy controls vs APAP no ALI	0.0662	0.9997	0.837	> 0.9999	0.465
CKD vs Healthy Controls	0.9999	0.0063	0.0054	0.9989	< 0.0001
Non-APAP ALI vs Healthy controls	< 0.0001	0.0005	0.2988	0.5164	> 0.9999
APAP ALI vs CKD	< 0.0001	< 0.0001	0.0004	0.420	0.0001

Table 3.3: ALT and miRNA measurements from six cohorts of patients, healthy controls (n=25), APAP-overdosed patients presenting no liver injury (APAP no ALI, n=6), chronic kidney disease patients (CKD, n=22), liver injury patients not caused by APAP (non-APAP ALI, n=11) and APAP-overdosed patients presenting liver injury (n=53). *P* values determined by Kruskall-Wallis multiple comparison test.

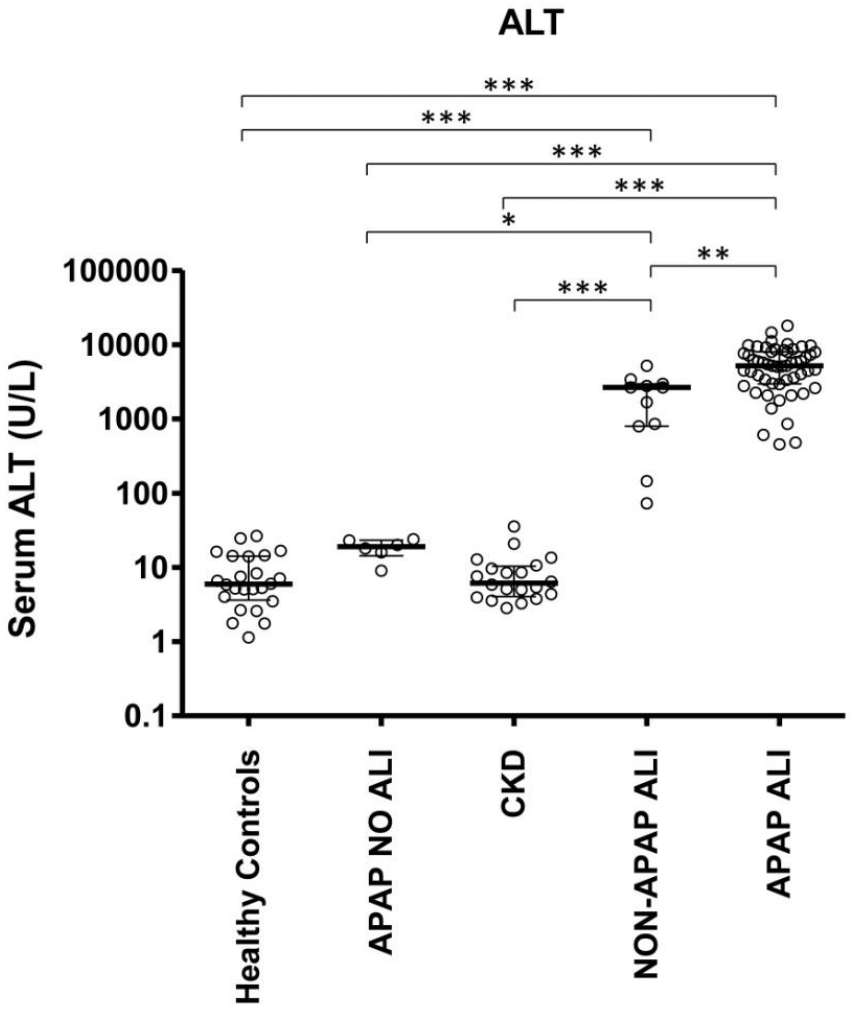

Figure 3.1: Circulating serum ALT activities are significantly higher in patients with ALI. Dynamic ranges of serum ALT activities were evaluated in human serum in grouped controls (n = 25), APAP no ALI patients (n = 6), CKD patients (n = 22), non-APAP ALI patients (n = 11), and APAP ALI patients (n = 53). Each open spot represents an individual serum ALT activity. Bars represent the interquartile range (25th and 75th percentiles) from the median (horizontal line). The data is shown in table 3.3.

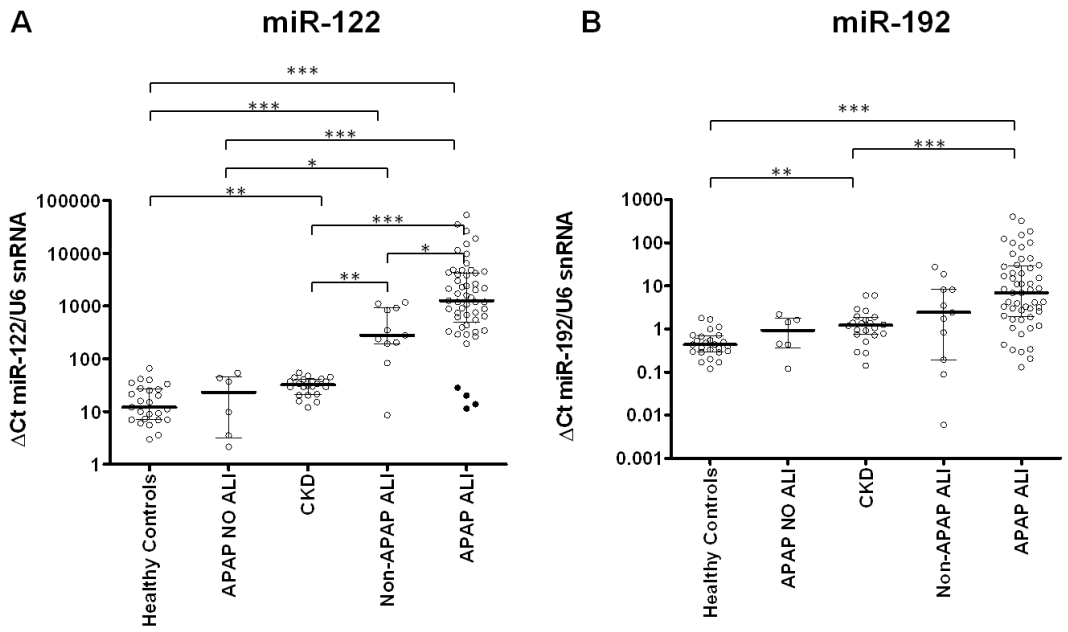

Figure 3.2: Circulating liver-enriched miR-122 and miR-192 species are significantly higher in patients with APAP ALI. Relative dynamic ranges of two liver-enriched miRNA species were evaluated in human serum or plasma in grouped controls (n = 25), APAP no ALI patients (n = 6), CKD patients (n = 22), non-APAP ALI patients (n = 11), and APAP ALI patients (n = 53). Panels show the relative levels of circulating (A) miR-122 and (B) miR-192 across six cohorts. Bars represent the interquartile range (25th, 75th percentiles) from the median (horizontal line). The data is shown in table 3.3. Four patients who had miR-122 levels within the normal range are highlighted by closed circles (panel A). Clinical data from these patients is presented in table 3.4

Study #	ALT (U/L)	miR-122 (ΔCt)	INR	HE Grade	Day Death	Creatinine (μmol/L)
Patient 61	2188	8.574	2.3	4	2	246
Patient 64	3386	11.432	1.8	4	Survived	234
Patient 63	482	13.785	2.2	3	Survived	179
Patient 68	1385	20.112	N/A	0	Survived	N/A

Table 3.4: Clinical analysis of 4 patients with serum miR-122 levels in the normal range

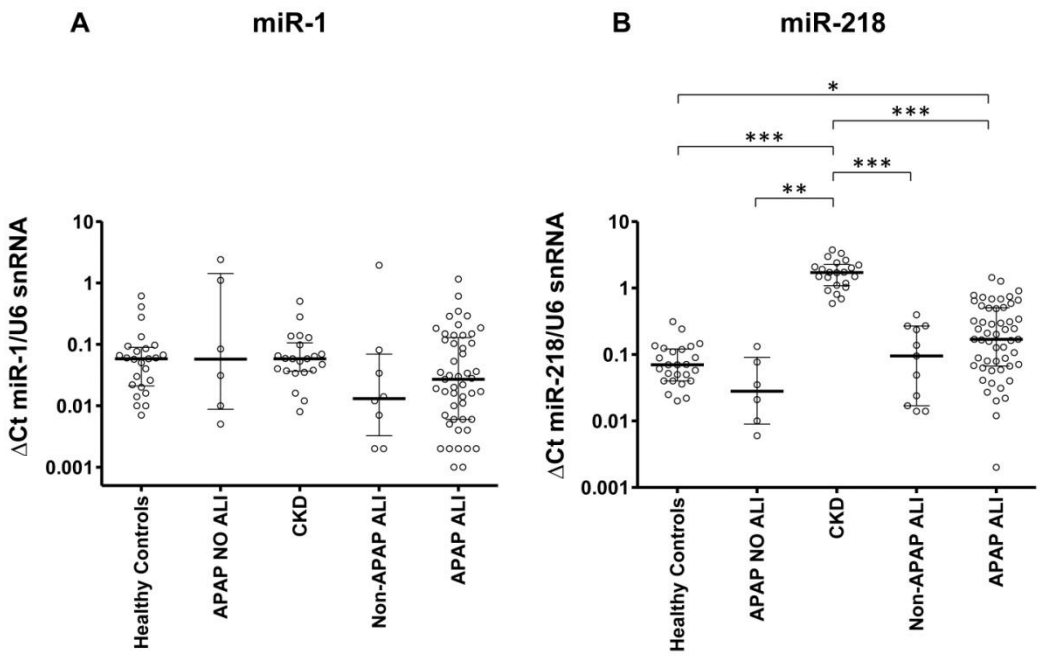

Figure. 3.3: Circulating muscle-enriched miR-1 is not significantly higher in patients with ALI, compared to healthy controls, and brain-enriched miR-218 is significantly higher in APAP ALI patients over a small dynamic range, compared to healthy controls. Relative dynamic ranges of a heart-enriched (miR-1) and a brain-enriched (miR-218) miRNA was evaluated in human serum or plasma in grouped controls (n = 25), APAP no ALI patients (n = 6), CKD patients (n = 22), non-APAP ALI patients (n = 11), and APAP ALI patients (n = 53). Panels show the relative levels of circulating miR-1 (A) and miR-218 (B) across six cohorts. Each open spot represents an individual relative amount of miRNA (ΔCt). Bars represent the interquartile range (25th, 75th percentiles) from the median (horizontal line). The data is shown in table 3.3.

3.3.2 miR-122 Correlates With ALTs, But Not Prothrombin Time or Total Bilirubin Concentration, in APAP ALI Patients.

To assess the performance of the two liver-enriched miRNAs as markers of liver injury, the relative abundance of each miRNA was compared against serum ALT activity. Serum miR-122 showed a statistically significant correlation (figure 3.4A) with ALT activity (P = 0.0004, Pearson R = 0.47), whereas miR-192 (figure 3.4B) showed no significant correlation (P = 0.14, Pearson R = 0.20). When the two non-liver-enriched miRNAs were plotted against ALT, miR-1 showed no significant correlation (P = 0.46, Pearson R = -0.10) (figure 4C) and miR-218 showed a significant positive correlation over a small dynamic range (P = 0.004, Pearson R = 0.39) (figure 3.4D). In the same serum samples, we plotted the relative abundance of miR-122 versus prothrombin time and total serum bilirubin concentration (figures 3.5A-B), clinical markers of liver function, and serum creatinine levels (figure 5C), the standard marker of kidney function. There was no statistical correlation between miR-122 abundance and prothrombin time (Pearson R = 0.14, P = 0.34, figure 3.5A), total bilirubin concentration (Pearson R = 0.10, P = 0.48, figure 3.5B), or serum creatinine (Pearson R = -0.16, P = 0.25, figure 3.5C).

3.3.3 Day 1 miR-122 Levels and Outcome in APAP ALI Patients

To determine the predictive value of miR-122, miRNA abundance in serum samples obtained from APAP ALI patients on day 1 was assessed relative to outcome: Whether that person met Kings College Criteria (KCC) for liver transplantation (figure 3.6A) and recovery versus poor outcome (died/required liver transplant) (figure 3.6B). In patients satisfying KCC, miR-122 levels and serum ALT activities were 96.3% and 11.4% higher, respectively, compared to those that did not meet KCC (miR-122: 6,848 ± 3,144 versus 3,488 ± 1,018, P = 0.15; ALT: 6,123 ± 694 versus 5,496 ± 658, P = 0.46). The average (mean ± standard error) miR-122 levels and serum ALT activities were 110% and 3.5% higher, respectively, in patients who had poor outcome, compared to those who recovered

(miR-122: 7,522 ± 3,966 versus 3,576 ± 928, *P* = 0.39; ALT: 5,863 ± 890 versus 5,664 ± 590, *P* = 0.93).

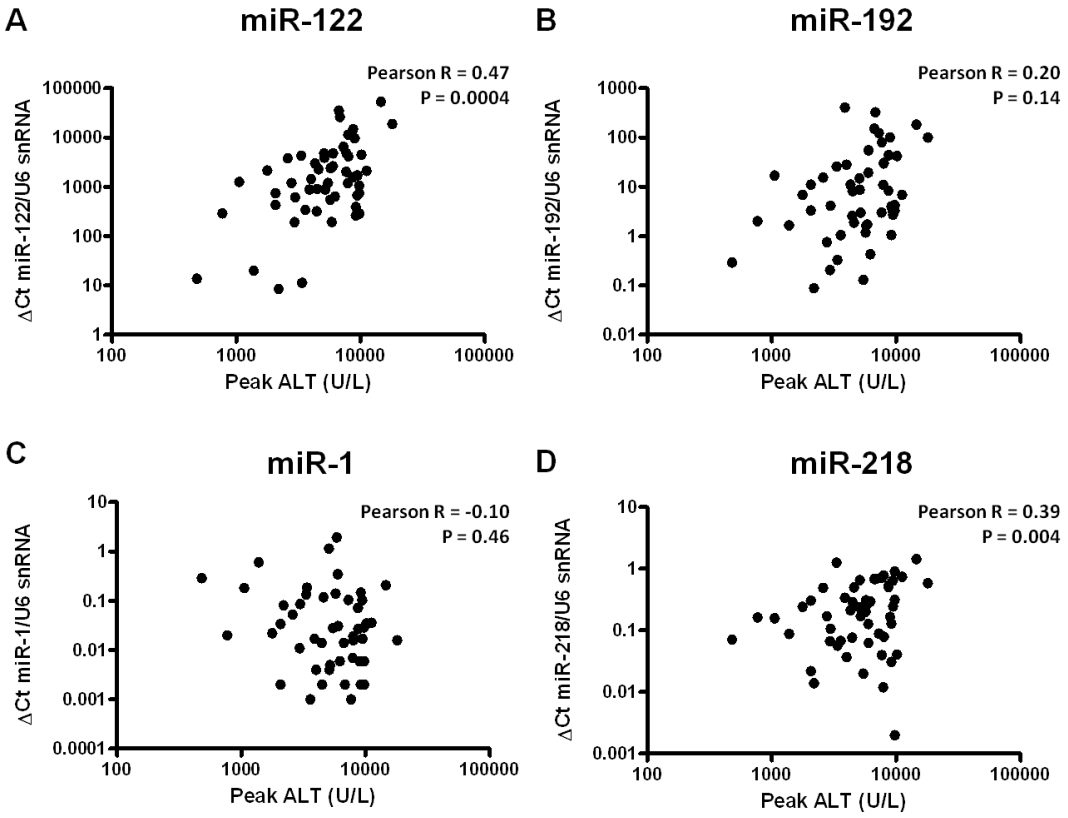

Figure 3.4: Liver-enriched miR-122 levels and brain-enriched miR-218 levels significantly correlate with peak serum ALT activity in APAP ALI patients. Correlation between relative miRNA abundances and ALTs from APAP-induced ALI patients (A) miR-122, (B) miR-192, (C) miR-1, and (D) miR-218. Scatter graphs show the correlation between the relative abundance of each miRNA (ΔCt) versus the serum ALT activity in that sample. Pearson R values (statistical P values) are 0.47 (P = 0.0004), 0.20 (P = 0.14), -0.10 (P = 0.46), and 0.39 (P = 0.004) for miR-122, miR-192, miR-1, and miR-218, respectively, versus serum ALT (Pearson's correlation test).

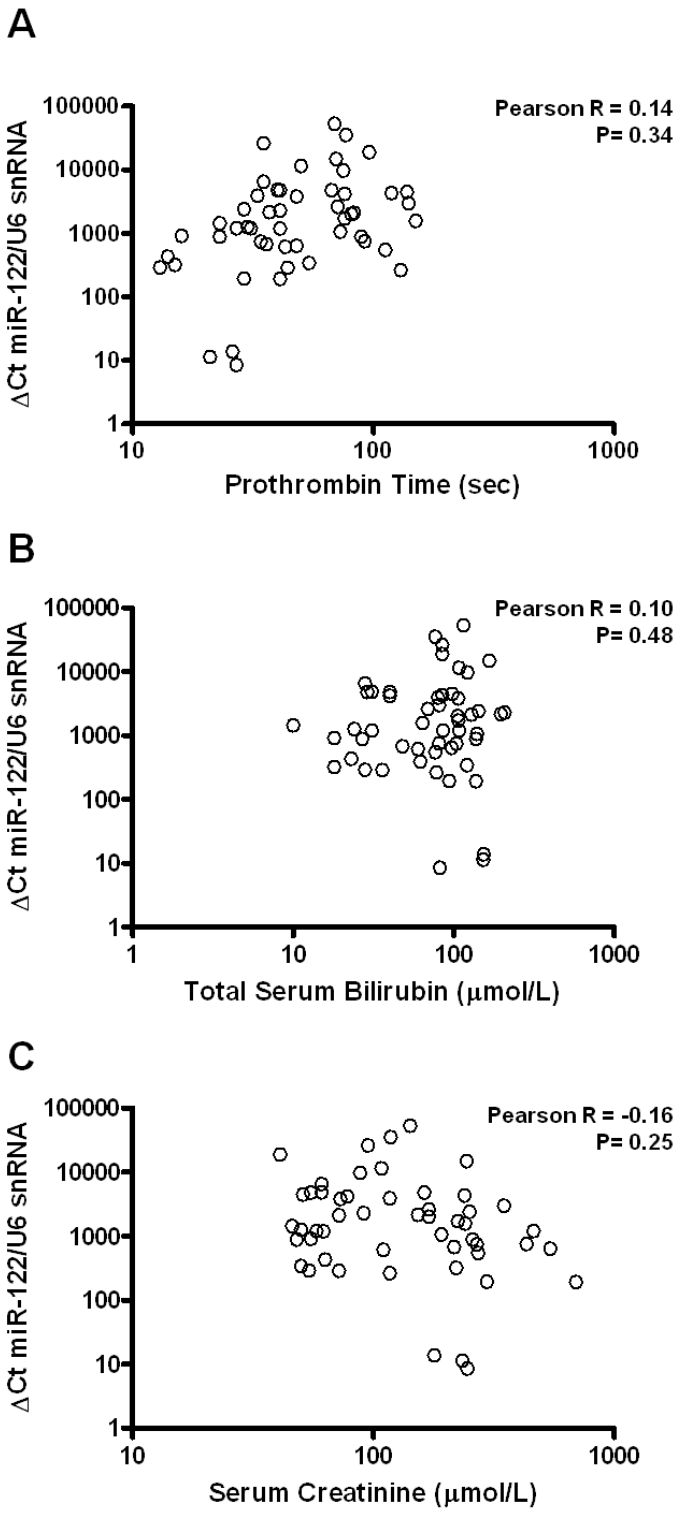

Figure 3.5: Circulating liver-enriched miR-122 does not correlate with prothrombin time, total serum bilirubin concentrations, or serum creatinine levels. Blood was taken from each patient on day 1 of the study. Prothrombin time, serum bilirubin levels, serum creatinine, and serum miRNAs were measured as described. Scatter graphs show the correlation between the relative abundance of miR-122 versus (A) prothrombin time, (B) total serum bilirubin, and (C) serum creatinine. Pearson R values (statistical probabilities) are 0.14 (P = 0.34), 0.10 (P = 0.48) and -0.16 (P = 0.25) for prothrombin time, total serum bilirubin concentration,and serum creatinine, respectively (Pearson's correlation test).

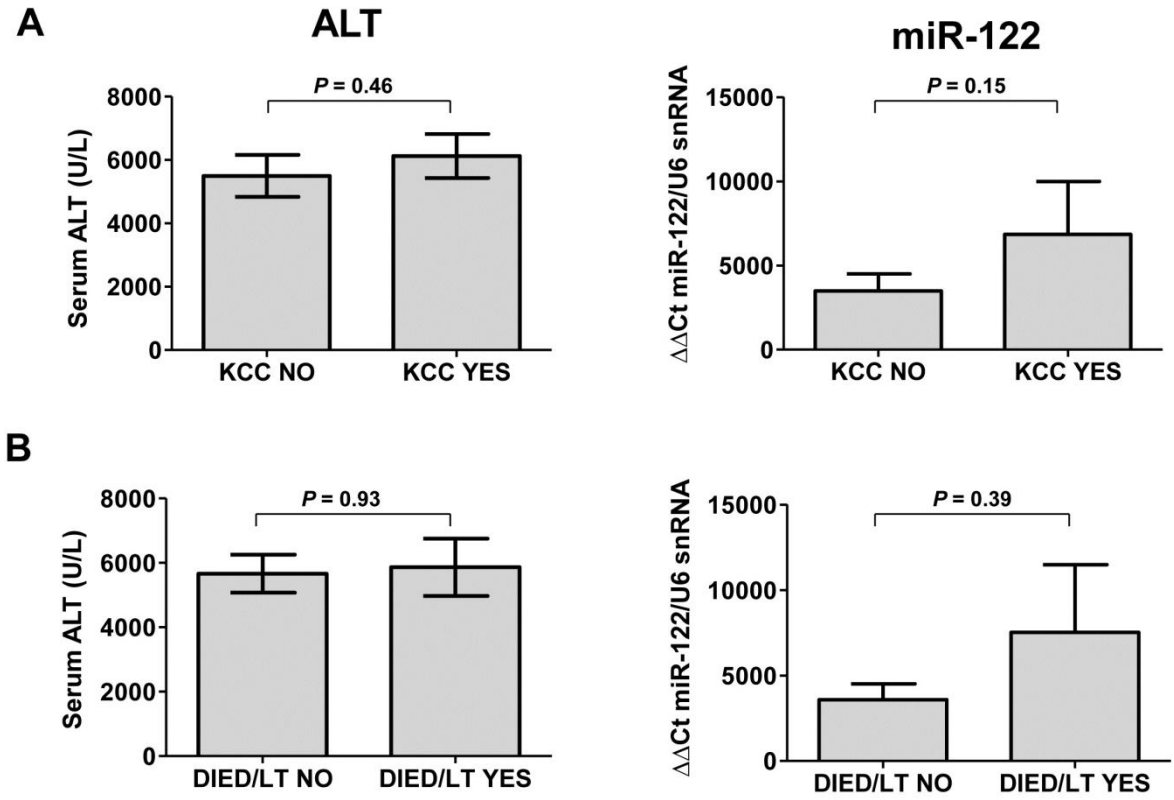

Figure 3.6: Day One miR-122 levels and outcome in APAP ALI patients. The data for each biomarker (ALT - left, miR-122 - right) was categorized into groups based on patient outcome. (A) Patients who satisfied Kings College Hospital Criteria (KCC) for liver transplant during the study. The average day one (mean ± standard error) ALT values (U/L) for patients who meet KCC criteria and those who do not meet KCC are 6123 ± 694 vs 5496 ± 658 respectively ($P = 0.46$). The average day one miR-122 values (ΔΔCt) for patients who meet KCC criteria and those who do not meet KCC are 6848 ± 3144 and 3488 ± 1018 respectively ($P = 0.15$). (B) Day one serum ALT data is not predictive of outcome in patients who have poor outcome (death or liver transplant). The average day one (mean ± standard error) ALT values (U/L) for patients who recovered and those who died/required liver transplantation are 5664 ± 590 and 5863 ± 890 respectively ($P = 0.93$). Average relative miR-122 levels (ΔΔCt) in patients who survived and those who died/required liver transplantation are 3576 ± 928 and 7522 ± 3966 respectively ($P = 0.39$, Mann-Whitney U test). Columns represent means, error bars represent standard error.

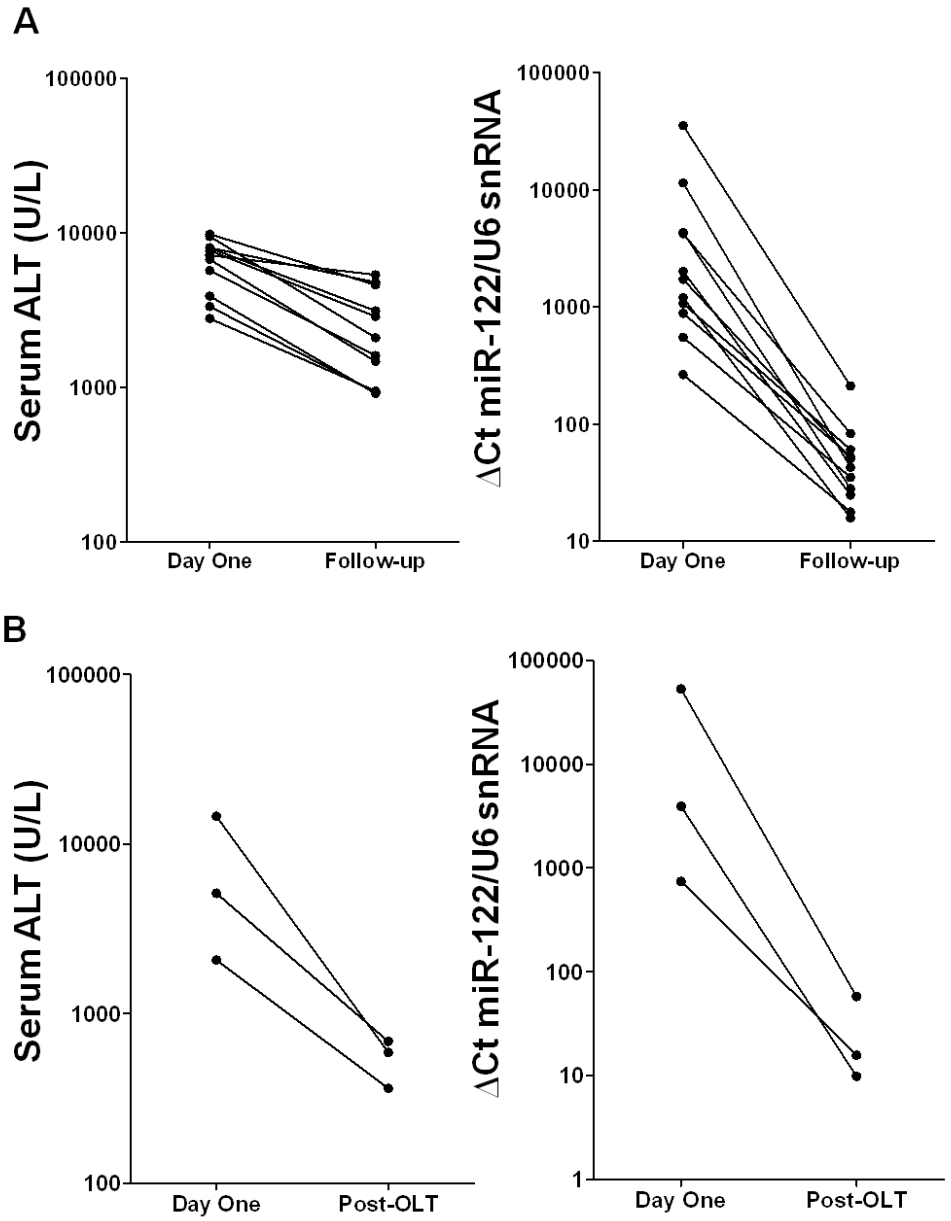

Figure. 3.7: Longitudinal analysis of circulating biomarkers in APAP ALI patients. (A) miR-122 (right) levels return to baseline sooner than serum ALT activity (left). Eleven APAP ALI patients had their blood taken on day one of the study and again between days three and seven. Serum ALT activity and relative miR-122 abundance was measured (as described) to understand the disposition of these biomarkers in a longitudinal fashion. Average (mean ± standard error) serum ALT activity values for day one and follow-up analysis are 6583 ± 719 and 2603 ± 500 U/L respectively. Average miR-122 ΔΔCt values for day one and follow-up analysis are 5734 ± 3115 and 56.8 ± 16.6 respectively (B) miR-122 levels return to baseline after liver transplantation. Three APAP ALI patients who required orthotopic liver transplantation had their blood taken on day one of the study and again after liver transplantation to understand the effects of invasive surgery on the abundance of these circulatory biomarkers. Average (mean ± standard error) serum ALT activity values for day one and post-transplantation analysis are 7256 ± 3766 and 546 ± 95.8 respectively. Average relative miR-122 levels (ΔΔCt) for day one and post-transplantation analysis are 19301 ± 16989 and 27.9 ± 15.2 respectively. Each closed spot represents the individual value for ALT activity or relative miR-122 abundance with a solid line connecting the values from the same patient between day one and follow-up (A) or post transplantation (B) analysis.

3.3.4 miR-122 Levels Return to Baseline Before Serum ALT Activity in APAP ALI Patients Both With and Without Liver Transplantation

We selected 11 APAP-poisoned patients, based on day 1 analysis, with a range of ALTs (2,782-9,760 U/L) and relative miR- 122 concentrations (ΔCt 264-35,364). These patients had blood retaken between days 3 and 7, and the same biomarkers were analyzed. There was an average (mean ± standard error) 62.2% ± 5.1% reduction in serum ALT activity (2,603 ± 500 versus 6,583 ± 719), whereas relative miR-122 abundance exhibited an average 96.9% ± 0.8% reduction (56.8 ± 16.6 versus 5,734 ± 3,115) (figure 3.7A). Furthermore, 3 APAP ALI patients required orthotopic liver transplantation. Blood was taken on day 1 and after transplantation. Serum ALT activity had reduced by 88.3% ± 4%, on average, but still remained above baseline (546 ± 95.8 versus 7,256 ± 3,766), whereas miR-122 levels had reduced by 99.1% ± 0.65%, on average, and returned to baseline (ΔCt 27.9 ± 15.2 versus 19,301 ± 16,989) (figure 3.7B).

3.3.5 Circulating day one miR-218 levels are significantly higher in patients who develop grade 4 encephalopathy patients compared to grade 0 patients.

The APAP-ALI cohort was stratified into groups based on the patient's encephalopathy grade, either at admission or the maximal grade that was reached during the study. We focused on grade 4 patients versus grade 0 patients to determine whether day one circulating miR-122 (figure 3.8A) or miR-218 (figure 3.8B) levels could distinguish patients based on their maximum encephalopathy grade at presentation to hospital (figure 3.8 left panels) or at a later time during the study (figure 3.8 right panels). Only day one miR-218 levels could statistically distinguish patients who developed a maximum grade 4 encephalopathy during the study (P=0.02) (figure 3.8B).

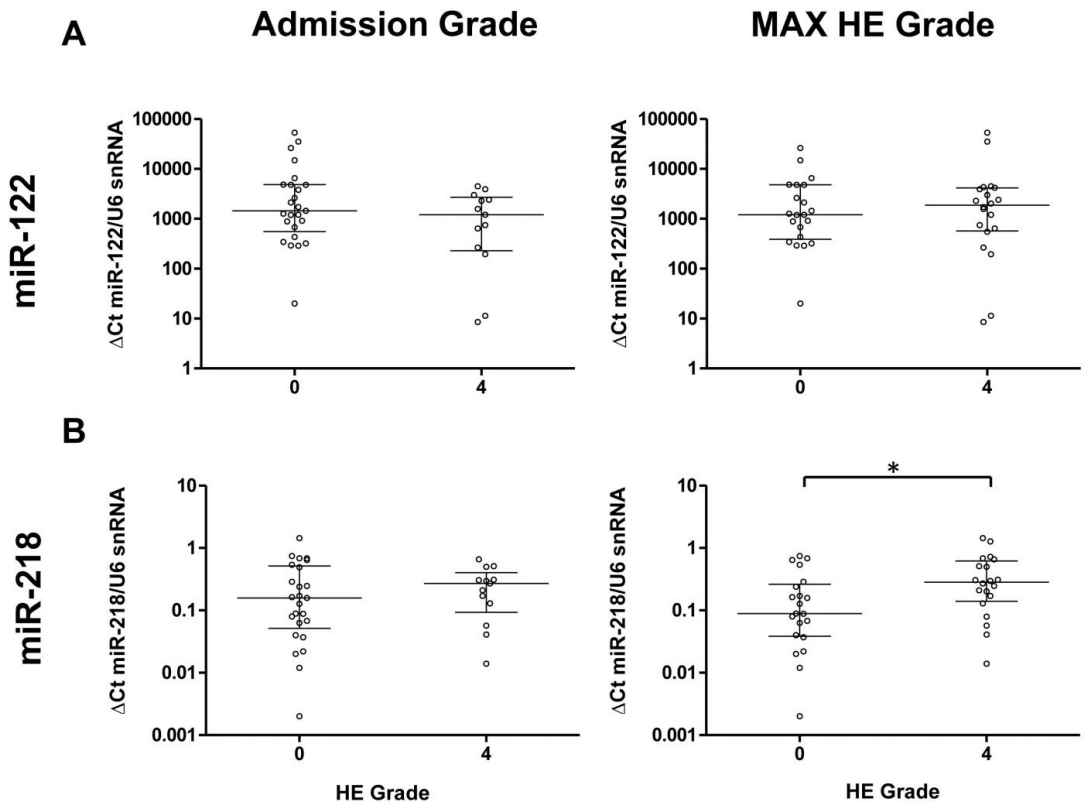

Figure 3.8: Day One miR-218 levels are significantly higher in patients who exhibited a maximum grade 4 encephalopathy during the study compared to grade 0 patients. Panels show individual day one serum miR-122 levels (A) and miR-218 levels (B) from APAP ALI patients categorized into either Grade 0 or Grade 4 encephalopathy. Analyses are based on encephalopathy grade on admission (Admission Grade, left) or the maximum encephalopathy grade reached during the study (MAX HE Grade, right). Each open spot represents an individual relative miRNA level. The bars represent the interquartile range (25^{th}, 75^{th} percentiles) from the median (horizontal line). Median (25^{th}, 75^{th} percentiles) miRNA ΔΔCt values [grade 4 vs grade 0] in admission HE grade categories are 1201 (229, 2700) vs 1453 (554, 4829) and 0.271 (0.093, 0.4040) vs 0.158 (0.052, 0.516) for miR-122 and miR-218 respectively. In maximum HE grade patients, ΔCt values are 1868 (523, 4141) vs 1201 (387, 4796) and 0.284 (0.139, 0.620) vs 0.089 (0.039, 0.263) for miR-122 and miR-218 respectively. Day One miR-218 levels in the grade 4 MAX HE group are statistically different to grade 0 patients ($P = 0.02$, Mann-Whitney U test). No other comparisons are statistically significant.

3.3.6 Biological and bio-analytical variability and reproducibility

To assess the biological variation for miR-122 and the reference species, U6 snRNA, raw Ct values obtained from healthy volunteers and APAP ALI patients were grouped and compared (figure 3.9A; table 3.5). To assess bioanalytical variability, four control and four APAP ALI serum samples were selected at random. Small RNA was extracted and purified from each sample three times before miR-122 was reverse transcribed and measured via qPCR separately. Mean Ct values (± standard deviation) are shown in table 3.6 and figure 3.9B. miR-122 levels are reproduced within 2.86 Ct values, with the greatest %CV = 4.9%.

	Healthy (Ct Range [%CV])	ALI (Ct Range [%CV])
U6 snRNA	**29.1-33.1** (3.5%)	**29.6 -36.3** (4.9%)
miR-122	**26.8 -28.2** (1.4%)	**17.6-27.4** (12.2%)

Table 3.5: Ct value range for U6 snRNA and miR-122 in healthy controls and ALI cohorts

	Mean miR-122 Ct (± SD)
Control 1	**29.7 ± 0.53**
Control 2	**30.3 ± 0.24**
Control 3	**31.1 ± 1.54**
Control 4	**31.5 ± 0.47**
APAP ALI 1	**22.6 ± 0.60**
APAP ALI 2	**21.8 ± 0.33**
APAP ALI 3	**19.5 ± 0.36**
APAP ALI 3	**21.7 ± 0.43**

Table 3.6: miR-122 Ct values in selected control and APAP ALI patients

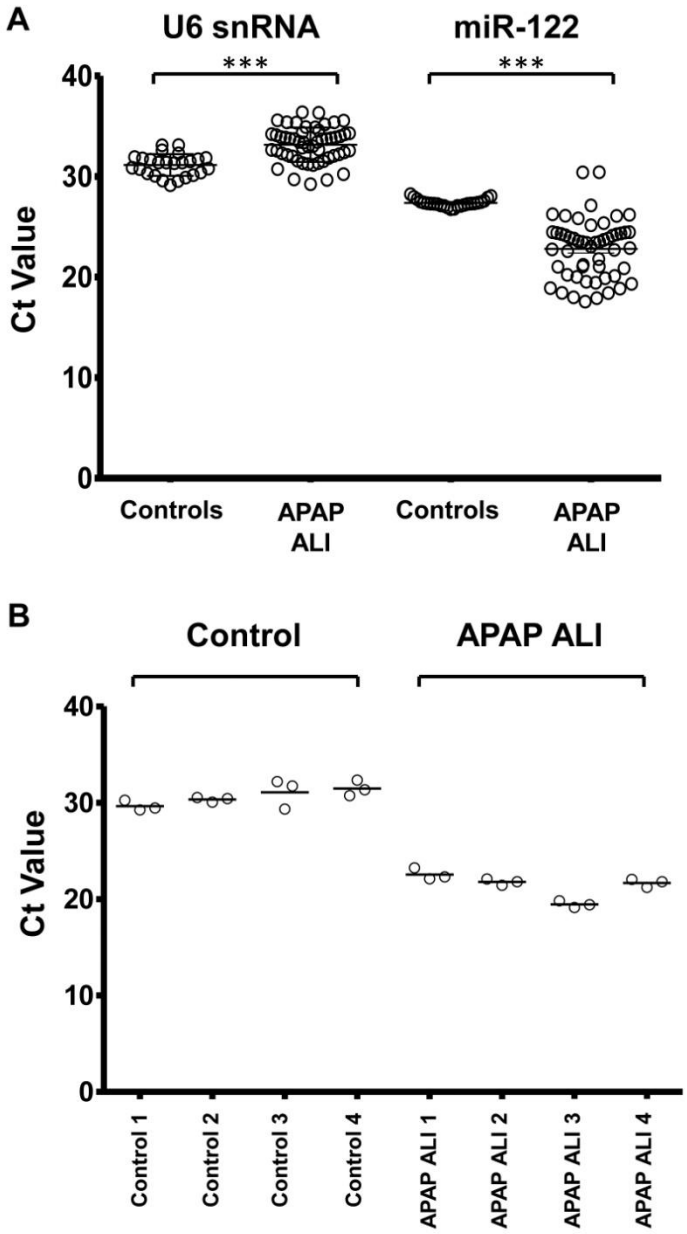

Figure 3.9: Assay variability and reproducibility. The variation in Ct values of U6 snRNA (left) and miR-122 (right) are shown in the control and APAP ALI cohort (A). The bars represent the standard deviation from the mean (horizontal line). The range of U6 snRNA Ct Values (%CV) are 29.1-33.1 (3.5%) and 29.6 -36.3 (4.9%) for controls and APAP ALI patients respectively. The range of miR-122 Ct Values (%CV) are 26.8 -28.2 (1.4%) and 17.6-27.4 (12.2%) for controls and APAP ALI patients respectively. In a separate experiment (B), we selected four healthy control samples at random (left) and four APAP ALI patients with high relative miR-122 levels (right, ΔΔCt 19016-53231) and extracted miRNA (as described) three times to test the reproducibility of miR-122 analysis in our assay. An open circle represents a single miR-122 replicate Ct value around the mean (horizontal line). miR-122 levels are reproduced within 2.86 Ct values, with the greatest %CV = 4.9%.*** $P < 0.001$ (Student t-test).

3.3.7 Endogenous and exogenous normaliser performance

The performance of the reference species, U6 snRNA, was tested by comparing raw Ct values in grouped controls (n=25) and APAP ALI patients (n=53) (figure 3.9A). A modest but statistically significant difference was observed in U6 snRNA Ct values between controls and APAP ALI patients ($P < 0.001$). After correspondence with Qi et al, two alternative reference species were identified (let-7d and miR-374a) (Qi et al, 2012). To test the performance of alternative endogenous circulating reference species, hsa-let-7d-5p and hsa-miR-374a-3p, was measured alongside U6 snRNA in further analysis. Fifteen healthy control serum samples and fifteen ALI serum samples were selected at random. Small RNA was extracted again from these samples as described. An exogenous reference species, *Caenorhabditis elegans*-specific lin-4 was added to compare endogenous versus exogenous normalisation strategies (figure 3.10) A statistically significant difference was observed between groups (healthy controls vs ALI patients) for both hsa-let-7d (figure 3.10A, $P<0.001$) and U6 snRNA (figure 3.10C, table 3.7, $P<0.001$). Although, no statistical difference was observed between groups for miR-374a-3p (figure 3.10B), the %CV was high (7.21%), had low mean abundance (Ct=40.1) and was undetected in 6 samples. The exogenous normaliser provided low variation in both groups (CV < 2%) and did not provide a statistical difference between groups.

	Healthy Ct value range (%CV)	ALI Ct value range (%CV)
hsa-let-7d-5p	**31.2 - 33.3** (1.74%)	**32.5 - 36.7** (2.99%)
has-miR-374a-3p	**36.4 - 46.2** (7.58%)	**37.6 - undetected** (7.21%)
U6 snRNA	**31.0 - 35.2** (3.55%)	**34.9 - 40.9** (4.69%)
cel-lin-4-5p	**34.7 - 36.4** (1.51%)	**34.1 - 36.6** (1.88%)

Table 3.7: Ct values and coefficients of variation (%CV) of different normalisers in healthy and ALI cohorts.

To further test the impact of applying different normalisers to the miRNA data set, the original miR-122 Ct values were normalised using four different reference species measured in the same samples; let-7d (figure 3.11A), miR-374a-3p (figure 3.11B), U6 snRNA (figure 3.11C) and cel-lin-4 (figure 3.11D). The data is shown in table 3.8.

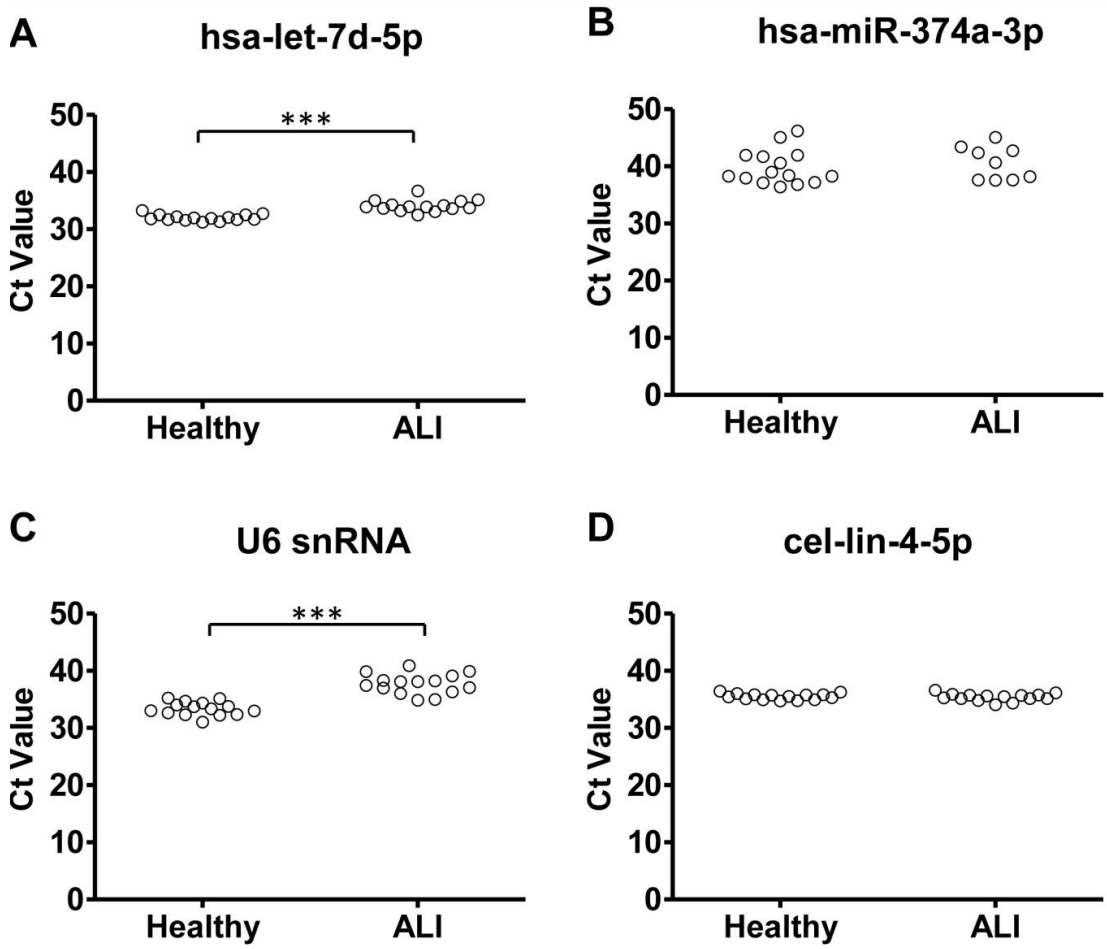

Figure 3.10: Profiling endogenous miRNA normalizers in healthy and ALI patient sera. Individual serum miRNAs were assayed from 15 randomly selected healthy controls and ALI patients from our study using TaqMan human microRNA assays (Applied Biosystems, Foster City, CA). To serve as an exogenous control species, 5 lL of a 10 fM solution of cel-lin-4-5p was added to each denatured serum sample during RNA extraction. The Ct values of hsa-let-7d-5p (A), hsa-miR-374a-3p (B), U6 snRNA (C), and cel-lin-4-5p (D) are shown in panels in grouped healthy controls and ALI patients. Each open spot represents an individual Ct value.

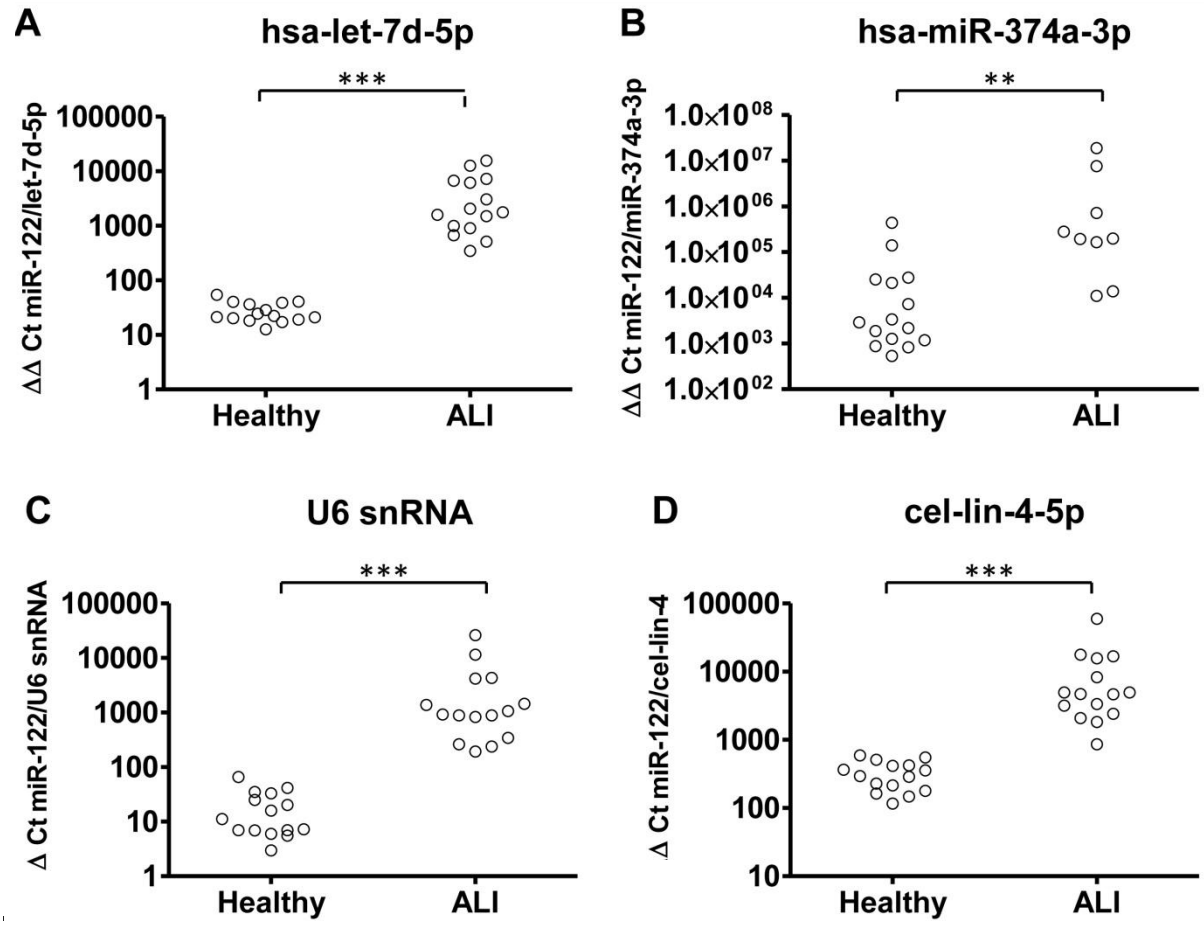

Figure 3.11 Circulating liver-enriched miR-122 is significantly higher in ALI patients regardless of the normalization strategy applied. Panels show the relative dynamic range of circulating miR-122 in grouped controls (n = 15) and ALI patients (n = 15) when normalized with hsa-let-7d-5p (E), hsa-miR-374a-3p (F), U6 snRNA (G), and cel-lin-4-5p (H). The expression of serum miR-122 was significantly higher in ALI patients compared to healthy controls irrespective of the normalization strategy applied. ***P < 0.001, **P < 0.01 (Mann-Whitney U test).

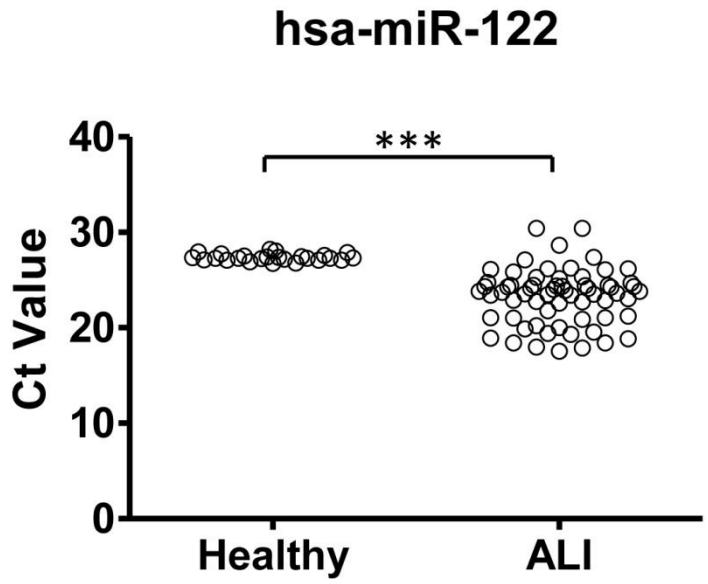

Figure 3.12 miR-122 levels are significantly different between healthy controls and ALI patients when normalisation is removed. Nonnormalized serum miR-122 Ct values show a highly significant difference between healthy controls and ALI patients. The variation in Ct values of serum miR-122 in healthy controls and ALI patients are shown in groups. The median (25th, 75th percentile) miR-122 Ct values are 27.3 (27.1, 27.5) and 23.8 (21.1, 24.6) for controls and ALI patients, respectively. The range of miR-122 Ct values (%CV) are 26.8-28.2 (1.4%) and 17.6-30.4 (12.4%) for controls and ALI patients, respectively. ***P < 0.001 (Mann-Whitney U test).

A statistical significant difference between healthy and ALI was observed between groups regardless of the normaliser used. Similar fold-increases, variations and levels of significance were observed between groups when let-7d, U6 snRNA or lin-4 was used to normalise the data.

Normaliser	Healthy (miR-122 **ΔCt** ± IQR)	ALI (miR-122 **ΔCt** ± IQR)
hsa-let-7d-5p	**22.3** (19.0, 38.9)	**1764** (907, 6724)
hsa-miR-374a-3p	**2906** (1184, 25268)	**199358** (89889, 4155000)
U6 snRNA	**11.2** (6.89, 33.1)	**923** (343, 4211)
cel-lin-4-5p	**294** (178, 420)	**4689** (2410, 15662)

Table 3.8: Relative miR-122 data (ΔCt) in healthy and ALI cohorts when applied with different normalisers

When the normalisation strategy is removed (Ct values alone), miR-122 levels in ALI patients are statistically significant ($P < 0.001$, figure 3.12). The median (25th, 75th percentile) miR-122 Ct values are 27.3 (27.1, 27.5) and 23.8 (21.1, 24.6) for controls and ALI patients, respectively. The ranges of miR-122 Ct values (%CV) were 26.8-28.2 (1.4%) and 17.6-30.4 (12.4%) for controls and ALI patients, respectively.

3.4 DISCUSSION

miR-122 is an abundant, liver-enriched miRNA species. It has been shown recently that circulating levels of miR-122 are significantly increased after ethanol and D-galactosamine treatment in rodents and in patients with viral hepatitis infection (Zhang et al, 2010) suggesting that miR-122 release into the circulation is a hallmark of liver injury developing from multiple aetiologies. Wang and colleagues showed recently that elevations in serum miR-122 and miR-192, another abundant liver miRNA, preceded significant rises in serum ALT activity, with respect to time and dose after APAP treatment in mice (Wang et al, 2009). These findings suggest that circulating miR-122 and miR-192 can be detected before marked cell death occurs in the liver and hold potential to be used as predictive markers of injury. Here, these candidate biomarkers were tested in healthy controls and a cohort of patients who have taken an overdose of APAP and developed injury. These markers were also measured in a control group of patients who had an APAP overdose with no detectable liver injury (prevented through NAC treatment) and a group of patients who had ALI independent of APAP ingestion (see table 3.2). Because of the importance of the specificity of potential biomarkers, the panel of miRNAs was in a cohort of CKD patients to test the performance of liver-specific miRNAs in patients who had an underlying pathological condition in another organ. Kidney injury frequently occurs in parallel with liver injury and has been reported to occur in isolation during APAP poisoning. In testing the reproducibility of the assay, very similar levels of miR-122 and U6 snRNA were observed across three separate extractions from different control and patient samples (figure 3.9B). With regard to

the normalization protocol, it is considered important to include an endogenous internal standard in miRNA measurement of patient samples to control for variations in sample handling and different extraction efficiencies. It was observed that U6 snRNA levels were, on average, slightly lower in APAP ALI patients (figure 3.9A), but this did not result in a significant distortion to all miRNA levels, as shown by consistent levels of miR-1 across all cohorts (figure 3.3A). The highly significant increase in miR-122 levels in APAP ALI patients was evident with normalisation (figure 3.2A) or when normalization was removed (figure 3.12). The choice of particular normalization control for miRNA assays currently varies between laboratories. Adding exogenous nonmammalian miRNAs (e.g., *Caenorhabditis elegans*–specific miR-39 or lin-4) into the extraction procedure is an approach used to correct for technical variation (Mitchell *et al*, 2008, Mahn *et al*, 2011, Arroyo *et al*, 2011). However, an endogenous species may be required to correct for biological variation, especially where samples are isolated from patients. Due to practicalities, biological sampling in the clinic may be subject to greater variation through inconsistent sampling methods, variable sample handling and storage, and necessary transport of samples from care units to laboratories. Using endogenous normalisers can compensate for this variation in a sample by providing a reference reading of an invariable small RNA species. Several different small RNA species have been utilized previously, including U6 snRNA (as in this study), RNU48, and miR-16, (Zhang *et al*, 2010, Wang *et al*, 2011, Wang *et al*, 2010) although one group has recently reported miR-122 analysis in human patients without normalization (Bihrer et al, 2011). More recently, Qi *et al* discovered a panel of invariable circulating miRNA species (hsa-miR-374a, hsa- miR374b and hsa-let-7d) with potentially superior stability and reduced variability between various clinical groups, compared to U6 snRNA (including young and aging healthy volunteers, patients with autoimmune disease and patients with malignant melanoma) (Qi *et al*, 2011). The performance of these novel normalisers was tested in a random selection of 15 healthy controls against 15 ALI serum samples. It was observed that at let-7d has low variation within healthy controls (CV 1.7%) and ALI patients (CV 3.0%) (figure 3.10A). However, in

common with U6 snRNA (figure 3.10C), we observed a modest but statistically significant difference in let-7d levels between healthy controls and ALI patients which supports our notion that many reference molecules may be perturbed in these very sick, acutely injured patients. The serum profile of miR-374a-3p was less promising, with high variation in controls (CV 7.58%) and ALI patients (CV 7.21%) and low mean abundance (Ct = 40.1) (figure 3.10B). Furthermore, miR-374a-3p was not detected in 6 ALI patients. It would be interesting to profile the related miR-374a-5p in light of the findings by Qi and colleagues, however, these assays are currently unavailable on the Taqman platform. As expected, the exogenous species (cel-lin-4) provided the least variation in controls (CV 1.5%) and ALI patients (CV 1.9%) whilst exhibiting no difference between groups (figure 3.10D), however this serves to correct for technical variation and not biological variation. cel-lin-4 is a *c.elegans*-specific miRNA, that plays an important role during development by targeting lin-41 mRNA during embryogenesis (Schulman et al, 2005). Although, lin-4 is described as *c-elegans*-specific, a mammalian variant does exist, miR-125b, which shares function with lin-4 (Schulman et al, 2005). However, the complementarily is not 100% (see figure 3.13), therefore the specificity of the taqman primers can distinguish mammalian and non-mammalian isoforms allowing consistent quantification of lin-4 in clinical samples.

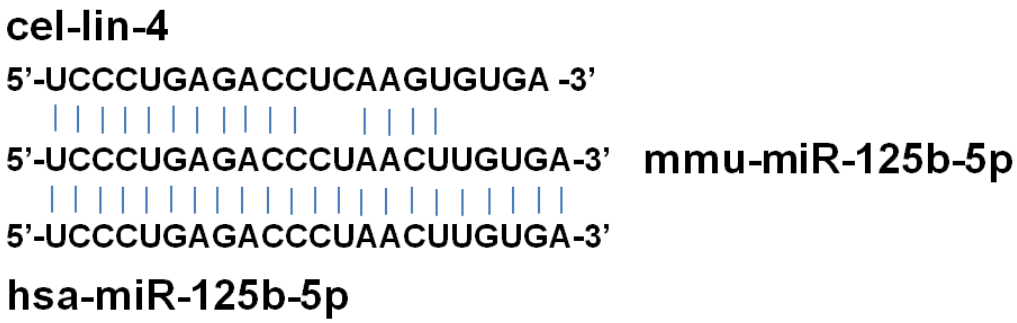

Figure 3.13: Sequence complementarily between c.elegans lin-4 and mammalian miR-125b species.

Nevertheless, regardless of the choice of normaliser applied, it is clear that miR-122 is raised in ALI patients compared to healthy controls (figures 3.11A-D). Moreover, a significant

difference was still observed when we remove normalization, a characteristic of miR-122 that may greatly simplify a future 'point of care' clinical assay (figure 3.12). These data support the use of endogenous normalisers and suggest that let-7d-5p in particular may add value as a reference species alongside or instead of U6 snRNA, in certain circulating miRNA studies. This work will now allow the field to test reference molecules in prospective studies and may ultimately provide a more robust and accurate analysis strategy for circulatory miRNA studies.

In the clinical study, the most abundant miRNA in every cohort analyzed was miR-122. This is not surprising, because miR-122 is highly abundant in the liver, comprising approximately 70% of the entire miRNA hepatic complement (Lagos-Quintana *et al*, 2002). In the panel, the next most abundant circulating miRNA was miR-192 (figure 3.2B), which is also enriched in the liver, but is also expressed in the kidney and in the gastrointestinal tract (Liang *et al*, 2007). The levels of miR-1 (expressed in muscle and cardiac tissues) were, on average, the least abundant. Levels of miR-218, which is enriched in brain (Wang et al, 2009) was more abundant than miR-1, but not as abundant as the liver enriched miRNAs in serum and plasma. Levels of miR-122 and miR-192 (liver-enriched miRNAs) were significantly higher in APAP-poisoned patients as were serum ALT activities (figures 3.2A-B). However, heart enriched miR-1 levels were not different from healthy controls (figure 3.3A). APAP ingestion alone is not sufficient to release high levels of hepatic miRNAs into the circulation, as shown in 6 patients who had taken an APAP overdose, but did not develop liver injury (figure 3.2A,B). MiR-122 was significantly higher in non-APAP ALI patients, compared to healthy controls. This confirms that the levels of miR-122, but not miR-192, are significantly higher in the circulation after multiple forms of liver injury, including hepatitis and malignancy (see table 3.2), suggesting that miR- 122 holds superior diagnostic potential over miR-192. Furthermore, miR-218, the brain-enriched miRNA, exhibited a small, but significant, elevation in the circulation of APAP ALI patients (figure 3.2D). For comparison, miR-218 levels in non-APAP ALI patients did not differ from healthy controls. Liver-enriched miRNAs were slightly higher in CKD patients (figure 3.2),

compared to healthy controls, but ALT levels did not differ (figure 3.1). ALT tissue expression is mainly hepatic, but isoforms are present in other human tissues (e.g., muscle) (Glinghammar *et al* 2009, Lindblom *et al* 2007). Increased serum ALT activity has been noted in individuals after extreme-endurance exercise regimens highlighting potential contributing factors for false positives (Skenderi *et al*, 2006, Koutedakis *et al*, 1993). Zhang *et al*. have shown recently that serum ALTs are higher in patients with polymyositis and after exercise-induced muscle damage without a concomitant rise in miR-122, (Zhang *et al*, 2010) further highlighting the possible additional benefit of miR-122 in diagnosing liver injury. Therefore, it will be necessary, in further work, to define changes in circulating miRNA levels that are of actual, rather than merely of statistical significance, analogous to the use of multiples of ULN in ALT measurements.

Four subjects from the ALI cohort presented with miR-122 levels in the normal range (figure 3.2A) despite having ALI (ALT > 3 X ULN; table 3.4). The presentation clinical chemistry data for these patients indicated, unexpectedly, that these patients were extremely ill. All patients had coagulopathy (INR >1.3), all had raised serum creatinine levels, and three patients presented with a HE grade > 2 (fourth patient - data not available). These data, taken together, suggest that these patients presented to hospital very late after drug ingestion. In fact, one subject in this group died on day 2 of the study. It is possible that the miR-122 signal has been missed in these patients due to the relatively short half-life of miR-122 in the blood. This may explain the unexpectedly low levels of miR-122 in this small group of extremely ill patients. This further highlights the urgent need to understand the kinetics of miR-122 in the blood of patients during both early and late phases of DILI.

It is shown, for the first time, that miR-122 levels are significantly correlated with peak serum ALT activity in a heterogeneous cohort of APAP-poisoned patients (figure 3.4A), suggesting that miR-122 can inform on human liver injury. The dynamic range of relative miR-122 levels among all the samples analyzed was, in fact, higher than that of ALT (ΔCt 0.154 53,231 versus 1.144-18,040 U/L). This could provide a key advantage, if it is possible to eliminate false positives and false negatives. Nevertheless, miR-122 did not correlate with

prothrombin time or total serum bilirubin levels, which are clinical markers of ALF (figure 3.5A,B). These disparities may be explained by the circulatory kinetics of these biomarkers during the cascade of toxicity (i.e., it is possible that miR-122 release is an earlier event than the cessation of hepatic-clotting factor production or heme-metabolism pertubations during ALF). It is also important to consider the circulatory half-lives of these biomarkers during toxicity. ALT has been reported to have a half-life of 48 ± 17 hours in patients with hepatitis-associated liver injury (Saheki *et al* 1990). Indeed, prothrombin time correlates with ALT activity in these patients (data not shown). The relatively long circulatory half-life of ALT may provide more of a window for correlation with both early markers (e.g., miR-122) and markers that present later (e.g., prothrombin time). To date, the circulatory half-life of miR-122 has not been ascertained in humans. Although the intracellular half-life of miR-122 has been estimated to be >24 hours (Gatfield *et al*, 2009), the data suggests that the circulatory half life of miR-122 is considerably less than that of ALT as serum levels return to baseline sooner than ALT in APAP-poisoned patients (figure 3.7A). miR-122 did not correlate with serum creatinine levels, a marker of kidney function (figure 3.5C). This is not surprising, because miR-122 is not abundantly expressed in kidney tissues (Liang *et al*, 2007). The muscle-enriched miRNA, miR-1, did not correlate with any of the markers in this study, suggesting that APAP toxicity did not cause a nonspecific elevation in circulating miRNA abundance (figure 3.4C). The brain-enriched miRNA, miR-218, correlated with serum ALT activity (figure 3.4D), although this was over a small dynamic range. This may be explained by the fact that APAP-induced ALF is associated with encephalopathy. We found that day 1 miR-218 levels were significantly higher in patients who reached a maximal encephalopathy grade 4 during the study, compared to grade 0 patients (Fig. 3.8B). It is also possible that miR-218 is present in the liver and other tissues at low levels, and that an increase in the circulation may be the result of APAP-induced damage in tissues, including the brain.

Current biomarkers of liver injury are not predictive of outcome. Here, the predictive value of miR-122 was tested. Serum miRNA levels were measured in samples obtained from

patients on day 1 of their admittance into the study against outcome criteria after day 30: poor outcome (i.e., non-survival or required transplantation) versus recovery and whether patients met KCC for transplantation. Day 1 miR-122 levels were not predictive of any outcome in this small sample set. However, the trend suggested that miR-122 was more predictive than ALT (figure 3.6), and it would be valuable to test this possibility in further studies. In summary, we show, for the first time, that liver-enriched miR-122 levels are raised and correlate with an existing biomarker of DILI in a heterogeneous group of ALI patients. Also, it is shown that circulating miR-122 returns to baseline before serum ALT, indicating that miR-122 has a shorter circulatory half-life. This data suggests that circulating miRNAs can provide a novel addition to the existing catalogue of biomarkers to detect and diagnose human liver injury. Future challenges will be to define the mechanisms of release of cellular miRNAs, establish whether their release has a functional adaptive role in response to injury, and to determine whether miR-122 can provide clinical prognostic value over current biomarkers of DILI in future, prospective, clinical trials and real-life clinical situations with other etiologies of liver disease.

CHAPTER FOUR

CIRCULATING miR-122 AS AN EARLY CLINICAL BIOMARKER OF PARACETAMOL-INDUCED LIVER INJURY

4.1 INTRODUCTION

Overdose of APAP is a common reason to attend hospital. Statistical evidence collected for the financial year 2010-2011 found that there were approximately 38,000 emergency room visits in England (NHS Information Centre - Hospital Episode Statistics for England. Inpatient statistics). Similarly, in the United States, there are over 100,000 calls to poison control centres which are attributed to an overdose of APAP (Lee, 2004). Early identification of APAP overdose and extent of APAP exposure is critical in the early management of patients in the clinic. If the appropriate therapy is not administered at the appropriate time, patients risk developing hepatotoxicity which may lead to life-threatening acute liver failure. If the patient presents within 4 hours of APAP ingestion, then activated charcoal can be administered orally to sequester APAP and reduce systemic absorption. However, many patients present after this time, when much of the dose had already been absorbed. The current clinical triage strategy involves measuring plasma APAP levels and assessing risk through use of the Rumack-Matthew nomogram which determines risk based on a circulating plasma half-life of 4 hours. However, an accurate time of ingestion is also required to determine risk which is often unreliable. If risk cannot be ruled out, then the patient will receive antidotal therapy through an intravenous NAC regimen. The full NAC regimen takes at least 20 hours to complete which not only causes patient discomfort but results in substantial hospital bed occupancy (47,000 bed days per annum in England). Furthermore, NAC therapy itself is associated with several ADRs encompassing minor skin reactions to serious systemic anaphylactoid responses. In total, it is estimated that up to 45% of patients suffer an ADR who receive NAC therapy (Kerr *et al*, 2005).

Clinical uncertainty exists in the utilisation of the Rumack-Matthew nomogram, which is prone to identifying false-positive and false-negative risk in APAP overdosed patients. A personalised biological approach is sought that identifies risk in patients and could supersede the current 'one-size-fits-all' strategy. The current catalogue of clinical biomarkers that detect liver injury include the serum aminotransferase enzymes (ALT, AST), bilirubin and

parameters of liver function such as prothrombin time. However, these markers rise relatively late after APAP administration when hepatocellular damage has already occurred. Although serum ALT activity is the gold standard marker for the detection of liver injury, the enzyme typically rises between 12-36 hours after APAP ingestion. This latent period prevents the use of ALT being used as an early predictive marker of injury and therefore cannot be used to assess risk.

Clearly, the identification and development of novel markers that rise at the earliest possible time after an APAP overdose is required in the clinic. Furthermore, novel markers are required that have enhanced liver specificity and reflect accurately the pathophysiological status of the liver. Such markers would provide the physician with a biological readout with which risk of hepatotoxicity could be assessed confidently soon after APAP ingestion. If high-risk patients could be identified in a personalised manner, this may allow safe discharge of low-risk patients without the need of administering time-consuming, unnecessary antidotal therapy. This type of approach would likely reduce both rate of NAC-related ADRs and reduce the clinical and financial burden of patient care.

Recently, miR-122 has been found to be a sensitive blood-based biomarker of APAP-induced liver injury in a mouse model (Wang et al, 2009). In this study, it was found that rises in miR-122 could be detected earlier than rises in ALT. Furthermore, miR-122 was raised at relatively low doses where ALT was not elevated suggesting that miR-122 provides substantial sensitivity for APAP-induced liver injury. Alongside these potential benefits, miR-122 also exhibits remarkable liver-enrichment in man (Liang et al, 2007). The clinical promise of this high-level enrichment was demonstrated by Zhang and colleagues who found that serum ALT activity provided false-positive readings for liver injury in patients with muscle-damage (Zhang et al, 2010).

In this chapter, it is hypothesised that miR-122 can serve as an early informative marker of liver injury in a cohort of APAP-overdosed patients who have presented early after APAP ingestion. Due to enhanced liver specificity and potentially earlier time of release, circulating

miR-122 holds promise to identify patients with ALI at presentation to the hospital emergency department.

4.2 PATIENTS AND METHODS

4.2.1 Patients

Patients (total N=129) were recruited from the Royal Infirmary of Edinburgh, UK (N=107) and the Royal Victoria Infirmary, Newcastle-Upon-Tyne, UK (N=22). Full informed consent was obtained; the study was approved by the local research ethics committee. Inclusion criteria were: adult with a clear history of excess paracetamol ingestion and a timed blood paracetamol concentration that was judged by the treating physician to necessitate hospital admission for intravenous NAC therapy, as per UK guidelines at the time of study (www.toxbase.org). Exclusion criteria were: patients detained under the Mental Health Act; patients with known permanent cognitive impairment; patients with a life-threatening illness; unreliable history of paracetamol overdose; patients who take anticoagulants therapeutically or have taken an overdose of anticoagulants; patients who, in the opinion of the responsible clinician/nurse, were unlikely to complete the full course of NAC. All patients completed the full course of NAC treatment. 97 patients were participants in the Scottish and Newcastle Antiemetic Pretreatment for Paracetamol Poisoning study (SNAP – EudraCT number 2009-017800-10), a randomised clinical trial designed to assess if ondansetron is effective in reducing nausea and vomiting in patients poisoned with paracetamol treated with NAC. As a pre-defined part of the SNAP trial protocol, blood samples were collected for biomarker evaluation.

4.2.2 Sample collection

In all 129 study participants, blood samples were collected at the time of first presentation to hospital, before NAC (and for SNAP study participants, ondansetron or placebo) therapy had commenced. Plasma was separated and the samples were stored at -80^{0}C until analysis. For all study participants, demographic data and blood results were recorded. ALI was defined as peak serum ALT activity greater than 3x the upper limit of the normal range (>150 IU/L), the

UK indication for continuing acetylcysteine therapy after completion of the initial regimen (www.toxbase.org) at the time of study.

4.2.3 Clinical chemistry measurements

Plasma or serum was obtained via pulse centrifugation from blood that had been allowed to clot overnight. Serum ALT levels, total bilirubin, serum creatinine, serum alkaline phophatase (ALP), serum gamma glutamyl-transpeptidase (GGT) and international normalised ratio (INR) determintion were all determined in the respective hospital laboratory after blood sampling, according to the standard hospital laboratory practice.

4.2.4 miRNA extraction

miRNA was extracted using an miRNeasy kit (Qiagen, Venlo, Netherlands), following the manufacturer's instructions, with minor modifications. Briefly, 40 µL of biofluid was made up to 200 µL with nuclease-free water, then combined with 700 µL of QIAzol. The sample was mixed and left for 5 minutes before the addition of 140 µL of chloroform. Samples were then mixed vigorously for 15 seconds and centrifuged at 12,000 g for 15 minutes at 4 °C. Equal volumes (350 µL) of the upper aqueous phase and 70% ethanol were mixed in a fresh microtube before adding the total volume to an miRNeasy minispin column. The column was centrifuged at 8,000g for 15 seconds at room temperature. The flow-through, containing the small RNA fraction, including the miRNA complement, was mixed with 450 µL of 100% ethanol. The elute was then purified using a MinElute kit (Qiagen, Venlo, Netherlands).

4.2.5 miRNA purification

The small RNA elution mixture was applied to a MinElute column, 700 µL at a time. The immobilized RNA was then washed with various buffers before a final 80 % ethanol wash. The

column was then dried by centrifugation. The small RNA fraction was eluted in 14 µL of nuclease-free water and stored at -80 °C.

4.2.6 Quantitative Polymerase Chain Reaction Analysis.

miRNA levels were measured using Taqman-based quantitative polymerase chain reaction (qPCR). The small RNA elute was reverse transcribed using specific stem-loop reverse-transcription RT primers (Applied Biosystems, Foster City, CA) for each miRNA species, following the manufacturer's instructions. Next, 2 µL of RNA was used to produce the complementary DNA (cDNA) template in a total volume of 15 µL. Then, 1.33 µL of cDNA was used in the PCR mixture with specific stem-loop PCR primers (Applied Biosystems, Foster City, CA) in a total volume of 20 µL. Levels of miRNA were measured by the fluorescent signal produced from the Taqman probes on an ABI Prism 7000 (Applied Biosystems). miRNA levels were normalised to levels of hsa-let-7d, an invariable blood based miRNA species for biological standardisation, as described elsewhere (Qi et al, 2011).

4.2.7 Plasma HMGB1 measurement

NB: This analysis was performed by Dr Dan Antoine in collaborative work within the CDSS. Total HMGB1 was measured by ELISA according to the manufacturer's instructions. A chicken anti-HMGB1 antibody was used as a catcher antibody (1 µg/well). Linear regression was used to determine the concentration of HMGB1 in each sample by comparison to known standards. A fluorescent signal was produced by 3,3',5,5'-tetramethyl-benzidine turnover using a peroxidise linked anti-HMGB1 antibody.

4.2.8 Plasma keratin 18 (K-18) measurement

NB: This analysis was performed by Dr Dan Antoine in collaborative work within the CDSS. K18 (apoptosis) and K18 (necrosis) were determined using the M30 (apoptosis) and M65 (total: apoptosis and necrosis) ELISAs respectively, according to the manufacturer's guidelines (Peviva AB, Bromma, Sweden). Linear regression was used to determine the concentration of CK in both assays by comparison to known standards. A fluorescent signal was produced by 3,3',5,5'-tetramethyl-benzidine turnover using a peroxidise linked anti-K-18 antibody. The full-length K-18 (necrosis) data was obtained by subtracting the apoptosis K-18

assay data (M30 ELISA) from the total K-18 data (M65 ELISA) as performed previously (Antoine et al, 2012).

4.2.9 Glutamate dehydrogenase (GLDH) measurement

NB: This analysis was performed by Dan Antoine in collaborative work within the CDSS. GLDH levels were measured photo-optically using the DGKC kit as previously (Randox Laboratories, Kearneysville, WV, USA) (Harrill et al, 2012). A decrease in absorbance was measured in each sample caused by the oxidation of nicotinamide adenine dinucleotide at 340 nm, as per the manufacturer's protocol.

4.2. Statistical analysis

Data are presented as median and range or inter-quartile range. Each data set was analysed for non-normality using a Shapiro-Wilk test. For two non-normal data sets, comparisons were made using the Mann-Whitney U test. The Kruskall-Wallis test was used to determine significance between more than two non-normal sample groups. All calculations were performed using StatsDirect statistical software. For correlative analysis, Pearson's Correlation test, R^2 and Receiver Operator Characteristic (ROC) curve analysis was carried out using the GraphPad PRISM software. Results were considered significant when $p<0.05$.

4.3 RESULTS

4.3.1 Plasma miR-122 at hospital presentation correlated with subsequent liver injury

In the cohort, there were 51 men (40 %) and 78 women (60 %) with a median age of 34 years (Table 1). Fifty four percent of this cohort had at least one risk factor for APAP-induced ALI. The median time (interquartile range, IQR) from APAP ingestion to first blood sample collection was 8.0 h (6.0-15.0 h). The median admittance blood paracetamol concentration was 120.0 mg/L (IQR, 63.0-179.0). From timed plasma paracetamol concentrations, the Rumack-Matthew nomogram indicated that all 129 patients required NAC therapy. The median (IQR) clinical chemistry values at first hospital presentation were: serum creatinine: 67.0 µmol/L (60.0-81.5), bilirubin: 5.0µmol/L (7.0-11.0), serum ALT activity: 22.0IU/L (16.0-57.5), serum ALP activity: 75.0IU/L (60.5-94.5), serum GGT activity: 24.0IU/L (15.0-46.0) and an INR of 1.0 (0.9-1.1). The number of patients presenting with a serum ALT activity less than 3xULN was 98 (75%) with 32 (25%) patients more than 3xULN. The number of patients presenting with an international normalised ratio < 1.5 was 107 (83%) with 19 (17%) presenting with an INR > 1.5. No patients required liver transplantation or developed encephalopathy.

Plasma miR-122 levels were measured in plasma obtained at the point of hospital admission, before NAC treatment had begun but when a time blood paracetamol concentration had indicated the requirement for NAC therapy. A Pearson correlation analysis was performed on values obtained from miR-122 against the peak serum ALT activity during patient hospitalisation. The presentation serum miR-122, significantly correlated with peak ALT activity values (P <0.0001, Fig 4.1A). The correlation coefficients (R^2) was 0.14, and the Pearson R values (95% CI) was 0.37 (0.21-0.52).

Then, a Pearson correlation analysis was performed from miR-122 values at first presentation against the peak INR value reached during patient hospitalization. The presentation values for

plasma miR-122 significantly correlated with peak INR values ($P < 0.0001$, figures 4.1B). The correlation coefficient (R^2) was 0.24 and the Pearson R value (95% CI) was 0.49 (0.34-0.61).

Number	129
Sex (Male : Female)	51:78
Age (Years)	34 (24.5 – 47.0)
Risk Factors (% of cohort)	54
Amount of APAP ingested (g)	18.0 (13.0 – 25.0)
Time from ingestion to first blood sample (Hr)	8.0 (6.0 – 15.0)
Admission paracetamol concentration (mg/L)	120.0 (63.0 – 179.0)
Admission serum creatinine (µmol/L)	67.0 (60.0 – 81.5)
Admission bilirubin (µmol/L)	5.0 (7.0 – 11.0)
Admission ALT activity (IU/L)	22.0 (16.0 – 57.5)
Admission ALP activity (IU/L)	75.0 (60.5 – 94.5)
Admission GGT activity (IU/L)	24.0 (15.0 – 46.0)
Admission INR	1.0 (0.9 – 1.1)
Number with Admission ALT < ULN	94
Number with peak ALT > 3x ULN	32
Number with peak ALT > 1000 U/L	20
Number with admission INR < 1.5	107
Number with peak INR > 1.5	19

Table 4.1: Clinical parameters of the patient cohort. Various clinical parameters of the patient cohort who present early after APAP ingestion. Abbreviations: ALT, alanine aminotransferase; ALP, alkaline phosphatise; GGT, gamma glutamyl transpeptidase; INR, International Normalised Ratio; ULN, upper limit of normal.

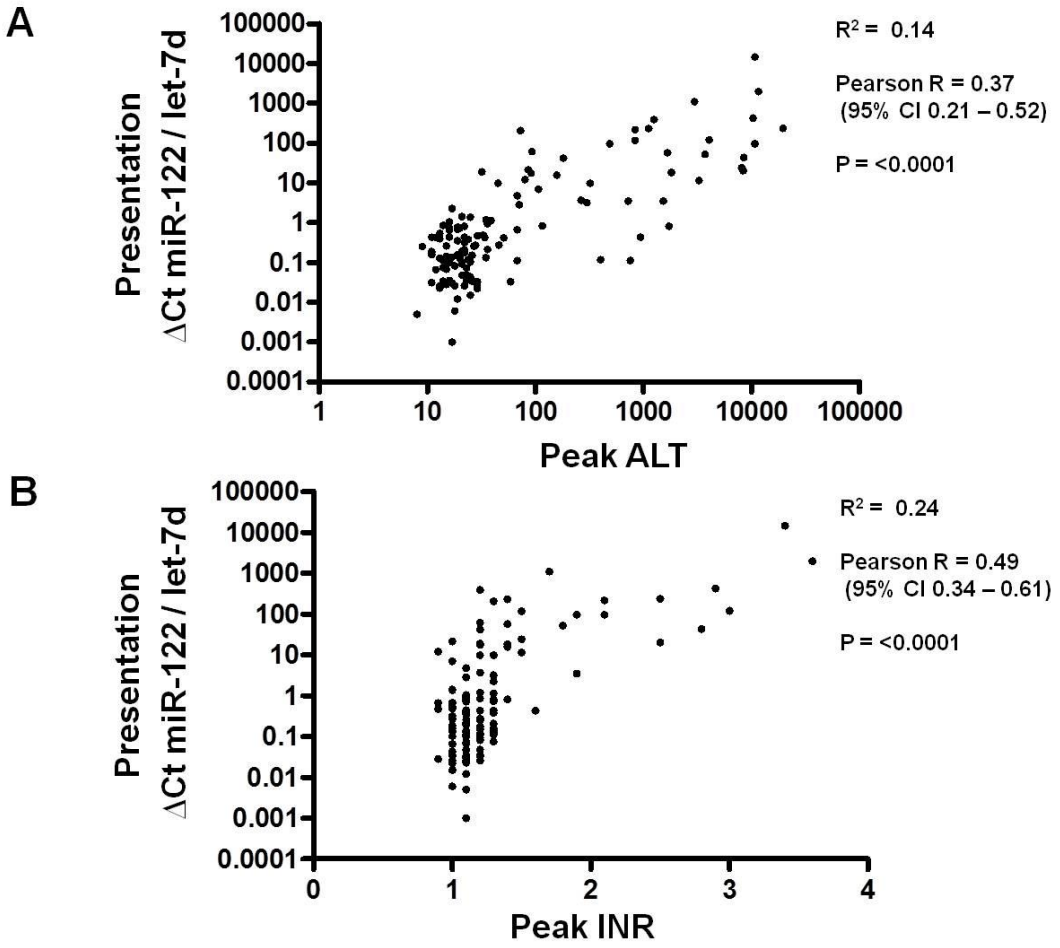

Figure 4.1 : Plasma miR-122 levels at hospital admission significantly correlate with peak serum ALT activity and peak INR values. miR-122 levels were measured in patients who presented early (median time = 8 hours) after APAP overdose (n=129) and correlated against the peak ALT value (A) or peak INR value (B) from each respective patient during their hospital admission. Each closed circle represents values from individual patients. Presentation miR-122 levels significantly correlated with peak ALT (P<0.0001) and peak INR values (P<0.0001) (Pearson correlation test). The R^2 values (Pearson R with 95% CI) were 0.14 (0.37, from 0.21 to 0.52) and 0.24 (0.49, from 0.34 to 0.61).

4.3.2 In patients with a normal ALT activity on first hospital presentation, plasma miR-122, are higher in those who develop ALI

From the cohort of 129 paracetamol overdose patients, the cohort was stratified to focus on the 94 patients who presented with a normal serum ALT activity (<50U/L) to determine if miR-122 is more sensitive than ALT at detecting ALI. Of these patients, 11 (12%) developed ALI (> 3 x ULN serum ALT activity; median peak ALT (IQR) 403 (266, 1532) during their hospitalization whereas 83 (88%) patients did not develop ALI at any time during the study (serum ALT activity remained < 3xULN). Plasma miR-122 levels were significantly higher at presentation in patients who developed ALI compared to those that did not (P<0.0001) (figure 4.2A; table 4.2). In contrast, presentation ALT levels did not identify patients who developed ALI (*P*=0.27, figure 4.3B; table 4.2).

	ALT < 3 x ULN	ALT > 3 x ULN
miR-122 (median ΔCt + IQR)	**0.16** (0.05-0.43)	**3.48** (0.81-15.56)
ALT (median U/L + IQR)	**19** (14, 25)	**21** (12, 30)

Table 4.2: Admission relative miR-122 levels (ΔCt) and serum ALT activity in patients who do not develop liver injury and patients who subsequently develop liver injury

A ROC curve analysis was performed on these groups to provide a robust test of sensitivity and specificity for presentation plasma miR-122 (figure 4.2 C) and presentation serum ALT activity (figure 4.2 D). Plasma miR-122 performed with high AUC values (and sensitivity at 90% specificity); 0.87 (0.72) suggesting that miR-122 could separate patients with and without ALI at a time when serum ALT activity was normal (P<0.0001). In accordance with the data, the AUC values (and sensitivity at 90% specificity) for serum ALT were lower; 0.6 (0.18) confirming that presentation serum ALT activity did not identify patients who develop injury (P=0.26).

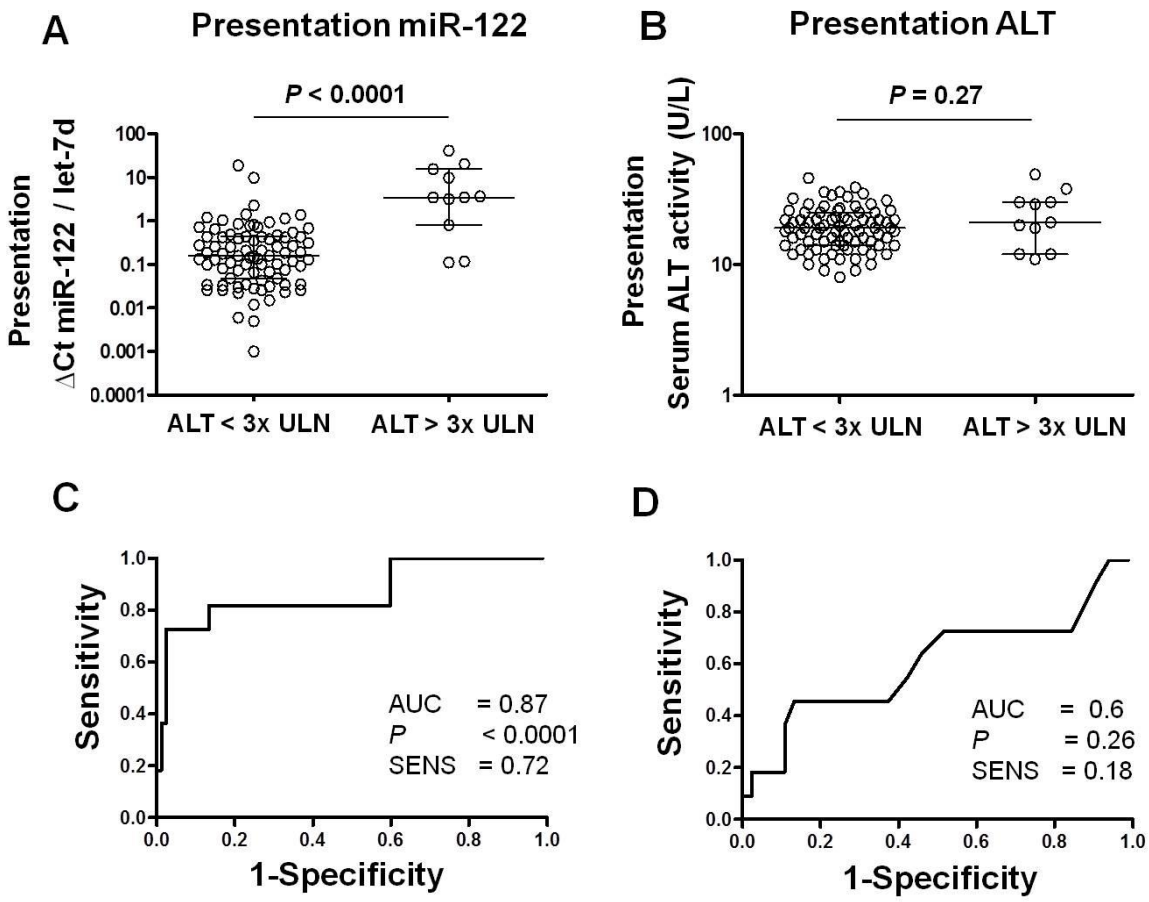

Figure 4.2 : Plasma miR-122 levels at hospital admission are significantly higher in patients who develop ALI. Presentation plasma miR-122 levels were measured in patients who presented with a normal ALT range (<50 U/L) (n=94). The patients were grouped into those who developed ALI (ALT > 3x ULN) during their hospitalisation (n=11) and those who did not develop ALI (ALT < 3x ULN) (n=83). The panels show the presentation plasma miR-122 levels (A) and presentation serum ALT activity (B) in each group of patients. Each open circle represents the value measured from individual patients. The horizontal line represents the median between the whiskers (IQR). ROC curves were generated from the grouped data. Panels show plasma miR-122 (C) and serum ALT activity (D). The AUCs (and sensitivity at 90% specificity) were 0.87 (0.72) and 0.6 (0.18) for plasma miR-122 and serum ALT respectively.

4.3.3 In patients with a normal ALT activity on first hospital presentation, plasma miR-122 levels are higher in patients who develop APAP-induced coagulopathy (INR>1.3)

From the cohort of 129 paracetamol overdose patients, the cohort was stratified to focus on the 94 patients who presented with a normal serum ALT activity (<50U/L) to determine if miR-122 is more sensitive than ALT. Of these patients, 6 (6%) developed coagulopathy (INR > 1.3) median peak INR (IQR) 1.5 (1.4, 2.0) during their hospitalization whereas 88 (94%) patients did not develop coagulopathy at any time during the study (serum ALT activity remained < 3xULN). Plasma miR-122 levels were significantly higher in patients who developed coagulopathy compared to those that did not (P = 0.0038) (figure 4.3A; table 4.3). In contrast, presentation ALT levels did not identify patients who developed coagulopathy (P = 0.26, figure 4.3B, table 4.3).

	INR ≤ 1.3	INR > 1.3
miR-122 (median ΔCt + IQR)	**0.17** (0.05, 0.53)	**3.48** (0.62, 17.94)
ALT (median U/L + IQR)	**19** (14, 25)	**21** (17.3, 40.8)

Table 4.3: Admission relative miR-122 levels (ΔCt) and serum ALT activity in patients who do not develop coagulopathy and patients who subsequently develop coagulopathy

A ROC curve analysis was performed on these groups to provide a robust test of sensitivity and specificity for presentation plasma miR-122 (figure 4.3 C) and presentation serum ALT activity (figure 4.3 D). Plasma miR-122 performed with high AUC values (and sensitivity at 90% specificity); 0.89 (0.6) suggesting that miR-122 could identify patients who develop coagulopathy at a time when serum ALT activity was normal (P = 0.0038). In accordance with the data, the AUC values (and sensitivity at 90% specificity) for serum ALT were lower; 0.63 (0.33) confirming that presentation serum ALT activity did not identify patients who develop injury (P=0.27).

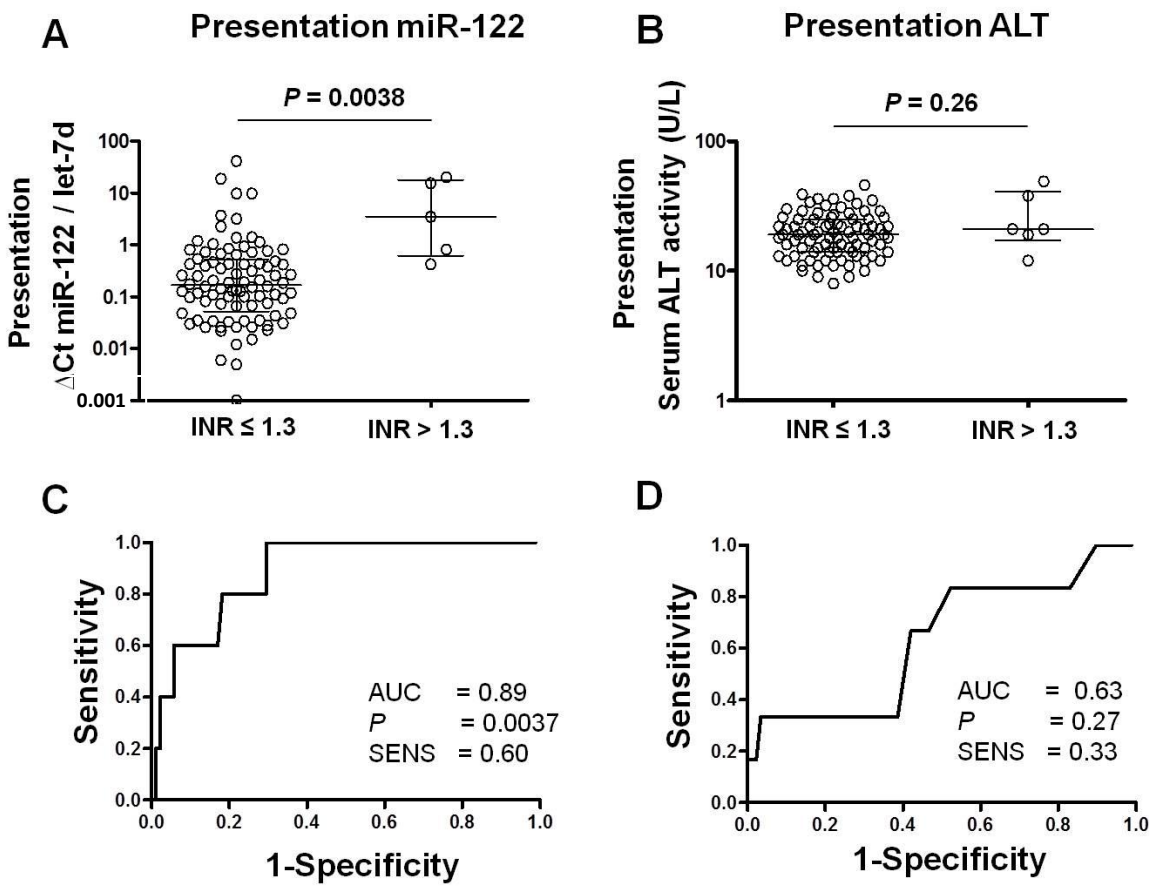

Figure 4.3: Plasma miR-122 levels at hospital admission are significantly higher in patients who develop APAP-induced coagulopathy. Presentation plasma miR-122 levels were measured in patients who presented with a normal ALT range (<50 U/L) (n=94). The patients were grouped into those who developed coagulaopathy (INR > 1.3) during their hospitalisation (n=6) and those who did not develop ALI (INR ≤ 1.3) (n=88). The panels show the presentation plasma miR-122 levels (A) and presentation serum ALT activity (B) in each group of patients. Each open circle represents the value measured from individual patients. The horizontal line represents the median between the whiskers (IQR). ROC curves were generated from the grouped data. Panels show plasma miR-122 (C) and serum ALT activity (D). The AUCs (and sensitivity at 90% specificity) were 0.87 (0.72) and 0.6 (0.18) for plasma miR-122 and serum ALT respectively.

4.3.4 Circulating miR-122 is superior to serum ALT activity in identifying ALI in patients whose first blood sample was within 8 hours of overdose

From the cohort of 129 paracetamol overdose patients, the group was stratified to focus on 63 patients who presented within 8 hours of APAP ingestion to determine whether miR-122 could detect early ALI. Of these patients, 11 (17%) subsequently developed liver injury (> 3xULN serum ALT activity; median peak ALT (IQR) 487 U/L (266, 942 U/L) during their hospitalization whereas 52 (83%) patients did not develop liver injury at any time during the study (serum ALT activity remained < 3xULN). First presentation levels of miR-122 was significantly higher in patients who developed ALI compared to those that did not (*P*=0.0013) (figure 4.4B, table 4.4). In contrast, presentation ALT values were not different in patients who developed liver injury compared to those that did not (*P*=0.5) (figure 4.4A, table 4). We performed a ROC curve analysis (figures 4.4 C-D) which demonstrated the following AUC (and sensitivity at 90% specificity) values: 0.81 (0.45) for plasma miR-122 and 0.56 (0.09) for serum ALT.

	8H NO ALI	8H ALI
miR-122 (median ΔCt + IQR)	**0.19** (0.07-0.73)	**3.69** (0.43-96.0)
ALT (median U/L + IQR)	**20** (15 – 28)	**21** (12-56) U/L

Table 4.4: miR-122 levels (ΔCt) and serum ALT activity in patients who presented to hospital within 8 hours of APAP overdose who did or did not subsequently develop ALI.

Furthermore, the median (IQR) plasma APAP concentration was not significant between patients that did and did not develop ALI; 177.0 (139.0-208.0) vs 165 (123.0-204.8) mg/l (*P*=0.68) (figure 4.5A). Also, back-extrapolation of the presentation paracetamol concentration to 4h was also not significant between patients that did and did not develop ALI; 179.0 (165.0-354.0) vs 269.4 (179.7-351.0) mg/l (*P*=0.43) (figure 4.5B). Consistent with there being no statistical difference in plasma paracetamol concentration between groups, the ROC curve analysis for paracetamol concentration produced an AUC (and sensitivity at 90% specificity) value at presentation of 0.54 (0.18, P=0.68, figure 4.5C) and at 4h of 0.58 (0.18, P=0.43, figure 4.5D).

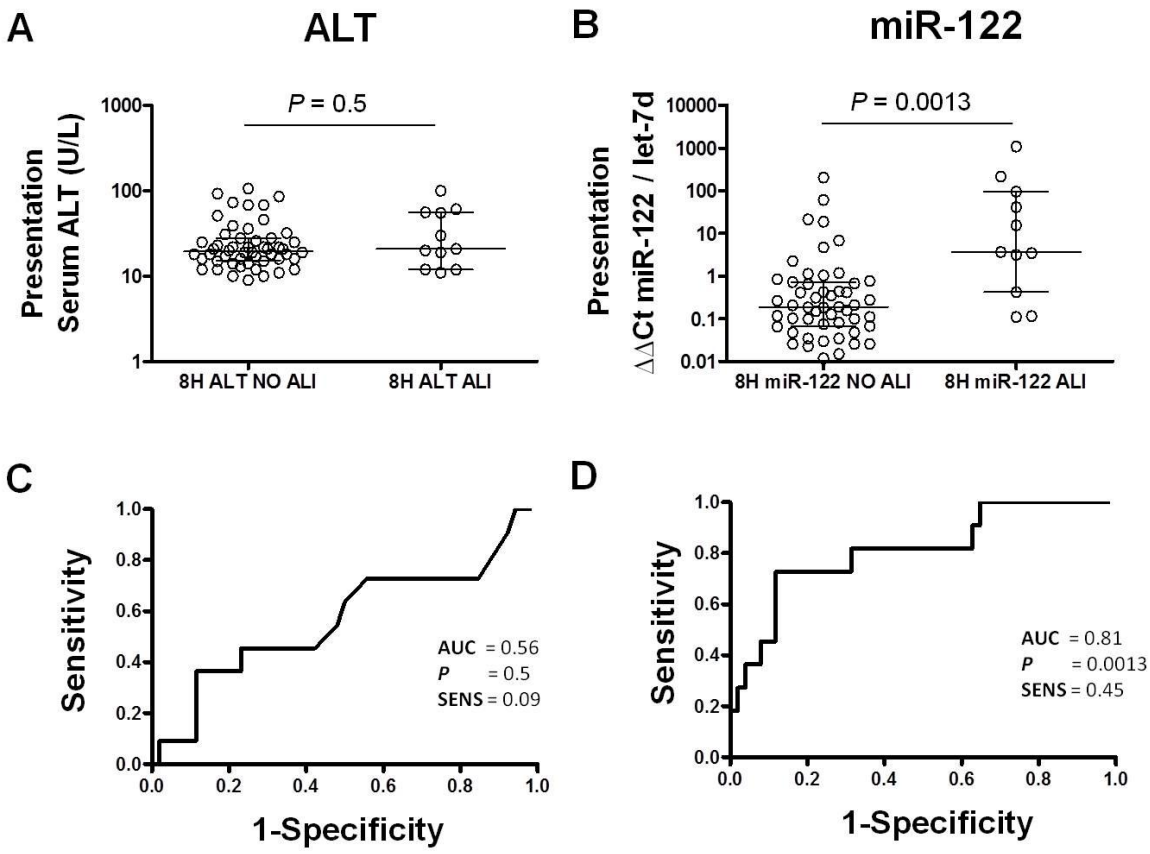

Figure 4.4: miR-122 is superior over ALT in detecting ALI in APAP overdose patients who present within 8 hours. miR-122 levels were measured in all patients who presented within 8 hours (n=63). The patients were grouped into those who developed liver injury (ALT > 3x ULN) (n=11) and those who did not develop injury (n=52). The panels show the levels of serum ALT activity (A) or relative miR-122 levels (B) in both groups. Each open circle represents the value from individual patients. The median serum ALT activities (IQR) for patients who developed injury and for patients that did not develop ALI were 21 (12-56) U/L vs 20 (15 – 28) respectively. A ROC curve was produced for ALT (C) and miR-122 (D). The AUC values (sensitivity at 90% specificity) were 0.81 (0.45) for plasma miR-122 and 0.56 (0.09) for serum ALT.

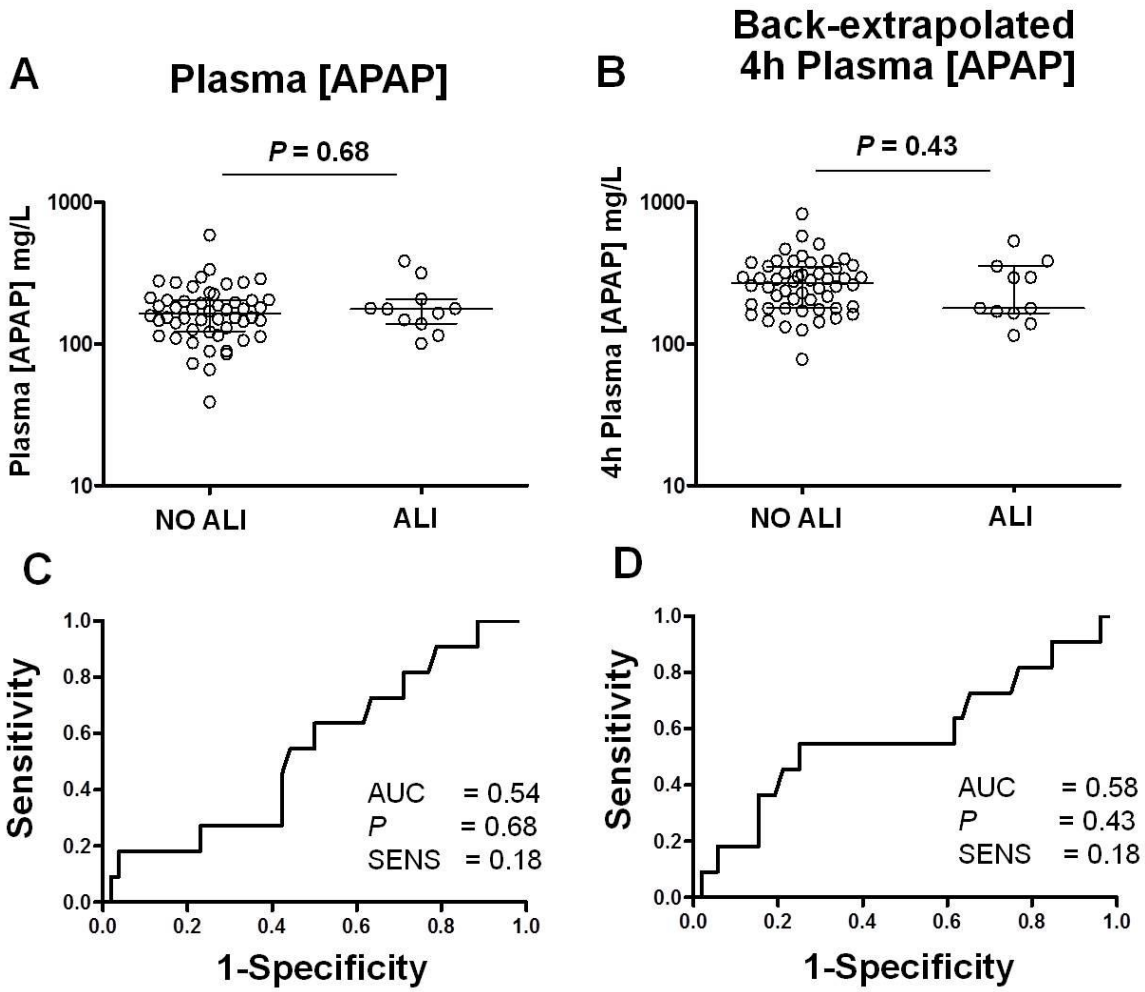

Figure 4.5: Presentation plasma APAP concentration or back-extrapolated 4-hour plasma APAP concentration does not identify patients who develop liver injury. Plasma APAP concentration was measured on plasma samples taken at admission. The patients who presented within 8 hours were grouped into those that developed liver injury (ALT > 3x ULN) and those that did not develop liver injury (ALT remained < 3x ULN). The absolute plasma APAP levels (A) and the plasma levels that were back-extrapolated to 4 hours (B) were plotted to determine if circulating APAP concentration could distinguish patients who develop liver injury. The median (IQR) plasma APAP values for patients who developed ALI and those that did not develop ALI were 177.0 (139.0-208.0) vs 165 (123.0-204.8) mg/l respectively. The median (IQR) back-extrapolated 4h plasma APAP values for patients who developed ALI and those that did not develop ALI were 179.0 (165.0-354.0) vs 269.4 (179.7-351.0) respectively. A ROC curve was produced for admission plasma APAP contration (C) and back-extrapolated 4h plasma APAP concentration (D). The AUC values (sensitivity at 90% specificity) were 0.54 (0.18) and 0.58 (0.18) for admission plasma APAP concentration and back-extrapolated plasma APAP concentration.

4.3.5 Circulating miR-122 strongly correlates with HMGB1 and necrosis keratin-18

Plasma miR-122, HMGB1, necrosis keratin-18, apoptosis keratin-18 and GLDH levels were measured in plasma obtained at the point of hospital admission, before NAC treatment had begun but when a time blood paracetamol concentration had indicated the requirement for NAC therapy (n=129). A Pearson correlation test was performed with plasma miR-122 versus each of the novel mechanistic biomarkers of ALI (HMGB1, necrosis keratin-18, apoptosis keratin-18 and GLDH). The correlation coefficients (*P* values) were 0.21 ($P < 0.0001$) and 0.19 ($P < 0.0001$), 0.06 ($P = 0.005$), 0.08 ($P = 0.0012$) between plasma miR-122 and HMGB1 (figure 4.6A), necrosis keratin-18 (figure 4.4B), apoptosis keratin-18 (figure 4.5C) and GLDH (figure 4.6D) respectively. The Pearson R values (95% CI) were 0.46 (0.31 - 0.59), 0.43 (0.28 - 0.57), 0.25 (0.08 to 0.41) and 0.29 (0.12 to 0.44) between miR-122 and HMGB1, necrosis keratin-18, apoptosis keratin-18 and GLDH respectively.

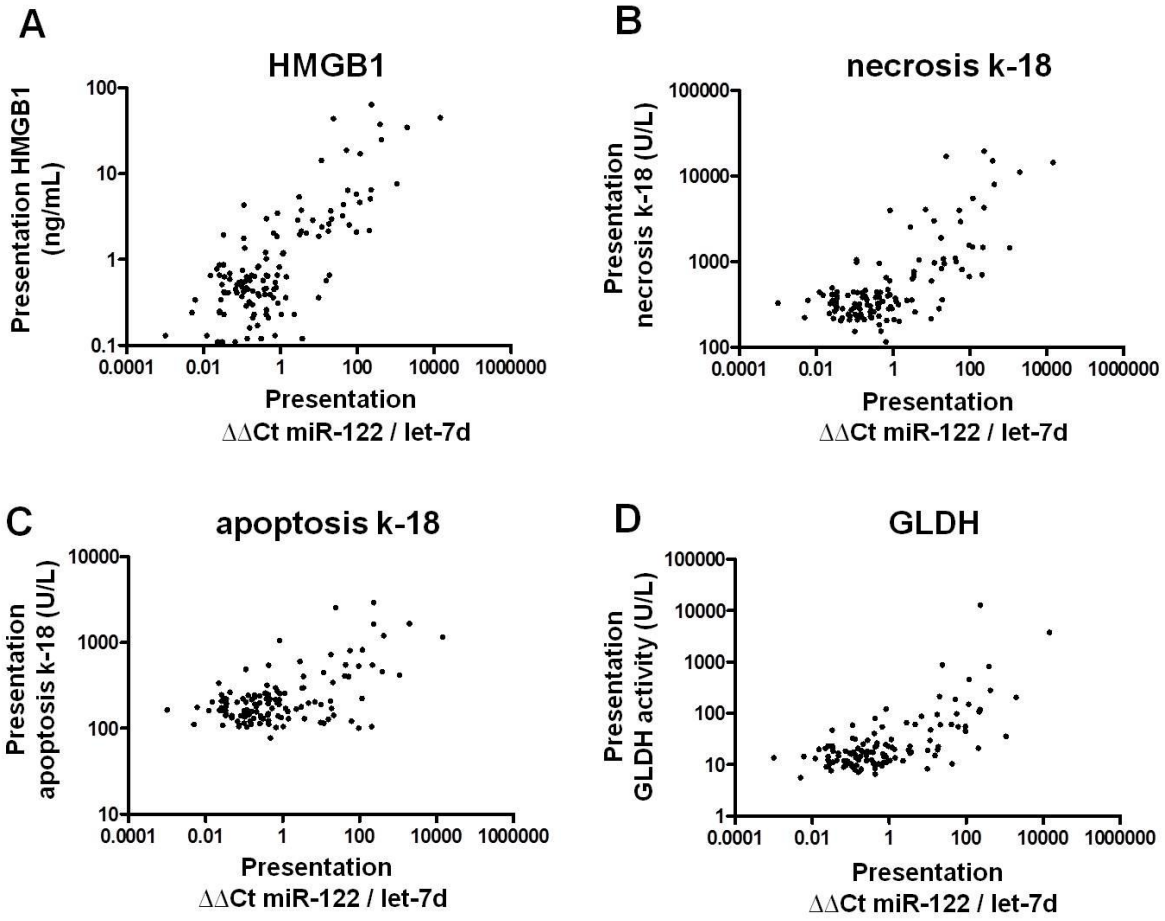

E

Biomarker	Pearson R (95% CI)	P-value	R^2
HMGB1	0.46 (0.31 to 0.59)	<0.0001	0.21
Necrosis k-18	0.43 (0.28 to 0.57)	<0.0001	0.19
Apoptosis k-18	0.25 (0.08 to 0.41)	0.005	0.06
GLDH	0.29 (0.12 to 0.44)	0.0012	0.08

Figure 4.6 : Presentation plasma miR-122 correlates well with presentation HMGB1 and necrosis keratin-18. Plasma miR-122 levels. HMGB1, necrosis keratin-18 was measured on plasma samples taken at admission (n=129). The patients who presented within 8 hours were grouped into those that developed liver injury (ALT > 3x ULN) and those that did not develop liver injury (ALT remained < 3x ULN). The presentation plasma miR-122 levels are plotted against HMGB1 (A), necrosis keratin-18 (B), apoptosis keratin-18 (C) and GLDH (D). Each closed circle represents an individual patient values. The correlation coefficients (R^2), statistical probabilities (P-values) and Pearson R values (95% CI) are tabularised in panel E.

4.3.6 Longitudinal analysis of miR-122 and ALT in individual APAP-overdose patients

From the cohort of 129 APAP overdose patients, 10 patients were selected on an individual basis; 7 patients who developed ALI during their hospitalisation, median peak ALT (IQR) 1122 (755, 1729), and 3 patients who did not develop ALI. All 10 patients had blood taken at admission to hospital where plasma APAP concentrations indicated that all 10 patients required NAC therapy. In total, three blood samples were taken from each patient; at presentation, 12 hours after the start of NAC therapy, and 20.25 hours after the start of NAC therapy. From these samples, plasma miR-122 and serum ALT activity was measured as described in order to measure each marker longitudinally. Patient characteristics, admission plasma APAP concentrations, serum ALT activities and plasma miR-122 values at admission, 12 hours after the start of NAC therapy and 20.25 after the start of NAC therapy are tabulated in table 4.2. The data from individual patients is expressed graphically in figure 4.7 A-J.

Patient ID	Age	Sex	ALI?	Plasma APAP at admission (mg/L)	Time post OD at admission (h)	Blood 1 (admission)		Blood 2 (admission + 12h)		Blood 3 (admission + 20.25h)	
						ALT (U/L)	miR-122/let7d (ΔCt)	ALT (U/L)	miR-122/let7d (ΔCt)	ALT (U/L)	miR-122/let7d (ΔCt)
X21	46	F	Y	10	19	184	232.325	1032	3541.14	1122	1669.27
X34	22	M	Y	17	20	87	18.189	863	105.786	1504	157.586
11041	29	F	Y	177	8	61	217.519	306	27.002	531	16.111
11067	17	M	Y	70	14	38	0.812	71	0.395	318	21.781
12023	53	F	Y	46	16	80	56.689	360	1.061	480	57.68
FV1	36	M	Y	386	4	12	0.111	755	471.136	662	20.393
FV2	63	F	Y	120	10	30	3.47	53	10.966	319	57.083
11006	31	F	N	148	8	18	0.73	17	0.76	20	0.35
11008	43	M	N	254	8	12	0.648	16	0.125	15	0.087
11009	42	M	N	37	11	26	0.022	28	0.455	29	0.485

Table 4.2: Patient characteristics, admission plasma APAP levels and serial serum ALT activity and plasma miR-122 levels in 10 individual patients.

Abbreviations: ALI, acute liver injury, APAP, paracetamol, ALT, alanine aminotransferase.

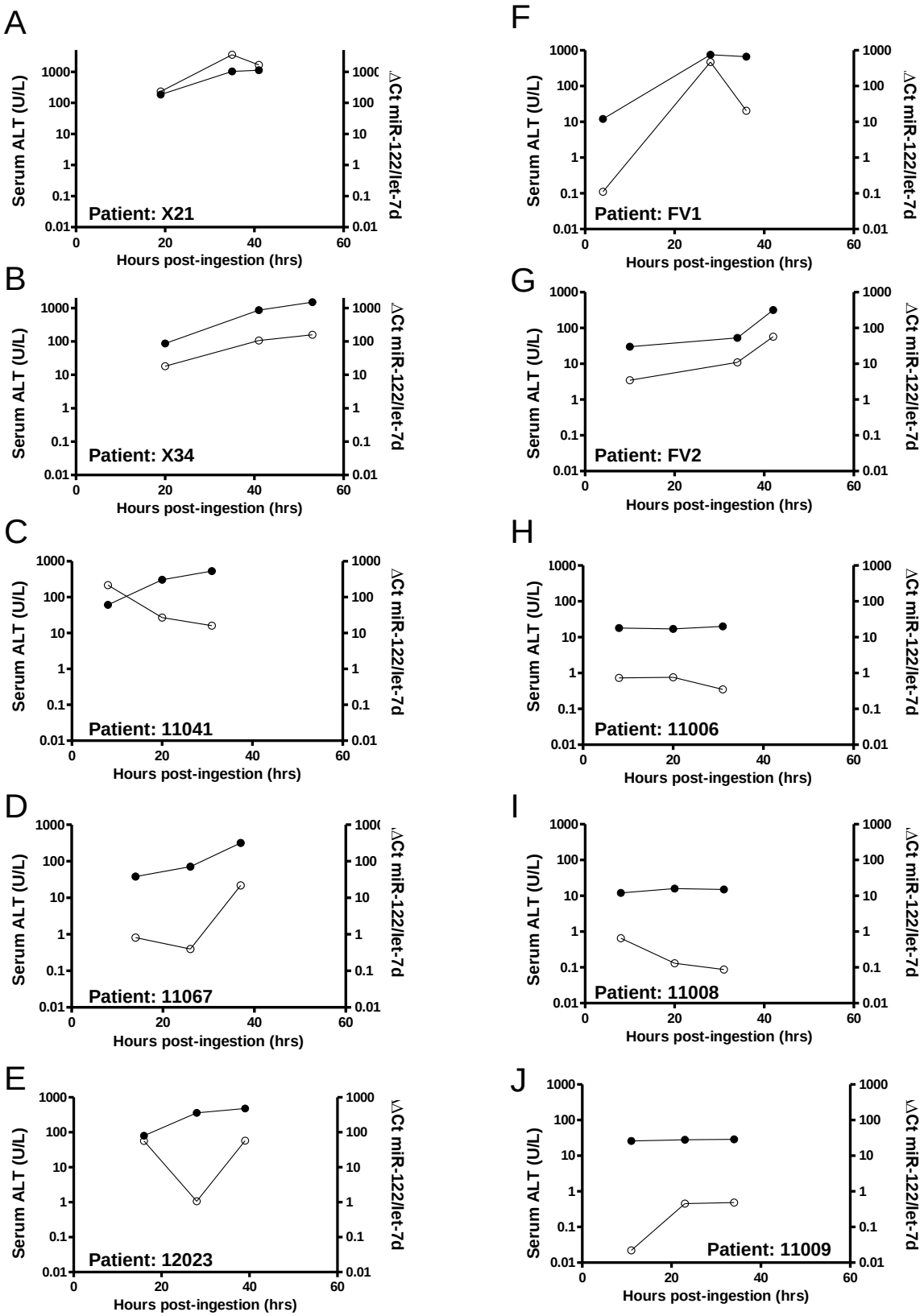

Figure 4.7: Longitudinal measurement of plasma miR-122 and serum ALT activity in 10 individual APAP overdose patients. All 10 patients required NAC therapy based on plasma APAP concentration. All 10 patients had blood taken on admission, 12 hours after the start of NAC therapy and 20.25 hours after the start of NAC therapy. Each panel shows serum ALT values (closed circles) and plasma miR-122 values (open circles) from individual patients. Seven individual patients developed ALI (panels A-G) and three individual patients did not develop ALI (panels H-J).

4.4 Discussion

There is an urgent requirement in the clinic to identify and develop novel biomarkers of ALI that show enhanced liver-specificity, and/or improved sensitivity over currently-used markers. The current validated method to assess liver integrity combines measurement of circulating aminotransferase activity with markers of liver function; either prothrombin time (PT), or PT normalised to the INR score. However, limitations with the currently-used clinical biomarkers of DILI are widely recognised, including lengthy time from drug exposure to detection, lack of tissue specificity and unacceptable rates of false positives/negatives. In a wider sense, there is also a need to develop novel markers for other forms of DILI, in particular that of idiosyncratic DILI which may be the result of chronic exposure to a drug. In this chapter, the work builds upon previous clinical investigations in chapter 3 by testing the earliness and sensitivity of miR-122 against the current gold standard marker of liver injury, ALT.

Work by Wang and colleagues in a mouse model of APAP-induced ALI found that circulating levels of liver-enriched miRNAs were elevated earlier than serum ALT activity (Wang et al, 2009). Furthermore, this work also suggested that miR-122 was potentially more sensitive than ALT, as rises could be detected at lower toxic doses of APAP compared to serum ALT activity. However, whether this increased sensitivity is truly biological, or perhaps technical (i.e. improved bioanalytical sensitivity), has not been fully tested. In this chapter, plasma miR-122 and serum ALT were tested in a cohort of patients who presented early after APAP overdose (median presentation time after overdose = 8 hours). In these patients, miR-122 significantly correlates with both peak ALT levels and peak INR score (figures 4.1 A-B, $P < 0.0001$). This suggests that there is clinical promise in the early measurement of miR-122 to identify patients who are likely to develop liver injury, or coagulopathy (a functional marker of advanced liver injury). This finding supports data from

other APAP-overdose cohorts (see chapter 3) where day one miR-122 levels are 96% higher in patients who subsequently meet KCC for liver transplantation during their hospitalisation, although due to variation between groups this fell short of statistical significance (P=0.15). These data suggest that measurement of miR-122 holds clinical utility to predict liver injury at emergency room presentation.

This data also shows that miR-122 is significantly raised (P<0.0001) in patients on admission to hospital who subsequently develop ALI (ALT > 3 x ULN) (figure 4.2A). In the same samples, the presentation serum ALT activity reading was in the normal range and did not identify which patients would develop ALI (P = 0.27, figure 4.2B). Importantly, presentation miR-122 provided superior separation between patients who develop ALI and those who do not (sensitivity at 90% specificity = 0.72), as shown in ROC curve analysis (figure 4.2C) over presentation serum ALT activity (sensitivity at 90% specificity = 0.18) (figure 4.2D). Similarly, miR-122 also identified patients who develop coagulopathy (an indicator of more severe poisoning) (figure 4.3A) whilst serum ALT activity could not (figure 4.3B). These data together suggest that, at presentation, a raised miR-122 reading may identify patients who not only develop ALI, but develop a decrease in liver function, which is associated with severe poisoning and poor outcome. If these findings can be validated and limits of normal ranges identified for miR-122 (analogous to 3 x ULN for ALT), then miR-122 holds promise as an early predictive marker for liver injury, and as a tool to highlight patients who may need more intensive therapy. Furthermore, chemical measurement of plasma APAP concentration within the first 8 hours of APAP overdose, either taken alone or back-extrapolated to 4 hours could not identify patients who develop liver injury (figure 4.5A-B). Plasma paracetamol concentration at admission is currently used to assess risk through the use of the Rumack-Matthew nomogram to highlight which patients are likely to require antidotal therapy, provided by NAC infusion. This finding supports the notion that a biological parameter would be better suited to identify risk in

patients on an individual basis, rather than using a fixed chemical threshold for all patients. Further development is necessary to validate these findings in multi-centre prospective clinical studies to test the predictivity of miR-122 during APAP-induced ALI.

To specifically test the earliness of miR-122 and ALT, the cohort was stratified for those patients who presented within 8 hours (n=63). Within this time, all patients presented with a serum ALT activity below 3 x ULN; median ALT (IQR) 20 U/L (15, 31 U/L). Green and colleagues found that serum ALT activity does not rise in the first 12 hours after an acute APAP overdose in the majority of patients (Green et al, 2010). In this chapter, the data shows that in patients who present within 8 hours, the presentation serum ALT activity is below 3x ULN, even in patients who develop liver injury later (figure 4.4A). In contrast to this, plasma miR-122 levels were already raised in patients who presented within 8 hours of APAP ingestion who develop liver injury (figure 4.4B). This finding builds upon previously published data in a mouse-model of APAP-induced ALI where miR-122 levels were raised at 1 hour after APAP exposure, before increases in serum ALT activity (Wang et al, 2009). Furthermore, data presented in chapter 2 also shows earlier increases of circulating miR-122 compared to ALT in a different mouse model (CD-1) of APAP-induced ALI . These findings allow one to speculate on release mechanisms of biomarkers from injured or dying hepatocytes. The release mechanism of ALT has not been extensively studied; however, it is considered that ALT is passively leaked into the circulation once the hepatocyte loses membrane integrity (Rafter et al, 2012). It is likely that a population of hepatic miR-122 is also lost through the same passive mechanism, but this does not explain how miR-122 is detected before ALT in animal and human forms of APAP-induced ALI. Circulating miRNAs have been to found to exist either enveloped in exosomes and other small cell-derived vesicular bodies, or in complexes with auxiliary proteins. This circulating cargo is thought to confer stability to circulating miRNAs which exhibit remarkable durability in serum/plasma; a matrix rich in RNase activity. Arroyo and colleagues found that circulating

miR-122 existed almost exclusively bound to argonaute 2 proteins in plasma and serum from healthy volunteers (Arroyo et al, 2011). However, in a mouse-model of APAP-induced ALI, time-dependant increases in miR-122 was observed in both exosome-rich and protein-rich serum fractions (Bala et al, 2012). This suggests that the nature of circulating miR-122 may indeed change during conditions of liver disease. Despite this, the exact nature of early release of miR-122 remains elusive. It is possible that miR-122 release may be bi-phasic with an early active release in response to stress, followed by massive late release during hepatocellular necrosis. However, this urgently requires experimental testing.

In this cohort of patients, several novel mechanistic markers of liver injury were also measured, including HMGB1, full-length keratin-18 (necrosis K-18), caspase-cleaved keratin-18 (apoptosis K-18) and GLDH. HMGB1 is a nuclear protein that exhibits proinflammatory activity through the activation of toll-like receptors (TLRs) or receptor for advance glycation end-products (RAGE). Hyper-acetylated HMGB1 has been found to be released from activated monocytes and macrophages, while hypoacetylated HMGB1 is released from necrotic cells. HMGB1 is a known damage-associated molecular pattern (DAMP) molecule and has been shown to contribute to APAP-induced ALI through modulation of the immune response to inflammation (Scaffidi et al, 2002). Keratins are intermediate filament proteins found in a vast array of cell types. During apoptosis-mediated cell death, keratin-18 is cleaved in a precise manner. The caspase-cleaved fragment can be measured in the circulation as a surrogate marker of apoptotic cell death. The circulating full-length keratin-18 filament is associated with necrotic cell death. While both HMGB1 and keratin-18 offer no liver-specificity, they can be used as robust mechanistic indicators of cell death when used in combination. More recently, it has been shown that circulating forms of HMGB1 and keratin-18 can be used as mechanistic markers of APAP-induced ALI in pre-clinical models and in patients (Antoine et al, 2009, Antoine et al 2010, Craig et al, 2011, Antoine et al 2012,). Furthermore, GLDH is an enzymatic marker of liver injury that has been suggested to be a more sensitive blood-based marker of APAP-induced ALI in rats

(O'Brien et al, 2002). GLDH can also provide mechanistic insight due to the large stores of GLDH within the mitochondria. Indeed, GLDH has recently been used specifically as a circulating marker of mitochondrial damage during APAP-induced ALI (McGill et al, 2012).

Therefore, in a collaborative effort within the CDSS, these novel mechanistic markers were measured in the same samples from all patients within this study. Here, in this chapter, the data is focussed on the correlative analysis between miR-122 and the novel panel of mechanistic markers (HMGB1, necrosis K-18, apoptosis K-18 and GLDH) in an attempt to gain insight behind the mode of cell death associated with miR-122 release. The data shows that presentation plasma miR-122 correlates most strongly with HMGB1 and necrosis K-18 ($R^2 = 0.21$, $P<0.0001$ and $R^2 = 0.19$, $P<0.0001$) respectively (figure 4.6 A-B). These markers are mechanistic indicators of necrotic cell death, which is recognised as the predominant form of cell death during APAP-induced ALI (Lawson et al, 1999; Gujral et al, 2002). Furthermore, in a cohort of hepatitis C infected patients, miR-122 is described as a marker of necroinflammation associating closely with ALT and histological activity index (HAI) score (Bihrer *et al*, 2011). These data suggest that the circulating miR-122 release is closely associated with necrotic cell death. Moreover, the data shows that miR-122 also correlates with apoptosis K-18, albeit with less strength and significance ($R^2 = 0.06$, $P = 0.005$) than the necrotic markers (figure 4.6 C-D). The role of apoptosis in APAP-induced ALI is controversial. In animal models of APAP-induced ALI, apoptosis is considered to play a negligible role in hepatotoxicity. This is based on lack of caspase-activation, morphological findings and the fact that caspase-inhibitors do not protect against injury (Gujral et al, 2002; Jaeschke et al, 2006). However, it should be noted that animal models of APAP-induced ALI were fasted prior to APAP exposure. Nutritional status has a profound impact on hepatic ATP stores, and therefore, the ability of hepatocytes to fully commit to apoptosis. More recent evidence has found that apoptosis may play a modest role in APAP-induced liver injury under certain conditions (Antoine et al, 2010, Antoine et al, 2012). Nevertheless, in this study, circulating caspase-cleaved K-18 fragments are clearly raised in some patients

alongside miR-122 (figure 4.6C). Further studies are necessary to delineate the specific release mechanisms and kinetics of miR-122 and other liver-enriched miRNAs into the blood during specific conditions of apoptosis and necrosis.

Here, the data also shows that miR-122 correlates with serum GLDH activity (figure 4.6D). The mitochondrion represents a key intracellular target for NAPQI, the toxic metabolite of APAP. It has been shown that inhibition of manganese superoxide dismutase (MnSOD, a critical mitochondrial defence enzyme) and subsequent mitochondrial stress, plays a key role in APAP-induced ALI (Agarwal *et al*, 2011, Ramachandran *et al* 2011). Here, GLDH (a mitochondrial-enriched enzyme) is used as a circulating marker of mitochondrial damage. Although the correlation between miR-122 and GLDH was significant ($P = 0.012$), the correlation was weaker than with the necrotic markers ($R^2 = 0.08$). Circulating GLDH and ALT enzymes may share a similar release mechanism and/or exhibit similar times of release. Therefore, like ALT, GLDH may not be an early clinical marker of APAP-induced ALI. This represents a clear hypothesis to test in future work.

It is also important to consider the kinetics of circulating markers during the evolution of hepatoxicity. In a separate cohort of APAP-induced ALI patients (see chapter 3), circulating miR-122 appears to return to baseline earlier than ALT, which has been estimated to have a circulatory half life of approximately 48 hours (Saheki *et al*, 1990). Here, we selected 10 individuals from this cohort (n=129); 7 of whom developed ALI and 3 of whom did not develop ALI. All 10 patients had blood taken at admission (for patient characteristics see table 4.2) where plasma APAP concentrations had indicated the need for NAC therapy. Further blood samples were taken 12 hours and 20.25 after the start of NAC therapy in each individual. Circulating miR-122 and ALT activity was measured in plasma or serum. Firstly, in three patients who do not develop ALI, neither serum ALT nor plasma miR-122 is raised at any time (figure 4.7 H-J). This is important to show that both markers remained low and in accordance with each other, which may provide added confidence if used in parallel. Furthermore, in most patients who did develop ALI (patients X21, X34, 11067, FV1, FV2,

figure 4.7 A, B, D, F, G), plasma miR-122 tracks serum ALT activity closely. However, in two patients (patients 11041 and 12023, figure 4.7 C and E) plasma miR-122 and ALT were dissociated. In patient 11041, miR-122 levels were highest at presentation (ΔCt 217.6) before decreasing at 12 hours (ΔCt 27.0) and 20.25 hours (ΔCt 16.1) thereafter. However, serum ALT activity was lowest at presentation (61 U/L) before rising at 12 hours (306 U/L) and 20.25 hours (531 U/L) thereafter. A delayed presentation of ALT and longer circulatory half-life may account for delayed increase and opposite trend in this patient; it should be noted that miR-122 levels were relatively high at all three time-points. Without histological examination of a liver biopsy from these patients, it is impossible to state what the true degree of liver injury was at each time. However, this analysis shows that plasma miR-122 levels and serum ALT activity may be different in certain conditions.

In summary, the data obtained from this cohort supports previous pre-clinical data where histological changes can support circulatory biomarker data. Now, the challenge is to build upon these findings and further develop miR-122 as a clinical marker. One important challenge will be to define normal miR-122 levels in a heterogenous group of patients so a threshold can be set, beyond which ALI can be diagnosed with confidence. Another challenge is the need to develop and test a clinical assay that can be used between different clinical laboratories. Whilst qPCR offers good bioanalytical sensitivity, the entire assay can take up to 8 hours from patient sampling to result. There is a pressing need for a fast, robust, and sensitive clinical assay for the measurement of circulating miRNAs that can be used routinely at the bed-side, given that APAP-induced ALI can develop rapidly. In general, the findings presented here in this retrospective study are underpinned by the heterogeneity of the cohort, with respect to dose ingested and time to presentation. Therefore, these data should add to the body of evidence for the development of circulating miR-122 as a clinical biomarker of APAP-induced ALI.

In conclusion, the data presented here suggest that miR-122 is an early marker of APAP-induced ALI that can outperform existing markers of liver injury in patients at emergency

room presentation. Furthermore, miR-122 also holds promise in the ability to predict injury, including severe injury (coagulopathy) in APAP-induced ALI patients at presentation. However, none of the patients in this cohort required a liver transplant or died, so further testing is required to test miR-122 against patient outcome. Circulating miR-122 has the potential to refine patient care in a number of ways. In prospective clinical trials, circulating miR-122 could be included in the patient inclusion criteria to test novel treatment strategies, i.e. in the identification of low and high-risk patient groups using a biological personalised strategy. The use of such an approach, if successful, may reduce unnecessary administration of protracted NAC therapy. Furthermore, miR-122 may allow earlier exclusion of injury in patients in APAP-induced ALI patients, rather than reliance on late markers of liver function which are used currently. If injury can be confidently excluded in well patients, this could significantly reduce bed occupancy and reduce the clinical burden of APAP-induced ALI. The key point is that this retrospective study and other studies (see chapter 3) provide the first justification of the use of miR-122 to be included in future clinical trials to test the ability of this marker to detect APAP-induced ALI early, and predict hard-clinical outcomes.

CHAPTER FIVE

THE ROLE OF CIRCADIAN RHYTHMS IN DILI

5.1 Introduction

Circadian (derived from latin, *circa diem*) rhythms are defined at rhythms in biological or biochemical events that have a periodicity of approximately 24 hours. Circadian rhythms are distinct from other biological rhythms such as ultradian rhythms (biological rhythms with a periodicity less than 24 hours, e.g. 90 minute cycles of R.E.M. sleep) and infradian rhythms (biological rhythms with a periodicity longer than 24 hours, e.g. menstruation cycles). Many intrinsic physiological processes exhibit a daily cyclic pattern, e.g. heart rate, blood pressure, body temperature and metabolism all show time-of-day differences in their level or activity. This is considered to confer an advantage to organisms to allow anticipatory rather than reactionary behaviour to stimuli such as food availability (Gehring & Rosbash, 2003). Circadian rhythms are observed throughout nature; plants, animals and bacteria show 24-hour rhythms in their biology. Furthermore, in man, it is accepted that the wellbeing of individuals is dependent on functioning and unperturbed circadian biology. For example, studies have shown that rotating shift workers are at more risk of developing cancer and cardiovascular disease due to a constantly disrupted circadian system (Schernhammer et al, 2001, Boggild & Knutsson, 1999). Furthermore, there is a strong link between sleep disorders and other morbidities such as metabolic syndrome and depression (Ford & Kamerow, 1989, Punjabi & Polotsky, 2005). This growing body of evidence suggests that the effects of circadian regulation are extensive on core physiology.

The evidence governing the complex coordination of circadian physiology is still evolving. A major breakthrough occurred in early 1990's upon the discovery of the first clock gene in mice (Vitaterna et al, 1994). This provided a genetic basis (rather than simply being a behavioural phenomenon) behind circadian regulation. Since then, many clock genes and their variants have been found in species as diverse as bacteria and humans. A master clock exists in the suprachiasmatic nuclei (SCN) region of the brain, which has been found to orchestrate the dynamics of peripheral clocks in numerous cell types, including hepatocytes (Schibler & Sassone-Corsi, 2002). Light information is sensed by photoreceptive regions of

the retina and relayed to the SCN via the retinohypothalmic tract (Berson *et al*, 2002). The rhythmicity of light availability entrains the master clock exquisitely to a twenty four hour period. Peripheral clock synchronisation is achieved by direct neuronal signalling and from cyclic release of melatonin from the pineal gland with other glucocorticoids also being implicated (Arnedt & Skene, 2005). This, essentially, provides peripheral organs with a timing cue (zeitgeber) in relation to the environment and geophysical time. The clock machinery is consistent between central and peripheral clocks, with Bmal1 and Clock proteins forming an active heterodimer to upregulate the expression of Cryptochrome (*CRY1-2*) and Period (*PER1-3*) genes and a catalogue of other genes containing E-Box motifs. When the concentrations of CRY and PER genes reach a threshold in the cytoplasm, they dimerise, move to the nucleus and attenuate the effects of Bmal1-Clock, completing the negative feedback circuit (Reppert & Weaver, 2002). When one considers that the period of this intrinsic oscillation is twenty-four hours, the basis of the biologic clock can be envisaged.

Recently, other zeitgebers have been implicated in entrainment of peripheral organs, especially in the liver where food availability acts as the dominant timing cue (Suter & Schibler, 2009). Food intake, which ultimately determines the energy status of the cell, can affect the stability of core clock gene products and alter the dynamics of the clock directly. The AMP:ATP ratio in the hepatocyte, essentially the cellular energy status, can be sensed by liver kinases including LKB (Lamia *et al*, 2009). Such kinases phosphorylate AMPK which targets CRY1, a key transcription factor in the core clock machinery, for proteasomal degradation. Not only can food availability affect clock gene dynamics but it can actively change hepatic rhythmic gene expression (Vollmers *et al*, 2009). It is likely that other regulatory mechanisms will also emerge as additional sensory pathways that confirms nutrient intake as the dominant zeitgeber in the liver.

Circadian regulation influences many aspects of molecular physiology including metabolism and cell cycle control (Rutter et al, 2002, Matsuo et al, 2003). The detoxification systems of the liver and kidney are regulated through central and peripheral circadian coordination. It becomes evident that the disposition of some drugs may not remain constant over the course of the day. Almost every aspect of drug disposition, from absorption to excretion has the potential to change over a daily cycle (Bruguerolle, 1998). This may explain how the presentation of some adverse drug reactions in patients appears to be dependent on the time of day at which the drug was administered. This has been reported with indomethacin, 5-fluorouracil and a number of angiotensin-converting-enzyme (ACE) inhibitors (Levi et al, 1985, Levi et al, 1995, Ohmori & Fujimura, 2005) suggesting that this effect is independent of chemical structure or drug class. Other compounds have exhibited diurnal rhythmicity in tolerance when tested in laboratory rodent models including cyclosporine and loratidine (Magnus *et al*, 1985, Dridi *et al*, 2005). The term 'chronopharmacology' is now used to describe how drug response can change over the circadian phase.

APAP is a widely studied analgesic and antipyretic drug that is very well tolerated at sub-toxic doses. APAP, however, is considered a model hepatotoxicant in overdose and mechanisms of toxicity have been well characterised. Overdoses of APAP overwhelm the intrinsic clearance pathways of glucuronidation and sulfation in the hepatocyte, allowing APAP to be bioactivated through several cytochrome P450s (CYPs) to form n-acetyl-p-benzoquinoneimine (NAPQI), a reactive metabolite (Nelson, 1995, Dahlin *et al*, 1984). This reactive metabolite is sequestered by hepatic stores of glutathione (GSH), a sulfhydryl-containing antioxidant, and then excreted as a nontoxic mercapturate (Yuan & Kaplowitz, 2009). Intracellular stores of GSH are rapidly depleted after a toxic insult which allows NAPQI to bind to macromolecules in the cell and initiate a cascade of hepatotoxicity (Jaeschke & Bajt, 2006; Jaeschke *et al*, 2006; Park *et al*, 2005). It has been shown previously that the hepatotoxicity of paracetamol follows a circadian rhythm (Matsunaga et al, 2004). Key biological determinants of APAP-mediated hepatotoxicity, such as hepatic

glutathione (GSH) content, have been reported to oscillate over a twenty-four hour period which may explain the temporal difference in toxicity (Jaeschke & Wendel, 1985).

In the present work, hepatotoxicity was investigated following morning and evening administration of a single dose of either APAP (350 mg/kg, i.p.) or furosemide (FS) (400 mg/kg, i.p.) to the young CD-1 mouse. These model hepatotoxins were selected based on their mechanism of injury; APAP depleted GSH which is an obligatory event in the manifestation of hepatotoxicity whereas FS causes injury independent of GSH depletion. DILI was assessed through a series of conventional and emerging biomarkers of hepatotoxicity, including serum ALT activity and circulating miRNAs. After characterising archetypal clock gene expression in our rodent model over time, hepatic GSH dynamics and temporal Cyp2e1 levels were measured across the light-phase. Separately, the safety of a common vehicle, polyethylene glycol-400 (PEG-400) was assessed for its safety in DILI studies.

The overall goal of this part of the thesis is to improve our understanding of the area of chronotoxicology. A firm understanding of the key determinants of drug disposition could potentially improve the therapeutic index of many drugs and reduce ADRs in patients.

5.2 Materials & Methods

5.2.1 Animal Experiments.

The protocols described were performed according to the regulations defined in the project licence granted under the Animals (Scientific Procedures) Act 1986 and approved by the University of Liverpool Animal ethics committee. All animals were purchased from Charles River (Manston, UK) and housed at constant temperature and humidity with free access to food and water. All animals were allowed to acclimatise to a 12-hour light-dark cycle (lights on: 08:00 (ZT00)/lights off: 20:00 (ZT12)) for at least 14 days prior to experimentation. Mice were humanely culled via rising concentration of CO^2 before exsanguinations according to the Humane Killing of Animals Under Schedule 1 to the Animals (Scientific Procedures) 1 Act 1986.

5.2.2 Dosing regimen.

For normal circadian analysis, male CD-1 mice (5-7 weeks old, n=5/6 per group, 30-40g, fed *ad libitum*) were culled via schedule 1 as described at 09:00 (ZT01), 13:00 (ZT05), 17:00 (ZT09) and 21:00 (ZT13). Blood was obtained via cardiac puncture. Tissues were harvested and snap frozen on liquid nitrogen for storage at -80°C until use. For toxicity experiments, male CD-1 mice (5-7 weeks old, n=6, 30-40g, fed *ad libitum*) were administered a single i.p. dose of APAP (350 mg/kg, in warmed saline) or FS (400 mg/kg, in warmed PBS, pH 8.0) or vehicle alone using a 25-gauge needle at either 09:00 (ZT01) or 21:00 (ZT13). In some experiments, PEG-400 was used as a vehicle for FS administration. All mice were culled 8 hours after dosing via a rising CO_2 concentration. Blood was extracted immediately via cardiac puncture. Livers were removed, rinsed in phosphate-buffered saline (PBS), and one large lobe was semi-homogenised before being snap frozen in liquid nitrogen. Tissues were stored at -80°C until use.

5.2.3 Serum ALT Activity Determination

Blood was collected in microtubes and allowed to clot overnight at 4 °C. The blood clot was initially separated and serum removed by centrifugation (1500g, 5 mins, 4 °C). Residual red blood cells were pelleted by centrifugation (10,000g, 5 mins, 4 °C) to yield cell-free supernatant. Serum ALT levels were determined immediately (to prevent freeze-thawing effects) using a Thermo Infinity ALT Liquid stable reagent-based (Thermo, Waltham, MA) kinetic assay, at 37°C, according to the manufacturer's instructions.

5.2.4 Determination of temporal hepatic GSH abundance.

The kinetic 5,5'dithiobis(2-nitrobenzoic acid)-GSH disulfide recycling assay was used to determine hepatic GSH abundance from normal mouse livers excised at 09:00 (ZT01), 13:00 (ZT05), 17:00 (ZT09) and 21:00 (ZT13). The method used is described by Vandeputte *et al*, 1994.

5.2.5 Determination of total protein concentration.

Total protein concentration was determined using the method described by Lowry *et al* (1951).

5.2.6 Immunoblotting

Immunoblotting was performed against Cyp2e1. Briefly snap-frozen livers were homogenised in PBS. After total protein concentration was determined, pools were generated for each time point (ZT01, ZT05, ZT09, ZT13) from six individual liver homogenates. From pooled homogenates, 10 µg of protein was added to a 10 % homemade

acrylamide gel and run (1.5 h, 125 V) before being transferred to a nitrocellulose film (1 h, 100V). Films were blocked with 10 % (w/v) non-fat milk overnight before ponceau red staining to ensure sufficient protein transfer. Membranes were then cut at the appropriate molecular weight to separate β-actin (loading control) from Cyp2e1. Each film was treated with primary antibody overnight (anti-Cyp2e1, raised in mouse, BD Gentest, San Jose, CA). Films were washed (0.1 % TWEEN/1% TBS buffer) before secondary antibody treatment (1 hour). Films were washed again and treated with Lumiglo chemiluminescent reagent (New England Biolabs, Ipswich, MA) for 5 min, before exposure to ECL Hyperfilm (Amersham, Chalfont St. Giles, UK).

5.2.6 Total RNA extraction.

Total RNA was obtained using a phase-extraction method as described by Chomczynski & Sacchi 1987. Briefly, liver tissue (50 mg) excised from mice at 09:00 (ZT01), 13:00 (ZT05), 17:00 (ZT09) and 21:00 (ZT13) was lysed in Trizol reagent (Invitrogen, Carlsbad, CA) as per the manufacturer's instructions. RNA was DNase treated using the DNA-free kit (Ambion, Carlsbad, CA) before spectrophotometric quantification via Nanodrop (Nanodrop technologies, Wilmington, DE), cDNA was generated using the imPromptII reverse transcription system (Promega, Fitchburg, WI) by using 2 µg of RNA as per the manufacturer's instructions.

5.2.7 Temporal clock gene expression analysis.

Expression of seven clock genes was analysed. Briefly, clock genes were co-amplified sequentially by quantitative polymerase chain reaction (qPCR) with a reference housekeeping gene, glyceraldehyde 3-phosphate dehydrogenase (GAPDH) as described by Kitteringham *et al*, 2000. The selected clock genes and their respective primer pairs are

summarised in table 1. Primers were bought from Eurofins MWG Operon (Ebersberg, Germany). qPCR was performed using the SYBR ® Green I JumpStart Taq polymerase kit (Sigma Aldrich, Poole, UK) on an AbiPrism7000 (Applied Biosystems, Carlsbad, CA).

5.2.8 miRNA extraction

miRNA was extracted using an miRNeasy kit (Qiagen, Venlo, Netherlands), following the manufacturer's instructions, with minor modifications. Briefly, 40 µL of biofluid was made up to 200 µL with nuclease-free water, then combined with 700 µL of QIAzol. The sample was mixed and left for 5 minutes before the addition of 140 µL of chloroform. In some experiments, 10µL of cel-lin-4 (5fM) was added to denatured serum before the addition of chloroform (to serve as exogenous control). Samples were then mixed vigorously for 15 seconds and centrifuged at 12,000 g for 15 minutes at 4 °C. Equal volumes (350 µL) of the upper aqueous phase and 70% ethanol were mixed in a fresh microtube before adding the total volume to an miRNeasy minispin column. The column was centrifuged at 8,000g for 15 seconds at room temperature. The flow-through, containing the small RNA fraction, including the miRNA complement, was mixed with 450 µL of 100% ethanol. The elute was then purified using a MinElute kit (Qiagen, Venlo, Netherlands).

5.2.9 miRNA purification

The small RNA elution mixture was applied to a MinElute column, 700 µL at a time. The immobilized RNA was then washed with various buffers before a final 80 % ethanol wash. The

column was then dried by centrifugation. The small RNA fraction was eluted in 14 µL of nuclease-free water and stored at -80 °C.

5.2.10 Quantitative Polymerase Chain Reaction Analysis (miRNA).

miRNA levels were measured using Taqman-based quantitative polymerase chain reaction (qPCR). The small RNA elute was reverse transcribed using specific stem-loop reverse-transcription RT primers (Applied Biosystems, Foster City, CA) for each target miRNA species, following the manufacturer's instructions. Next, 2 µL of RNA was used to produce the complementary DNA (cDNA) template in a total volume of 15 µL. Then, 1.33 µL of cDNA was used in the PCR mixture with specific stem-loop PCR primers (Applied Biosystems, Foster City, CA) in a total volume of 20 µL. Levels of miRNA were measured by the fluorescent signal produced from the Taqman probes on an ABI Prism 7000 (Applied Biosystems). All samples were assayed in duplicate. miRNA levels were normalized to levels of U6 snRNA, a ubiquitous small nuclear RNA (snRNA) species used as an endogenous control, as described elsewhere (Zhang et al, 2010).

Gene	Primer	Nucleotide sequence
Bmal1	F	TCATTGATGCCAAGACTGGA
	R	ACTGAAGGCCTGTTGCACTT
CRY	F	CGGACAGCCACCTCTAACAT
	R	GACAGAGGGGTCATGCACTT
DBP	F	ACCGTGGAGGTGCTAATGAC
	R	TGGTTGAGGCTTCAGTTCCT
Per2	F	CAGGCTGAGTTCCCTAGTCG
	R	ACTGCCTCTGGACTGGAAGA
Rev-erb-a	F	AGCCGCACAACCTACAGTCT
	R	CAGCTCCTCCTCGGTAAGTG
ROR-gamma	F	GAAGGCAAATACGGTGGTGT
	R	GGGCAATCTCATCCTCAGAA
Sirt1	F	GATACCTTGGAGCAGGTTGC
	R	CTCCACGAACAGCTTCACAA
GAPDH	F	CAAGGTCATCCATGACAACTTTG
	R	GGGCCDTCCACAGTCTTCTG

Table 5.1: Primer sequences used for qPCR analysis of clock gene expression.

5.3 Results

5.3.1 Large changes in hepatic clock gene expression occurs over the light-phase of the day

Total RNA was extracted from livers (n=6) which were harvested at ZT01, ZT05, ZT09 and ZT13. From this, expression of six clock genes (BMAL1, REV-ERBα, PER2, CRY1, RORɣ, SIRT1) and one circadian gene (DBP) was measured. For normalisation, GAPDH provided a consistent baseline across all time points. All data was compared to the ZT01 timepoint; fold-changes and *P*-values for each gene in shown in below (table 5.2). Large differences in expression was observed for DBP (45-fold change, at ZT09), REV-ERBα (16-fold change, at ZT05) and BMAL1 (41-fold change, at ZT09) (figure 5.1). BMAL1 and its inhibitor REV-ERBα showed an anti-phase relationship. Furthermore, CRY1 (-2.4 fold change) and PER2 (5.4 fold change) showed more modest yet significant maximal changes in expression at ZT05 and ZT13 respectively. RORɣ and SIRT1 did not show any significant difference in expression during the light-phase.

Clock Gene	ZT01 vs ZT05		ZT01 vs ZT09		ZT01 vs ZT13	
	Mean Fold Change	*P*-value	Mean Fold Change	*P*-value	Mean Fold Change	*P*-value
BMAL1	-3.6	P = 0.0002	-40.5	P < 0.0001	-3.9	P < 0.0001
Cry1	-2.4	P < 0.0001	-2.1	P = 0.0004	1.2	P = 0.3131
DBP	31.8	P < 0.0001	44.6	P < 0.0001	7.0	P = 0.0078
PER2	2.0	P = 0.2001	3.6	P = 0.0012	5.4	P < 0.0001
REV-ERB	15.7	P < 0.0001	1.3	P = 0.5897	-3.8	P = 0.001
RORɣ	1.5	P = 0.5616	1.2	P = 0.7709	2.0	P = 0.1556
SIRT1	1.1	P = 0.8181	-1.0	P = 0.3843	-1.3	P = 0.1017

Table 5.2: Average fold changes and *P*-values of hepatic clock gene expression

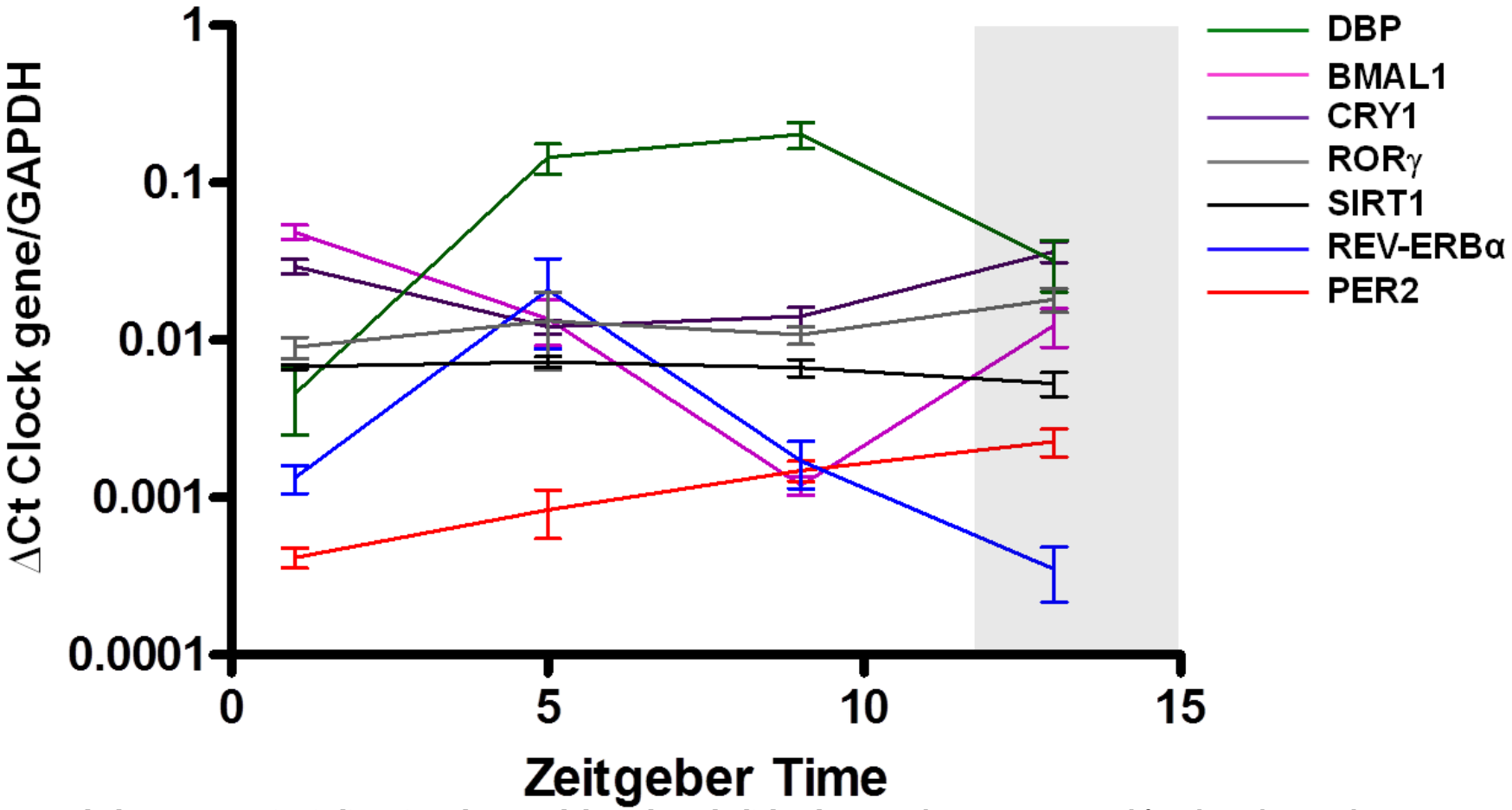

Figure 5.1: Clock gene expression in liver tissue harvested throughout the light-phase. Total RNA was extracted from livers harvested at ZT01, ZT05, ZT09 and ZT13 (n=6). Each gene was measured by qPCR on SYBR Green I platform using primer sequences in Table 5.1. The panel shows the relative levels of expression (ΔCt) normalised to GAPDH). The average ΔCt and S.E.M. is plotted for each group. Coloured lines connect the mean ΔCt between groups for each gene where DBP (green line), BMAL1 (pink line), CRY1 (purple line), RORɣ (grey line), SIRT1 (black line), REV-ERBα (blue line) and PER2 (red line). The shaded area indicates when lights were switched off (from ZT12). Fold-changes and P-values are shown in table 5.2. Kruskall-Wallis test.

5.3.2 Extent of APAP and FS-induced liver injury is dependent on the time of day of administration

To investigate the effect of time-of-day of administration on the extent of liver injury caused by two model hepatotoxins, mice (n=6) were administered a single dose of either APAP (350 mg/kg, i.p., in warm saline) or FS (400 mg/kg, i.p., in warm PBS, pH 8.0) for 8 hours. Serum was extracted (as described). Serum ALT activity analysis was performed immediately to prevent unnecessary freeze-thawing of the samples. For miR-122 analysis, U6 snRNA (for APAP) and lin-4 (for FS) provided standardisation.

For APAP, two mice died unexpectedly from toxicity after evening treatment with APAP providing n=4 for this group. All other mice survived providing n=6 in other groups. Biomarker analysis showed that mice are more sensitive to APAP after evening administration. (figure 5.2A; table 5.3). Average serum ALTs were 26-fold higher after evening APAP administration compared to morning, although due to variation provided by one animal that did not develop severe hepatotoxicity in the evening group (ALT=151), this fell short of statistical significance (P=0.11). Likewise, average serum miR-122 values were 18.3-fold higher after evening administration compared to morning administration, with variation between animals accounting for the lack of statistical significance (P=0.08). Together, with the increased mortality rate observed in mice (33% vs 0% for evening and morning administration of APAP respectively), it is concluded that mice were more sensitive to APAP after evening (ZT13) administration compared to morning administration (ZT01).

For FS, all mice survived providing n=6 in all treatment groups. FS generally produced a milder injury after 8 hours compared to APAP (average APAP ALT = 4357, average FS ALT = 352). Biomarker analysis showed that mice were more sensitive to FS after morning exposure. Average serum ALTs were 4.4-fold higher after morning administration (P=0.022) (figure 5.2D; table 5.4). Likewise, serum miR-122 levels were 2.6-fold higher

after morning administration, although this did not reach statistical significance (*P*=0.08) (figure 5.2E; table 5.4).

	ZT01		**ZT13**	
	Control	**APAP**	**Control**	**APAP**
ALT (Median U/L ± IQR)	**18.5** (11.1, 26.1)	**380** (59.6, 662)	**29.6** (17.4, 45.7)	**12785** (2846, 15281)
miR-122 (Median ΔCt ± IQR)	**2.95** (1.87, 9.50)	**88.8** (18.3, 159)	**9.3** (6.4, 20.4)	**1779** (256.7, 3147)

Table 5.3: Serum miR-122 levels and serum ALT activity in control and APAP treated mice when administered in the morning (ZT01) or in the evening (ZT13)

	ZT01		**ZT13**	
	Control	**FS**	**Control**	**FS**
ALT (Median U/L ± IQR)	**12.8** (8.3, 37.4)	**562** (149, 924)	**17.9** (11.7, 32.9)	**69.2** (36.4, 226)
miR-122 (Median ΔCt ± IQR)	**683** (372, 9240)	**40471** (10320, 64111)	**1830** (291, 4379)	**8864** (1614, 26995)

Table 5.4: Serum miR-122 levels and serum ALT activity in control and FS treated mice when administered in the morning (ZT01) or in the evening (ZT13)

Serum ALTs and Serum miR-122 levels correlated significantly for APAP-induced ALI ($P<0.0001$, $R^2=0.76$, figure 5.2C) and FS-induced ALI ($P<0.0001$, $R^2=0.78$, figure 5.2F).

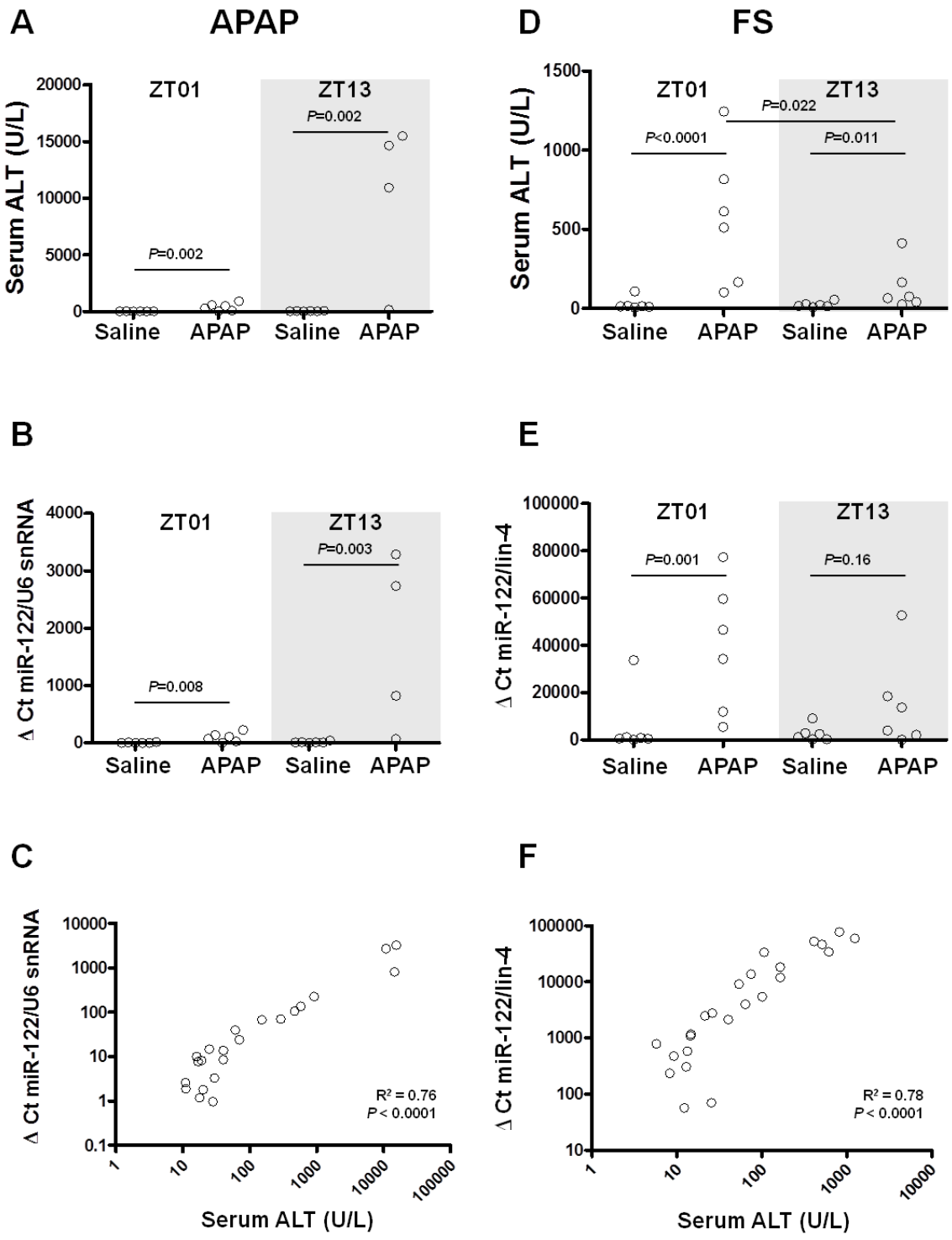

Figure 5.2: APAP and FS-induced liver injury is dependent on the time of day of administration. Serum ALT activity and serum miR-122 levels were measured from mice treated with either APAP (350 mg/kg, i.p.) or FS (400 mg/kg, i.p.). Each open circle represents an individual biomarker value. Statistical P-values are shown in the panels. Panels show grouped controls (saline-treated) vs drug-treated at ZT01 (white background) or ZT13 (shaded background). Serum ALTs are shown in panels A (APAP) and D (FS). Serum miR-122 levels are shown in panels B (APAP) and E (FS). Biomarker correlations are shown in panels C (APAP) and F (FS).

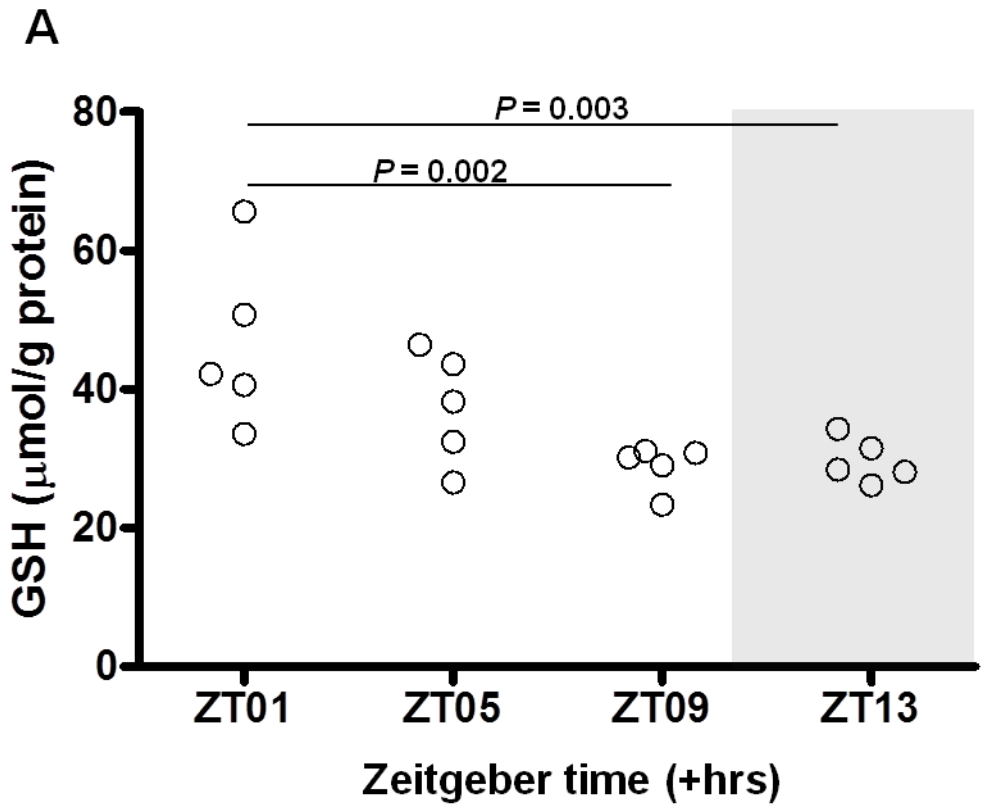

Figure 5.3: Hepatic GSH levels follow a circadian rhythm. Hepatic GSH levels were measured in individual mice culled at ZT01, ZT05, ZT09 and ZT13 (n=5). The panel shows grouped data where each open circle represents an individual GSH value obtained for each mouse. The shaded area indicates the dark-phase (starting at ZT12). Statistical significance is assigned in the panel (Kruskall-Wallis test).

5.3.3 Hepatic GSH levels are higher in the morning than in the evening.

Livers were harvested from normal untreated mice at ZT01, ZT05, ZT09 and ZT13 (n=5) before being snap-frozen on nitrogen and stored at -80°C until use. Hepatic GSH was measured from 50 mg tissue as described. Hepatic GSH levels were standardised to protein levels using the Lowry method. Levels were highest at ZT1 and declined at ZT05 exhibiting a 20% drop (figure 5.3; table 5.5). Hepatic GSH levels reached a nadir at ZT09 with a 38% drop (compared to ZT01) and levels remained 36% lower at ZT13. Statistical significance was observed between ZT01 vs ZT09 (P = 0.002) and ZT13 (P = 0.003).

	ZT01	ZT05	ZT09	ZT13
GSH µmol/g protein (+SD)	**46.6** (12.3)	**37.4** (8.1)	**28.9** (3.2)	**29.7** (3.2)

Table 5.5: GSH levels over the circadian phase

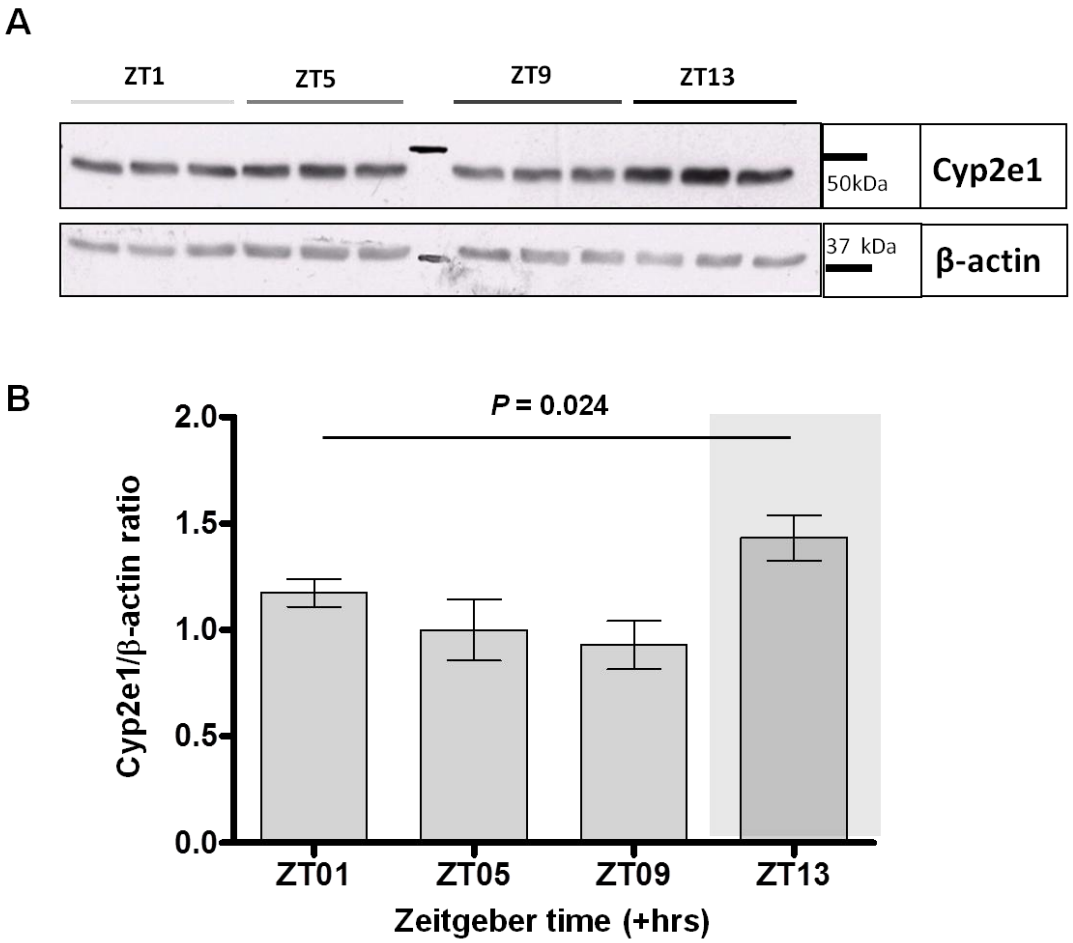

Figure 5.4: Hepatic CYP2E1 levels follow a circadian rhythm. Cyp2e1 levels were probed in pooled liver homogenates using a specific Cyp2e1 antibody. Each sample was run in triplicate on the same gel. β-actin levels ensured equal loading. A typical blot showing Cyp2e1 and β-actin are represented in panel A. Densitometric analysis of this blot is shown in panel B. Gray bars represent the mean ratio between Cyp2e1 and β-actin, and the bars represent the SD. The shaded area indicates the dark-phase. Statistical significance is assigned in the panel (Two-way ANOVA). Average (SD) densitometry ratios were 1.17 (0.07), 1.00 (0.14). 0.93 (0.11) and 1.43 (0.11) for ZT01, ZT05, ZT09 and ZT13 respectively.

5.3.4 Hepatic Cyp2e1 levels are higher at ZT13 compared to ZT01

To investigate the circadian variation in hepatic Cyp2e1 levels, livers were extracted at ZT01, ZT05, ZT09 and ZT13 (n=6). Liver homogenates were generated from individual mice, in PBS. Pools were generated for each group based on extraction time, with an equal amount of protein from individual samples contributing to the pool. Hepatic Cyp2e1 was measured via immunoblotting as described. Protein levels were visualised on autoradiography film (figure 5.4A) and then semi-quantified by densitometry (5.4B). To ensure equal protein loading, β-actin was also measured. Densitometric analysis of Cyp2e1 was standardised against β-actin. The immunoblot was repeated 3 times to ensure reproducibility. This data shows that hepatic Cyp2e1 levels were 22% higher in mice at ZT13 compared to ZT01 (P=0.024).

5.3.5 PEG-400 is an unsuitable vehicle for DILI studies

PEG-400 was investigated for hepatotoxicity after unexpected rises in serum ALT activity were observed during DILI studies. PEG-400 was used as the vehicle of choice due to apparent superior safety over DMSO and the poor solubility of FS in corn oil and aqueous preparations. FS chronotoxicity studies, we observed rises (> 50 U/L) in serum ALT activity (figure 5.5A) after morning (mean ALT = 80.8) and evening dosing (mean ALT = 319.8). In one mouse, a serum ALT activity of 968 was recorded, suggesting substantial liver injury had occurred. Serum miR-122 levels were also measured to rule out non-specific ALT rises. In the same animals, mean miR-122 levels after morning and evening dosing were ΔCt 0.06 and 15.51 respectively (figure 5.5B). The animal with high ALT exhibited a serum miR-122 ΔCt of 89.3.

To rule out batch-specific effects (with respect to mouse batch and chemical batch), new batches of PEG were tested from two suppliers (Sigma-Aldrich and Fisher Scientific) in a separate mouse experiment. Furthermore, in one group, PEG was diluted 2:1 with saline (this concentration dissolves FS) to test if hepatotoxicity could be abolished with a more physiological vehicle. The data shows that serum ALTs were raised in all mice (n=4) treated with PEG from either suppler (Aldrich - mean ALT = 421 U/L; Fisher - mean ALT = 362 U/L) (figure 5.5C). Serum ALTs were also raised in all mice administered with the 66% PEG (v/v) (mean ALT = 162), although this was significantly lower than the 100% (Sigma) group $P = 0.02$.

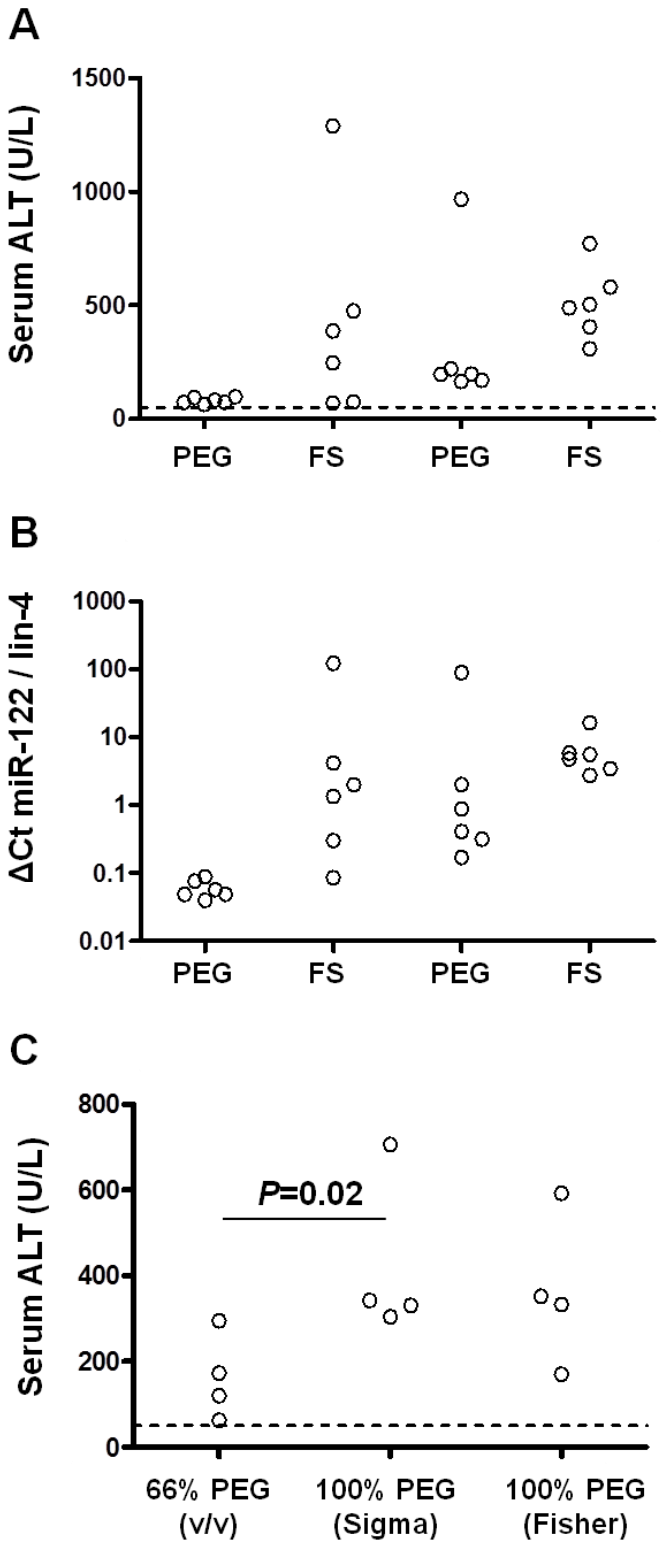

Figure 5.5: PEG-400 causes serum ALT rises independent of time of day or batch. In chronotoxicity studies using FS, PEG was administered to mice as vehicle controls. Serum ALTs are raised in mice who received PEG only. Panels show serum ALT activity (A) and serum miR-122 levels (B) in groups receiving PEG and PEG/FS at morning or evening. The dashed line in panels A and C indicates the ULN for ALT activity in mice. Panel C shows serum ALT activities in a separate batch of mice administered 66% or 100% (v/v) from different suppliers. Statistical significance is displayed in the panel (Kruskall-Wallis test).

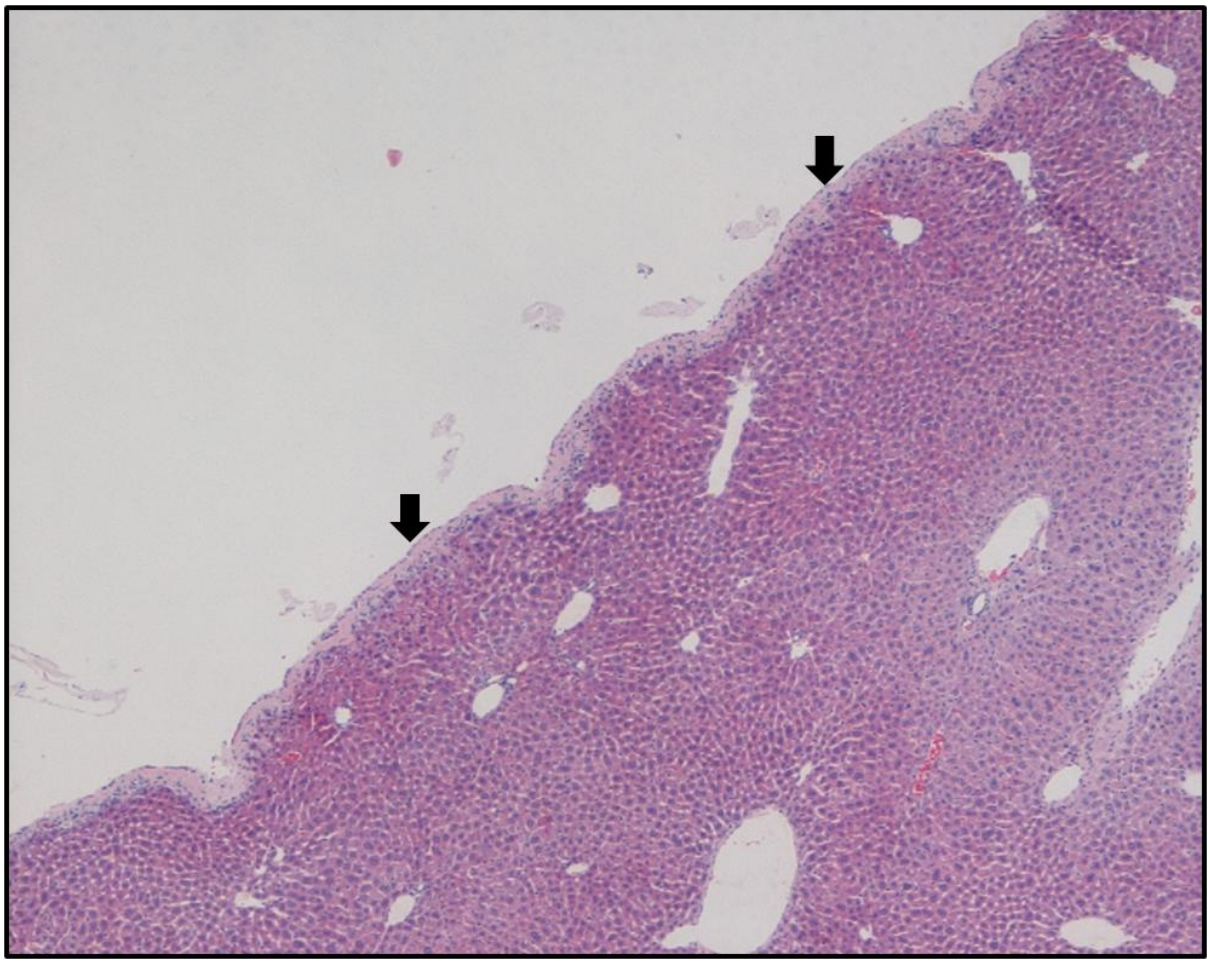

Figure 5.6: PEG-400 causes one- to two-cell deep subcapsular hepatic necrosis in mice. Formalin-fixed liver sections of the right lobe were stained with H&E. The image shows the edge of a liver section, including the liver capsule. One- to two-cell deep subcapsular necrosis is visible (black arrows). Magnification = 4x.

PEG-induced hepatotoxicity was confirmed by histology in FFPE preparations derived from formalin-fixed livers. Histology revealed one- to two-cell deep subcapsular necrosis in all control animals administered PEG-400 (figure 5.6) which account for the rises in circulating ALT and miR-122 levels.

5.4 Discussion

Circadian rhythms regulate many physiological processes and metabolic systems including those implicated in drug disposition. Many drugs are known to exert differences in efficacy and/or toxicity depending on the time-of-day they are administered, which can be attributed to circadian fluctuations in a drug's pharmacokinetics or pharmacodynamics. Circadian rhythms are regulated at the molecular level by clock genes which exhibit substantial temporal changes in expression over the circadian phase. In this chapter, we confirm that in untreated young mice, robust, high-amplitude oscillations were observed in the expression of clock genes and genes known to be regulated directly by the clock (figure 5.1). The genes which expressed the largest change in expression in the time-frame analysed were DBP, BMAL1 and REV-ERBα, three genes which are known to exhibit large circadian variations in expression. This suggests that the effects of the biological clock on key transcription factors can be substantial. DBP, and other related PAR-domain basic leucine zipper (PAR bZip) transcription factors have been implicated in regulating the transcription of many genes including those directly involved in drug disposition (Gachon *et al*, 2006). The expression of PER2 and CRY1 showed milder variations over this time-frame whilst SIRT1 and RORɣ remained consistent over all times analysed. The phases and amplitudes of the clock gene expression in our model were in accordance with other published mouse models (Zhang et al, 2009). This data confirms that the young CD-1 male mouse model is an applicable model for us to study the role of circadian rhythms in DILI.

Chronotoxicity of two model hepatotoxins was then assessed by morning and evening administration of fixed toxic doses of either APAP (350 mg/kg) or FS (400 mg/kg) in the young mouse model (figure 5.2). APAP is an analgesic compound known to cause centrilobular necrosus in man and rodent models. FS is a potent loop diuretic which causes centrilobular necrosis in mice, but not in man. In contrast to APAP, FS does not cause GSH

during the evolution of hepatotoxicity. These hepatotoxins were used as chemical tools to study the role of circadian rhythms on DILI and selected based on their disparate toxic mechanisms. The data shows that there is a clear difference in murine sensitivity to APAP between morning and evening administration. Evening administration (ZT13) of APAP caused more severe liver injury than morning administration, as determined by two circulating biomarkers of hepatotoxicity: serum ALT activity and serum miR-122 levels. This time-of-day dependent toxic response in mice has been reported by other groups who also show increased sensitivity in the early dark-phase (Matsunaga *et al*, 2004, Kim & Lee *et al*, 1998). The differences in chronotoxicity were previously attributed to rhythmic levels of Cyp2e1 and hepatic GSH. In this chapter, further experiments set out to confirm whether these changes are applicable in our model.

In contrast, the chronotoxicity exhibited by FS was different to APAP. FS produced a more mild toxicity after 8 hours and this was slightly more pronounced after morning administration. The metabolism of FS has yet to be fully elucidated in mice. However, it is known that FS does not deplete GSH and a pan-CYP inhibitor protects against hepatotoxicity (Williams et al, 2007). This suggests that toxicity is mediated by a chemically-reactive metabolite, possibly an epoxide or dialdehyde derivative of FS. Clearly, an understanding of the enzymology of FS metabolism is required to further investigate the basis for the chronotoxicity observed with FS. However, this time-of-day dependence on toxicity is much more modest in comparison to APAP. APAP chronotoxicity can be attributed largely to the circadian rhythm of hepatic GSH levels which is a key determinant of APAP-induced hepatotoxicity. However, this does not seem important in FS-induced hepatotoxicity.

To explore the molecular basis of these observations, the levels of Cyp2e1 were measured in pooled liver homogenates generated from six mice per time-point over the light-phase (ZT01-ZT13). We observed that hepatic Cyp2e1 levels were constant over the early light phase but increased approximately 20% during the early dark phase (figure 5.4). These data suggest that the metabolism of APAP may not remain consistent over the day. Higher levels of Cyp2e1 during the early dark phase suggests that there is a greater propensity for APAP to undergo bioactivation and form the toxic metabolite. Previously published data shows that Cyp2e1 levels follow a circadian rhythm in mouse liver (Matsunaga et al, 2008). The same report shows that HNF1α, a circadian nuclear transcription factor, is implicated in the periodical transcription of Cyp2e1 as mRNA and protein levels increase steadily in the early dark phase in accordance with the data shown here. Furthermore, an alternative theory suggests that a shift from carbohydrate metabolism to a more lipolytic energy source may account for increased Cyp2e1 production (Bruckner et al, 2002). Mice are nocturnal animals and rest during the day, therefore they do not feed and switch energy sources to maintain glucose homeostasis. A by-product of lipid metabolism is ketone formation (including acetone) which has been detected in mouse serum at an early evening time-point (Bruckner et al, 2002). Acetone and other ketones are known to induce Cyp2e1 expression (Forkert *et al*, 1994). The circadian nature of Cyp2e1 levels may lie at a crossroads between clock-mediated transcriptional regulation via HNF1α and daily exposure to inducers of Cyp2e1 due to feeding rhythms. To further explore the molecular basis governing the circadian rhythm behind APAP-induced ALI, a global proteomic analysis is warranted to identify other candidate determinants that may contribute to the chronotoxicity of APAP and other drugs. However, a transgenic model may be needed to fully elucidate the role of the hepatic clock during DILI, due to cross-talk between feeding rhythms and entrainment of the hepatic clock.

Hepatic GSH levels were measured in mice with access to food and water *ad libitum* at time points from early light-phase to early dark-phase. GSH is one of the most important antioxidants as it sequesters many electrophilic species including NAPQI, the reactive metabolite of APAP. It is found abundantly in the liver where it acts as a multifunctional peptide, maintaining thiol status, providing antioxidant defence and detoxifying toxic species. GSH status in the hepatocyte is therefore considered a function of the detoxification potential of the liver. We observed that GSH abundance in the hepatocyte was highest in early morning and decreased steadily until ZT9 where it remained low through to ZT13 (figure 5.3). To understand why GSH levels were not constant we considered that the synthesis of GSH may not be static over a daily cycle. Two important factors which determine the rate GSH synthesis are constituent amino acid availability and GSH-generating enzyme activities (Lu, 2009). Methionine, an essential sulphur-containing amino acid derived from the diet, is implicated in the formation of cysteine, one of the constituent amino acids that comprise GSH. Cycles of methionine availability (feeding patterns) may contribute to the oscillatory nature of hepatic GSH levels throughout the day. Studies have shown that GSH can be depleted by either starvation or feeding on a protein-free diet (Jaeschke & Wendel, 1985), suggesting that methionine availability is a key determinant of hepatic GSH levels. Clearly, the circadian rhythm in hepatic GSH levels is an important feature that may influence the chronotoxicity of many hepatotoxins. Further work is required to measure Cyp2e1 activity over the circadian phase to test if changes in the levels of Cyp2e1 correlate with changes in Cyp2e1 activity.

The solubility of FS is extremely poor in aqueous vehicles (< 1 mg/mL). Previous studies using FS have used a variety of organic or oil-based solvents, including 10% DMSO and corn oil (Francois *et al*, 2007, Randle *et al*, 2007). However, DMSO is an inappropriate vehicle to study FS-induced liver injury due to DMSO-mediated white cell infiltration in the liver (Masson et al, 2008). Furthermore, corn oil is also unsuitable as large volumes would

be required to be dosed i.p. to deliver the appropriate amount of FS needed to evoke toxicity. Therefore, PEG-400 was used as a vehicle to administer FS, as used previously (Williams et al, 2007). However, an unexpected increase in serum ALT activity and elevated serum miRNA levels were observed in mice treated with PEG-400 alone, indicative of liver injury (figure 5.5). Subsequent studies using different batches of PEG confirmed these findings and apparent hepatotoxicity followed a dose-response trend. Finally, PEG-induced hepatotoxicity was confirmed via histopathology (figure 5.6). PEG-400 causes subcapsular necrosis in mice and therefore should not be considered as an appropriate vehicle for use in pre-clinical DILI studies. A non-toxic vehicle was identified in alkaline PBS (pH 8.0), which did not cause necrosis in any mice, as used by McGill *et al*, 2012. This safer vehicle was used in subsequent chronotoxicity studies shown in figure 5.2. Mechanistic studies using FS can now be performed in mouse models within the CDSS through use of a non-toxic vehicle.

In summary, a mouse model which is routinely used within the CDSS has an active liver-clock and exhibits high-amplitude circadian variations in clock genes and clock-controlled genes (i.e. DBP). This provides an appropriate model in which to study the time-of-day dependence on drug response. Using two model hepatotoxins, the data shows that mice are profoundly more sensitive to APAP when administered in the early dark-phase. In contrast, FS shows a milder injury with pronounced toxicity occurring after morning dosing. We have confirmed that GSH levels are highest in the early light-phase and reach a nadir at late light phase and early dark phase. Furthermore, Cyp2e1, the oxidative enzyme which yields the chemically reactive metabolite, has a higher abundance at early dark-phase which may promote the transformation of APAP to NAPQI and contribute to dark-phase hepatotoxicity. In this chapter, a safer vehicle was also identified for FS administration. A previously-used vehicle, PEG-400, is hepatotoxic and should not be considered appropriate for DILI studies in mice. These data together increase the understanding of the toxicity profile of two model hepatotoxins which should result in improvements in the design of toxicity experiments. This work provides a platform to further explore the mechanistic basis of chronotoxicity in

model hepatotoxins that may be applicable to other drugs associated with hepatotoxicity. Identifying the most appropriate time of day to administer drugs could provide enhanced efficacy or reduced risk in patients. Major advances have already been achieved in the cancer field with safer chemotherapy regimens based on refined rhythmic circadian administration optimised to improve drug tolerance in patients (Levi et al, 1997, Mormont & Levi, 2003). It remains to be seen if the same strategy can be applied to other drugs associated with risks of hepatotoxicity and other ADRs.

CHAPTER SIX

Concluding Discussion

6.1 Introduction

As discussed earlier, ADRs have a significant impact on patient health, healthcare systems and represent a major impediment in the generation of new medicines, being a main cause of drug attrition in pre-clinical settings (Kola & Landis, 2004; Lazarou et al, 1998; Pirmohamed et al, 2004). Despite a worldwide effort to investigate the reasons that underpin the formation of DILI, the casual mechanisms remain controversial and poorly defined. Clearly, better tools and more appropriate models are required to drive translational research in pre-clinical and clinical settings, in order to bridge DILI between molecule (i.e. defining chemical liabilities in NCEs), mouse (i.e. more appropriate models of DILI) and man (i.e. a better understanding of the relationship between drugs and patient populations). One of the most important tools needed to help advance research in the field of DILI is identification and development of novel biomarkers of liver injury. Identification of sensitive and specific markers of DILI is required *in vitro*, *in vivo* and in the clinic, so that they can complement or supersede the existing catalogue of biomarkers.

The existing set of validated DILI biomarkers in the clinic (and in the laboratory), are limited to the circulating aminotransferases (AST/ALT), and markers of functional impairment such as prothrombin time/INR or serum bilirubin. Whilst these markers have been validated for use in the clinic, limitations are recognised with these markers which impede research in drug development and similarly cause uncertainty in patient management in the clinic. The "gold-standard" marker of DILI is serum ALT activity. This enzyme is a good sensitive marker of DILI; however it lacks true liver-specificity as isoforms are expressed at moderate levels in the muscle tissue leading to the risk of false positives. Furthermore, in the clinic, whilst serum ALT activity is increased before markers of liver function impairment like prothrombin time, there is a distinct latent period in the first 12-18 hours that occurs with toxic doses of APAP, a model hepatotoxin that causes rapid centrilobular necrosis and potentially fatal ALF. Blood sampling within this latent time frame does not indicate any liver injury, even in patients who later develop substantial

hepatotoxicity. Biomarkers that rise at the earliest possible time would benefit the physician in identifying or ruling out injury in patients early. Furthermore, in the laboratory, despite a larger set of markers that are utilised to detect liver injury, none have superseded ALT. Clearly, novel markers have the potential to improve on these limitations that exist presently with the current set of markers. Whilst identifying and developing new DILI markers will be challenging, the advantages of doing so will benefit patients, clinicians and the pharmaceutical industry.

6.2 Circulating miR-122 as a novel marker of DILI

MiRNAs are small (approx 22 nucleotides in length) non-coding RNA species that have an important regulatory role in cells. MiRNAs have recently emerged as a promising class of biomarkers for a range of pathologies due to high abundances in cells, remarkable tissue enrichment and extracellular stability. To date, the potential of circulating miRNAs have been assessed in many disease settings such as cancer (Mitchell et al, 2008), Myocardial infarction (D'Alessandra et al, 2010), stroke (Gan et al, 2012), nephrotoxicity (Lorenzen et al, 2011) and hepatitis (Zhang et al, 2010). With respect to DILI, it was shown in a recent publication that circulating levels of liver-specific miRNAs (most notably miR-122 and miR-192) are substantially raised after toxic APAP exposure in mice (Wang et al, 2009).

The aim of this thesis was to further investigate the role of circulating miRNAs as potential markers of DILI. Using a similar approach to Wang and colleagues, the sensitivity of circulating miRNAs was tested in parallel to ALT, albeit in a younger CD-1 strain with *ad libitum* access to food. Despite the low-powered study, it was clear that rises in circulating miRNAs occurred early after APAP administration resulting in a statistically significant rise at 2 hours when ALT had not yet risen (see chapter 2). This finding confirms the earlier detection of miR-122 using *in vivo* models. However, using the same model, a sensitivity

study did not show miR-122 performed better than ALT, although this may be attributed to the exposure time used in the original study, where time may have been a factor.

Also in chapter 2, *in situ* hybridisation studies were performed in healthy liver and liver exposed to toxic doses of APAP which revealed that miR-122 is lost early from liver tissue, which coincides with early detection in blood. This data also shows that loss of miR-122 is associated with cells that are not yet necrotic. This finding raises the suggestion that early release of miR-122 is mediated through an active mechanism, although it is likely that miR-122 is also lost passively via necrosis when more severe hepatotoxicity develops later. It is possible that hepatocytes are triggered into preferential loss of miR-122 as a means to drive proliferation and regenerate injured cells, due to the regulation of miR-122 on proliferation pathways. Furthermore, it has recently been shown that the form of circulating miR-122 is dependent on the mechanism of injury (Bala *et al*, 2012). Further studies are warranted to test the relationship between circulating forms of miR-122 and how they change over time as hepatotoxicity evolves.

In this thesis, the potential of circulating liver-enriched miRNAs to serve as informative clinical markers of liver injury was assessed retrospectively in two independent cohorts of APAP-overdose patients. The first cohort included a very heterogeneous group of 53 patients who presented at different times with various exposures of APAP. Some of these patients developed fatal liver failure, whilst others spontaneously recovered after transient rises in ALT. As discussed in chapter 3, the major conclusions from this study were: i) liver specific miRNAs (miR-122 and miR-192) are raised in two ALI cohorts, ii) miR-122 levels did not correlate with functional markers of liver impairment in the same samples, and iii) miR-122 levels returned to baseline sooner than serum ALT activity in follow-up analysis. These data provide the first evidence in man that liver-enriched miRNAs hold potential as biomarkers of DILI. However, because it is clear from this study that miR-122 did not correlate with markers of liver function, the dynamics/kinetics of circulating miR-122 during ALI deserve further investigation.

In order to further investigate miR-122 as a clinical marker of DILI, a separate patient cohort was characterised (see chapter 4). This cohort was distinct from the previous patient cohort in that the majority of these patients presented early after APAP overdose when serum ALT was in the normal range. None of these patients required liver transplantation, or died from severe toxicity. However, all patients required NAC therapy as indicated by presentation plasma APAP concentration. This study showed that miR-122 was raised earlier than ALT in a subgroup of patients who subsequently developed liver injury. Also, when miR-122 or ALT was not raised in patients, they did not develop injury at any time due to therapeutic intervention with NAC. These findings suggest that further development of miR-122 as a novel clinical marker of APAP-induced ALI is warranted, as this biomarker has the potential to provide the physician with an early indication of risk of a patient developing serious hepatotoxicity. A high miR-122 reading on admission, even if serum ALT activity is within the normal range might indicate that the patient is likely to develop liver injury at a later time and should be treated accordingly. Vice versa, if the presentation miR-122 is low in parallel with ALT, then the patient might be at lower risk of developing liver injury, and may even require less rigorous antidotal therapy, which could reduce costs and the likelihood of developing ADRs associated with antidotal therapy. Clearly, these are hypotheses which can be tested in prospective clinical studies.

6.3 miRNAs - bioanaltyical perspectives

Here, we took advantage of a taqman-based qPCR method that shows great analytical sensitivity (miRNA amplification) with the specificity of stem-loop primers that can discriminate between one nucleotide in the amplicon. Even so, questions remain about the most efficient strategy to quantify miRNAs: One consideration must be the starting biological matrix which is assayed; two major options being serum or plasma. Serum is the cell-free supernatant that is obtained after blood has clotted and the clot has been removed

via centrifugation. Plasma is the cell-free supernatant of blood that has not clotted due to the presence of an anticoagulant, and cells are removed via centrifugation. The purity of the resulting supernatant is an important factor to consider. Specific miRNAs are enriched in blood cells, therefore a thorough and consistent protocol is required with meticulous sample preparation. Substantial haemolysis due to red blood cell carry over or inappropriate sample handling/storage can lead to increases in baseline plasma miRNA levels. This can be a confounding factor: for example miR-16 is a popular choice of endogenous normaliser and also found at appreciable levels in red blood cells (Kirschner *et al*, 2011). Clearly, haemolysis could impinge on the utility of this miRNA to serve as a reference species. Serum is the most common blood-based fraction which is obtained from pre-clinical animals in the laboratory, and frequently in the clinic for serum ALT analysis. Importantly, it has been shown that miR-122 levels specifically do not differ considerably between serum and plasma in humans (Arroyo et al, 2011), but this has only been ascertained in healthy individuals and not in cases of liver injury where the circulating forms of miRNAs may be biologically different (Bala et al, 2012). Clearly, this represents a hypothesis that can be tested for in future work.

Plasma is sometimes used clinically to measure certain analytes such as glucose. For plasma, the main issue that needs to be considered is the choice of anticoagulant used. The major concern with plasma is the use of the popular anticoagulant heparin, which is a potent PCR inhibitor (Kroh et al, 2010). All heparinised plasma samples are incompatible with qPCR analysis and cannot be used for miRNA measurement, heparinase treatment of plasma can reduce the impact but other anticoagulants should be sought in the first instance (Kim *et al*, 2012). A side-by-side analysis of serum and plasma using various anticoagulants found that sodium fluoride/potassium oxalate (NaF/KOx) (commonly used for glucose analysis) provided the sensitivity for miR-16 and miR-223. Levels of these endogenous miRNAs were higher in NaF/KOx plasma tubes compared to EDTA plasma, sodium citrate plasma, serum and heparinised plasma. Intriguingly, the use of NaF/KOx tubes also improved the

sensitivity of exogenous 'spiked-in' miRNA species. This was not attributed to anticoagulant effects on PCR efficiency or RNA stability. Therefore, it is possible that NaF/KOx may improve the efficiency of the reverse transcription.

Another consideration is selection of starting volume of serum/plasma. Due to the abundance of miRNAs in serum and plasma coupled with the amplification technology of qPCR, miRNAs can be detected easily from very small volumes, as low as 10 µL (Kim *et al*, 2012). The same article found that increasing the starting volume from 50 µL to 200 µL did not increase the sensitivity of detection. In fact, paradoxically, miR-16 levels were lower when RNA was extracted using 200 µL of serum or plasma compared to 50 µL. This counterintuitive finding suggests that molecules that interfere with the qPCR assay are inherent in blood, and by reducing the starting volume, these molecules get diluted below a threshold that reduces this interference.

Thirdly, consideration should be given to the method of quantification. A standard curve is sometimes used against test samples to determine absolute copy number of target miRNAs. The risk of contamination is a factor when the same miRNA is used for the standard curve and samples, especially considering the relative copy numbers typically used for standard curve dilutions. A less risky approach is to create a standard curve using a non-biological (synthetic) miRNA to use as a surrogate for the miRNA of interest (analagous to the use of a serum albumin standard curve in protein determination assays). However, RNA extraction and reverse transcription may not be 100% efficient and the copy number generated by using absolute quantification is not likely to be relevant to the actual biological level. Another approach is to use a reference species to standardise to, and use relative quantification via the 2^-(ΔΔCt) method, similar to the use of GADPH or actin for mRNA measurement. The advantage of this approach is the ability to utilise endogenous normalisers as a reference to control for biological and technical variation in serum/plasma simultaenously. To date, no universal normaliser exists and many reference species have been used in this rapidly evolving field including U6 snRNA (Zhang et al, 2010), let-7d (Qi et al), miR-16 (Wang et

al, 2010) and miR-24 (Baraniskin et al, 2011) among others. From correspondence between our group and Qi and colleagues (Qi et al, 2012), let-7d was highlighted as a potentially superior normaliser over U6 snRNA with less variation between patient groups. Qi *et al* found that U6 snRNA levels were significantly different among young and aged subjects, however, no relationship existed between U6 snRNA and age in the APAP-induced ALI cohort (n=53; data not shown). An alternative quantification approach for circulating miRNA studies is through use of the addition of 'spiked-in' exogenous normalisers. Usually, this method involves the addition of a synthetic or non-mammalian miRNA species that is added to denatured serum/plasma samples. Care should be given as exogenous 'naked' miRNA exhibits altered biological stability, and must only be added when the biofluid is fully denatured (ectopic miRNAs degrades immediately when introduced to non-dentaured serum, Mitchell *et al*, 2008). Using exogenous miRNAs as a reference is an increasingly popular approach as it offers extremely low variation between samples. However, whilst this is an excellent approach to control for technical variation, it does not control for biological variation. In the clinical samples here studied, it was important to use an endogenous normalisation approach to control for biological variation through use of U6 snRNA and later let-7d. Since the samples were generated in the clinic, this provides greater risk of inter-sample variation through inconsistent sampling technique, processing, storage and shipment of samples between laboratories. Typically, 5% of clinical samples that were assayed in the studies contained within this thesis had degraded miRNA and were not used for further analysis.

Other biological/bioanalytical variables that should be investigated in future work include the effects of circadian rhythm on circulating miRNA levels, fed versus fasted subjects (particularly with respect to lipid content in the blood after fatty meals), white blood cell count effects (i.e. in HIV patients) and sampling method (optimisation of needle gauge used in phlebotomy/site of blood draw).

6.4 Establishment of miR-122 as a clinical biomarker of DILI

One of the short-term challenges to further develop miR-122 as a clinical marker will be to identify baselines and limits of normal for miR-122 in healthy volunteers so that "a rise" can be set against a clear reference, analogous to 50 U/L which is used for serum ALT activity in the clinic. This can only be done in prospective studies with clear sampling protocols in place before a large *n*-number of patients can be profiled. Before then, a consistent bioanalytical method needs to be approved and universally accepted in the field. Currently, by far the most popular method for miRNA quantification is based around end-point or qPCR. Whilst this technique offers high-sensitivity and high-specificity, a typical assay takes at least 6 hours to complete, from sample RNA extraction to amplification, quantification and analysis. This time frame is incongruous to the needs of the clinic. As described, APAP-induced ALI is a very rapid illness that can lead to potentially fatal ALF if the correct clinical decision is not made in a timely fashion. In particular for APAP-induced ALI, the correct decision must be made quickly in the early-phase post APAP-ingestion, as soon as possible after emergency room presentation. Therefore, a robust, cost-effective and rapid bioanalytical method is needed for miRNA quantification in the clinic. From a bioanalytical perspective, time-consuming amplification-based technology is unsuitable. Therefore, a method to detect miRNAs directly in the femtomolar range is required. Despite this huge challenge, several novel methods of direct, fast miRNA quantification have been described with high potential for use in clinical scenarios (reviewed in de Plannell-Sageur & Rodicio, 2011). Promising methods for direct miRNA quantification include solution-phase bioluminescene (*Renilla* luciferase-quantum dot and DNA hybridisation; Cissell et al, 2008a), fluorescence correlation spectrometry (DNA-based probe with fluorescence label; Neely *et a*l, 2006), and bioluminescence miRNA detection (protein complementation and DNA hybridization; Cissell et al, 2008b). Clearly, these methods need to be developed further and tested against existing techniques of miRNA detection to ensure novel assays are

sensitive, specific and robust. Ultimately, any technique for miRNA detection/measurement in the clinic will require full validation by regulatory bodies.

The data contained herein suggests that circulating miR-122 are at least as informative as ALT in both pre-clinical models and clinical settings of APAP-induced ALI. Coupled with superior liver-enrichment, high bioanalytical sensitivity, non-invasive sampling source, relatively inexpensive assay costs and low sampling volume, high mammalian conservation, miR-122 holds real potential to be a powerful translational biomarker of DILI. Clearly, further development of this biomarker is warranted. So far, this biomarker has been assessed in settings of acute liver injury. It remains to be seen if miR-122 can be as informative in chronic disease states or in idiosyncratic cases of DILI. This represents a clear hypothesis that can be tested in future work. At the moment, there is lack of knowledge on baselines and dynamic ranges of circulating levels of miRNAs in patients and in pre-clinical species. Currently, an international consortium (Safer and Faster Evidence-Based Translation, SAFE-T) developed by the Innovative Medicines Initiative (IMI) is facilitating research into a panel of exploratory biomarkers including miR-122. This should augment the development and provide a platform for the clinical validation of miR-122 as a biomarker of DILI.

6.5 The role of circadian rhythms in drug safety

Circadian rhythms have been found to regulate core biology in mammalian species (as well as in plants and bacteria) in a profound way. The extent of circadian regulation at the molecular level is extensive with 2-10% of the transcriptome exhibiting circadian variation (Kornmann et al, 2001; Panda et al, 2002). A number of publications have highlighted that genes implicated in drug disposition (including drug metabolism) exhibit circadian variation at the mRNA or protein level. For example, in mice devoid of three clock-controlled PAR bZIP transcription factors (DBP, TEF HELF), many genes involved in xenobiotic metabolism were found to be significantly underexpressed including members of the CYP450 superfamily (Cyp2a4/5, Cyp2b9, Cyp2b10, Cyp2c37, Cyp2c50), carboxylesterases

(Ces1, Ces3), UGTs (UGT2b37) GSTs (Gstα3, Gstθ1), aldehyde dehydrogenases (Aldh1a1, Aldh1a7) and drug transporters (MRP4, BCRP1) (Gachon et al, 2006). This work suggests that a catalogue of genes involved in xenobiotic detoxification is regulated directly by the hepatic molecular clock. Clearly, this is likely to have implications on the time-of-day variation in drug response.

A number of drugs have shown to exhibit circadian variation in safety and efficacy in the clinic. A pharmacokinetic study of a sustained-release theophylline preparation found that it exhibited marked pharmacokinetic circadian variation in asthmatic children; levels were substantially lower when administered in the morning compared to evening dosing (Smolensky et al, 1987). Moreover, in cancer patients, a pronounced circadian rhythm in plasma 5-fluorouracil (5-FU) concentration exists despite constant rate intravenous infusion (Petit et al, 1988; Metzger et al, 1994). Circadian variation in drug response also occurs in pre-clinical animals. This is exemplified by the diurnal variation observed in halothane-induced sleeping time which is doubled during the light phase compared to the dark phase (Turnbull & Watkins, 1976). Furthermore, the toxicity of archetypal hepatotoxins APAP and carbon tetrachloride also show significant circadian variation (Matsunaga et al 2004; Bruckner et al, 2002).

Here, the potential chronotoxicity of two model hepatotoxins were assessed in a young CD-1 mouse model. In this model, four out of six core clock genes showed high-amplitude (up to 40-fold changes) time-of-day variation in expression. Furthermore, a direct clock-controlled PAR bZIP transcription factor known to be drive the expression of drug-processing genes, DBP, also showed marked circadian variation (up to 45-fold change in expression). The toxicity of both APAP and FS showed time-of-day dependence on toxicity. A moderately toxic dose of APAP (350 mg/kg) produced 26-fold higher levels of serum ALT activity after evening administration compared to morning administration. Serum miR-122 levels correlated with serum ALTs and also were 18-fold higher after evening administration compared to morning administration. These findings coupled with the increased lethality of

this 'moderate' dose of APAP (33% evening vs 0% morning) shows that APAP-induced ALT also shows circadian toxicity in the young CD-1 male mouse. This finding corroborates other mouse studies where toxic doses of APAP produced more severe injury after evening administration (Matsunaga et al, 2004). In comparison, the toxicity evoked by FS showed a reverse pattern in chronotoxicity, serum ALT and miR-122 levels were 4.4-fold and 2.8-fold higher after morning administration compared to evening administration. The observation that FS was not more toxic in the evening fits with the hypothesis that GSH does not deplete hepatic GSH. Interestingly, FS also shows circadian rhythm in its pharmacology in the rat (Stoynev *et al*, 1986) but it is not known if this is associated with the circadian rhythm in hepatotoxicity. Currently, there is a lack of knowledge with respect to the metabolism of FS in rodents. A pan-CYP inhibitor protects against FS-induced ALI in rodents which suggests toxicity is manifested through production of a CRM. Future work is required to characterise the metabolism of FS in the mouse in order to explore the mechanisms behind FS chronotoxicity. Furthermore, it is likely that the model is under severe pharmacological stress (400 mg/kg is 100-fold higher dose than pharmacological levels) in the kidney. It is currently unknown if this is a function of hepatotoxicity.

To explain these observations, we confirmed that a circadian rhythm exists in hepatic GSH levels in our model which reflects previously published work (Jaeshke & Wendel, 1985; Matsunaga et al, 2004). The circadian variation in GSH levels is likely to reflect the circadian rhythm in feeding as it has been shown that switching the natural feeding time to day-time feeding (during the rest phase of the mouse) reverses the periodicity of the GSH cycle (Matsunaga et al, 2004). It is difficult to study the role of the hepatic clock in isolation due to the myriad of networks which govern circadian regulation such as rhythms in behaviour and temperature. For example, feeding rhythms have been shown to act as a zeitgeber on the molecular oscillator in hepatocytes. Periodical feeding rhythms cause rhythms in the energy levels in hepatocytes (AMP:ATP). This can be sensed by liver kinases including LKB (Lamia *et al*, 2009). Such kinases phosphorylate AMPK which target *bona*

fide clock genes such as CRY1 for proteasomal degradation. Not only can food availability affect clock gene dynamics but it can actively change hepatic rhythmic gene expression (Vollmers *et al*, 2009). To study the role of the molecular clock in isolation, a liver-specific conditional transgenic is currently being assessed within the CDSS. Using such an approach, the molecular clocks should be abrogated in a liver-specific fashion due to the engineering of the model (based on Kornmann et al, 2009). This will allow us to test the system using model hepatotoxins with and without a functioning hepatic clock.

Also, in normal CD-1 mice, hepatic Cyp2e1 levels were 20% higher in the evening compared to morning levels. This is likely to play a role in the toxicity of APAP, as this CYP isozyme plays a major role in the conversion of APAP to the toxic metabolite, NAPQI. Further work will be to ascertain if these changes at the protein level correlate with Cyp2e1 activity. Previously, it has been shown that Cyp2e1 levels at the mRNA and protein are higher during the early dark phase in rodents (Matsunaga et al, 2008; Bruckner et al 2002). This has been attributed to rhythmic levels of HNF1α, a circadian nuclear transcription factor known to regulate Cyp2e1 expression (Matsunaga et al, 2008). Furthermore, serum acetone levels follow a circadian rhythm which peak in the early dark phase. Acetone may play a role in Cyp2e1 circadian rhythm due to its ability to induce Cyp2e1 (Forkert et al, 1994). It will be worthwhile in future work to characterise the circadian profile of other Cyp450s at the mRNA, protein and activity level in rodent models, notably Cyp3a and Cyp1a isoforms which may play a role in APAP-induced ALI. A detailed knowledge of the circadian profile of a catalogue of genes implicated in drug disposition (particularly genes involved in phase I, phase II and phase III drug metabolism) will help predict chronotoxicity *in vivo* models. To this end, a global proteomic analysis of liver tissue harvested over the circadian phase may help explore the molecular mechanisms governing the chronotoxicity with APAP, FS and other drugs.

These studies show that knowledge of the circadian profile at the molecular levels of key determinants that ultimately effect drug response can explain the time-of-day variation

observed with drugs. Identifying the most appropriate time of day to administer drugs could provide enhanced efficacy or reduced risk in patients. Major advances have already been achieved in the cancer field with safer chemotherapy regimens based on refined rhythmic circadian administration optimised to improve drug tolerance in patients (Levi et al, 1997; Mormont & Levi, 2003). Similar methodologies could be applied to other drugs currently used in the clinic that are associated with poor efficacy or limited by safety issues. Chronopharmacology studies may also become standard practice in the development of NCEs to identify the optimal time for drug administration in order to maximise efficacy and minimise toxicity. Essentially, a better understanding in the dynamics of the molecular clock and how it affects drug response may improve the risk:benefit ratio of drugs in clinical and pre-clinical settings.

6.5 Final comments

The hypotheses that were addressed in this thesis were:

- Circulating liver-enriched miRNAs can be used as biomarkers of liver injury in an APAP model of DILI and a FS model of DILI.

Comment: Circulating miR-122 was able to inform on both APAP-induced ALI and FS-induced ALI in a young CD-1 mouse model. Circulating miR-122 correlated with the gold-standard marker of ALT, providing sensitive and specific detection of liver injury.

- Circulating liver-enriched miRNAs can be used as sensitive, non-invasive biomarkers to detect DILI in a heterogeneous cohort of APAP-overdose patients.

Comment: For the first time, it is shown that serum levels of liver-enriched miRNAs (miR-122 and miR-192) are raised in a cohort of patients with varying degrees of APAP-induced ALI. Most promising was serum miR-122 levels which correlated with serum ALT and exhibited reduced circulatory half-life.

- Circulating liver-enriched miRNAs can detect APAP-induced ALI before ALT and can predict patients who will develop acute liver failure.

Comment: In a separate cohort of specific patients who presented early after APAP overdose, miR-122 was raised before serum ALT. Most strikingly, miR-122 was raised in the patients who later developed liver injury (as determined by peak serum ALT activity) and developed coagulopathy (as determined by peak INR). If it can be shown in prospective clinical studies that miR-122 can predict peak INR (a marker of ALF), then analysis of miR-122 has potential to be routinely used in the clinic and help drive clinical decision making.

- APAP and FS murine models of DILI show distinct time-of-day dependence on severity of toxicity.

Comment: In a routinely-used murine model of DILI, both APAP and FS show time-of-day dependence on severity of hepatotoxicity. Strikingly, APAP exhibits severe lethal toxicity when a moderate dose is administered during the evening. In contrast, FS, which confers toxicity through a different mechanism, shows a reversed circadian rhythm in hepatotoxicity. For APAP, chronotoxicity can be associated with diurnal rhythms in hepatic GSH levels and Cyp2e1 content.

BIBLIOGRAPHY

Adler M, Hoffmann D, Ellinger-Ziegelbauer H, Hewitt P, Matheis K, Mulrane L, Gallagher WM, et al. Assessment of candidate biomarkers of drug-induced hepatobiliary injury in preclinical toxicity studies. Toxicol Lett 2010; **196**(1): 1-11.

Agarwal R, MacMillan-Crow LA, Rafferty TM, Saba H, Roberts DW, Fifer EK, James LP, et al. Acetaminophen-induced hepatotoxicity in mice occurs with inhibition of activity and nitration of mitochondrial manganese superoxide dismutase. J Pharmacol Exp Ther 2011; **337**(1): 110-116.

Agress CM, Jacobs HI, Glassner HF, Lederer MA, Clark WG, Wroblewski F, Karmen A, et al. Serum transaminase levels in experimental myocardial infarction. Circulation 1955; **11**(5): 711-713.

Akhtar RA, Reddy AB, Maywood ES, Clayton JD, King VM, Smith AG, Gant TW, et al. Circadian cycling of the mouse liver transcriptome, as revealed by cDNA microarray, is driven by the suprachiasmatic nucleus. Current Biology 2002; **12**(7): 540-550.

Aleksunes LM, Campion SN, Goedken MJ, Manautou JE. Acquired resistance to acetaminophen hepatotoxicity is associated with induction of multidrug resistance-associated protein 4 (Mrp4) in proliferating hepatocytes. Toxicological Sciences 2008; **104**(2): 261-273.

Altuvia Y, Landgraf P, Lithwick G, Elefant N, Pfeffer S, Aravin A, Brownstein MJ, et al. Clustering and conservation patterns of human microRNAs. Nucleic Acids Res 2005; **33**(8): 2697-2706.

Amacher DE. The discovery and development of proteomic safety biomarkers for the detection of drug-induced liver toxicity. Toxicol Appl Pharmacol 2010; **245**(1): 134-142.

Amacher DE. Serum transaminase elevations as indicators of hepatic injury following the administration of drugs. Regulatory Toxicology and Pharmacology 1998; **27**(2): 119-130.

Anand AC, Nightingale P, Neuberger JM. Early indicators of prognosis in fulminant hepatic failure: An assessment of the king's criteria. J Hepatol 1997; **26**(1): 62-68.

Antoine DJ, Jenkins RE, Dear JW, Williams DP, McGill MR, Sharpe MR, Craig DG, et al. Molecular forms of HMGB1 and keratin-18 as mechanistic biomarkers for mode of cell death and prognosis during clinical acetaminophen hepatotoxicity. J Hepatol 2012; **56**(5): 1070-1079.

Antoine DJ, Williams DP, Jenkins AK, Regan SL, Sathish JG, Kitteringham NR, Park BK. High-mobility group box-1 protein and keratin-18, circulating serum proteins informative of acetaminophen-induced necrosis and apoptosis in vivo. Toxicological Sciences 2009; **112**(2): 521-531.

Antoine DJ, Williams DP, Kipar A, Laverty H, Kevin Park B. Diet restriction inhibits apoptosis and HMGB1

oxidation and promotes inflammatory cell recruitment during acetaminophen hepatotoxicity. Molecular Medicine 2010; **16**(11-12): 479-490.

Arasu P, Wightman B, Ruvkun G. Temporal regulation of lin-14 by the antagonistic action of two other heterochronic genes, lin-4 and lin-28. Genes and Development 1991; **5**(10): 1825-1833.

Arendt J, Skene DJ. Melatonin as a chronobiotic. Sleep Medicine Reviews 2005; **9**(1): 25-39.

Arroyo JD, Chevillet JR, Kroh EM, Ruf IK, Pritchard CC, Gibson DF, Mitchell PS, et al. Argonaute2 complexes carry a population of circulating microRNAs independent of vesicles in human plasma. Proc Natl Acad Sci U S A 2011; **108**(12): 5003-5008.

Bajt ML, Knight TR, Lemasters JJ, Jaeschke H. Acetaminophen-induced oxidant stress and cell injury in cultured mouse hepatocytes: Protection by N-acetyl cycteine. Toxicological Sciences 2004; **80**(2): 343-349.

Bala S, Petrasek J, Mundkur S, Catalano D, Levin I, Ward J, Alao H, et al. Circulating microRNAs in exosomes indicate hepatocyte injury and inflammation in alcoholic, drug-induced, and inflammatory liver diseases. Hepatology 2012; .

Balsalobre A, Damiola F, Schibler U. A serum shock induces circadian gene expression in mammalian tissue culture cells. Cell 1998; **93**(6): 929-937.

Baraniskin A, Kuhnhenn J, Schlegel U, Chan A, Deckert M, Gold R, Maghnouj A, et al. Identification of microRNAs in the cerebrospinal fluid as marker for primary diffuse large B-cell lymphoma of the central nervous system. Blood 2011; **117**(11): 3140-3146.

Bartel DP. MicroRNAs: Genomics, biogenesis, mechanism, and function. Cell 2004; **116**(2): 281-297.

Bartolone JB, Birge RB, Bulera SJ, Bruno MK, Nishanian EV, Cohen SD, Khairallah EA. Purification, antibody production, and partial amino acid sequence of the 58-kDa acetaminophen-binding liver proteins. Toxicol Appl Pharmacol 1992; **113**(1): 19-29.

Basyuk E, Suavet F, Doglio A, Bordonné R, Bertrand E. Human let-7 stem-loop precursors harbor features of RNase III cleavage products. Nucleic Acids Res 2003; **31**(22): 6593-6597.

Bateman DN. Limiting paracetamol pack size: Has it worked in the UK? Clin Toxicol 2009; **47**(6): 536-541.

Bernal W, Wendon J, Rela M, Heaton N, Williams R. Use and outcome of liver transplantation in acetaminophen-induced acute liver failure. Hepatology 1998; **27**(4): 1050-1055.

Berson DM, Dunn FA, Takao M. Phototransduction by retinal ganglion cells that set the circadian clock. Science 2002; **295**(5557): 1070-1073.

Bihrer V, Friedrich-Rust M, Kronenberger B, Forestier N, Haupenthal J, Shi Y, Peveling-Oberhag J, et al. Serum miR-122 as a biomarker of necroinflammation in patients with chronic hepatitis C virus infection. Am J Gastroenterol

2011; .

Blazka ME, Elwell MR, Holladay SD, Wilson RE, Luster MI. Histopathology of acetaminophen-induced liver changes: Role of interleukin 1α and tumor necrosis factor α. Toxicol Pathol 1996; **24**(2): 181-189.

Bøggild H, Knutsson A. Shift work, risk factors and cardiovascular disease. Scandinavian Journal of Work, Environment and Health 1999; **25**(2): 85-99.

Bourdi M, Korrapati MC, Chakraborty M, Yee SB, Pohl LR. Protective role of c-jun N-terminal kinase 2 in acetaminophen-induced liver injury. Biochem Biophys Res Commun 2008; **374**(1): 6-10.

Bourdi M, Masubuchi Y, Reilly TP, Amouzadeh HR, Martin JL, George JW, Shah AG, et al. Protection against acetaminophen-induced liver injury and lethality by interleukin 10: Role of inducible nitric oxide synthase. Hepatology 2002; **35**(2): 289-298.

Bourdi M, Reilly TP, Elkahloun AG, George JW, Pohla LR. Macrophage migration inhibitory factor in drug-induced liver injury: A role in susceptibility and stress responsiveness. Biochem Biophys Res Commun 2002; **294**(2): 225-230.

Brown SA, Ripperger J, Kadener S, Fleury-Olela F, Vilbois F, Rosbash M, Schibler U. Cell biology: PERIOD1-associated proteins modulate the negative limb of the mammalian circadian oscillator. Science 2005; **308**(5722): 693-696.

Bruckner JV, Ramanathan R, Lee KM, Muralidhara S. Mechanisms of circadian rhythmicity of carbon tetrachloride hepatotoxicity. J Pharmacol Exp Ther 2002; **300**(1): 273-281.

Bruguerolle B. Chronopharmacokinetics: Current status. Clin Pharmacokinet 1998; **35**(2): 83-94.

Bulera SJ, Birge RB, Cohen SD, Khairallah EA. Identification of the mouse liver 44-kDa acetaminophen-binding protein as a subunit of glutamine synthetase. Toxicol Appl Pharmacol 1995; **134**(2): 313-320.

Chang J, Nicolas E, Marks D, Sander C, Lerro A, Buendia MA, Xu C, et al. miR-122, a mammalian liver-specific microRNA, is processed from hcr mRNA and may downregulate the high affinity cationic amino acid transporter CAT-1. RNA biology 2004; **1**(2): 106-113.

Chassard D, Bruguerolle B. Chronobiology and anesthesia. Anesthesiology 2004; **100**(2): 413-427.

Chen W, Koenigs LL, Thompson SJ, Peter RM, Rettie AE, Trager WF, Nelson SD. Oxidation of acetaminophen to its toxic quinone imine and nontoxic catechol metabolites by baculovirus-expressed and purified human cytochromes P450 2E1 and 2A6. Chem Res Toxicol 1998; **11**(4): 295-301.

Chendrimada TP, Gregory RI, Kumaraswamy E, Norman J, Cooch N, Nishikura K, Shiekhattar R. TRBP recruits the dicer complex to Ago2 for microRNA processing and gene silencing. Nature 2005; **436**(7051): 740-744.

Chomczynski P, Sacchi N. Single-step method of RNA isolation by acid guanidinium thiocyanate-phenol-chloroform

extraction. Anal Biochem 1987; **162**(1): 156-159.

Chyka PA, Seger D. Position paper: Single-dose activated charcoal. Journal of Toxicology - Clinical Toxicology 2005; **43**(2): 61-87.

Cissell KA, Campbell S, Deo SK. Rapid, single-step nucleic acid detection. Analytical and Bioanalytical Chemistry 2008; **391**(7): 2577-2581.

Cissell KA, Rahimi Y, Shrestha S, Hunt EA, Deo SK. Bioluminescence-based detection of microRNA, miR21 in breast cancer cells. Anal Chem 2008; **80**(7): 2319-2325.

Cohen SD, Khairallah EA. Selective protein arylation and acetaminophen-induced hepatotoxicity. Drug Metab Rev 1997; **29**(1-2): 59-77.

Coles B, Wilson I, Wardman P, Hinson JA, Nelson SD, Ketterer B. The spontaneous and enzymatic reaction of N-acetyl-p-benzoquinonimine with glutathione: A stopped-flow kinetic study. Arch Biochem Biophys 1988; **264**(1): 253-260.

Corcoran GB, Chung S-, Salazar DE. Early inhibition of the na +/K +-ATPase ion pump during acetaminophen-induced hepatotoxicity in rat. Biochem Biophys Res Commun 1987; **149**(1): 203-207.

Coulouarn C, Factor VM, Andersen JB, Durkin ME, Thorgeirsson SS. Loss of miR-122 expression in liver cancer correlates with suppression of the hepatic phenotype and gain of metastatic properties. Oncogene 2009; **28**(40): 3526-3536.

Craig DGN, Lee A, Hayes PC, Simpson KJ. Review article: The current management of acute liver failure. Alimentary Pharmacology and Therapeutics 2010; **31**(3): 345-358.

Craig DGN, Lee P, Pryde EA, Masterton GS, Hayes PC, Simpson KJ. Circulating apoptotic and necrotic cell death markers in patients with acute liver injury. Liver International 2011; **31**(8): 1127-1136.

Dahlin DC, Miwa GT, Lu AY, Nelson SD. N-acetyl-p-benzoquinone imine: A cytochrome P-450-mediated oxidation product of acetaminophen. Proc Natl Acad Sci U S A 1984; **81**(5): 1327-1331.

D'Alessandra Y, Devanna P, Limana F, Straino S, Di Carlo A, Brambilla PG, Rubino M, et al. Circulating microRNAs are new and sensitive biomarkers of myocardial infarction. Eur Heart J 2010; **31**(22): 2765-2773.

Danielson PB. The cytochrome P450 superfamily: Biochemistry, evolution and drug metabolism in humans. Curr Drug Metab 2002; **3**(6): 561-597.

Davis DC, Potter WZ, Jollow DJ, Mitchell JR. Species differences in hepatic glutathione depletion, covalent binding and hepatic necrosis after acetaminophen. Life Sci 1974; **14**(11): 2099-2109.

De Planell-Saguer M, Rodicio MC. Analytical aspects of microRNA in diagnostics: A review. Anal Chim Acta 2011; **699**(2): 134-152.

De Ritis F, Coltorti M, Giusti G. Diagnostic value and pathogenetic significance of transaminase activity changes in viral hepatitis. Minerva Med 1956; **47**(7): 167-171.

Dear JW. New marker for paracetamol poisoningrevolution or evolution. Clin Toxicol 2010; **48**(8): 785-786.

Denicola A, Radi R. Peroxynitrite and drug-dependent toxicity. Toxicology 2005; **208**(2): 273-288.

Donahower BC, McCullough SS, Hennings L, Simpson PM, Stowe CD, Saad AG, Kurten RC, et al. Human recombinant vascular endothelial growth factor reduces necrosis and enhances hepatocyte regeneration in a mouse model of acetaminophen toxicity. J Pharmacol Exp Ther 2010; **334**(1): 33-43.

Dowsley TF, Forkert P-, Benesch LA, Bolton JL. Reaction of glutathione with the electrophilic metabolites of 1,1-dichloroethylene. Chem Biol Interact 1995; **95**(3): 227-244.

Dridi D, Boughattas NA, Aouam K, Reinberg A, Ben Attia M. Circadian time-dependent differences in murine tolerance to the antihistaminic agent loratadine. Chronobiol Int 2005; **22**(3): 499-514.

El-Hassan H, Anwar K, Macanas-Pirard P, Crabtree M, Chow SC, Johnson VL, Lee PC, et al. Involvement of mitochondria in acetaminophen-induced apoptosis and hepatic injury: Roles of cytochrome c, bax, bid, and caspases. Toxicol Appl Pharmacol 2003; **191**(2): 118-129.

Elms AR, Owen KP, Albertson TE, Sutter ME. Fatal myocardial infarction associated with intravenous N-acetylcysteine error. International Journal of Emergency Medicine 2011; **4**(1).

Enomoto A, Itoh K, Nagayoshi E, Haruta J, Kimura T, O'Connor T, Harada T, et al. High sensitivity of Nrf2 knockout mice to acetaminophen hepatotoxicity associated with decreased expression of ARE-regulated drug metabolizing enzymes and antioxidant genes. Toxicological Sciences 2001; **59**(1): 169-177.

Esau C, Davis S, Murray SF, Yu XX, Pandey SK, Pear M, Watts L, et al. miR-122 regulation of lipid metabolism revealed by in vivo antisense targeting. Cell Metabolism 2006; **3**(2): 87-98.

Etxagibel A, Julià MR, Brotons A, Company MM, Dolz C. Drug-induced hepatitis superimposed on the presence of anti-SLA antibody: A case report. Journal of Medical Case Reports 2008; **2**.

Ferner RE, Dear JW, Bateman DN. Management of paracetamol poisoning. BMJ 2011; **342**.

Fishbane S, Durham JH, Marzo K, Rudnick M. N-acetylcysteine in the prevention of radiocontrast-induced nephropathy. Journal of the American Society of Nephrology 2004; **15**(2): 251-260.

Fontana RJ. Acute liver failure including acetaminophen overdose. Med Clin North Am 2008; **92**(4): 761-794.

Ford DE, Kamerow DB. Epidemiologic study of sleep disturbances and psychiatric disorders. an opportunity for prevention? J Am Med Assoc 1989; **262**(11): 1479-1484.

Forkert P-, Chen S, Jackson AC. In situ hybridization analysis of hepatic cytochrome P450 2E1 messenger ribonucleic acid in mice: Modulation of expression by acetone. Laboratory Investigation 1995; **72**(1): 92-99.

Forkert PG, Redza ZM, Mangos S, Park SS, Tam S-. Induction and regulation of Cyp2e1 in murine liver after acute and chronic acetone administration. Drug Metab Disposition 1994; **22**(2): 248-253.

Francois H, Facemire C, Kumar A, Audoly L, Koller B, Coffman T. Role of microsomal prostaglandin E synthase 1 in the kidney. Journal of the American Society of Nephrology 2007; **18**(5): 1466-1475.

Freedman MS, Lucas RJ, Soni B, Von Schantz M, Muñoz M, David-Gray Z, Foster R. Regulation of mammalian circadian behavior by non-rod, non-cone, ocular photoreceptors. Science 1999; **284**(5413): 502-504.

Fujimoto K, Kumagai K, Ito K, Arakawa S, Ando Y, Oda S-, Yamoto T, et al. Sensitivity of liver injury in heterozygous sod2 knockout mice treated with troglitazone or acetaminophen. Toxicol Pathol 2009; **37**(2): 193-200.

Gachon F, Olela FF, Schaad O, Descombes P, Schibler U. The circadian PAR-domain basic leucine zipper transcription factors DBP, TEF, and HLF modulate basal and inducible xenobiotic detoxification. Cell Metabolism 2006; **4**(1): 25-36.

Gatfield D, Le Martelot G, Vejnar CE, Gerlach D, Schaad O, Fleury-Olela F, Ruskeepää A-, et al. Integration of microRNA miR-122 in hepatic circadian gene expression. Genes and Development 2009; **23**(11): 1313-1326.

Gehring W, Rosbash M. The coevolution of blue-light photoreception and circadian rhythms. J Mol Evol 2003; **57**(SUPPL. 1): S286-S289.

Gibson GG & Skett P. Introduction to drug metabolism, 3rd edition, 2001, Cheltenham: Nelson Thornes

Gipp JJ, Chang C, Mulcahy RT. Cloning and nucleotide sequence of a full-length cDNA for human liver γ-glutamylcysteine synthetase. Biochem Biophys Res Commun 1992; **185**(1): 29-35.

Girard M, Jacquemin E, Munnich A, Lyonnet S, Henrion-Caude A. miR-122, a paradigm for the role of microRNAs in the liver. J Hepatol 2008; **48**(4): 648-656.

Giri S, Nieber K, Bader A. Hepatotoxicity and hepatic metabolism of available drugs: Current problems and possible solutions in preclinical stages. Expert Opinion on Drug Metabolism and Toxicology 2010; **6**(8): 895-917.

Glinghammar B, Rafter I, Lindström A-, Hedberg JJ, Andersson HB, Lindblom P, Berg A-, et al. Detection of the mitochondrial and catalytically active alanine aminotransferase in human tissues and plasma. Int J Mol Med 2009; **23**(5): 621-631.

Goldfrank's Toxicologic Emergencies. New York ; London: McGraw-Hill, 2006.

Goldring CEP, Kitteringham NR, Elsby R, Randle LE, Clement YN, Williams DP, McMahon M, et al. Activation of hepatic Nrf2 in vivo by acetaminophen in CD-1 mice. Hepatology 2004; **39**(5): 1267-1276.

Gonzalez FJ, Gelboin HV. Role of human cytochrome P-450s in risk assessment and susceptibility to environmentally based disease. J Toxicol Environ Health 1993; **40**(2-3): 289-308.

Gorbacheva VY, Kondratov RV, Zhang R, Cherukuri S, Gudkov AV, Takahashi JS, Antoch MP. Circadian

sensitivity to the chemotherapeutic agent cyclophosphamide depends on the functional status of the CLOCK/BMAL1 transactivation complex. Proc Natl Acad Sci U S A 2005; **102**(9): 3407-3412.

Grabowski H, Vernon J, DiMasi JA. Returns on research and development for 1990s new drug introductions. Pharmacoeconomics 2002; **20**(SUPPL. 3): 11-29.

Green TJ, Sivilotti MLA, Langmann C, Yarema M, Juurlink D, Burns MJ, Johnson DW. When do the aminotransferases rise after acute acetaminophen overdose. Clin Toxicol 2010; **48**(8): 787-792.

Guengerich FP. Cytochrome P450s and other enzymes in drug metabolism and toxicity. AAPS Journal 2006; **8**(1): E105-E111.

Guengerich FP, Kim D-, Iwasaki M. Role of human cytochrome P-450 IIE1 in the oxidation of many low molecular weight cancer suspects. Chem Res Toxicol 1991; **4**(2): 168-179.

Guerri C, Grisolia S. Influence of prolonged ethanol intake on the levels and turnover of alcohol and aldehyde dehydrogenases and glutathione. Adv Exp Med Biol 1980; **126**: 365-384.

Gujral JS, Knight TR, Farhood A, Bajt ML, Jaeschke H. Mode of cell death after acetaminophen overdose in mice: Apoptosis or oncotic necrosis? Toxicological Sciences 2002; **67**(2): 322-328. Guo H, Brewer JM, Lehman MN, Bittman EL. Suprachiasmatic regulation of circadian rhythms of gene expression in hamster peripheral organs: Effects of transplanting the pacemaker. Journal of Neuroscience 2006; **26**(24): 6406-6412.

Hawkins LC, Edwards JN, Dargan PI. Impact of restricting paracetamol pack sizes on paracetamol poisoning in the united kingdom: A review of the literature. Drug Safety 2007; **30**(6): 465-479.

Henderson CJ, Wolf CR, Kitteringham N, Powell H, Otto D, Park BK. Increased resistance to acetaminophen hepatotoxicity in mice lacking glutathione S-transferase pi. Proc Natl Acad Sci U S A 2000; **97**(23): 12741-12745.

Hengstler JG, Van Der Burg B, Steinberg P, Oesch F. Interspecies differences in cancer susceptibility and toxicity. Drug Metab Rev 1999; **31**(4): 917-970.

Hinson JA, Pohl LR, Monks TJ, Gillette JR. Acetaminophen-induced hepatotoxicity. Life Sci 1981; **29**(2): 107-116.

Hogaboam CM, Bone-Larson CL, Steinhauser ML, Matsukawa A, Gosling J, Boring L, Charo IF, et al. Exaggerated hepatic injury due to acetaminophen challenge in mice lacking C-C chemokine receptor 2. Am J Pathol 2000; **156**(4): 1245-1252.

Holme JA, Hongslo JK, Bjorge C, Nelson SD. Comparative cytotoxic effects of acetaminophen (N-acetyl-p-aminophenol), a non-hepatotoxic regioisomer acetyl-m-aminophenol and their postulated reactive hydroquinone and quinone metabolites in monolayer cultures of mouse hepatocytes. Biochem Pharmacol 1991; **42**(5): 1137-1142.

Hsu S-, Wang B, Kota J, Yu J, Costinean S, Kutay H, Yu L, et al. Essential metabolic, anti-inflammatory, and anti-tumorigenic functions of miR-122 in liver. J Clin Invest 2012; **122**(8): 2871-2883.

Im J-, Jung B-, Kim S-, Lee K-, Lee J-. Per3, a circadian gene, is required for Chk2 activation in human cells. FEBS Lett 2010; **584**(23): 4731-4734.

Ingelman-Sundberg M. Polymorphism of cytochrome P450 and xenobiotic toxicity. Toxicology 2002; **181-182**: 447-452.

Ishida Y, Kondo T, Ohshima T, Fujiwara H, Iwakura Y, Mukaida N. A pivotal involvement of IFN-γ in the pathogenesis of acetaminophen-induced acute liver injury. FASEB Journal 2002; **16**(10): 1227-1236.

Ishida Y, Kondo T, Tsuneyama K, Lu P, Takayasu T, Mukaida N. The pathogenic roles of tumor necrosis factor receptor p55 in acetaminophen-induced liver injury in mice. J Leukoc Biol 2004; **75**(1): 59-67.

Ishida Y, Yokoyama C, Inatomi T, Yagita K, Dong X, Yan L, Yamaguchi S, et al. Circadian rhythm of aromatic L-amino acid decarboxylase in the rat suprachiasmatic nucleus: Gene expression and decarboxylating activity in clock oscillating cells. Genes to Cells 2002; **7**(5): 447-459.

Jaeschke H, Bajt ML. Intracellular signaling mechanisms of acetaminophen-induced liver cell death. Toxicological Sciences 2006; **89**(1): 31-41.

Jaeschke H, Cover C, Bajt ML. Role of caspases in acetaminophen-induced liver injury. Life Sci 2006; **78**(15): 1670-1676.

Jaeschke H, Knight TR, Bajt ML. The role of oxidant stress and reactive nitrogen species in acetaminophen hepatotoxicity. Toxicol Lett 2003; **144**(3): 279-288.

Jaeschke H, McGill MR, Ramachandran A. Oxidant stress, mitochondria, and cell death mechanisms in drug-induced liver injury: Lessons learned from acetaminophen hepatotoxicity. Drug Metab Rev 2012; **44**(1): 88-106.

Jaeschke H, Wendel A. Diurnal fluctuation and pharmacological alteration of mouse organ glutathione content. Biochem Pharmacol 1985; **34**(7): 1029-1033.

James LP, Mayeux PR, Hinson JA. Acetaminophen-induced hepatotoxicity. Drug Metab Disposition 2003; **31**(12): 1499-1506.

Jeffery WH, Lafferty WE. Acute renal failure after acetaminophen overdose: Report of two cases. Am J Hosp Pharm 1981; **38**(9): 1355-1358.

Jollow DJ, Mitchell JR, Potter WZ. Acetaminophen induced hepatic necrosis. II. role of covalent binding in vivo. J Pharmacol Exp Ther 1973; **187**(1): 195-202.

Jollow DJ, Mitchell JR, Zampaglione N, Gillette JR. Bromobenzene induced liver necrosis. protective role of glutathione and evidence for 3,4 bromobenzene oxide as the hepatotoxic metabolite. Pharmacology 1974; **11**(3): 151-169.

Jollow DJ, Thorgeirsson SS, Potter WZ. Acetaminophen induced hepatic necrosis. VI. metabolic disposition of toxic

and nontoxic doses of acetaminophen. Pharmacology 1974; **12**(4-5): 251-271.

Jones AL. Mechanism of action and value of N-acetylcysteine in the treatment of early and late acetaminophen poisoning: A critical review. Journal of Toxicology - Clinical Toxicology 1998; **36**(4): 277-285.

Jordan CD, Flood JG, Laposata M, Lewandrowski KB. Normal reference laboratory values. N Engl J Med 1992; **327**(10): 718-724.

Ju C, Reilly TP, Bourdi M, Radonovich MF, Brady JN, George JW, Pohl LR. Protective role of kupffer cells in acetaminophen-induced hepatic injury in mice. Chem Res Toxicol 2002; **15**(12): 1504-1513.

Kaplowitz N. Idiosyncratic drug hepatotoxicity. Nature Reviews Drug Discovery 2005; **4**(6): 489-499.

Kerr F, Dawson A, Whyte IM, Buckley N, Murray L, Graudins A, Chan B, et al. The australasian clinical toxicology investigators collaboration randomized trial of different loading infusion rates of N-acetylcysteine. Ann Emerg Med 2005; **45**(4): 402-408.

Kim D-, Linnstaedt S, Palma J, Park JC, Ntrivalas E, Kwak-Kim JYH, Gilman-Sachs A, et al. Plasma components affect accuracy of circulating cancer-related microRNA quantitation. Journal of Molecular Diagnostics 2012; **14**(1): 71-80.

Kim YC, Lee SJ. Temporal variation in hepatotoxicity and metabolism of acetaminophen in mice. Toxicology 1998; **128**(1): 53-61.

Kim Y-, Kim VN. Processing of intronic microRNAs. EMBO J 2007; **26**(3): 775-783.

Kirschner MB, Kao SC, Edelman JJ, Armstrong NJ, Vallely MP, van Zandwijk N, Reid G. Haemolysis during sample preparation alters microRNA content of plasma. PLoS ONE 2011; **6**(9).

Kitteringham NR, Powell H, Clement YN, Dodd CC, Tettey JN, Pirmohamed M, Smith DA, et al. Hepatocellular response to chemical stress in CD-1 mice: Induction of early genes and γ-glutamylcysteine synthetase. Hepatology 2000; **32**(2): 321-333.

Kola I, Landis J. Can the pharmaceutical industry reduce attrition rates? Nature Reviews Drug Discovery 2004; **3**(8): 711-715.

Kornmann B, Schaad O, Bujard H, Takahashi JS, Schibler U. System-driven and oscillator-dependent circadian transcription in mice with a conditionally active liver clock. PLoS biology 2007; **5**(2).

Koutedakis Y, Raafat A, Sharp NCC, Rosmarin MN, Beard MJ, Robbins SW. Serum enzyme activities in individuals with different levels of physical fitness. J Sports Med Phys Fitness 1993; **33**(3): 252-257.

Kroh EM, Parkin RK, Mitchell PS, Tewari M. Analysis of circulating microRNA biomarkers in plasma and serum using quantitative reverse transcription-PCR (qRT-PCR). Methods 2010; **50**(4): 298-301.

Kumar D, Wingate D, Ruckebusch Y. Circadian variation in the propagation velocity of the migrating motor

complex. Gastroenterology 1986; **91**(4): 926-930.

Kutay H, Bai S, Datta J, Motiwala T, Pogribny I, Frankel W, Jacob ST, et al. Downregulation of miR-122 in the rodent and human hepatocellular carcinomas. J Cell Biochem 2006; **99**(3): 671-678.

Labbe G, Pessayre D, Fromenty B. Drug-induced liver injury through mitochondrial dysfunction: Mechanisms and detection during preclinical safety studies. Fundamental and Clinical Pharmacology 2008; **22**(4): 335-353.

Lagos-Quintana M, Rauhut R, Yalcin A, Meyer J, Lendeckel W, Tuschl T. Identification of tissue-specific MicroRNAs from mouse. Current Biology 2002; **12**(9): 735-739.

Lamia KA, Sachdeva UM, Di Tacchio L, Williams EC, Alvarez JG, Egan DF, Vasquez DS, et al. AMPK regulates the circadian clock by cryptochrome phosphorylation and degradation. Science 2009; **326**(5951): 437-440.

Landin JS, Cohen SD, Khairallah EA. Identification of a 54-kDa mitochondrial acetaminophen-binding protein as aldehyde dehydrogenase. Toxicol Appl Pharmacol 1996; **141**(1): 299-307. Larson AM, Polson J, Fontana RJ, Davern TJ, Lalani E, Hynan LS, Reisch JS, et al. Acetaminophen-induced acute liver failure: Results of a united states multicenter, prospective study. Hepatology 2005; **42**(6): 1364-1372.

Laskin DL, Gardner CR, Price VF, Jollow DJ. Modulation of macrophage functioning abrogates the acute hepatotoxicity of acetaminophen. Hepatology 1995; **21**(4): 1045-1050.

Lasser KE, Allen PD, Woolhandler SJ, Himmelstein DU, Wolfe SM, Bor DH. Timing of new black box warnings and withdrawals for prescription medications. J Am Med Assoc 2002; **287**(17): 2215-2220.

Laterza OF, Lim L, Garrett-Engele PW, Vlasakova K, Muniappa N, Tanaka WK, Johnson JM, et al. Plasma microRNAs as sensitive and specific biomarkers of tissue injury. Clin Chem 2009; **55**(11): 1977-1983.

Lawson JA, Fisher MA, Simmons CA, Farhood A, Jaeschke H. Inhibition of fas receptor (CD95)-induced hepatic caspase activation and apoptosis by acetaminophen in mice. Toxicol Appl Pharmacol 1999; **156**(3): 179-186.

Lazarou J, Pomeranz BH, Corey PN. Incidence of adverse drug reactions in hospitalized patients: A meta- analysis of prospective studies. J Am Med Assoc 1998; **279**(15): 1200-1205.

Lee H, Chen R, Lee Y, Yoo S, Lee C. Essential roles of CKIδ and CKIε in the mammalian circadian clock. Proc Natl Acad Sci U S A 2009; **106**(50): 21359-21364.

Lee RC, Feinbaum RL, Ambros V. The C. elegans heterochronic gene lin-4 encodes small RNAs with antisense complementarity to lin-14. Cell 1993; **75**(5): 843-854.

Lee SST, Buters JTM, Pineau T, Fernandez-Salguero P, Gonzalez FJ. Role of CYP2E1 in the hepatotoxicity of acetaminophen. J Biol Chem 1996; **271**(20): 12063-12067.

Lee WM. Acetaminophen-related acute liver failure in the united states. Hepatology Research 2008; **38**(SUPPL. 1): S3-S8.

Lee WM. Acetaminophen and the U.S. acute liver failure study group: Lowering the risks of hepatic failure. Hepatology 2004; **40**(1): 6-9.

Lee WM. Acute liver failure in the united states. Semin Liver Dis 2003; **23**(3): 217-226.

Lee Y, Ahn C, Han J, Choi H, Kim J, Yim J, Lee J, et al. The nuclear RNase III drosha initiates microRNA processing. Nature 2003; **425**(6956): 415-419.

Lemmer B, Nold G. Circadian changes in estimated hepatic blood flow in healthy subjects. Br J Clin Pharmacol 1991; **32**(5): 627-629.

Levi F, Giacchetti S, Adam R, Zidani R, Metzger G, Misset J-. Chronomodulation of chemotherapy against metastatic colorectal cancer. European Journal of Cancer Part A: General Topics 1995; **31**(7-8): 1264-1270.

Levi F, Le Louarn C, Reinberg A. Timing optimizes sustained-release indomethacin treatment of osteoarthritis. Clin Pharmacol Ther 1985; **37**(1): 77-84.

Levi F, Misset J-, Brienza S, Adam R, Metzger G, Itzakhi M, Caussanel J-, et al. A chronopharmacologic phase II clinical trial with 5-fluorouracil, folinic acid, and oxaliplatin using an ambulatory multichannel programmable pump: High antitumor effectiveness against metastatic colorectal cancer. Cancer 1992; **69**(4): 893-900.

Levi F, Schibler U. Circadian Rhythms: Mechanisms and Therapeutic Implications. , 2007:593-628.

Lévi F, Zidani R, Misset J-. Randomised multicentre trial of chronotherapy with oxaliplatin, fluorouracil, and folinic acid in metastatic colorectal cancer. Lancet 1997; **350**(9079): 681-686.

Li Z-, Xi Y, Zhu W-, Zeng C, Zhang Z-, Guo Z-, Hao D-, et al. Positive regulation of hepatic miR-122 expression by HNF4α. J Hepatol 2011; **55**(3): 602-611.

Lim FL, Currie RA, Orphanides G, Moggs JG. Emerging evidence for the interrelationship of xenobiotic exposure and circadian rhythms: A review. Xenobiotica 2006; **36**(10-11): 1140-1151. Lindblom P, Rafter I, Copley C, Andersson U, Hedberg JJ, Berg A-, Samuelsson A, et al. Isoforms of alanine aminotransferases in human tissues and serum-differential tissue expression using novel antibodies. Arch Biochem Biophys 2007; **466**(1): 66-77.

Liu AC, Welsh DK, Ko CH, Tran HG, Zhang EE, Priest AA, Buhr ED, et al. Intercellular coupling confers robustness against mutations in the SCN circadian clock network. Cell 2007; **129**(3): 605-616.

Lowry OH, Rosebrough NJ, Farr AL, Randall RJ. Protein measurement with the folin phenol reagent. The Journal of biological chemistry 1951; **193**(1): 265-275.

Lu SC. Regulation of hepatic glutathione synthesis: Current concepts and controversies. FASEB Journal 1999; **13**(10): 1169-1183.

Magnus G, Cavallini M, Halberg F. Circadian toxicology of cyclosporin. Toxicol Appl Pharmacol 1985; **77**(1): 181-185.

Mah SM, Buske C, Humphries RK, Kuchenbauer F. Mirna*: A passenger stranded in RNA-induced silencing complex? Crit Rev Eukaryot Gene Expr 2010; **20**(2): 141-148.

Mahn R, Heukamp LC, Rogenhofer S, Von Ruecker A, Müller SC, Ellinger J. Circulating microRNAs (miRNA) in serum of patients with prostate cancer. Urology 2011; **77**(5): 1265.e9-1265.e16.

Makin AJ, Wendon J, Williams R. A 7-year experience of severe acetaminophen-induced hepatotoxicity (1987-1993). Gastroenterology 1995; **109**(6): 1907-1916.

Mallal S, Nolan D, Witt C, Masel G, Martin AM, Moore C, Sayer D, et al. Association between presence of HLA-B*5701, HLA-DR7, and HLA-DQ3 and hypersensitivity to HIV-1 reverse-transcriptase inhibitor abacavir. Lancet 2002; **359**(9308): 727-732.

Mallal S, Phillips E, Carosi G, Molina J-, Workman C, Tomažiè J, Jägel-Guedes E, et al. HLA-B*5701 screening for hypersensitivity to abacavir. N Engl J Med 2008; **358**(6): 568-579.

Mandenius C-, Andersson TB, Alves PM, Batzl-Hartmann C, Björquist P, Carrondo MJT, Chesne C, et al. Toward preclinical predictive drug testing for metabolism and hepatotoxicity by using in vitro models derived from human embryonic stem cells and human cell lines - A report on the vitrocellomics EU-project. ATLA Alternatives to Laboratory Animals 2011; **39**(2): 147-171.

Masson MJ, Carpenter LD, Graf ML, Pohl LR. Pathogenic role of natural killer T and natural killer cells in acetaminophen-induced liver injury in mice is dependent on the presence of dimethyl sulfoxide. Hepatology 2008; **48**(3): 889-897.

Masubuchi Y, Bourdi M, Reilly TP, Graf MLM, George JW, Pohl LR. Role of interleukin-6 in hepatic heat shock protein expression and protection against acetaminophen-induced liver disease. Biochem Biophys Res Commun 2003; **304**(1): 207-212.

Matsunaga N, Ikeda M, Takiguchi T, Koyanagi S, Ohdo S. The molecular mechanism regulating 24-hour rhythm of CYP2E1 expression in the mouse liver. Hepatology 2008; **48**(1): 240-251.

Matsunaga N, Nakamura N, Yoneda N, Qin T, Terazono H, To H, Higuchi S, et al. Influence of feeding schedule on 24-h rhythm of hepatotoxicity induced by acetaminophen in mice. J Pharmacol Exp Ther 2004; **311**(2): 594-600.

Matsuo T, Yamaguchi S, Mitsui S, Emi A, Shimoda F, Okamura H. Control mechanism of the circadian clock for timing of cell division in vivo. Science 2003; **302**(5643): 255-259.

Maywood ES, Reddy AB, Wong GKY, O'Neill JS, O'Brien JA, McMahon DG, Harmar AJ, et al. Synchronization and maintenance of timekeeping in suprachiasmatic circadian clock cells by neuropeptidergic signaling. Current Biology 2006; **16**(6): 599-605.

McGill MR, Sharpe MR, Williams CD, Taha M, Curry SC, Jaeschke H. The mechanism underlying acetaminophen-

induced hepatotoxicity in humans and mice involves mitochondrial damage and nuclear DNA fragmentation. J Clin Invest 2012; **122**(4): 1574-1583.

Meister A. Glutathione metabolism and its selective modification. J Biol Chem 1988; **263**(33): 17205-17208.

Mercer AE, Regan SL, Hirst CM, Graham EE, Antoine DJ, Benson CA, Williams DP, et al. Functional and toxicological consequences of metabolic bioactivation of methapyrilene via thiophene S-oxidation: Induction of cell defence, apoptosis and hepatic necrosis. Toxicol Appl Pharmacol 2009; **239**(3): 297-305.

Meredith MJ, Reed DJ. Status of the mitochondrial pool of glutathione in the isolated hepatocyte. J Biol Chem 1982; **257**(7): 3747-3753.

Meredith TJ, Newman B, Goulding R. Paracetamol poisoning in children. Br Med J 1978; **2**(6135): 478-479.

Metzger G, Massari C, Etienne M-, Comisso M, Brienza S, Touitou Y, Milano G, et al. Spontaneous or imposed circadian changes in plasma concentrations of 5-fluorouracil coadministered with folinic acid and oxaliplatin: Relationship with mucosal toxicity in patients with cancer. Clin Pharmacol Ther 1994; **56**(2): 190-201.

Michael SL, Pumford NR, Mayeux PR, Niesman MR, Hinson JA. Pretreatment of mice with macrophage inactivators decreases acetaminophen hepatotoxicity and the formation of reactive oxygen and nitrogen species. Hepatology 1999; **30**(1): 186-195.

Mitchell I, Bihari D, Chang R, Wendon J, Williams R. Earlier identification of patients at risk from acetaminophen-induced acute liver failure. Crit Care Med 1998; **26**(2): 279-284.

Mitchell JR, Jollow DJ, Potter WZ. Acetaminophen induced hepatic necrosis. I. role of drug metabolism. J Pharmacol Exp Ther 1973; **187**(1): 185-194.

Mitchell JR, Nelson WL, Potter WZ. Metabolic activation of furosemide to a chemically reactive hepatotoxic metabolite. J Pharmacol Exp Ther 1976; **199**(1): 41-52.

Mitchell JR, Potter WZ, Hinson JA, Jollow DJ. Hepatic necrosis caused by furosemide. Nature 1974; **251**(5475): 508-510.

Mitchell JR, Thorgeirrson SS, Potter WZ. Acetaminophen induced hepatic injury: Protective role of glutathione in man and rationale for therapy. Clin Pharmacol Ther 1974; **16**(4): 676-684.

Mitchell PS, Parkin RK, Kroh EM, Fritz BR, Wyman SK, Pogosova-Agadjanyan EL, Peterson A, et al. Circulating microRNAs as stable blood-based markers for cancer detection. Proc Natl Acad Sci U S A 2008; **105**(30): 10513-10518.

Mittelbrunn M, Gutiérrez-Vázquez C, Villarroya-Beltri C, González S, Sánchez-Cabo F, González MÁ, Bernad A, et al. Unidirectional transfer of microRNA-loaded exosomes from T cells to antigen-presenting cells. Nature Communications 2011; **2**(1).

Moore JG, Halberg F. Circadian rhythm of gastric acid secretion in men with active duodenal ulcer. Dig Dis Sci 1986; **31**(11): 1185-1191.

Mormont M-, Levi F. Cancer chronotherapy: Principles, applications, and perspectives. Cancer 2003; **97**(1): 155-169.

Murphy R, Swartz R, Watkins PB. Severe acetaminophen toxicity in a patient receiving isoniazid. Ann Intern Med 1990; **113**(10): 799-800.

Nagoshi E, Saini C, Bauer C, Laroche T, Naef F, Schibler U. Circadian gene expression in individual fibroblasts: Cell-autonomous and self-sustained oscillators pass time to daughter cells. Cell 2004; **119**(5): 693-705.

Nakagawa H, Maeda S, Hikiba Y, Ohmae T, Shibata W, Yanai A, Sakamoto K, et al. Deletion of apoptosis signal-regulating kinase 1 attenuates acetaminophen-induced liver injury by inhibiting c-jun N-terminal kinase activation. Gastroenterology 2008; **135**(4): 1311-1321.

Neely LA, Patel S, Garver J, Gallo M, Hackett M, McLaughlin S, Nadel M, et al. A single-molecule method for the quantitation of microRNA gene expression. Nature Methods 2006; **3**(1): 41-46.

Nelson SD. Mechanisms of the formation and disposition of reactive metabolites that can cause acute liver injury. Drug Metab Rev 1995; **27**(1-2): 147-177.

Nolan CM, Sandblom RE, Thummel KE, Slattery JT, Nelson SD. Hepatotoxicity associated with acetaminophen usage in patients receiving multiple drug therapy for tuberculosis. Chest 1994; **105**(2): 408-411.

O'Brien PJ, Slaughter MR, Polley SR, Kramer K. Advantages of glutamate dehydrogenase as a blood biomarker of acute hepatic injury in rats. Lab Anim 2002; **36**(3): 313-321.

Ohmori M, Fujimura A. ACE inhibitors and chronotherapy. Clin Exp Hypertens 2005; **27**(2-3): 179-185.

Ostapowicz G, Fontana RJ, Schioødt FV, Larson A, Davern TJ, Han SHB, McCashland TM, et al. Results of a prospective study of acute liver failure at 17 tertiary care centers in the united states. Ann Intern Med 2002; **137**(12): 947-954.

Ozer J, Ratner M, Shaw M, Bailey W, Schomaker S. The current state of serum biomarkers of hepatotoxicity. Toxicology 2008; **245**(3): 194-205.

Panda S, Antoch MP, Miller BH, Su AI, Schook AB, Straume M, Schultz PG, et al. Coordinated transcription of key pathways in the mouse by the circadian clock. Cell 2002; **109**(3): 307-320.

Park BK, Kitteringham NR, Maggs JL, Pirmohamed M, Williams DP. The Role of Metabolic Activation in Drug-Induced Hepatotoxicity. , 2005:177-202.

Pasquinelli AE, Reinhart BJ, Slack F, Martindale MQ, Kuroda MI, Maller B, Hayward DC, et al. Conservation of the sequence and temporal expression of let-7 heterochronic regulatory RNA. Nature 2000; **408**(6808): 86-89.

Patten CJ, Thomas PE, Guy RL, Lee M, Gonzalez FJ, Guengerich FP, Yang CS. Cytochrome P450 enzymes involved

in acetaminophen activation by rat and human liver microsomes and their kinetics. Chem Res Toxicol 1993; **6**(4): 511-518.

Petit E, Milano G, Levi F, Thyss A, Bailleul F, Schneider M. Circadian rhythm-varying plasma concentration of 5-fluorouracil during a five-day continuous venous infusion at a constant rate in cancer patients. Cancer Res 1988; **48**(6): 1676-1679.

Pirmohamed M, James S, Meakin S, Green C, Scott AK, Walley TJ, Farrar K, et al. Adverse drug reactions as cause of admission to hospital: Prospective analysis of 18 820 patients. Br Med J 2004; **329**(7456): 15-19.

Prescott LF. Paracetamol poisoning. prevention of liver damage. Medecine et Chirurgie Digestives 1979; **8**(5): 391-393.

Prescott LF, Matthew H. Cysteamine for paracetamol overdosage. Lancet 1974; **1**(7864): 998.

Pryor WA, Squadrito GL. The chemistry of peroxynitrite: A product from the reaction of nitric oxide with superoxide. American Journal of Physiology - Lung Cellular and Molecular Physiology 1995; **268**(5 12-5): L699-L722.

Ptolemy AS, Rifai N. What is a biomarker? research investments and lack of clinical integration necessitate a review of biomarker terminology and validation schema. Scand J Clin Lab Invest 2010; **70**(SUPPL. 242): 6-14.

Punjabi NM, Polotsky VY. Disorders of glucose metabolism in sleep apnea. J Appl Physiol 2005; **99**(5): 1998-2007.

Qi R, Weiland M, Gao XH, Zhou L, Mi QS. Identification of endogenous normalizers for serum microRNAs by microarray profiling: U6 small nuclear RNA is not a reliable normalizer. Hepatology 2012; **55**(5): 1640-2; author reply 1642-3.

Qiu Y, Benet LZ, Burlingame AL. Identification of the hepatic protein targets of reactive metabolites of acetaminophen in vivo in mice using two-dimensional gel electrophoresis and mass spectrometry. J Biol Chem 1998; **273**(28): 17940-17953.

Rafter I, Graberg T, Kotronen A, Strommer L, Mattson CM, Kim RW, Ehrenborg E, et al. Isoform-specific alanine aminotransferase measurement can distinguish hepatic from extrahepatic injury in humans. Int J Mol Med 2012; **30**(5): 1241-1249.

Ralph MR, Foster RG, Davis FC, Menaker M. Transplanted suprachiasmatic nucleus determines circadian period. Science 1990; **247**(4945): 975-978.

Ramachandran A, Lebofsky M, Weinman SA, Jaeschke H. The impact of partial manganese superoxide dismutase (SOD2)-deficiency on mitochondrial oxidant stress, DNA fragmentation and liver injury during acetaminophen hepatotoxicity. Toxicol Appl Pharmacol 2011; **251**(3): 226-233.

Ramachandran S, Palanisamy V. Horizontal transfer of RNAs: Exosomes as mediators of intercellular communication. Wiley Interdisciplinary Reviews: RNA 2012; **3**(2): 286-293.

Randle LE, Goldring CEP, Benson CA, Metcalfe PN, Kitteringham NR, Park BK, Williams DP. Investigation of the effect of a panel of model hepatotoxins on the Nrf2-Keap1 defence response pathway in CD-1 mice. Toxicology 2008; **243**(3): 249-260.

Reilly TP, Brady JN, Marchick MR, Bourdi M, George JW, Radonovich MF, Pise-Masison CA, et al. A protective role for cyclooxygenase-2 in drug-induced liver injury in mice. Chem Res Toxicol 2001; **14**(12): 1620-1628.

Reinhart BJ, Slack FJ, Basson M, Pasquienelll AE, Bettlnger JC, Rougvle AE, Horvitz HR, et al. The 21-nucleotide let-7 RNA regulates developmental timing in caenorhabditis elegans. Nature 2000; **403**(6772): 901-906.

Reisman SA, Aleksunes LM, Klaassen CD. Oleanolic acid activates Nrf2 and protects from acetaminophen hepatotoxicity via Nrf2-dependent and Nrf2-independent processes. Biochem Pharmacol 2009; **77**(7): 1273-1282.

Reppert SM, Weaver DR. Coordination of circadian timing in mammals. Nature 2002; **418**(6901): 935-941.

Rex DK, Kumar S. Recognizing acetaminophen hepatotoxicity in chronic alcoholics. Postgrad Med 1992; **91**(4): 241-245.

Riordan SM, Williams R. Perspectives on liver failure: Past and future. Semin Liver Dis 2008; **28**(2): 137-141.

Ripperger JA, Schibler U. Rhythmic CLOCK-BMAL1 binding to multiple E-box motifs drives circadian dbp transcription and chromatin transitions. Nat Genet 2006; **38**(3): 369-374.

Roberts BJ, Song B-, Soh Y, Park SS, Shoaf SE. Ethanol induces CYP2E1 by protein stabilization: Role of ubiquitin conjugation in the rapid degradation of CYP2E1. J Biol Chem 1995; **270**(50): 29632-29635.

Rubbo H. Nitric oxide and peroxynitrite in lipid peroxidation. Medicina 1998; **58**(4): 361-366. Rumack BH, Bateman DN. Acetaminophen and acetylcysteine dose and duration: Past, present and future. Clin Toxicol 2012; **50**(2): 91-98.

Rumack BH, Matthew H. Acetaminophen poisoning and toxicity. Pediatrics 1975; **55**(6): 871-876.

Rumack BH, Peterson RC, Koch GG, Amara IA. Acetaminophen overdose. 662 cases with evaluation of oral acetylcysteine treatment. Arch Intern Med 1981; **141**(3): 380-385.

Rumack BH, Peterson RG. Acetaminophen overdose: Incidence, diagnosis, and management in 416 patients. Pediatrics 1978; **62**(5 II SUPPL.): 898-903.

Russo MW, Galanko JA, Shrestha R, Fried MW, Watkins P. Liver transplantation for acute liver failure from drug induced liver injury in the united states. Liver Transplantation 2004; **10**(8): 1018-1023.

Rutter J, Reick M, McKnight SL. Metabolism and the Control of Circadian Rhythms. , 2002:307-331.

Saheki T, Komorizono K, Miura T, Ichiki H, Yagi Y, Hashimoto S. Clearance of arginiosuccinate synthetase from the circulation in acute liver disease. Clin Biochem 1990; **23**(2): 139-141.

Scaffidi P, Misteli T, Bianchi ME. Release of chromatin protein HMGB1 by necrotic cells triggers inflammation. Nature 2002; **418**(6894): 191-195.

Schenker S, Speeg Jr. KV, Perez A, Finch J. The effects of food restriction in man on hepatic metabolism of acetaminophen. Clinical Nutrition 2001; **20**(2): 145-150.

Schernhammer ES, Laden F, Speizer FE, Willett WC, Hunter DJ, Kawachi I, Colditz GA. Rotating night shifts and risk of breast cancer in women participating in the nurses' health study. J Natl Cancer Inst 2001; **93**(20): 1563-1568.

Schibler U, Sassone-Corsi P. A web of circadian pacemakers. Cell 2002; **111**(7): 919-922. Schiødt FV, Rochling FA, Casey DL, Lee WM. Acetaminophen toxicity in an urban county hospital. N Engl J Med 1997; **337**(16): 1112-1117.

Schulman BR, Esquela-Kerscher A, Slack FJ. Reciprocal expression of lin-41 and the microRNAs let-7 and mir-125 during mouse embryogenesis. Developmental Dynamics 2005; **234**(4): 1046-54

Senior JR. How can 'hy's law' help the clinician? Pharmacoepidemiol Drug Saf 2006; **15**(4): 235-239.

Shakil AO, Kramer D, Mazariegos GV, Fung JJ, Rakela J. Acute liver failure: Clinical features, outcome analysis, and applicability of prognostic criteria. Liver Transplantation 2000; **6**(2): 163-169.

Shayiq RM, Roberts DW, Rothstein K, Snawder JE, Benson W, Ma X, Black M. Repeat exposure to incremental doses of acetaminophen provides protection against acetaminophen-induced lethality in mice: An explanation for high acetaminophen dosage in humans without hepatic injury. Hepatology 1999; **29**(2): 451-463.

Shi Q, Hong H, Senior J, Tong W. Biomarkers for drug-induced liver injury. Expert Review of Gastroenterology and Hepatology 2010; **4**(2): 225-234.

Simpson KJ, Bates CM, Henderson NC, Wigmore SJ, Garden OJ, Lee A, Pollok A, et al. The utilization of liver transplantation in the management of acute liver failure: Comparison between acetaminophen andnon-acetaminophen etiologies. Liver Transplantation 2009; **15**(6): 600-609. Skenderi KP, Kavouras SA, Anastasiou CA, Yiannakouris N, Matalas A-. Exertional rhabdomyolysis during a 246-km continuous running race. Med Sci Sports Exerc 2006; **38**(6): 1054-1057.

Slack FJ, Basson M, Liu Z, Ambros V, Horvitz HR, Ruvkun G. The lin-41 RBCC gene acts in the C. elegans heterochronic pathway between the let-7 regulatory RNA and the LIN-29 transcription factor. Mol Cell 2000; **5**(4): 659-669.

Smolensky MH, Scott PH, Harrist RB, Hiatt PH, Wong TK, Baenziger JC, Klank BJ, et al. Administration-time-dependency of the pharmacokinetic behavior and therapeutic effect of a once-a-day theophylline in asthmatic children. Chronobiol Int 1987; **4**(3): 435-447.

Stapelbroek JM, van Erpecum KJ, Klomp LWJ, Houwen RHJ. Liver disease associated with canalicular transport defects: Current and future therapies. J Hepatol 2010; **52**(2): 258-271.

Stravitz RT, Kramer DJ. Management of acute liver failure. Nature Reviews Gastroenterology and Hepatology 2009; **6**(9): 542-553.

Suter DM, Schibler U. Feeding the clock. Science 2009; **326**(5951): 378-379.

Testa B, Pedretti A, Vistoli G. Reactions and enzymes in the metabolism of drugs and other xenobiotics. Drug Discovery Today 2012; **17**(11-12): 549-560

Thummel KE, Lee CA, Kunze KL, Nelson SD, Slattery JT. Oxidation of acetaminophen to N-acetyl-p-aminobenzoquinone imine by human CYP3A4. Biochem Pharmacol 1993; **45**(8): 1563-1569.

Thummel KE, Slattery JT, Nelson SD, Lee CA, Pearson PG. Effect of ethanol on hepatotoxicity of acetaminophen in mice and on reactive metabolite formation by mouse and human liver microsomes. Toxicol Appl Pharmacol 1989; **100**(3): 391-397.

Tirmenstein MA, Nelson SD. Hepatotoxicity after 3′-hydroxyacetanilide administration to buthionine sulfoximine pretreated mice. Chem Res Toxicol 1991; **4**(2): 214-217.

Tsai W-, Hsu S-, Hsu C-, Lai T-, Chen S-, Shen R, Huang Y, et al. MicroRNA-122 plays a critical role in liver homeostasis and hepatocarcinogenesis. J Clin Invest 2012; **122**(8): 2884-2897.

Tsokos-Kuhn JO, Todd EL, McMillan-Wood JB, Mitchell JR. ATP-dependent calcium uptake by rat liver plasma membrane vesicle. effect of alkylating hepatotoxins in vivo. Mol Pharmacol 1985; **28**(1): 56-61.

Tujios S, Fontana RJ. Mechanisms of drug-induced liver injury: From bedside to bench. Nature Reviews Gastroenterology and Hepatology 2011; **8**(4): 202-211.

Turnbull MJ, Watkins JW. Determination of halothane induced sleeping time in the rat: Effect of prior administration of centrally active drugs. Br J Pharmacol 1976; **58**(1): 27-35.

Valadi H, Ekström K, Bossios A, Sjöstrand M, Lee JJ, Lötvall JO. Exosome-mediated transfer of mRNAs and microRNAs is a novel mechanism of genetic exchange between cells. Nat Cell Biol 2007; **9**(6): 654-659.

Vandeputte C, Guizon I, Genestie-Denis I, Vannier B, Lorenzon G. A microtiter plate assay for total glutathione and glutathione disulfide contents in cultured/isolated cells: Performance study of a new miniaturized protocol. Cell Biol Toxicol 1994; **10**(5-6): 415-421.

Vickers KC, Palmisano BT, Shoucri BM, Shamburek RD, Remaley AT. MicroRNAs are transported in plasma and delivered to recipient cells by high-density lipoproteins. Nat Cell Biol 2011; **13**(4): 423-435.

Vitaterna MH, King DP, Chang A-, Kernhauser JM, Lowrey PL, McDonald JD, Dove WF, et al. Mutagenesis and mapping of a mouse gene, clock, essential for circadian behavior. Science 1994; **264**(5159): 719-725.

Vollmers C, Gill S, DiTacchio L, Pulivarthy SR, Le HD, Panda S. Time of feeding and the intrinsic circadian clock drive rhythms in hepatic gene expression. Proc Natl Acad Sci U S A 2009; **106**(50): 21453-21458.

Wang F, Zheng Z, Guo J, Ding X. Correlation and quantitation of microRNA aberrant expression in tissues and sera from patients with breast tumor. Gynecol Oncol 2010; **119**(3): 586-593.

Wang K, Zhang S, Marzolf B, Troisch P, Brightman A, Hu Z, Hood LE, et al. Circulating microRNAs, potential biomarkers for drug-induced liver injury. Proc Natl Acad Sci U S A 2009; **106**(11): 4402-4407.

Wang K, Zhang S, Weber J, Baxter D, Galas DJ. Export of microRNAs and microRNA-protective protein by mammalian cells. Nucleic Acids Res 2010; **38**(20): 7248-7259.

Watkins PB, Kaplowitz N, Slattery JT, Colonese CR, Colucci SV, Stewart PW, Harris SC. Aminotransferase elevations in healthy adults receiving 4 grams of acetaminophen daily: A randomized controlled trial. J Am Med Assoc 2006; **296**(1): 87-93.

Wendel A, Feuerstein S, Konz KH. Acute paracetamol intoxication of starved mice leads to lipid peroxidation in vivo. Biochem Pharmacol 1979; **28**(13): 2051-2055.

Whitcomb DC, Block GD. Association of acetaminophen hepatotoxicity with fasting and ethanol use. J Am Med Assoc 1994; **272**(23): 1845-1850.

Wightman B, Ha I, Ruvkun G. Posttranscriptional regulation of the heterochronic gene lin-14 by lin-4 mediates temporal pattern formation in C. elegans. Cell 1993; **75**(5): 855-862.

Williams DP, Antoine DJ, Butler PJ, Jones R, Randle L, Payne A, Howard M, et al. The metabolism and toxicity of furosemide in the wistar rat and CD-1 mouse: A chemical and biochemical definition of the toxicophore. J Pharmacol Exp Ther 2007; **322**(3): 1208-1220.

Woodcock J, Buckman S, Goodsaid F, Walton MK, Zineh I. Qualifying biomarkers for use in drug development: A US food and drug administration overview. Expert Opinion on Medical Diagnostics 2011; **5**(5): 369-374.

Xu H, He JH, Xiao ZD, Zhang QQ, Chen YQ, Zhou H, Qu LH. Liver-enriched transcription factors regulate microRNA-122 that targets CUTL1 during liver development. Hepatology 2010; **52**(4): 1431-1442.

Yan N, Meister A. Amino acid sequence of rat kidney γ-glutamylcysteine synthetase. J Biol Chem 1990; **265**(3): 1588-1593.

Yang R-, Park S, Reagan WJ, Goldstein R, Zhong S, Lawton M, Rajamohan F, et al. Alanine aminotransferase isoenzymes: Molecular cloning and quantitative analysis of tissue expression in rats and serum elevation in liver toxicity. Hepatology 2009; **49**(2): 598-607.

Yohe HC, O'Hara KA, Hunt JA, Kitzmiller TJ, Wood SG, Bement JL, Bement WJ, et al. Involvement of toll-like receptor 4 in acetaminophen hepatotoxicity. American Journal of Physiology - Gastrointestinal and Liver Physiology 2006; **290**(6): G1269-G1279.

Yuan L, Kaplowitz N. Glutathione in liver diseases and hepatotoxicity. Mol Aspects Med 2009; **30**(1-2): 29-41.

Zamek-Gliszczynski MJ, Hoffmaster KA, Nezasa K-, Tallman MN, Brouwer KLR. Integration of hepatic drug transporters and phase II metabolizing enzymes: Mechanisms of hepatic excretion of sulfate, glucuronide, and

glutathione metabolites. European Journal of Pharmaceutical Sciences 2006; **27**(5): 447-486.

Zanello SB, Jackson DM, Holick MF. Expression of the circadian clock genes clock and period1 in human skin. J Invest Dermatol 2000; **115**(4): 757-760.

Zhang J, Huang W, Chua SS, Wei P, Moore DD. Modulation of acetaminophen-induced hepatotoxicity by the xenobiotic receptor CAR. Science 2002; **298**(5592): 422-424.

Zhang Y, Jia Y, Zheng R, Guo Y, Wang Y, Guo H, Fei M, et al. Plasma microRNA-122 as a biomarker for viral-, alcohol-, and chemical-related hepatic diseases. Clin Chem 2010; **56**(12): 1830-1838.